Extracellular vesicle engineering for drug delivery

Sander Kooijmans

Colofon

ISBN: 978-90-393-6544-1
Printed by: Proefschriftmaken.nl || Uitgeverij BOXPress
Cover design: Sander Kooijmans
Lay-out: Sander Kooijmans

The printing of this thesis was financially supported by Becton Dickinson Biosciences, Greiner Bio-One, and Sysmex Nederland.

Extracellular vesicle engineering for drug delivery

Modificatie van extracellulaire membraanblaasjes
voor geneesmiddelafgifte
(met een samenvatting in het Nederlands)

Proefschrift

ter verkrijging van de graad van doctor aan de Universiteit Utrecht
op gezag van de rector magnificus, prof.dr. G.J. van der Zwaan,
ingevolge het besluit van het college voor promoties in het openbaar te verdedigen
op dinsdag 5 juli 2016 des middags te 4.15 uur

door

Sander Alexander Antonius Kooijmans

geboren op 3 februari 1988 te West Maas en Waal

Promotoren: Prof. dr. R.M. Schiffelers
Prof. dr. W.W. van Solinge

Copromotor: Dr. P. Vader

This research is supported by a European Research Council starting grant (260627) "MINDS" in the FP7 ideas program of the European Union.

"Don't waste your time
or time will waste you"

Muse – Knights of Cydonia

Table of contents

CHAPTER 1

General introduction

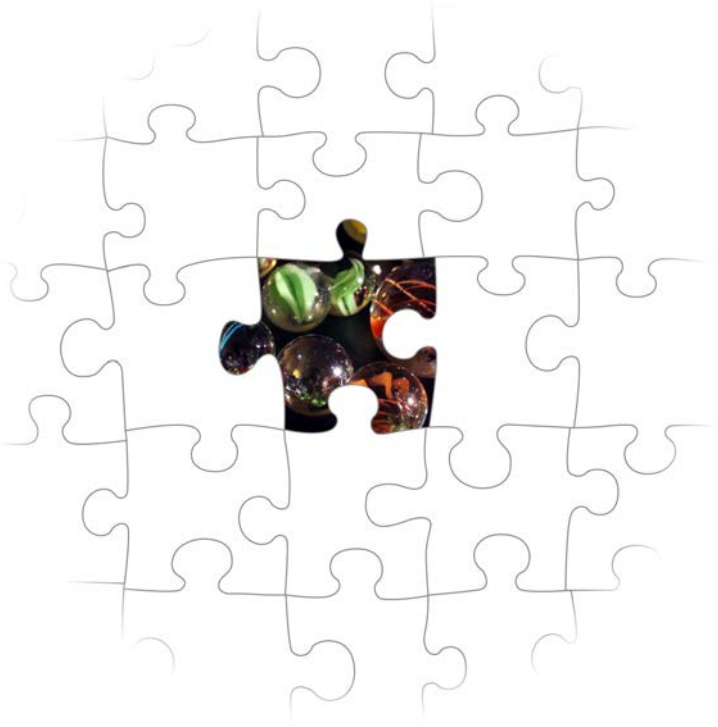

A hidden surprise

"How could I have been so stupid?" The thought of king Priam was overshadowed by an immense blow from the collapsing stables, set ablaze by the intruders. Groups of frightened people - those who were not completely intoxicated by the nightly celebrations - ran across the blackened streets in pointless attempts to flee their pursuers. The city, his beloved home, had fended off the attack for ten glorious years. He felt betrayed. The ongoing siege had come to an abrupt end when the cursed Greeks had given up and retreated from the field of battle. He had witnessed with his own eyes how they embarked their ships and sailed away. He should have known that it would not be this easy. The Greek offering of an immense, well-crafted wooden horse at the gates of the city had initially raised suspicion. However, misled by the treacherous words of Sinon and strengthened by the continuing Greek absence, his gut feeling had gradually shifted towards pride of his victory. The heavy gift was hauled into the city, whilst relief and joy filled the hearts of the city's inhabitants. From that moment onwards, the streets became the venue for celebrations whose extent exceeded any event in history. The festivities continued long after nightfall and brought sparkling feelings of victory to all. But then, in the middle of the night, suddenly misfortune had struck. Hidden Greek soldiers had swarmed out of the wooden horse, bringing death and destruction, and had opened the gates to the returning Greek army. With this dramatic twist of events, the war indeed had come to an end. The impenetrable city of Troy had fallen.

The above fragment could illustrate the thoughts of king Priam during the last moments of the Trojan War, which was waged around 1180 BC. This war, and more specifically the cunning use of the Trojan horse to breach Troy's walls, is still a rich source of inspiration for modern inventions. For example, the term 'Trojan horse' is currently used to refer to seemingly innocent, yet malicious software designed to gain access to protected computers when the 'gift' is accepted by their users. Here, the Trojan horse analogy will be used to clarify the aim of the research described in this thesis.

Treatment of cancer: seizing an impregnable fort

Despite intensive research over many decades, treatment of cancer with currently approved therapeutics often fails to stop disease progression. As a consequence, cancer is still a leading cause of death worldwide [1]. One of the reasons for the limited clinical success in cancer therapy is the unfavorable distribution of therapeutic agents in the body, characterized by poor drug penetration into the tumor tissue and high systemic exposure, resulting in dose-limiting toxicity [2]. These parameters can be improved by the incorporation of cytotoxic drugs in nanoparticulate delivery systems. The sizes of these systems generally range between 50 and 200 nm, which limits their premature renal clearance, but allows passive extravasation and accumulation in inflamed (tumor) tissues due to the enhanced-permeability-and-

retention (EPR) effect [3]. Furthermore, nanoparticles can be employed for the packaging and targeted delivery of therapeutic nucleic acids, such as small interfering (si)RNA. Although siRNA is considered a powerful potential therapeutic agent for the treatment of a variety of human diseases due to its ability to specifically knock down (disease-causing) genes, its physicochemical properties prevent entry into the cytosol of cells, where it exerts its function. Furthermore, siRNA is rapidly degraded upon intravenous administration. Hence, protective formulation into a suitable carrier system is mandatory to fully exploit the therapeutic potential of siRNA [4].

Over the past decades, a large variety of synthetic and viral carrier systems for siRNA (e.g. liposomes, micelles, polymers and virus-like particles) have been designed and evaluated in preclinical settings. Unfortunately, these ongoing efforts have translated into only a handful of nanoparticulate drug delivery systems undergoing clinical trials. The limited clinical success of these systems can often be attributed to poor *in vivo* performance, illustrated by undesired interactions with blood components, immunogenicity, off-target accumulation (e.g. in liver and spleen), and poor delivery efficiency [5-8].

A novel approach: construction of a biological Trojan horse

Almost half a century ago, it was first observed that platelets release small membrane-enclosed vesicles with procoagulant properties [9]. Initially, these were disregarded as biologically irrelevant artifacts resulting from storage of plasma, but over the years it became apparent that this view required revision. Currently, it is widely accepted that virtually all cells in the body constitutively release these vesicles into bodily fluids, including blood, urine, lymph, cerebrospinal fluid and other fluids. Vesicles can be classified according to their intracellular origin: larger vesicles (50-1000 nm) are generally believed to originate from budding from the plasma membrane (termed microvesicles or ectosomes), while smaller subsets (30-100 nm) are released upon fusion of large endosomal bodies with the plasma membrane (exosomes) [10, 11]. However, given the fact that in practice these classes show overlapping characteristics and cannot be completely separated, the term 'extracellular vesicles' (EVs) is used in this thesis to refer to both.

In the early days of EV research, EVs were considered to comprise complex mixtures of bioactive lipids and proteins, both soluble and membrane-bound. This view changed in 2007, when it was described that EVs also carry RNA, including mRNA and regulatory miRNA, which are structurally similar to siRNA [12]. Ongoing research provides mounting evidence that EVs harness the capacity to transfer their RNA to recipient cells, where it can induce phenotypical changes [12-18]. It is currently well established that, through their signaling and cargo-transferring properties, EVs function as mediators of intercellular communication. EVs have been shown to be involved a wide range of (patho)physiological processes, including immune modulation, cancer development and metastasis, coagulation, tissue regeneration and infectious diseases (reviewed in [10, 19]). The highly variable composition of EVs is dictated by

their producer cells, and may thus reflect cell state and origin. Hence, EVs have also been opted as valuable diagnostic tools, for example as 'liquid biopsies' to monitor disease progression and responses to therapy [20, 21].

The natural capacity of EVs to encapsulate, protect, transport and functionally deliver biological cargo to cells *in vivo* has also created excitement in the drug delivery field, and raised the question whether this natural delivery system could be hijacked for therapeutic purposes [22, 23]. Would it be possible to 'reprogram' EVs to convey therapeutic cargo specifically to diseased cells in an efficient and biocompatible manner, thereby functioning as biological Trojan horses? The feasibility of this idea is explored in this thesis.

In order to exploit EVs for drug delivery, their intrinsic properties may need to be engineered, given that these may not necessarily overlap with, or even interfere with their intended therapeutic application. For example, the presence of predefined cell-specific targeting moieties on EV surfaces could induce EV uptake by non-targeted (healthy) cells, resulting in off-target cargo delivery and corresponding side effects. Furthermore, therapeutic cargo (e.g. siRNA) needs to be stably incorporated, without compromising EV delivery performance. However, robust strategies to efficiently and reproducibly modify EV content for drug delivery purposes are still lacking. In this thesis, we therefore investigated the engineering of two aspects of EVs: loading of EVs with siRNA (**Chapters 2-3**), and (re)targeting of EVs to tumor cells using epidermal growth factor receptor (EGFR)-binding nanobodies (**Chapters 4-6**). Additionally, we discuss the possibility to borrow a leaf from nature's book to improve state-of-the-art synthetic drug delivery systems by incorporation of EV constituents (**Chapter 7**).

Outline of this thesis

In **Chapter 2**, we characterize the use of the frequently employed electroporation technique for the loading of siRNA into EVs. We employed a combination of RT-PCR, fluorescence spectroscopy and fluorescence fluctuation spectroscopy techniques to address misconceptions in the analysis of siRNA loading into EVs by electroporation. Furthermore, we attempted to optimize the electroporation protocol for the efficient incorporation of siRNA, while preserving EV integrity and colloidal stability.

Chapter 3 provides an overview of currently employed strategies to incorporate small RNAs into EVs, and discusses the advantages and potential pitfalls of each strategy. In addition, several challenges that need to be overcome for the generation of siRNA-loaded EVs are highlighted.

In **Chapter 4**, we describe a novel strategy to improve the targeting specificity of EVs to tumor cells. Anti-EGFR nanobodies were fused to glycosylphosphatidylinositol (GPI)-anchoring peptides and expressed in EV producer cells. The nanobody incorporation, morphology and

size of EVs secreted from these cells was analyzed. Furthermore, the effect of nanobody display on EV association and uptake by EGFR-overexpressing tumor cells was assessed. In addition, EV association with tumor cells under flow conditions was evaluated using a fluorescence microscopy-coupled perfusion setup.

A strategy to decorate EVs with targeting ligands after their isolation is presented in **Chapter 5**. Herein, we investigate the use of the post-insertion technique, adopted from the liposome field, to graft polyethylene glycol (PEG) coupled to anti-EGFR nanobodies on the surface of EVs. The effects of this modification on basal EV characteristics (size, morphology, integrity) were evaluated. We further assessed how insertion of PEG-nanobodies alter EV tumor cell specificity *in vitro*, and analyzed the circulation time and tissue distribution of modified EVs in tumor-bearing mice.

In **Chapter 6**, we optimized the expression and purification of recombinant anti-EGFR nanobodies fused with the phosphatidylserine (PS)-binding C1C2 domains of lactadherin. To test whether these proteins can serve as 'plug-and-play' tumor targeting ligands for isolated (PS-exposing) EVs, association of C1C2-nanobodies with PS, EGFR and EVs from two distinct sources was characterized. Furthermore, it was investigated whether decoration of these EVs with C1C2-nanobodies improved their specific association and internalization by EGFR-overexpressing tumor cells.

The idea to incorporate EV components into synthetic drug delivery systems, such as liposomes, to improve their biocompatibility and delivery efficiency, is discussed in **Chapter 7**. An overview of EV constituents (proteins, lipids and miRNAs) which may fulfill key roles for membrane stabilization, immune evasion, cell association, membrane fusion, and therapeutics effects is presented. These could be used as starting points for future research to 'EV-mimetic' drug delivery systems.

Chapter 8 provides a summarizing discussion of the findings in this thesis, and describes perspectives for the further development of EVs as drug delivery systems.

References

1. World Health Organization, All Cancers (excluding non-melanoma skin cancer) Estimated Incidence, Mortality and Prevalence Worldwide in 2012, accessible at http://globocan.iarc.fr/Pages/fact_sheets_cancer.aspx, accessed 23 February 2016.
2. A. Wicki, D. Witzigmann, V. Balasubramanian, J. Huwyler, Nanomedicine in cancer therapy: challenges, opportunities, and clinical applications, *J Control Release*, 200 (2015) 138-157.
3. H. Maeda, H. Nakamura, J. Fang, The EPR effect for macromolecular drug delivery to solid tumors: Improvement of tumor uptake, lowering of systemic toxicity, and distinct tumor imaging in vivo, *Adv Drug Deliv Rev*, 65 (2013) 71-79.
4. A. Schroeder, C.G. Levins, C. Cortez, R. Langer, D.G. Anderson, Lipid-based nanotherapeutics for siRNA delivery, *J Intern Med*, 267 (2010) 9-21.
5. V.J. Venditto, F.C. Szoka Jr, Cancer nanomedicines: so many papers and so few drugs!, *Adv Drug Deliv Rev*, (2013) 80-88.
6. H. Yin, R.L. Kanasty, A.A. Eltoukhy, A.J. Vegas, J.R. Dorkin, D.G. Anderson, Non-viral vectors for gene-based therapy, *Nat Rev Genet*, 15 (2014) 541-555.
7. J.L. Au, B.Z. Yeung, M.G. Wientjes, Z. Lu, Delivery of cancer therapeutics to extracellular and intracellular targets: Determinants, barriers, challenges and opportunities. , (2015) 280-301.
8. R. van der Meel, L.J. Vehmeijer, R.J. Kok, G. Storm, E.V. van Gaal, Ligand-targeted particulate nanomedicines undergoing clinical evaluation: current status, *Adv Drug Deliv Rev*, 65 (2013) 1284-1298.
9. P. Wolf, The nature and significance of platelet products in human plasma, *Br J Haematol*, 13 (1967) 269-288.
10. M. Colombo, G. Raposo, C. Thery, Biogenesis, secretion, and intercellular interactions of exosomes and other extracellular vesicles, *Annu Rev Cell Dev Biol*, 30 (2014) 255-289.
11. C. Thery, M. Ostrowski, E. Segura, Membrane vesicles as conveyors of immune responses, *Nat Rev Immunol*, 9 (2009) 581-593.
12. H. Valadi, K. Ekstrom, A. Bossios, M. Sjostrand, J.J. Lee, J.O. Lotvall, Exosome-mediated transfer of mRNAs and microRNAs is a novel mechanism of genetic exchange between cells, *Nat Cell Biol*, 9 (2007) 654-659.
13. A. Zomer, C. Maynard, F.J. Verweij, A. Kamermans, R. Schafer, E. Beerling*, et al.*, In Vivo imaging reveals extracellular vesicle-mediated phenocopying of metastatic behavior, *Cell*, 161 (2015) 1046-1057.
14. C.P. Lai, E.Y. Kim, C.E. Badr, R. Weissleder, T.R. Mempel, B.A. Tannous*, et al.*, Visualization and tracking of tumour extracellular vesicle delivery and RNA translation using multiplexed reporters, *Nat Commun*, 6 (2015) 7029.
15. M. Mittelbrunn, C. Gutierrez-Vazquez, C. Villarroya-Beltri, S. Gonzalez, F. Sanchez-Cabo, M.A. Gonzalez*, et al.*, Unidirectional transfer of microRNA-loaded exosomes from T cells to antigen-presenting cells, *Nat Commun*, 2 (2011) 282.
16. A. Montecalvo, A.T. Larregina, W.J. Shufesky, D. Beer Stolz, M.L. Sullivan, J.M. Karlsson*, et al.*, Mechanism of transfer of functional microRNAs between mouse dendritic cells via exosomes, *Blood*, 119 (2012) 756-766.

17. D.M. Pegtel, K. Cosmopoulos, D.A. Thorley-Lawson, M.A. van Eijndhoven, E.S. Hopmans, J.L. Lindenberg*, et al.*, Functional delivery of viral miRNAs via exosomes, *Proc Natl Acad Sci U S A*, 107 (2010) 6328-6333.

18. M.T. Le, P. Hamar, C. Guo, E. Basar, R. Perdigao-Henriques, L. Balaj*, et al.*, miR-200-containing extracellular vesicles promote breast cancer cell metastasis, *J Clin Invest*, 124 (2014) 5109-5128.

19. M. Yanez-Mo, P.R. Siljander, Z. Andreu, A.B. Zavec, F.E. Borras, E.I. Buzas*, et al.*, Biological properties of extracellular vesicles and their physiological functions, *J Extracell Vesicles*, 4 (2015) 27066.

20. R. van der Meel, M. Krawczyk-Durka, W.W. van Solinge, R.M. Schiffelers, Toward routine detection of extracellular vesicles in clinical samples, *Int J Lab Hematol*, 36 (2014) 244-253.

21. G. Fuhrmann, I.K. Herrmann, M.M. Stevens, Cell-derived vesicles for drug therapy and diagnostics: Opportunities and challenges, *Nano Today*, 10 (2015) 397-409.

22. S.M. van Dommelen, P. Vader, S. Lakhal, S.A. Kooijmans, W.W. van Solinge, M.J. Wood*, et al.*, Microvesicles and exosomes: opportunities for cell-derived membrane vesicles in drug delivery, *J Control Release*, 161 (2012) 635-644.

23. S. El-Andaloussi, I. Mager, X.O. Breakefield, M.J. Wood, Extracellular vesicles: biology and emerging therapeutic opportunities, *Nat Rev Drug Discov*, 12 (2013) 347-357.

CHAPTER 2

Electroporation-induced siRNA precipitation obscures the efficiency of siRNA loading into extracellular vesicles

Sander A. A. Kooijmans[1,*], Stephan Stremersch[2,*], Kevin Braeckmans[2,3], Stefaan de Smedt[2], An Hendrix[4], Matthew J. A. Wood[5], Raymond M. Schiffelers[1], Koen Raemdonck[2,#], Pieter Vader[2,5,#]

[1]Department of Clinical Chemistry and Haematology, University Medical Center Utrecht, Utrecht, The Netherlands; [2]Laboratory of General Biochemistry and Physical Pharmacy, Ghent University, Ghent, Belgium; [3]Centre for Nano- and Biophotonics, Ghent University, Ghent, Belgium; [4]Department of Radiation Oncology and Experimental Cancer Research, Laboratory of Experimental Cancer Research, Ghent University Hospital, Ghent, Belgium; [5]Department of Physiology, Anatomy and Genetics, University of Oxford, Oxford, UK

*These authors contributed equally to this work

#These authors contributed equally to this work

Journal of Controlled Release, 2013. 172(2), 229-38

Abstract

Extracellular vesicles (EVs) are specialised endogenous carriers of proteins and nucleic acids and are involved in intercellular communication. EVs are therefore proposed as candidate drug delivery systems for the delivery of nucleic acids and other macromolecules. However, the preparation of EV-based drug delivery systems is hampered by the lack of techniques to load the vesicles with nucleic acids. In this work we have now characterised in detail the use of an electroporation method for this purpose. When EVs were electroporated with fluorescently labelled siRNA, the siRNA retention was comparable with previously published results (20-25% based on fluorescence spectroscopy and fluorescence fluctuation spectroscopy), and electroporation with unlabelled siRNA resulted in significant siRNA retention in the EV pellet as measured by RT-PCR. Remarkably, when siRNA was electroporated in the absence of EVs, a similar or even greater siRNA retention was measured. Nanoparticle Tracking Analysis and confocal microscopy showed extensive formation of insoluble siRNA aggregates after electroporation, which could be dramatically reduced by addition of EDTA. Other strategies to reduce aggregate formation, including the use of cuvettes with conductive polymer electrodes and the use of an acidic citrate electroporation buffer, resulted in a more efficient reduction of siRNA precipitation than EDTA. However, under these conditions, siRNA retention was below 0.05% and no significant differences in siRNA retention could be measured between samples electroporated in the presence or absence of EVs. Our results show that electroporation of EVs with siRNA is accompanied by extensive siRNA aggregate formation, which may cause overestimation of the amount of siRNA actually loaded into EVs. Moreover, our data clearly illustrate that electroporation is far less efficient than previously described, and highlight the necessity for alternative methods to prepare siRNA-loaded EVs.

Introduction

Extracellular vesicles (EVs) are small endogenous phospholipid vesicles with typical diameters of 40-1000 nm, which are secreted from a variety of cell types. A well-studied subpopulation of EVs, mostly termed 'exosomes', originates from inward budding of endosomal membranes into large multivesicular bodies (MVBs). The 40-100 nm vesicles are secreted into the extracellular space upon fusion of the MVBs with the plasma membrane [1]. Alternatively, EVs may be formed and secreted by budding and fission of the plasma membrane. This subpopulation of EVs is believed to contain vesicles somewhat larger in size than exosomes (50-1000 nm) and is usually termed 'microvesicles' [1]. EVs can be isolated from cell culture supernatants or body fluids and are reported to be involved in intercellular communication [2-4]. During their biogenesis, EVs are loaded with a variety of biological cargoes, such as cytoskeleton proteins, membrane receptors, mRNAs and miRNAs [5, 6]. After secretion of the vesicles, the lipid bilayer protects against plasma and immune components, fixes the ratio between biological molecules and assists in functional delivery to target cells, where the vesicular content may provoke functional and phenotypical changes [7-9]. The small size of the vesicles may limit phagocytic uptake by the mononuclear phagocyte system and promotes extravasation through vessel fenestrations. Subsequently, (sub)populations of vesicles may deliver their cargo by direct fusion with the plasma membrane of target cells, circumventing the endosomal-lysosomal pathway and resulting in efficient release of the cargo in the cytoplasm [10]. These characteristics are very attractive for drug delivery purposes, especially in the case of nucleic acid-based drugs, given that endosomal escape is one of the major bottlenecks for the intracellular delivery of nucleic acids [11, 12]. Hence, in recent years the exploitation of endogenous EVs for the delivery of siRNA and miRNA has gained increasing attention.

Despite EVs being excellent drug delivery vehicle candidates, their practical use has been limited by the lack of techniques to load them with the desired therapeutics. Several strategies have been proposed to encapsulate siRNA or miRNA into EVs, including transfection-based approaches and electroporation. In the transfection-based approach, donor cells are transfected with a suitable expression vector, which induces overexpression of the desired short RNA. Subsequently, the RNA is incorporated into EVs and may be transferred to other cells. Using this technique, a number of reports have described the successful loading of a variety of siRNAs and miRNAs into EVs and showed their inhibitory effects in target cells [13-16]. Alternatively, donor cells can be directly transfected with the siRNA or miRNA of choice using conventional transfection reagents. This results in the secretion of EVs functionally loaded with the selected small RNAs. A number of groups have employed this technique and have shown promising results [17-22]. However, a disadvantage of this technique is that remainders of transfection reagents may influence the encapsulation process and the behaviour of the modified EVs. Furthermore, the levels of the desired small RNAs secreted in the vesicles may vary widely among sequences, and the basis for this phenomenon is unclear [23]. In addition, the transfected miRNA/siRNA may alter target gene expression in the donor cell, which

complicates the selection of feasible donor cells and target sequences. By loading short RNAs into EVs using electroporation, loading efficiency may be independent of the sequence of the small RNA that is incorporated into EVs. Two groups reported successful loading of EVs with exogenous siRNA by electroporation [24-26]. Wahlgren *et al.* demonstrated that the exogenous siRNA could be detected in up to 85.2% of the electroporated EVs (however no encapsulation efficiency was reported). Loaded EVs induced knockdown of the siRNA target genes when incubated with monocytes or lymphocytes [26]. Alvarez-Erviti *et al.* showed that approximately 25% of the electroporated siRNA was loaded into EVs and that retargeted EVs were functional *in vivo*, reducing expression of the *BACE1* target gene in mouse brains by 60% [24, 25].

Electroporation appears to maintain EV integrity and functionality with concomitant encapsulation of high levels of small RNAs. The reported high encapsulation efficiency after electroporation is intriguing, given that the introduction of nucleic acids into preformed carrier systems is challenging and not commonly performed. Efficient loading of drug delivery systems with nucleic acids is generally only achieved during assembly of the carriers [27]. The electroporation technique therefore may offer an elegant solution for the loading of EVs, as well as other preformed drug delivery systems, with siRNA. However, electroporation settings, buffers and equipment may vary among laboratories and may greatly influence electroporation results. Furthermore, the mechanism by which electroporation results in high encapsulation levels of siRNA into EVs remains unclear. In this work, we sought to further study and characterize the electroporation process for the loading of siRNA into EVs, in order to optimize the use of this technique to generate siRNA-loaded EVs.

Materials and methods

Materials

Optiprep was obtained from Sigma-Aldrich (Steinheim, Germany). Fluorescently labelled siRNAs (Cy5 and Cy3) were purchased from Eurogentec (Seraing, Belgium). Unlabelled siRNA was from Integrated DNA Technologies (Leuven, Belgium) and primers were obtained from Sigma-Aldrich (Steinheim, Germany). Micro BCA Protein Assay Kit was from Thermo Scientific (Rockford, IL). Electroporation cuvettes with aluminium electrodes were from Bio-Rad Laboratories, Inc (Hercules, CA) or Sigma-Aldrich (Steinheim, Germany) and cuvettes with conductive polymer electrodes (Nucleocuvettes™) and 4D-Nucleofector electroporation buffers were from Lonza (Basel, Schwitzerland). TRIzol Reagent, GlycoBlue, Taqman miRNA Reverse Transcription Kit, MicroAmp Optical 96-well plates and Lipofectamine 2000 were purchased from Life Technologies (Paisley, UK). Sterile cell culture materials were purchased from Greiner Bio-One (Alphen aan de Rijn, The Netherlands) and FastStart SYBR Green Master was obtained from Roche (Penzberg, Germany) and Rox passive reference dye was from Bio-

Rad Laboratories, Inc (Hercules, CA). pCMV-Luc vector was obtained from PlasmidFactory (Bielefeld, Germany) and pGL4.74[hRluc/TK] vector and Dual Luciferase Reporter Assay System kit were from Promega (Leiden, The Netherlands).

Cell culture and isolation of extracellular vesicles

Human embryonic kidney (HEK293T) and mouse neuroblastoma (Neuro2A) cell lines were maintained at 37˚C and 5% CO_2 in Dulbecco's Modified Eagle Medium (DMEM) supplemented with 10% fetal bovine serum (FBS) and penicillin/streptomycin. For EV production, cells were cultured for 24 hours after which medium was replaced by EV-depleted medium, which contained FBS depleted of EVs by overnight centrifugation at 100 000g. Cells were allowed to produce EVs for 48 hours, after which EVs were isolated by a standard differential centrifugation/filtration protocol. Briefly, medium was centrifuged for 10 min at 300g, followed by 10 min at 2000g to remove cells and cell debris. Subsequently medium was filtered through 0.2 µm syringe filters and EVs were pelleted by centrifugation for 70 min at 100 000g. Pellets were washed with phosphate buffered saline (PBS) and pelleted again by centrifugation for 70 min at 100 000g. Resulting pellets were resuspended in the desired electroporation buffer and yield was determined using a Micro BCA Protein Assay (Pierce) with bovine serum albumin (BSA) protein standards. Using this method, routinely 1-3 µg EVs per T175 flask were obtained from HEK293T cells and 3-10 µg EVs per flask were obtained from Neuro2A cells.

Electroporation buffers

Citric acid based buffer consisted of 18.6 mM citric acid and 29.4 mM disodium phosphate with a pH of 4.4. Phosphate-free buffer contained 125 mM sodium chloride, 5 mM potassium chloride, 1.5 mM calcium chloride, 10 mM glucose, and 20 mM HEPES adjusted to pH 7.4. Optiprep based buffer consisted of 21% Optiprep, 1.25 mM potassium phosphate and 25 mM potassium chloride adjusted to pH 7.2. Cytomix electroporation buffer consisted of 120 mM potassium chloride, 0.15 mM calcium chloride, 10 mM potassium phosphate, 25 mM HEPES, 2 mM EGTA and 5 mM magnesium chloride, adjusted to pH 7.6 with potassium hydroxide.

Electroporations

Electroporations were performed in 0.4 cm cuvettes with aluminium electrodes using a Bio-rad Gene Pulser I or II with capacitance extender set at 400 V and 125 µF. For every electroporation the sample volume was fixed at 200 µL, containing 3 µg EVs and 3 µg siRNA. When 100 µL cuvettes with electrodes of conductive polymer were used in the Bio-Rad Gene Pulser electroporator, a custom designed adapter was used to properly connect the electrodes to the electroporator, and sample volume was fixed at 100 µL. Electroporations of 16-well 20 µL Nucleocuvette™ strips were performed in a Lonza 4D-Nucleofector™ X unit. EVs where suspended in 4D-Nucleofector buffer P3 with supplement 1 and electroporated in a total volume of 20 µL containing

0.6 µg EVs and 0.6 µg siRNA. After electroporation, all electroporation cuvettes were incubated on ice for at least 30 min before further processing.

Nanoparticle Tracking Analysis

The size and concentration of particle aggregates was determined via nanoparticle tracking analysis (NTA) using a NanoSight LM10-HS instrument (NanoSight, Amesbury, UK). Prior to analysis, the samples were diluted 5-fold in deionized water. For each condition three independent samples were prepared and analysed. Per measurement a movie of 60 sec was recorded while sample was maintained at 22˚C. Particle aggregates from conductive polymer cuvettes were diluted 100-fold with PBS and analysed using a Nanosight LM10-HS instrument connected to a syringe pump device (Nanosight, Amesbury, UK). Flow was set at 20 and for each sample a 180 sec movie was recorded. All data was analysed with the NTA Analytical Software suite version 2.3.

Confocal microscopy

Confocal microscopy of aggregates containing Cy5-labelled siRNA was performed using a Nikon Cs1 confocal laser scanning module installed on a motorised Nikon TE2000-E inverted microscope (Nikon Benelux, Brussels, Belgium) equipped with an oil immersion objective lens (Plan Apo 60x, NA 1.4, Nikon, Japan). Samples were transferred directly from electroporation cuvettes into wells of a glass-bottomed 96-well plate (Greiner Bio-one, Frickenhausen, Germany) for analysis.

Fluorescence Fluctuation Spectroscopy

To assess the percentage of encapsulated Cy5-labelled siRNA (see Supplementary Table 1 for sequence) into EVs by electroporation, fluorescence fluctuation spectroscopy (FFS) was used as previously described [28]. Prior to analysis, the electroporated samples were diluted 10-fold in the respective buffer and 60 µL was transferred to the wells of a glass-bottomed 96 well plate (Greiner Bio-one, Frickenhausen, Germany). The focal volume was positioned in the sample and FFS measurements were performed during a 30s time-interval. A motorized Nikon TE2000-E inverted microscope, equipped with a water immersion objective lens (Plan Apo 60X, NA1.2, collar rim correction, Nikon) and a 637 nm laser line for the excitation of Cy5-siRNA, was used. The fluorescence intensity fluctuations were recorded with the fluorescence correlation spectrometer MicroTime 200 (picoquant GmbH, Berlin, Germany), equipped with SymPhoTime software. For each condition samples were prepared in triplicate. The fluorescence intensity of the baseline (i.e. the average fluorescence in the focal volume) in the fluctuation profiles was determined as previously described [28]. The siRNA complexation efficiency was subsequently calculated using equation 1.

Eq. 1 $$siRNA\ complexation\ efficiency\ (\%) = 100 - 100 \times \left[\frac{\bar{I}_{after\ electroporation} - \bar{I}_{medium}}{\bar{I}_{before\ electroporation} - \bar{I}_{medium}} \right]$$

Where $\bar{I}_{before\ electroporation}$ is the average intensity of the baseline after electroporation, $\bar{I}_{after\ electroporation}$ is the average intensity of the baseline before electroporation and $\bar{I}_{medium}$ is the average intensity of the baseline of the medium without fluorescently labelled siRNA.

Fluorescence spectroscopy

To evaluate the encapsulation of siRNA in EVs using fluorescence spectroscopy, 3 µg EVs were mixed with 3 µg Cy3-labelled siRNA (see Supplementary Table 1 for sequence) in Optiprep electroporation buffer and electroporated in 0.4 cm cuvettes with aluminium electrodes. Samples were diluted 10-fold with PBS and centrifuged for 70 min at 100 000g to remove unbound siRNA. Pellets were resuspended in PBS and siRNA fluorescence (excitation 560 nm; emission 610 nm) was determined using a fluorescence plate reader. A calibration curve of free Cy3-siRNA was used to calculate the percentage of encapsulation.

Quantitative reverse transcription polymerase chain reactions

Encapsulation of non-fluorescent siRNA (siLuc) in EVs was analysed by quantitative reverse transcription PCR (RT-PCR). After electroporation, samples were diluted 10x with PBS and centrifuged at 100 000g for 70 min to remove unbound siRNA. RNA was isolated from pellets with TRIzol Reagent according to manufacturer's recommendations, with minor modifications. In brief, pellets were dissolved in TRIzol and solution was spiked with 10 fmol of internal control siRNA (siGFP), followed by chloroform extraction. Isopropanol and 1 µL GlycoBlue were added to the aqueous phase and sample was stored overnight at -20˚C for maximal RNA recovery. RNA was pelleted by centrifugation at 12 000g and 4˚C for 30 min, washed with 80% ethanol and air dried. Dry RNA pellets were reconstituted in 20 µL nuclease-free water and stored at -20˚C until analysis. Standard solutions of siLuc and siGFP were prepared by serially diluting 10 µM stocks of both siRNAs in 10-fold dilution steps (range 10 µM – 100 pM). Standard solutions were also purified with TRIzol Reagent according to described protocol to ensure equal PCR efficiency among samples and standards.

Reverse transcription of standards and samples was performed in a GeneAmp PCR System 9700 (Applied Biosystems, Foster City, CA) thermocycler using a Taqman MicroRNA Reverse Transcription Kit, according to manufacturer's instructions. Each 7.5 µL reverse transcription reaction contained 1 µL of RNA template, 1 mM dNTPs, 1.9 U RNAse Inhibitor, 50 nM reverse stemloop primer (custom designed as described by Chen *et al.* [29], see Supplementary Table 1) and 25 U MultiScribe Reverse Transcriptase in 1x Reverse Transcription buffer.

Quantitative PCR was performed in 10 µL reactions containing 1 µL of reverse transcription product, 0.625 µM of sequence-specific forward primer, 0.625 µM of stemloop-specific reverse primer (see Supplementary Table 1) and 0.013 µL of Rox passive reference dye in 1x FastStart SYBR Green master. Reactions were prepared in MicroAmp Optical 96-well plates and were run on a Viia™ 7 Real Time PCR System (Applied Biosystems, Foster City, CA) using

the following settings: 10 min at 95˚C; 40 cycles of 15 sec at 95˚C, 30 sec at 60˚C and 20 sec at 72˚C; melting curve analysis; store at 4˚C. Amplification curves were analysed with Viia 7 software version 1.2.1 and Ct values were determined for siLuc and siGFP. Each plate contained a set of siLuc and siGFP standard solutions which were used to construct calibration curves (Supplementary Figure 1). Total copy number (Cn) of siLuc and siGFP in each sample was calculated and Cn_{siLuc} was normalised for Cn_{siGFP} using equation 2. From normalised Cn_{siLuc} the loading efficiency of siLuc in each sample was calculated. All electroporation samples for RT-PCR were prepared in triplicate and each RNA isolate was analysed in duplicate. Using this method, traces of siRNA could still be accurately quantified.

Eq. 2 $$Normalised\ Cn_{siLuc} = Cn_{siLuc} \times \frac{\overline{Cn}_{siGFP}}{Cn_{siGFP}}$$

where $\overline{Cn}_{siGFP}$ is the mean Cn_{siGFP} of all samples processed in the same experiment.

Statistical data analysis

When applicable, statistical data analysis was performed using IBM SPSS Statistics, version 20. Data was assessed for normality and equality of variance, and differences between two groups were analysed using independent samples t-tests. Comparisons between more than two groups were made using one-way ANOVA. Differences with values of $p < 0.05$ were considered statistically significant.

RESULTS

Quantification of siRNA loading into EVs by electroporation

When aiming to use endogenous EVs as nanosized carriers for the delivery of siRNA, it is essential to have an efficient siRNA loading method available. A recently proposed method [24, 25] described that approximately 25% of fluorescently labelled siRNA could be encapsulated in EVs by electroporation using optimized settings and reagents. To quantify the amount of retained siRNA in EVs, EVs were pelleted after electroporation and the amount of siRNA fluorescence in the pellet was assayed by fluorescence spectroscopy. When we repeated this experiment under similar experimental conditions (3 µg Cy3-siRNA and 3 µg EVs electroporated in an Optiprep based buffer), indeed a similar siRNA retention was obtained, regardless of EV source (Figure 1A). Similar to previously reported control conditions [24-26], when no electric pulse was applied, no Cy3-siRNA could be detected in the pellet, ruling out the possibility of non-specific binding of siRNA to the EV surface. However, when Cy3-siRNA was electroporated in the absence of EVs and centrifuged at 100 000g, a pellet containing 80-85% of the total fluorescent signal was obtained, indicating that other factors than encapsulation in EVs contribute to the observed siRNA retention. To validate these results, the same experiment

was repeated with unlabelled siRNA and analysed by RT-PCR. It was quantified that 3.7% of the siRNA was retained in the EV pellet after electroporation, independent of vesicle source (Figure 1B). Again, when electroporation was performed in the absence of EVs, a substantial portion of siRNA could be recovered from the pellet (2.3%). To further investigate this phenomenon, the encapsulation of Cy5-siRNA in EVs after electroporation was measured by FFS. Briefly, FFS is a microscopy based technique that monitors fluorescence intensity fluctuations in the excitation volume of a confocal microscope. The fluorescence fluctuations originate from the movement of fluorescently labelled molecules (e.g. Cy5-siRNA) in and out of the fixed excitation volume. The average fluorescence signal is proportional to the concentration of freely diffusing fluorescently labelled siRNA in solution. Complexation of siRNA into (nano)particles results in a decrease of the average fluorescence signal.

This can be used to quantify the siRNA complexation (see Materials and Methods section) without the need for sample pre-treatment, which has previously been demonstrated for lipo-and polyplexes [28, 30, 31]. When FFS was used to quantify Cy5-siRNA retention in EVs after electroporation, complexation efficiency appeared comparable to that observed by fluorescence spectroscopy (Figure 1C). Also in this assay, electroporation in the absence of EVs resulted in a slightly higher complexation of the fluorescent siRNA in detectable particles (24% of total siRNA). Thus, although absolute values differed between methods, the percentage of retained siRNA following electroporation in the absence of EVs was similar to (or even greater than) the retention obtained in the presence of EVs.

Taken together, these data suggest that electroporation causes siRNA to be retained in particles which could not be distinguished from EVs by FFS, and which co-sediment at centrifugal forces usually applied to pellet EVs. In order to better visualise this phenomenon, electroporated samples were analysed by confocal microscopy. After electroporation of Cy5-siRNA in the absence of EVs, an excessive number of irregularly shaped insoluble fluorescent aggregates could be detected (Figure 1D). Hence, siRNA appears to strongly aggregate when subjected to electroporation. This effect was not specific for the Optiprep based electroporation buffer, but was also observed for the previously described Cytomix electroporation buffer [26] by fluorescence spectroscopy, FFS and confocal microscopy (Supplementary Figure 2), albeit the extent of aggregation was slightly lower compared to the Optiprep based buffer.

Effect of EV concentration on siRNA precipitation

Interestingly, when increasing concentrations of EVs were added to the electroporation mixture, fluorescence of the EV pellet after electroporation decreased (Figure 1E). A similar effect was previously reported by Wahlgren *et al.* [26], who showed that the percentage of EVs containing fluorescently labelled siRNA after electroporation decreased from 85.2% to 0.073% when the EV concentration in the electroporation cuvettes was increased from 0.25 µg/µL to 4 µg/µL. These data suggest that the presence of EVs may reduce, but not necessarily remove the formation of siRNA aggregates after electroporation. To check the possibility that siRNA

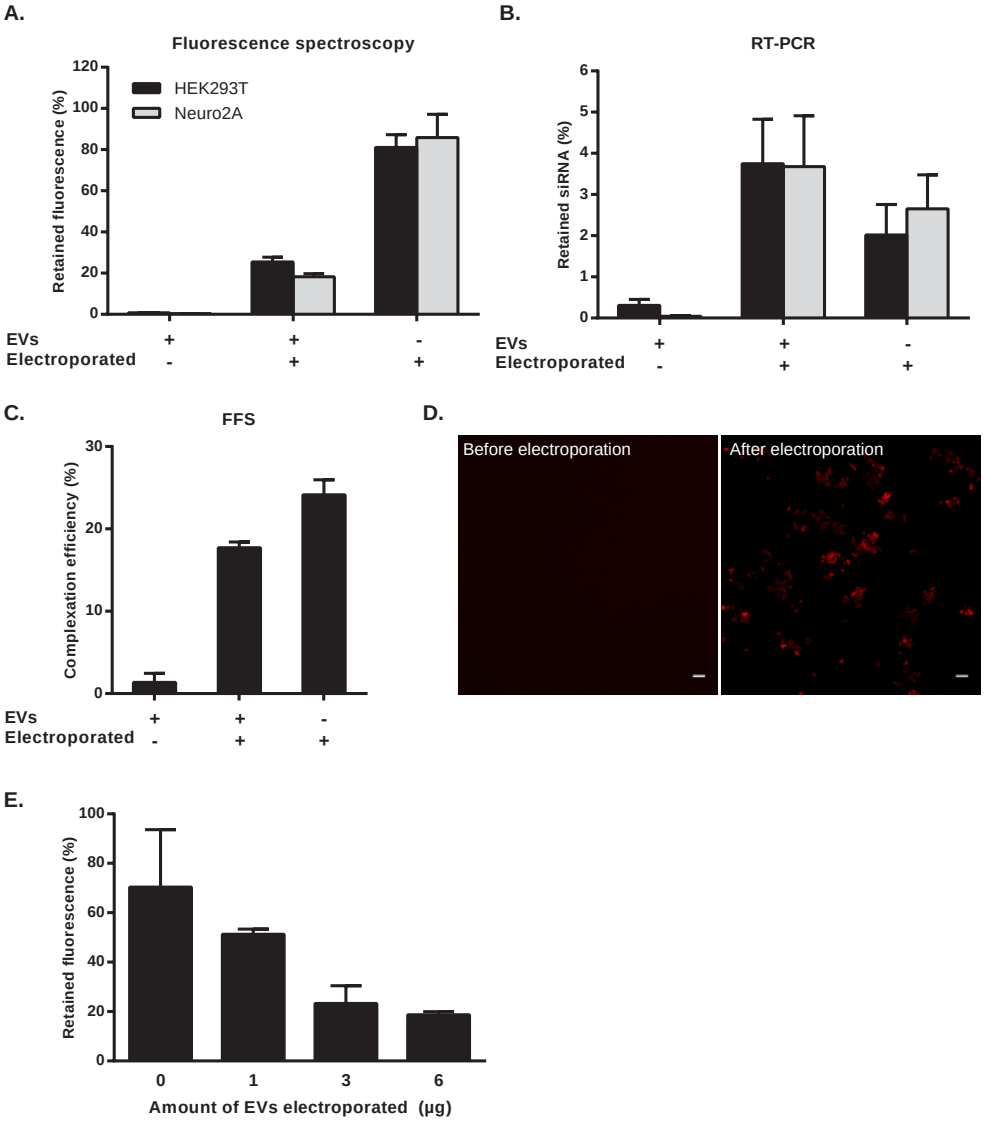

Figure 1: Precipitation of siRNA after electroporation in Optiprep electroporation buffer in the presence (+) or absence (-) of EVs from HEK293T (■) or Neuro2A (□). A: Retained percentage of Cy3-siRNA in 100 000g pellets before (-) or after (+) electroporation as measured by fluorescence spectroscopy. B: Retained percentage of unlabelled siRNA in 100 000g pellets as measured by RT-PCR. C: Complexation efficiency of Cy5-siRNA as measured by FFS. D: Confocal microscopy images of aggregate formation of Cy5-siRNA before (left) and after (right) electroporation in Optiprep electroporation buffer. Scale bars represent 10 µm. E: Retained percentage of Cy3-siRNA in 100 000g pellets in presence of increasing amounts of EVs as measured by fluorescence spectroscopy. All experiments were done in triplicate and data are presented as mean ± SEM.

aggregates might be loaded into EVs or otherwise associated with the vesicles, electroporated samples were floated on a sucrose gradient and the siRNA content of each fraction was analysed by RT-PCR (Supplementary Figure 3A-C). Here it was clearly observed that fractions containing the EV marker CD9 did not contain siRNA, suggesting that siRNA aggregates were not associated with EVs.

These data illustrate that, when not taken into account, electroporation-induced siRNA aggregation causes a severe overestimation of the amount of siRNA actually loaded into EVs. This aggregation needs to be prevented in order to quantitatively analyse siRNA encapsulation in EVs after electroporation and ultracentrifugation. Furthermore, the formation of siRNA aggregates might inhibit the loading of siRNA into EVs. Therefore, we investigated the mechanism by which siRNA aggregation occurs during electroporation.

Effect of EDTA on siRNA precipitation and loading efficiency

It has previously been described that electric discharges in electroporation cuvettes containing metal electrodes can cause the release of metal cations (e.g. Al-cations, Fe-cations) from the electrodes. These multivalent cations can react with phosphate and hydroxide anions present in the electroporation buffer and possibly nucleic acids, causing the formation of insoluble aggregates trapping nucleic acids [32]. Given that in our experiments cuvettes with aluminium electrodes were applied, it was hypothesized that these components caused the siRNA precipitation described in Figure 1.

To test this hypothesis, the Optiprep based buffer was electroporated without siRNA or EVs and the concentration of formed aggregates was measured by NTA (Figure 2A). It was confirmed that the buffer was particle-free before electroporation. Strikingly, after electroporation an average of $4x10^9$ particles per mL with a broad size distribution could be detected (Supplementary Figure 4). To point out the influence of aluminium cations in the formation of these aggregates, the same buffer was electroporated in the presence of increasing concentrations of EDTA. EDTA acts as a chelator and forms soluble complexes with aluminium ions, which may prevent interactions of these ions with buffer components and macromolecules.[32] Indeed, NTA revealed that the addition of EDTA to the electroporation buffer decreased particle formation during electroporation in a concentration-dependent manner (Figure 2A). Furthermore, when EVs and siRNA were electroporated in the presence of EDTA, RT-PCR showed a similar concentration-dependent inhibition of siRNA retention (Figure 2B). EDTA at 1 mM concentration reduced particle formation and siRNA precipitation by 98-99% in both experiments. Again similar results were found by FFS and fluorescence spectroscopy (Figures 2C and 2D, respectively). These observations are supported by results obtained using the Cytomix electroporation buffer (containing the chelator EGTA), which showed less aggregation after electroporation than using the Optiprep buffer (compare Supplementary Figure 2 and Figure 1). Under the aggregate-reducing conditions depicted in Figures 2C and 2D, retention was lower in the presence of EVs than in the absence of EVs (approximately 1%

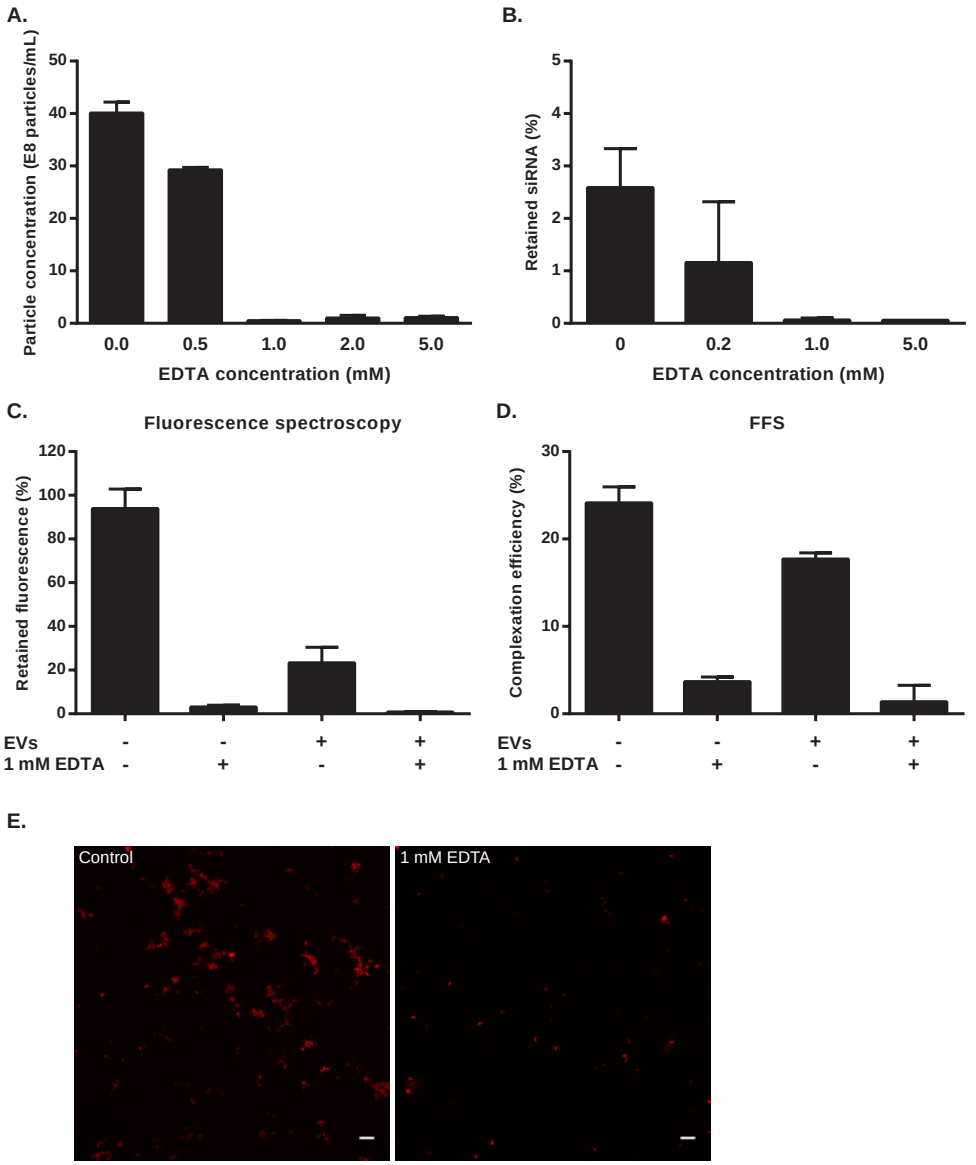

Figure 2: Addition of EDTA to Optiprep electroporation buffer affects aggregate formation and retention of siRNA. A: Concentration of particles in electroporation buffer after electroporation in presence of increasing concentrations of EDTA as measured by NTA. B: Percentage of retained unlabelled siRNA in 100 000g pellet after electroporation of Neuro2A EVs in the presence of increasing concentrations of EDTA as measured by RT-PCR. C: Percentage of retained Cy3-siRNA in 100 000g pellet after electroporation in the presence (+) or absence (-) of HEK293T EVs and 1 mM EDTA as measured by fluorescence spectroscopy. D: Complexation efficiency of Cy5-siRNA in HEK293T EVs after electroporation as measured by FFS. E: Confocal microscopy images of Cy5-siRNA in Optiprep electroporation buffer after electroporation in absence (left) or presence (right) of 1 mM EDTA. Scale bars represent 10 µm. All experiments were done in triplicate and data are presented as mean ± SEM.

versus 3%, respectively), supporting the previous finding that increasing concentrations of EVs inhibit aggregate formation. Together, these results strongly suggest that aluminium-induced aggregation, and not encapsulation into EVs, is responsible for the observed retention of siRNA as depicted in Figure 1.

Of note, while 1 mM EDTA strongly inhibited aggregate formation and reduced the observed retention of siRNA after electroporation, a minor amount of aggregates was still formed (Figure 2A), which could interfere with accurate determination of loading efficiency in the presence of EVs. These aggregates could be clearly distinguished from background by confocal microscopy (Figure 2E), and might account for the 1% siRNA retention observed with FFS and fluorescence spectroscopy when EVs were electroporated in the presence of EDTA (Figures 2C and 2D). Given that increasing EDTA concentrations above 1 mM could not completely inhibit this process (Figure 2A), our results suggest that chelation of aluminium ions is insufficient to completely inhibit the formation of siRNA aggregates. Therefore alternative methods to reduce background aggregate formation were investigated.

Effect of electroporation buffer on siRNA precipitation and loading efficiency

As both phosphate and hydroxide anions in the Optiprep buffer potentially contribute to aggregate formation, using a buffer devoid of these anions could possibly prevent siRNA precipitation. We first evaluated a phosphate-free electroporation buffer for the formation of aggregates. However, the amount of formed aggregates after electroporation in the presence of Cy5-siRNA was comparable to the amount in the Optiprep based buffer (Figure 3A, left panel). In addition, similar amounts of particles were formed after electroporation in the absence of siRNA (Figure 3B). This indicates that phosphate anions, in the concentration used in the Optiprep based buffer, likely play a minor role in the formation of aggregates. Dabbs *et al.* demonstrated that both acidic pH (implicating low hydroxide concentrations) and the presence of citric acid can prevent the formation of aluminium oxyhydroxide aggregates [33]. Therefore a citric acid based buffer (pH 4.4) was evaluated for aggregate formation after electroporation. Following electroporation of this buffer in the presence of Cy5-siRNA, no fluorescent aggregates could be detected and only minute amounts of particles could be measured via NTA (Figure 3A, right panel and 3B, respectively). In agreement with this result, FFS measurements showed near undetectable complexation following electroporation of Cy5-siRNA without EVs (Figure 3C). Hence, this buffer could potentially allow for precise measurements of encapsulation of siRNA in EVs. Nevertheless, after siRNA electroporation in the presence of EVs no encapsulation could be detected (Figure 3C).

However, it can not be excluded that EV integrity might have been compromised in this severe acidic environment, possibly reducing siRNA encapsulation. In order to avoid the formation of aggregates while maintaining physiological pH, we next investigated an alternative electroporation strategy.

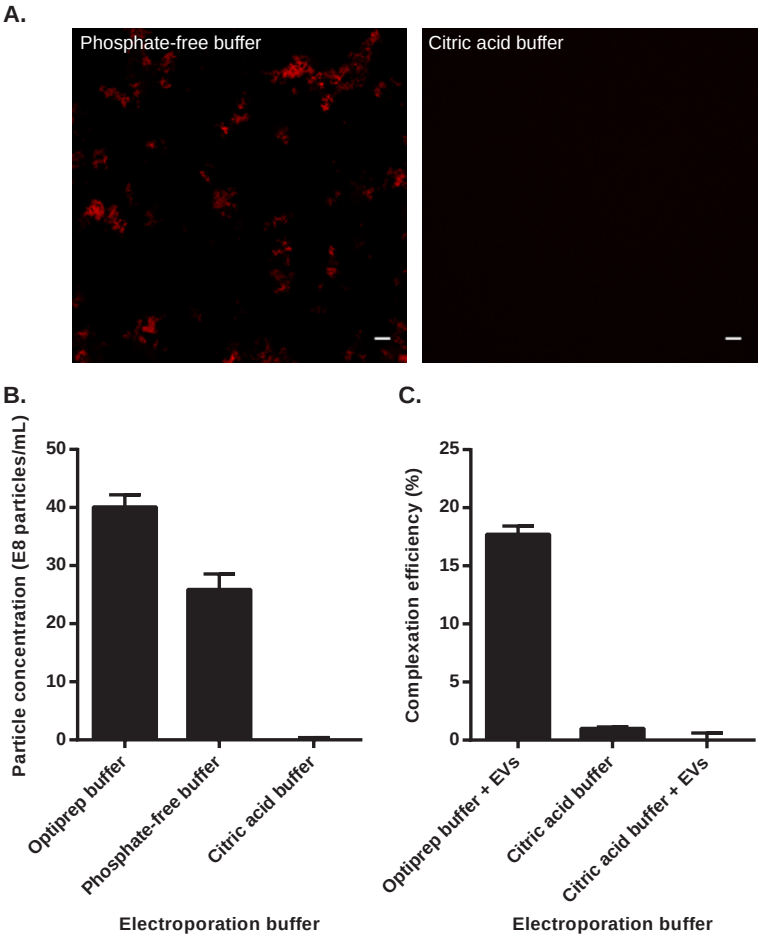

Figure 3: Effect of various electroporation buffers on the formation of aggregates after electroporation. A: Confocal microscopy images of phosphate-free buffer (left) and citric acid buffer (right) after electroporation in the presence of Cy5-siRNA. Scale bars represent 10 µm. B: Particle concentration after electroporation of Optiprep, phosphate-free and citric acid buffers, as measured by NTA. C: Complexation efficiency of Cy5-siRNA after electroporation in Optiprep or citric acid based buffer in the presence or absence of HEK293T EVs, as measured by FFS. All experiments were performed in triplicate and data are presented as mean ± SEM.

Effect of electrode material on siRNA precipitation loading efficiency

Given that metal ions released from the electrodes play an important role in the formation of oxyhydroxide precipitates, it was anticipated that the use of cuvettes with conductive polymer electrodes instead of metal electrodes could prevent aggregate formation. Such polymer cuvettes are commonly used in the Lonza Nucleofector™ technology. Particle formation in the Optiprep buffer after electroporation in these conductive polymer cuvettes was indeed dramatically reduced compared to conventional aluminium cuvettes (Figure 4A). This effect was

independent of the used voltage and capacitance during electroporation. Polymer cuvettes could thus be valuable for aggregate-free electroporation of EVs. To optimize loading of siRNA into EVs using these cuvettes, EVs were electroporated with unlabelled siRNA at varying EV:siRNA ratios and siRNA retention was determined by RT-PCR (Figure 4B). Unfortunately, only minor amounts of siRNA (maximally 0.09% of total siRNA) could be detected in EV pellets. In addition to siRNA:EV ratios, also electroporation settings of the Lonza 4D-Nucleofector were

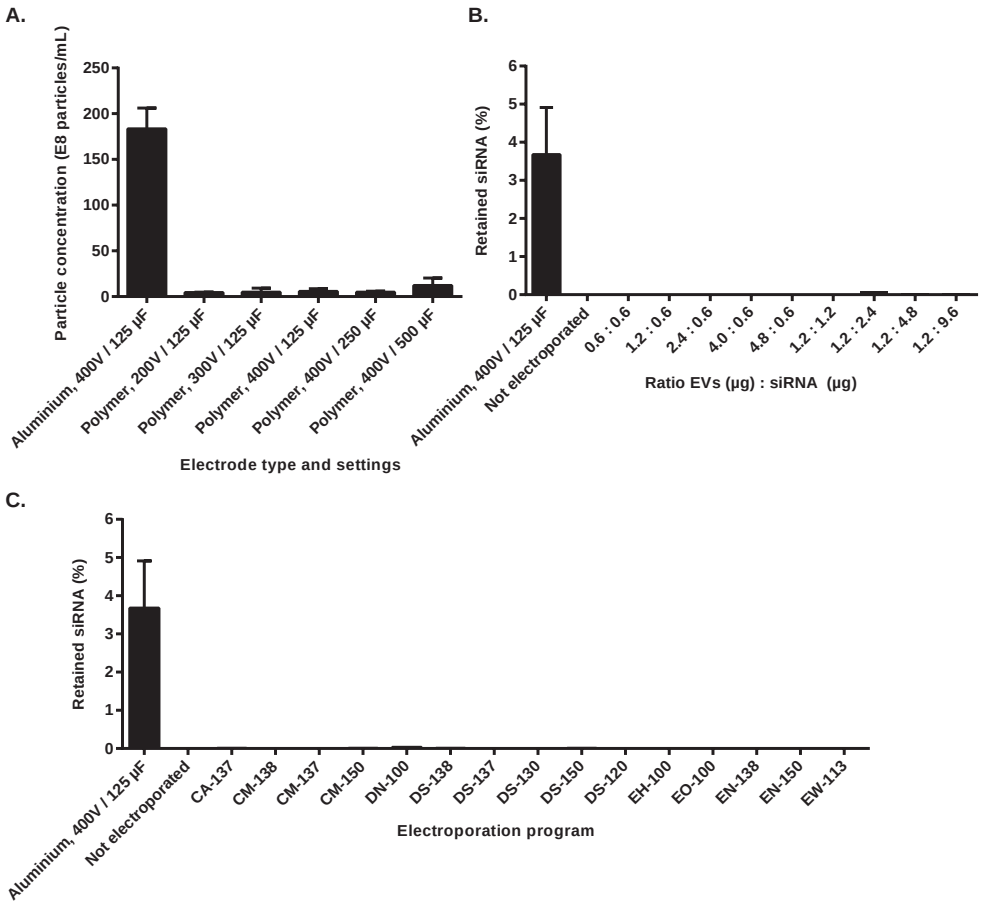

Figure 4: The use of cuvettes with conductive polymer electrodes instead of aluminium electrodes affects aggregate formation and siRNA retention in Neuro2A EVs. A: Concentration of particles in Optiprep electroporation buffer after electroporation in cuvettes with aluminium electrodes (at standard settings) or conductive polymer electrodes (at a range of voltages and capacitances), as measured by NTA. B: Percentage of retained unlabelled siRNA in 100 000g pellet at various EV : siRNA ratios after electroporation in a 4D-Nucleofector using the EH-100 program compared to electroporation in the Bio-Rad Gene Pulser, as measured by RT-PCR. C: Percentage of retained unlabelled siRNA in 100 000g pellet after electroporation of 0.6 µg EVs with 0.6 µg siRNA in the 4D-Nucleofector using various programs. Data in panel A are presented as mean ± SEM, n=3.

Table 1: Retained percentage of unlabelled siRNA in 100 000g pellets after electroporation of siRNA in the presence or absence of Neuro2A EVs in cuvettes with conductive polymer electrodes, as measured by RT-PCR. After electroporation in Optiprep electroporation buffer at 400 V and 125 µF, samples were centrifuged at 100 000g (washed once), or subsequently resuspended in PBS and centrifuged again (washed twice).

	Retained siRNA (%)[a]	
Sample	Washed once	Washed twice
siRNA, electroporated	0.2411 ± 0.0394	0.0008 ± 0.0005[b]
EVs + siRNA, not electroporated	0.0736 ± 0.0274	0.0001 ± 0.0001[b]
EVs + siRNA, electroporated	0.0856 ± 0.0255	0.0014 ± 0.0009[b]

[a]Data are presented as mean percentage of total siRNA ± SD, n = 3.

[b]Retained siRNA did not significantly differ among conditions when analysed by one-way ANOVA ($p = 0.099$).

optimised for the loading of siRNA in EVs. Again, using a variety of electroporation programs no marked siRNA retention could be measured (Figure 4C). None of the programs resulted in more than 0.04% of total siRNA retention in the EV pellet. These findings were confirmed by sucrose gradient flotation of EVs electroporated in conductive polymer cuvettes (Supplementary Figure 3D). To determine whether the small amounts of siRNA detected in the EV pellets after electroporation in conductive polymer cuvettes could be attributed to actual siRNA loading into EVs, samples were subjected to either one or two wash steps and siRNA in the pellets was quantified by RT-PCR (see Table 1). After two washes, no significant differences in siRNA retention could be measured between siRNA electroporated in the presence and absence of EVs, albeit siRNA was still detectable in both conditions (average Ct values of 21). Notably, after two washes the endogenous miRNAs miR-143 and miR-146a could still be detected in EV-containing samples (Ct values ranging from 31 to 34), indicating that EVs were not lost during the extensive wash procedure.

Given that siRNA associated with aluminium aggregates or EVs (even in extremely low concentrations) might still promote gene silencing effects when effectively delivered to cells, EVs electroporated in aluminium and conductive polymer cuvettes were tested in a luciferase reporter gene assay (Supplementary Figure 5). As expected by the lack of loading of siRNA into EVs after electroporation in conductive polymer cuvettes, no silencing effects were measured when washed EVs were added to the cells. Surprisingly, luciferase expression tended to be lower when cells were incubated with siRNA alone or siRNA with EVs after electroporation in aluminium cuvettes. However, similar effects were observed when non-specific control siRNA was used, suggesting a non-specific effect of aluminium aggregates on reporter gene expression or enzyme function.

Discussion

Taken together, these data provide conclusive evidence that electroporation can induce strong aggregation of siRNA, which might be mistakenly interpreted as encapsulation of siRNA into EVs if proper control experiments are omitted. Complex formation between metal ions from the electrodes and hydroxide ions from the electroporation buffer were shown to be the major cause of siRNA precipitation. While removal of one or both of these components (i.e. metal ions and/or hydroxide ions) almost completely inhibited this process, the loading efficiency of siRNA into EVs in these cases was found to be below 0.05%. Furthermore, similar siRNA retention was found when siRNA was electroporated in the absence of EVs. These data suggest that any siRNA measured after electroporation and washing of EVs can be attributed to traces of wash solution and not to actual loading of siRNA into EVs. This extremely inefficient encapsulation of siRNA could be expected when performing electroporations under these conditions. According to our NTA measurements and corresponding to a previous report [34], an electroporation volume of 200 µL with 15 µg/mL EVs contains approximately $2.5*10^{10}$ particles. Based on the size distribution of the EVs, and assuming they exist as perfect spherical structures in the electroporation buffer, the total volume of EVs can be calculated. When this calculation was performed using the EV size distributions commonly measured in our lab (median size of 110 nm), it was found that the total internal volume of EVs comprised 0.04% of the total electroporation volume (200 µL). Hence, assuming that loading of siRNA by electroporation occurs by passive diffusion of the macromolecules through pores in the EV membrane, no more than 0.04% of the siRNA molecules would be expected to enter the lumen of the EVs. In practice this is likely to be even lower, given that pores are only temporarily formed during electroporation and that the calculation is based on empty spherical structures, while EVs are dense particles already enriched in macromolecules. This theory is supported by the findings in this work, that show that when electroporation artefacts are effectively prevented, no encapsulation of siRNA into EVs could be detected. However, it should be noted that loading efficiencies might differ depending of the source of the EVs. Despite our findings that loading efficiencies were similar among EVs derived from two different cell lines, EVs derived from primary cells EVs may show different loading behaviour during electroporation.

In this work we show that extensive aggregate formation occurs during electroporation, resulting in precipitation of siRNA. This finding is consistent with a previous report, which showed that electric discharges through a solution cause DNA, RNA and some proteins to precipitate [32]. Furthermore, we showed that aggregate formation decreased with increasing concentrations of EVs. This effect may be due to the capturing of multivalent ions on the negatively charged EV membrane, or by changes in buffer conductivity upon addition of EVs. Interestingly, siRNA-aluminium complexes tended to reduce *Firefly* luciferase reporter expression in a commonly used reporter gene assay. The underlying biological mechanism for this phenomenon is unknown, however it is most likely not RNAi-mediated, given that complexed non-specific siRNA displayed similar effects. Our findings demonstrate the

importance of a variety of analysis techniques for the determination of loading efficiency. The main techniques used in this work (i.e. fluorescence spectroscopy, FFS and RT-PCR) revealed similar trends as a function of electroporation conditions, but absolute values for loading efficiency varied between fluorescence based measurements and RT-PCR. FFS and fluorescence spectroscopy generally showed over 5-fold higher siRNA retention or complexation than RT-PCR. The reason for this discrepancy is unclear. After electroporation siRNA could potentially be damaged due to association with metal ions, resulting in less copies to be detected via RT-PCR. Cleavage of ribonucleotides by metal ions has previously been described [35]. In addition, aggregation of siRNA may cause the critical 3' ends of siRNA to become unavailable for reverse transcription and subsequent PCR, resulting in low measured siRNA concentrations. However, stringent reducing conditions during RNA isolation are most likely to effectively disrupt such siRNA aggregates. Alternatively, fluorescently labelled siRNA might be more prone to aggregation than unlabelled siRNA. Nevertheless, these discrepancies warrant the use of multiple analysis techniques and controls to adequately measure loading of siRNA in nanoparticles.

In conclusion, in contrast to previous reports we show that electroporation of siRNA into EVs results in extensive precipitation of siRNA. Due to this process, encapsulation efficiency is easily overestimated when commonly used electroporation conditions and analysis techniques are employed. Our data further show that electroporation is far less efficient than previously believed. This work highlights an important complication of the electroporation technique and demonstrates the necessity for alternative methods to load EVs with macromolecules such as siRNA, in order to maximise their therapeutic activity.

Acknowledgements

The work of SAAK and RMS on cell-derived membrane vesicles is supported by a European Research Council starting grant (260627) "MINDS" in the FP7 ideas program of the European Union. SS and KR are doctoral and postdoctoral fellows respectively of the Research Foundation – Flanders (FWO). Financial support by the Ghent University Special Research Fund and the Research Foundation – Flanders is acknowledged with gratitude. The work of PV is supported by a Rubicon grant from the Netherlands Organization for Scientific Research (NWO), The Hague, The Netherlands.

References

1. G. Camussi, M.C. Deregibus, S. Bruno, V. Cantaluppi, L. Biancone, Exosomes/microvesicles as a mechanism of cell-to-cell communication, *Kidney Int*, 78 (2010) 838-848.
2. C. Lasser, V.S. Alikhani, K. Ekstrom, M. Eldh, P.T. Paredes, A. Bossios*, et al.*, Human saliva, plasma and breast milk exosomes contain RNA: uptake by macrophages, *J Transl Med*, 9 (2011) 9.
3. C. Thery, M. Ostrowski, E. Segura, Membrane vesicles as conveyors of immune responses, *Nat Rev Immunol*, 9 (2009) 581-593.
4. M. Record, C. Subra, S. Silvente-Poirot, M. Poirot, Exosomes as intercellular signalosomes and pharmacological effectors, *Biochem Pharmacol*, 81 (2011) 1171-1182.
5. H. Valadi, K. Ekstrom, A. Bossios, M. Sjostrand, J.J. Lee, J.O. Lotvall, Exosome-mediated transfer of mRNAs and microRNAs is a novel mechanism of genetic exchange between cells, *Nat Cell Biol*, 9 (2007) 654-659.
6. R.J. Simpson, S.S. Jensen, J.W. Lim, Proteomic profiling of exosomes: current perspectives, *Proteomics*, 8 (2008) 4083-4099.
7. K. Al-Nedawi, B. Meehan, J. Micallef, V. Lhotak, L. May, A. Guha*, et al.*, Intercellular transfer of the oncogenic receptor EGFRvIII by microvesicles derived from tumour cells, *Nat Cell Biol*, 10 (2008) 619-624.
8. J. Skog, T. Wurdinger, S. van Rijn, D.H. Meijer, L. Gainche, M. Sena-Esteves*, et al.*, Glioblastoma microvesicles transport RNA and proteins that promote tumour growth and provide diagnostic biomarkers, *Nat Cell Biol*, 10 (2008) 1470-1476.
9. A. Montecalvo, A.T. Larregina, W.J. Shufesky, D. Beer Stolz, M.L. Sullivan, J.M. Karlsson*, et al.*, Mechanism of transfer of functional microRNAs between mouse dendritic cells via exosomes, *Blood*, 119 (2012) 756-766.
10. J.G. van den Boorn, M. Schlee, C. Coch, G. Hartmann, SiRNA delivery with exosome nanoparticles, *Nat Biotechnol*, 29 (2011) 325-326.
11. S.A. Kooijmans, P. Vader, S.M. van Dommelen, W.W. van Solinge, R.M. Schiffelers, Exosome mimetics: a novel class of drug delivery systems, *Int J Nanomedicine*, 7 (2012) 1525-1541.
12. S.M. van Dommelen, P. Vader, S. Lakhal, S.A. Kooijmans, W.W. van Solinge, M.J. Wood*, et al.*, Microvesicles and exosomes: opportunities for cell-derived membrane vesicles in drug delivery, *J Control Release*, 161 (2012) 635-644.
13. N. Kosaka, H. Iguchi, Y. Yoshioka, F. Takeshita, Y. Matsuki, T. Ochiya, Secretory mechanisms and intercellular transfer of microRNAs in living cells, *J Biol Chem*, 285 (2010) 17442-17452.
14. N. Kosaka, H. Iguchi, Y. Yoshioka, K. Hagiwara, F. Takeshita, T. Ochiya, Competitive interactions of cancer cells and normal cells via secretory microRNAs, *J Biol Chem*, 287 (2012) 1397-1405.
15. Q. Pan, V. Ramakrishnaiah, S. Henry, S. Fouraschen, P.E. de Ruiter, J. Kwekkeboom*, et al.*, Hepatic cell-to-cell transmission of small silencing RNA can extend the therapeutic reach of RNA interference (RNAi), *Gut*, 61 (2012) 1330-1339.
16. S.D. Olson, A. Kambal, K. Pollock, G.M. Mitchell, H. Stewart, S. Kalomoiris*, et al.*, Examination of mesenchymal stem cell-mediated RNAi transfer to Huntington's disease affected neuronal cells for reduction of huntingtin, *Mol Cell Neurosci*, 49 (2012) 271-281.
17. S.S. Luo, O. Ishibashi, G. Ishikawa, T. Ishikawa, A. Katayama, T. Mishima*, et al.*, Human villous trophoblasts express and secrete placenta-specific microRNAs into maternal circulation via exosomes, *Biol Reprod*, 81 (2009) 717-729.

18. Y. Akao, A. Iio, T. Itoh, S. Noguchi, Y. Itoh, Y. Ohtsuki*, et al.*, Microvesicle-mediated RNA molecule delivery system using monocytes/macrophages, *Mol Ther*, 19 (2011) 395-399.

19. M. Yang, J. Chen, F. Su, B. Yu, F. Su, L. Lin*, et al.*, Microvesicles secreted by macrophages shuttle invasion-potentiating microRNAs into breast cancer cells, *Mol Cancer*, 10 (2011) 117.

20. P. Mocharla, S. Briand, G. Giannotti, C. Dorries, P. Jakob, F. Paneni*, et al.*, AngiomiR-126 expression and secretion from circulating CD34+ and CD14+ PBMCs: role for proangiogenic effects and alterations in type 2 diabetics, *Blood*, 121 (2013) 226-236.

21. S. Ohno, M. Takanashi, K. Sudo, S. Ueda, A. Ishikawa, N. Matsuyama*, et al.*, Systemically Injected Exosomes Targeted to EGFR Deliver Antitumor MicroRNA to Breast Cancer Cells, *Mol Ther*, 21 (2013) 185-191.

22. Y. Zhang, D. Liu, X. Chen, J. Li, L. Li, Z. Bian*, et al.*, Secreted monocytic miR-150 enhances targeted endothelial cell migration, *Mol Cell*, 39 (2010) 133-144.

23. A.O. Batagov, V.A. Kuznetsov, I.V. Kurochkin, Identification of nucleotide patterns enriched in secreted RNAs as putative cis-acting elements targeting them to exosome nano-vesicles, *BMC Genomics*, 12 Suppl 3 (2011) S18.

24. L. Alvarez-Erviti, Y. Seow, H. Yin, C. Betts, S. Lakhal, M.J. Wood, Delivery of siRNA to the mouse brain by systemic injection of targeted exosomes, *Nat Biotechnol*, 29 (2011) 341-345.

25. S. El-Andaloussi, Y. Lee, S. Lakhal-Littleton, J. Li, Y. Seow, C. Gardiner*, et al.*, Exosome-mediated delivery of siRNA in vitro and in vivo, *Nat Protoc*, 7 (2012) 2112-2126.

26. J. Wahlgren, L.K.T. De, M. Brisslert, F. Vaziri Sani, E. Telemo, P. Sunnerhagen*, et al.*, Plasma exosomes can deliver exogenous short interfering RNA to monocytes and lymphocytes, *Nucleic Acids Res*, 40 (2012) e130.

27. X. Yuan, S. Naguib, Z. Wu, Recent advances of siRNA delivery by nanoparticles, *Expert Opin Drug Deliv*, 8 (2011) 521-536.

28. K. Buyens, B. Lucas, K. Raemdonck, K. Braeckmans, J. Vercammen, J. Hendrix*, et al.*, A fast and sensitive method for measuring the integrity of siRNA-carrier complexes in full human serum, *J Control Release*, 126 (2008) 67-76.

29. C. Chen, D.A. Ridzon, A.J. Broomer, Z. Zhou, D.H. Lee, J.T. Nguyen*, et al.*, Real-time quantification of microRNAs by stem-loop RT-PCR, *Nucleic Acids Res*, 33 (2005) e179.

30. K. Buyens, J. Demeester, S.S. De Smedt, N.N. Sanders, Elucidating the encapsulation of short interfering RNA in PEGylated cationic liposomes, *Langmuir*, 25 (2009) 4886-4891.

31. K. Raemdonck, B. Naeye, K. Buyens, R.E. Vandenbroucke, A. Høgset, J. Demeester*, et al.*, Biodegradable Dextran Nanogels for RNA Interference: Focusing on Endosomal Escape and Intracellular siRNA Delivery, *Advanced Functional Materials*, 19 (2009) 1406-1415.

32. R. Stapulionis, Electric pulse-induced precipitation of biological macromolecules in electroporation, *Bioelectrochem Bioenerg*, 48 (1999) 249-254.

33. D.M. Dabbs, U. Ramachandran, S. Lu, J. Liu, L.Q. Wang, I.A. Aksay, Inhibition of aluminum oxyhydroxide precipitation with citric acid, *Langmuir*, 21 (2005) 11690-11695.

34. J. Webber, A. Clayton, How pure are your vesicles?, *Journal of Extracellular Vesicles*, 2 (2013) 19861.

35. R. Breslow, D.L. Huang, Effects of metal ions, including Mg2+ and lanthanides, on the cleavage of ribonucleotides and RNA model compounds, *Proc Natl Acad Sci U S A*, 88 (1991) 4080-4083.

SUPPLEMENTARY METHODS

Fractionation using sucrose gradients

EVs were electroporated in Optiprep based buffer as described before, using 15 µg/mL EVs and 15 µg/mL siLuc in 200 µL total volume for cuvettes with aluminium electrodes, or 100 µL total volume for cuvettes with conductive polymer electrodes. After electroporation, duplicate samples were combined to 400 µL electroporation samples (corresponding to 6 µg EVs/siLuc) and mixed with 1.5 mL of 2.5 M sucrose in PBS in SW40 tubes (Beckman Instruments). Samples were overlaid with a linear gradient of 0.4-2 M sucrose in PBS in SW40 tubes (Beckman Instruments) and centrifuged for 15 hours at 202 000g. Gradient fractions of 1 mL were collected from the top of the gradients and sucrose densities measured by refractometry. Subsequent fractions were pooled in pairs of two and 60 µL aliquots were collected for RNA isolation. Each 60 µL aliquot was mixed with 300 µL Trizol, RNA was isolated, and RT-PCR was performed according to method described before. The siRNA content of each fraction was expressed as a relative concentration compared to the fraction with the lowest sucrose density (top fraction), using Equation 1. Remainders of pooled sucrose fractions (1940 µL) were diluted to 4 mL with PBS and centrifuged at 100 000g for 70 min. Pellets were dissolved in 25 µL sample buffer for Western blot analysis.

Eq. 1 $$relative\ siRNA\ concentration_{fraction\ X} = \frac{Cn_{fraction\ X}}{Cn_{fraction\ top}}$$

where $Cn_{fraction\ X}$ is the measured copy number of siRNA in the 60 µL sample of fraction X and $Cn_{fraction\ top}$ is the measured copy number of siRNA in the 60 µL sample of the top fraction of the gradient.

Immunoblotting

Stored samples were heated to 95˚C for 10 min, snap cooled on ice and subjected to 12% SDS-PAGE. Proteins were electrotransferred to Immobilon-FL polyvinylidene difluoride (PVDF) membranes (Millipore). Blots were blocked with 50% v/v Odyssey Blocking Buffer (LI-COR Biosciences) in Tris buffered saline (TBS). CD9 immunolabelling was performed with 50% v/v Odyssey Blocking Buffer in TBS containing 0.1% Tween 20 and rabbit anti-CD9 antibody (Abcam, ab92726, 1:4000 dilution). Primary antibodies were probed with Alexa Fluor 680-conjugated anti-rabbit antibodies (Invitrogen, 1:7500 dilution) and bands were visualised using an Odyssey Infrared Imager (LI-COR Biosciences, Leusden, the Netherlands) at 700 nm.

Dual luciferase reporter assay

Neuro2A cells were transfected during 24 hours with a combination of pCMV-Luc and pGL4.74[hRluc/TK] (driving expression of *Firefly* luciferase and *Renilla* luciferase, respectively) using Lipofectamine 2000 according to manufacturer's instructions. Subsequently cells were

washed with PBS, trypsinised and seeded in a gelatin-coated 96-well plate at a density of $3*10^4$ cells per well. Cells were allowed to attach for 24 hours, and medium was replaced with EV-depleted medium. 3 µg of siRNA against *Firefly* luciferase (siLuc) or non-specific control (NC) siRNA was electroporated in the presence or absence of 3 µg Neuro2A EVs in Optiprep based electroporation buffer at 400V and 125 µF, diluted with 4 mL PBS and centrifuged at 100 000g for 70 min. Pellets were resuspended in 50 µL PBS and added to the cells. As controls, 10 pmol of both siRNAs were complexed with Lipofectamine 2000 according to manufacturer's instructions and added to the cells in antibiotic-free medium. Cells were incubated for 48 hours and lysed with Passive Lysis Buffer (Promega). Lysates were mixed with substrates from the Dual Luciferase Reporter Assay System kit (Promega) according to manufacturer's instructions and activities of both luciferases were sequentially measured at room temperature for 5s using a SpectraMax L luminescence microplate reader (Molecular Devices). *Firefly* luciferase activity was normalised to *Renilla* luciferase activity and expressed as a percentage of normalised *Firefly* luciferase activity in untreated cells. All conditions were tested in triplicate.

Supplementary Figures

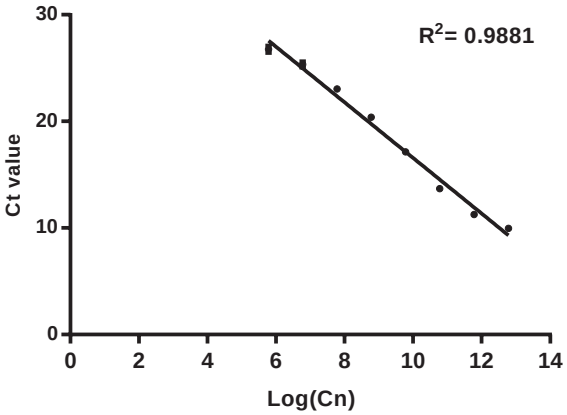

Supplementary Figure 1: RT-PCR calibration curve of siRNA (siLuc). After serial dilution, siRNA was purified with TRIzol Reagent to ensure good comparison with electroporation samples. Data are presented as mean ± SD and RT-PCRs were performed in duplicate.

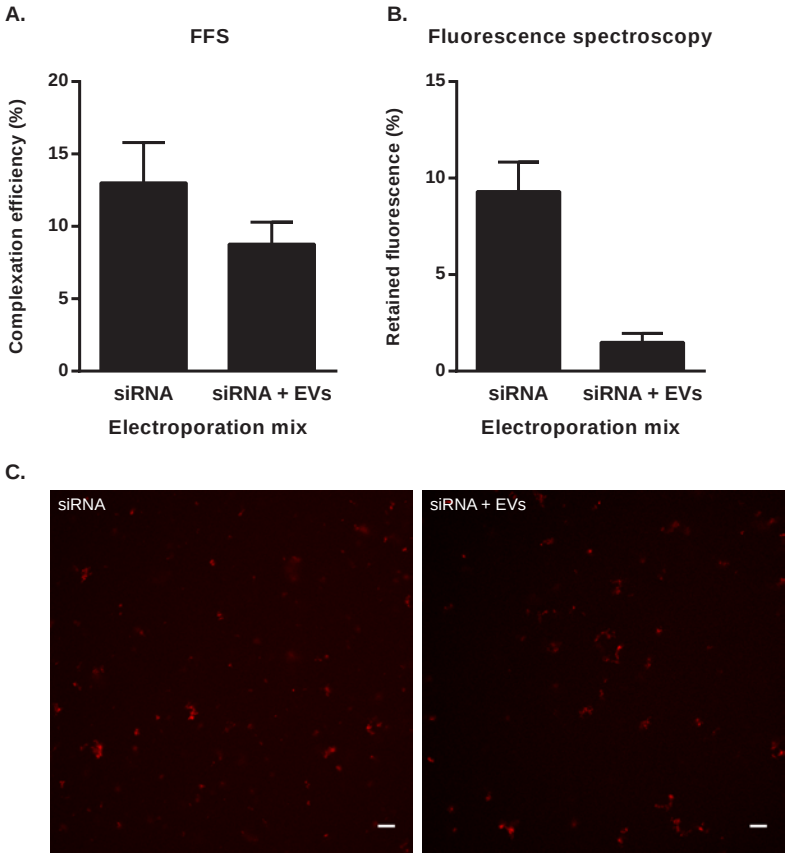

Supplementary Figure 2: Precipitation of siRNA after electroporation in Cytomix electroporation buffer. A: Complexation efficiency of Cy5-siRNA after electroporation in the absence or presence of HEK293T EVs, as measured by FFS. B: Retained percentage of Cy3-siRNA in 100 000g pellets after electroporation in the absence or presence of HEK293T EVs, as measured by fluorescence spectroscopy. C: Confocal microscopy images of Cy5-siRNA after electroporation in the absence (left) or presence (right) of HEK293T EVs. Scale bars represent 10 µm. All experiments were performed in triplicate and data are presented as mean ± SEM.

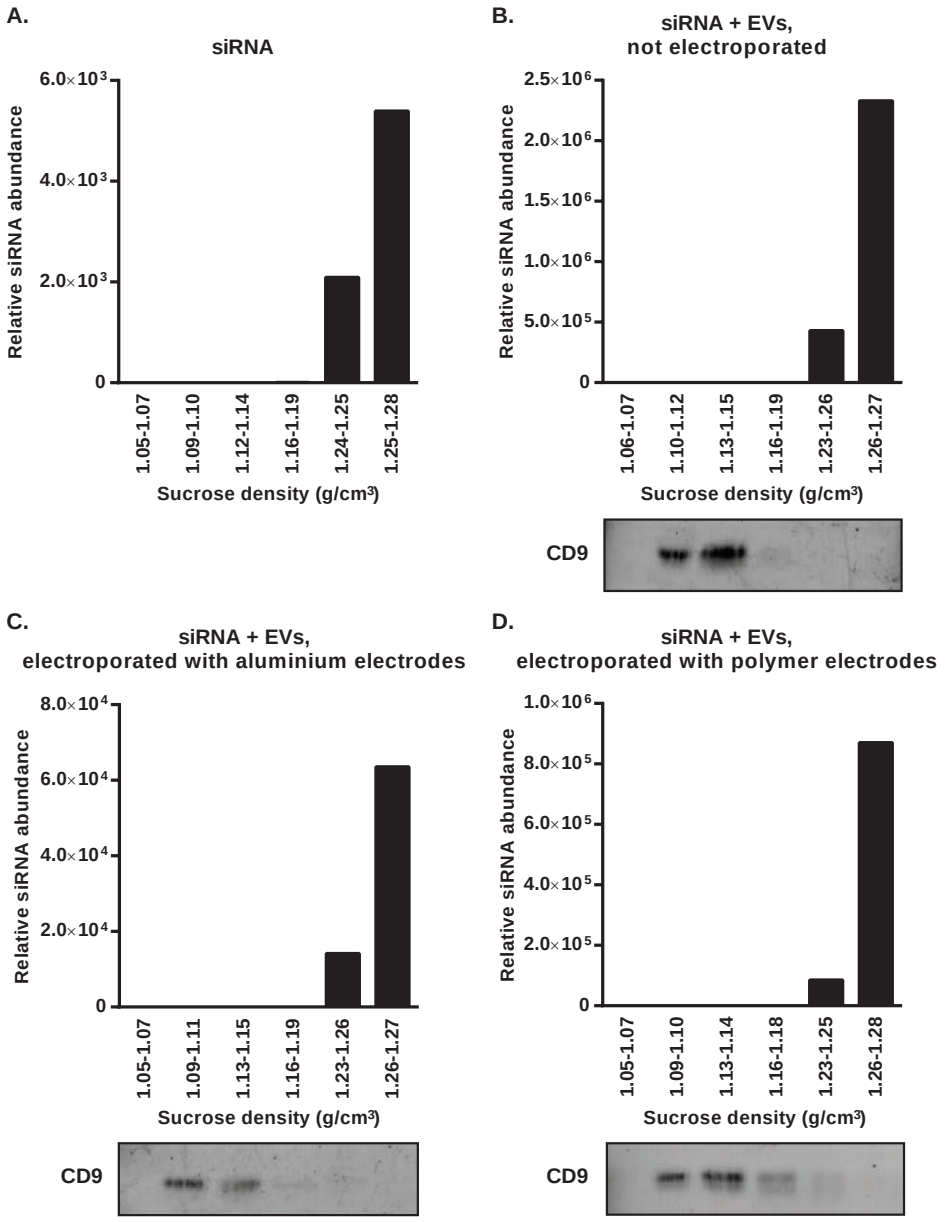

Supplementary Figure 3: Fractionation of electroporation samples on sucrose gradients. Unlabelled siRNA was electroporated in Optiprep buffer in the absence (A) or presence (B-D) of Neuro2A EVs in cuvettes with aluminium electrodes (A, C) or conductive polymer electrodes (D) at 400V and 125 µF. Electroporation samples were floated on a sucrose gradient according to 'Supplementary methods'. RT-PCR was used to determine relative concentrations of siRNA in each sucrose fraction compared to siRNA concentrations in fractions with the lowest sucrose density (bar charts). Western blots show the presence of the EV marker CD9 in the 100 000g pellet of each fraction. Bars in bar charts correspond to lanes on Western blots below. Most representative data of three independent experiments is shown.

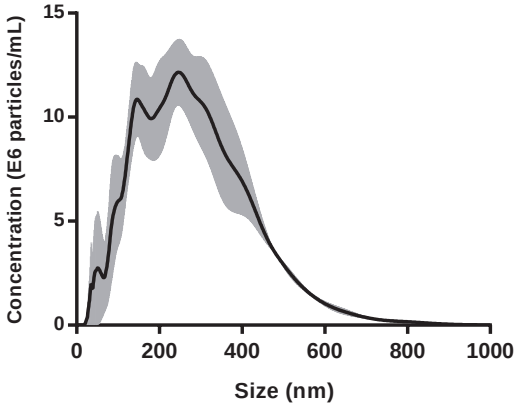

Supplementary Figure 4: Size distribution of Cy5-siRNA aggregates in Optiprep buffer after electroporation, as measured by NTA. Experiment was performed in triplicate and data are presented as mean ± SEM (grey area).

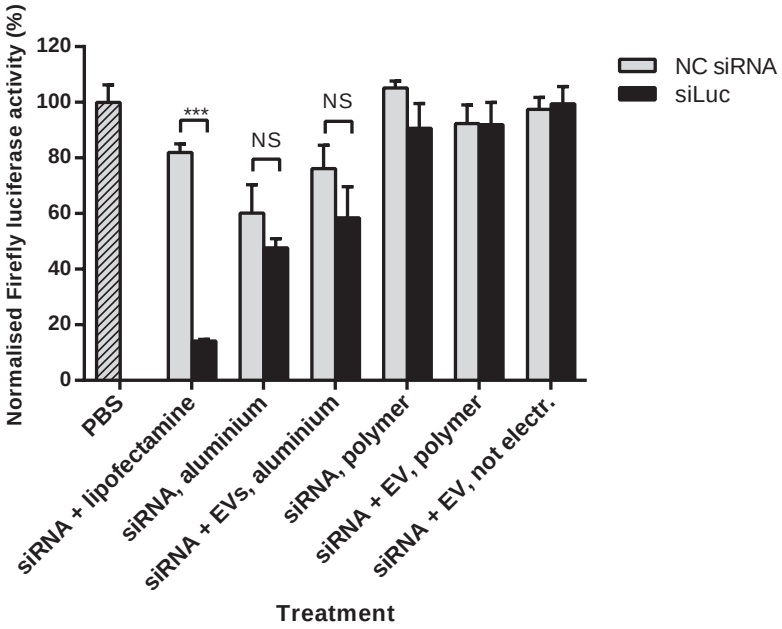

Supplementary Figure 5: Percentage of reporter gene silencing by electroporation samples, electroporated with non-specific control siRNA (NC siRNA, □) or Firefly luciferase-specific siRNA (siLuc, ■). Neuro2A cells expressing Firefly luciferase and Renilla luciferase were incubated with siRNA which was electroporated in the presence or absence of Neuro2A EVs in cuvettes with aluminium or conductive polymer electrodes at 400V and 125 µF. Controls included transfection of siRNA using Lipofectamine 2000 and siRNA mixed with EVs (not electroporated). After 48 hours, activities of both luciferases were analysed and Firefly luciferase activity was normalised to Renilla luciferase activity. Normalised Firefly luciferase activities are expressed as a percentage of activity in cells treated with PBS (mean ± SEM, n = 3 – 6). Significant differences between NC siRNA and siLuc were determined using independent samples t-tests and are indicated with *** ($p < 0.001$). NS: not significant.

Supplementary Table

Supplementary Table 1: Sequences of used siRNAs and primers.

Name	Sequence (5′-3′)	Modifications
siRNAs & synthetic miRNAs		
siRNA 1 (sense)	UGCGCUACGAUCGACGAUUGdTdT	5′ Cy5
siRNA 1 (antisense)	CAUCGUCGAUCGUAGCGCAdTdT	None
siRNA 2 (sense)	CAGAAGACUGUGGAUGGCCdTdT	5′ Cy3
siRNA 2 (antisense)	GGCCAUCCACAGUCUUCUGdGdG	None
siLuc (sense)	GAUUAUGUCCGGUUAUGUACG	None
siLuc (antisense)	UACAUAACCGGACAUAAUCGG	None
NC siRNA (sense)	UGCGCUACGAUCGACGAUGdTdT	None
NC siRNA (antisense)	CAUCGUCGAUCGUAGCGCAdTdT	None
siGFP (antisense only)	GGACUUGAAGAAGUCGUGCUU	None
Primers		
Reverse_stemloop_siLuc	GTCGTATCCAGTGCAGGGTCCGAGGTATTCGCAC TGGATACGACCCGATT	None
Reverse_stemloop_siGFP	GTCGTATCCAGTGCAGGGTCCGAGGTATTCGCAC TGGATACGACAAGCAC	None
Reverse_miR-143	GTCGTATCCAGTGCAGGGTCCGAGGTATTCGCAC TGGATACGACGAGCTA	None
Reverse_miR-146a	GTCGTATCCAGTGCAGGGTCCGAGGTATTCGCAC TGGATACGACAACCCA	None
Forward_siLuc	CCGCTAATACATAACCGGACAT	None
Forward_siGFP	CCGCTAAGGACTTGAAGAAGTC	None
Forward_miR-143	CGCTAATGAGATGAAGCACTG	None
Forward_miR-146a	CGCTAATGAGAACTGAATTCC	None
Reverse_stemloop	GTGCAGGGTCCGAGGT	None

CHAPTER 3

New considerations in the preparation of nucleic acid-loaded extracellular vesicles

Sander A. A. Kooijmans[1,*], Stephan Stremersch[2,*], Koen Raemdonck[2,#], Pieter Vader[1,3,#]

[1]Department of Clinical Chemistry and Haematology, University Medical Center Utrecht, Utrecht, The Netherlands; [2]Laboratory of General Biochemistry and Physical Pharmacy, Ghent University, Ghent, Belgium; [3]Department of Physiology, Anatomy and Genetics, University of Oxford, Oxford, UK

*These authors contributed equally to this work

#These authors contributed equally to this work

Therapeutic Delivery, 2014. 5(2), 105-7

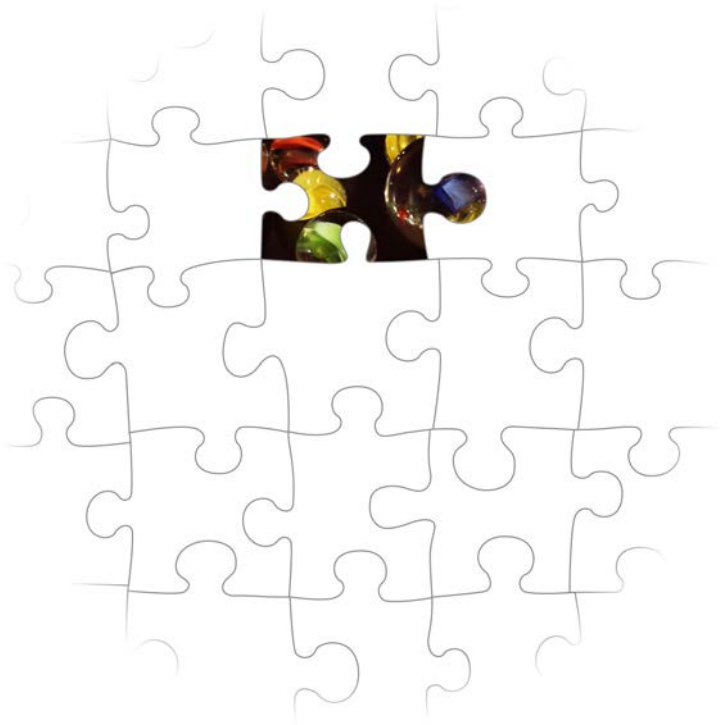

Introduction

RNA interference (RNAi) has emerged as a promising novel therapeutic strategy to selectively silence disease-causing genes. Successful RNAi depends on effective delivery of its mediator, short interfering (si)RNA, to the cytosol of the target cell. Different systems have already been proposed for siRNA delivery, including viral and non-viral systems, however due to lack of efficiency or issues related to toxicity and/or immunogenicity, they remain unsatisfactory [1].

Extracellular vesicles (EVs) are membrane-surrounded structures released by cells and are important mediators of cell-to-cell communication. They contain a variety of biological molecules, including miRNA, which can be transferred to other cells, leading to suppression of target genes in recipient cells [2, 3]. The fact that EVs appear to be nature's way to deliver functional small RNA molecules has created much excitement in the drug delivery field, as it may be possible to harness EVs for therapeutic siRNA delivery [4]. However, in order to realise this, methods for loading siRNA into EVs must be developed. Two different loading methods can be envisioned: (1) Extracellularly, after EV isolation, and (2) intracellularly, during EV formation.

Extracellular loading of RNA into EVs

The first approach comprises loading of EVs after their isolation from conditioned cell culture medium or bodily fluids. If successful, such an approach would allow for a controlled loading process and enable loading of all EVs produced. Unfortunately, for loading purified EVs with exogenous small RNAs without compromising their functionality, limited approaches are available.

Of the currently used nucleic acid delivery vehicles, liposomes appear the most analogous to EVs, especially from a physicochemical point of view. Hence, reflection on almost five decades of research on liposomal drug delivery systems could provide some valuable clues on siRNA loading methods [5]. It is important to note that liposomal nucleic acid delivery generally involves electrostatic complexation of the negatively charged siRNA via cationic lipids which are notorious for their *in vitro* and in vivo toxicity. However, EVs are known to carry a negative surface charge, hence precluding electrostatic siRNA complexation. Precomplexation of siRNA via cationic liposomes followed by fusion with isolated EVs has been evaluated for EV loading with siRNA by Wahlgren *et al.*. However, this approach appeared to be impractical as the EVs could not be purified from the remaining transfection liposomes/micelles, making it impossible to determine the location of the siRNA and the associated success of this loading method [6]. Passive loading of siRNA into (negatively charged) liposomes requires the addition of the nucleic acids before liposome formation which is not feasible for isolated EVs and as a rule entails low encapsulation efficiencies. In addition, the inherent complex composition of EVs, containing proteins next to lipids, rules out the use of organic solvent based methods or repeated freeze-thaw cycles because of potential interference with protein stability and (partial) loss of functionality.

Bryniarski and colleagues reported that mere incubation of miR-150 with exosome-like nanovesicles released by tolerised suppressor T-cells derived from miR-150 deficient mice, could restore the immunosuppressive effects seen with exosome-like nanovesicles from wild type mice [7]. Although this "loading" approach has not been thoroughly characterized yet, one can imagine that the miRNA remains associated to the EV surface and is therefore prone to enzymatic degradation, can easily detach from the EVs in complex biological media and possibly interferes with the inherent tropism of the EVs. Ideally, the loaded nucleic acids are encapsulated in the core of the isolated EVs as this mimics their natural localization and likely leads to the most optimal intracellular delivery. In a first effort towards such intravesicular loading, Alvarez-Erviti and colleagues used electroporation of EV/siRNA mixtures to induce transient pores in the EV membrane, allowing the siRNA to migrate through the lipid bilayer. Using this approach, siRNA encapsulation efficiencies up to 25% were reported [8]. Likewise, Wahlgren *et al.* demonstrated that nearly 90% of monocyte-derived vesicles effectively contained the siRNA of interest after electroporation [6]. Importantly, duplication of these experiments under similar experimental conditions revealed that the aforementioned siRNA encapsulation was largely due to unspecific aggregate formation, independent of the presence of extracellular vesicles [9]. The latter aggregates resulted from the interaction of multivalent cations, released from the metal electrodes in the electroporation cuvettes, with hydroxyl anions present in the electroporation buffer and were shown to co-precipitate siRNA. After blocking aggregate formation, by virtue of an acidic citrate electroporation buffer or the use of polymer based electroporation cuvettes, no significant encapsulation of siRNA could be measured [9]. Taken together, these results demonstrate the necessity for alternative methods to load EVs with siRNA.

Intracellular loading of RNA into EVs

In addition to methods for extracellular siRNA loading of EVs, also approaches for intracellular loading have been described. Such strategies make use of endogenous mechanisms for small RNA loading into EVs, by expressing the siRNA of interest in EV-producing cells. In a study by Kosaka *et al.*, cells were transiently transfected with a siRNA-expressing vector, and siRNA was shown to be released into the cell culture medium [10]. Importantly, siRNAs released from the cells were functionally transferred to recipient cells. Similar findings have been reported by other groups using a variety of co-cultured cell lines [11, 12]. Although these results suggest the feasibility of this approach, it is important to consider that small RNAs are released from cells via multiple pathways. In fact, it has been reported that the majority of released miRNAs are not associated with EVs but with protective protein complexes such as Argonaute-2 complexes [13]. It remains unclear whether protein complexes are also capable of transferring small RNAs to recipient cells. Nevertheless, when performing co-culture experiments to study small RNA transfer between cells, the presence of other secretory pathways, besides EVs, should be taken into account. Possibly, the use of 50-300 kDa cut-off filters may aid in discrimination

between EV- and protein-associated small RNA. In addition, experiments in which samples are treated with proteases (e.g. proteinase K) or detergents (e.g. Triton X-100, NP-40) followed by incubation with RNases may provide solid clues about the whereabouts of the small RNA of interest [14].

As an alternative to inducing siRNA expression in cells to stimulate siRNA secretion and encapsulation into EVs, host cells can be transfected directly with synthetic small RNAs. Several groups have reported that after transfection of donor cells, small RNAs are detectable in cell culture supernatants and in isolated EVs, and can be functionally transferred to recipient cells [15-17]. This approach is particularly useful for loading EVs with fluorescently labelled small RNAs, so that RNA uptake by recipient cells and RNA loading into EVs can be traced [17]. However, an important consideration when employing this method is the localization of the transfection reagent. It is conceivable that transfection reagent remains partly associated with the transfected small RNAs and is (co-)secreted in the culture medium. This may significantly affect not only the uptake behaviour of the released small RNAs, but also their localization in either EVs or protein complexes. Furthermore, complexes of transfection reagent and small RNA may be mistakenly interpreted as EV-encapsulated small RNA due to their co-precipitation with EVs at high centrifugal forces. To prevent confounding results when analysing the presence or behaviour of nucleic acids in EVs after transfection, it is advisable to purify EVs using stringent protocols.

The cellular mechanisms through which small RNAs are sorted into EVs are still unclear, which provides a drawback for intracellular loading of EVs with siRNA. It can be anticipated that EV loading efficiency will depend on siRNA sequence and cell type, as some small RNAs appear to be preferentially secreted into EVs, while others are retained within the host cell [18]. Furthermore, RNA species may be differentially distributed among EV subsets and this distribution may change depending on cell type and state [19]. Advances have been made towards identification of specific intracellular "zip code sequences" that target RNAs towards encapsulation in EVs [20], but tools to guarantee efficient RNA loading are still lacking, especially for small RNAs. Therefore, the loading of EVs with siRNA using the endogenous cellular machinery may need to be optimized for every individual siRNA sequence. Examples of parameters which may be modified to enhance siRNA secretion into EVs include knockdown of pathways directing siRNA away from EVs, cell stimulation or starvation, co-expression or knockdown of siRNA targets, and enhancement of siRNA expression levels.

Despite exciting progress since the first discovery of EVs as natural RNA carriers, realization of their therapeutic siRNA delivery potential awaits establishment of efficient, well-controlled and reproducible methods for loading. Increasing our understanding of the endogenous mechanisms that drive small RNA sorting into EVs may provide clues for siRNA loading optimization, which will prove critical for successful development of EVs as siRNA delivery systems.

References

1. R. Kanasty, J.R. Dorkin, A. Vegas, D. Anderson, Delivery materials for siRNA therapeutics, *Nat Mater*, 12 (2013) 967-977.
2. H. Valadi, K. Ekstrom, A. Bossios, M. Sjostrand, J.J. Lee, J.O. Lotvall, Exosome-mediated transfer of mRNAs and microRNAs is a novel mechanism of genetic exchange between cells, *Nat Cell Biol*, 9 (2007) 654-659.
3. D.M. Pegtel, K. Cosmopoulos, D.A. Thorley-Lawson, M.A. van Eijndhoven, E.S. Hopmans, J.L. Lindenberg*, et al.*, Functional delivery of viral miRNAs via exosomes, *Proc Natl Acad Sci U S A*, 107 (2010) 6328-6333.
4. S.M. van Dommelen, P. Vader, S. Lakhal, S.A. Kooijmans, W.W. van Solinge, M.J. Wood*, et al.*, Microvesicles and exosomes: opportunities for cell-derived membrane vesicles in drug delivery, *J Control Release*, 161 (2012) 635-644.
5. T.M. Allen, P.R. Cullis, Liposomal drug delivery systems: from concept to clinical applications, *Adv Drug Deliv Rev*, 65 (2013) 36-48.
6. J. Wahlgren, L.K.T. De, M. Brisslert, F. Vaziri Sani, E. Telemo, P. Sunnerhagen*, et al.*, Plasma exosomes can deliver exogenous short interfering RNA to monocytes and lymphocytes, *Nucleic Acids Res*, 40 (2012) e130.
7. K. Bryniarski, W. Ptak, A. Jayakumar, K. Pullmann, M.J. Caplan, A. Chairoungdua*, et al.*, Antigen-specific, antibody-coated, exosome-like nanovesicles deliver suppressor T-cell microRNA-150 to effector T cells to inhibit contact sensitivity, *J Allergy Clin Immunol*, 132 (2013) 170-181.
8. L. Alvarez-Erviti, Y. Seow, H. Yin, C. Betts, S. Lakhal, M.J. Wood, Delivery of siRNA to the mouse brain by systemic injection of targeted exosomes, *Nat Biotechnol*, 29 (2011) 341-345.
9. S.A. Kooijmans, S. Stremersch, K. Braeckmans, S.C. de Smedt, A. Hendrix, M.J. Wood*, et al.*, Electroporation-induced siRNA precipitation obscures the efficiency of siRNA loading into extracellular vesicles, *J Control Release*, 172 (2013) 229-238.
10. N. Kosaka, H. Iguchi, Y. Yoshioka, F. Takeshita, Y. Matsuki, T. Ochiya, Secretory mechanisms and intercellular transfer of microRNAs in living cells, *J Biol Chem*, 285 (2010) 17442-17452.
11. Q. Pan, V. Ramakrishnaiah, S. Henry, S. Fouraschen, P.E. de Ruiter, J. Kwekkeboom*, et al.*, Hepatic cell-to-cell transmission of small silencing RNA can extend the therapeutic reach of RNA interference (RNAi), *Gut*, 61 (2012) 1330-1339.
12. S.D. Olson, A. Kambal, K. Pollock, G.M. Mitchell, H. Stewart, S. Kalomoiris*, et al.*, Examination of mesenchymal stem cell-mediated RNAi transfer to Huntington's disease affected neuronal cells for reduction of huntingtin, *Mol Cell Neurosci*, 49 (2012) 271-281.
13. A. Turchinovich, L. Weiz, A. Langheinz, B. Burwinkel, Characterization of extracellular circulating microRNA, *Nucleic Acids Res*, 39 (2011) 7223-7233.
14. T.C. Roberts, C. Godfrey, G. McClorey, P. Vader, D. Briggs, C. Gardiner*, et al.*, Extracellular microRNAs are dynamic non-vesicular biomarkers of muscle turnover, *Nucleic Acids Res*, 41 (2013) 9500-9513.
15. S. Ohno, M. Takanashi, K. Sudo, S. Ueda, A. Ishikawa, N. Matsuyama*, et al.*, Systemically Injected Exosomes Targeted to EGFR Deliver Antitumor MicroRNA to Breast Cancer Cells, *Mol Ther*, 21 (2013) 185-191.
16. M. Yang, J. Chen, F. Su, B. Yu, F. Su, L. Lin*, et al.*, Microvesicles secreted by macrophages shuttle invasion-potentiating microRNAs into breast cancer cells, *Mol Cancer*, 10 (2011) 117.
17. Y. Zhang, D. Liu, X. Chen, J. Li, L. Li, Z. Bian*, et al.*, Secreted monocytic miR-150 enhances targeted endothelial cell migration, *Mol Cell*, 39 (2010) 133-144.

18. J. Guduric-Fuchs, A. O'Connor, B. Camp, C.L. O'Neill, R.J. Medina, D.A. Simpson, Selective extracellular vesicle-mediated export of an overlapping set of microRNAs from multiple cell types, *BMC Genomics*, 13 (2012) 357.

19. R. Crescitelli, C. Lasser, T.G. Szabo, A. Kittel, M. Eldh, I. Dianzani*, et al.*, Distinct RNA profiles in subpopulations of extracellular vesicles: apoptotic bodies, microvesicles and exosomes, *J Extracell Vesicles*, 2 (2013).

20. M.F. Bolukbasi, A. Mizrak, G.B. Ozdener, S. Madlener, T. Strobel, E.P. Erkan*, et al.*, miR-1289 and "Zipcode"-like Sequence Enrich mRNAs in Microvesicles, *Mol Ther Nucleic Acids*, 1 (2012) e10.

CHAPTER 4

Display of GPI-anchored anti-EGFR nanobodies on extracellular vesicles promotes tumor cell targeting

S.A.A. Kooijmans[1], C. Gomez Aleza[1], S.R. Roffler[2], W.W. van Solinge[1], P. Vader[1], R.M. Schiffelers[1]

[1]Department of Clinical Chemistry and Haematology, University Medical Center Utrecht, Utrecht, The Netherlands; [2]Institute of Biomedical Sciences, Academia Sinica, Taipei, Taiwan

Journal of Extracellular Vesicles, 2016. 5, 31053

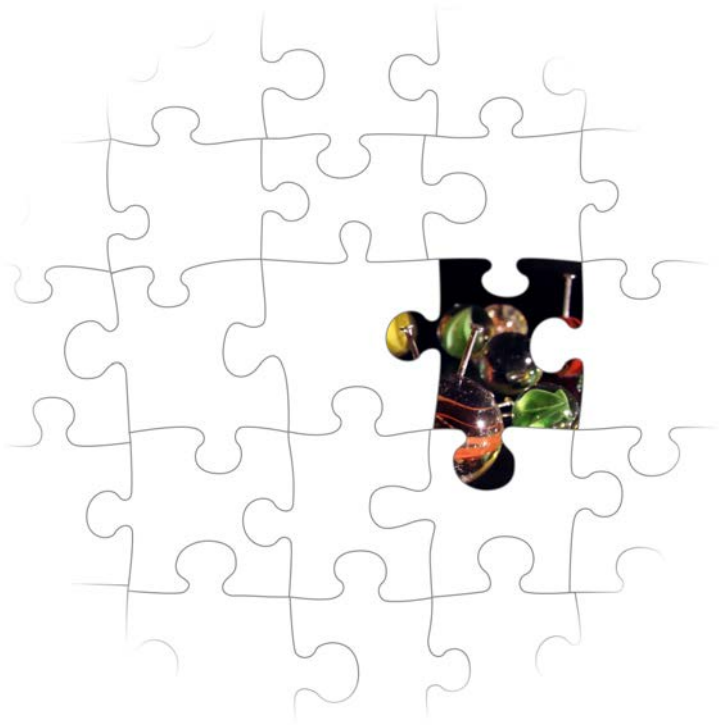

Abstract

Extracellular vesicles (EVs) are attractive candidate drug delivery systems due to their ability to functionally transport biological cargo to recipient cells. However, the apparent lack of target cell specificity of exogenously administered EVs limits their therapeutic applicability. In this study, we propose a novel method to equip EVs with targeting properties, in order to improve their interaction with tumor cells. EV producing cells were transfected with vectors encoding for anti-epidermal growth factor receptor (EGFR) nanobodies, which served as targeting ligands for tumor cells, fused to glycosylphosphatidylinositol (GPI) anchor signal peptides derived from decay-accelerating factor (DAF). EV analysis showed that GPI-linked nanobodies were successfully displayed on EV surfaces and were highly enriched in EVs compared with parent cells. Display of GPI-linked nanobodies on EVs did not alter general EV characteristics (i.e. morphology, size distribution and protein marker expression), but greatly improved EV binding to tumor cells dependent on EGFR density under static conditions. Moreover, nanobody-displaying EVs showed a significantly improved cell association to EGFR-expressing tumor cells under flow conditions, as determined using a live-cell fluorescence microscopy-coupled perfusion system. In conclusion, we show that nanobodies can be anchored on the surface of EVs via GPI, which alters their cell targeting behavior. Furthermore, this study highlights GPI-anchoring as a new tool in the EV toolbox, which may be applied for EV display of a variety of proteins, such as antibodies, reporter proteins and signaling molecules.

INTRODUCTION

Extracellular vesicles (EVs), including exosomes and microvesicles, are submicron lipid bilayer-surrounded vesicles containing proteins and nucleic acids, such as miRNAs and mRNAs. They are released from many, if not all, cell types in the body and are believed to play a role in intercellular communication [1, 2]. The ability of extracellular vesicles to selectively convey proteins, lipids and nucleic acids to cells has created excitement in the field of drug delivery, where efficient and targeted delivery of biomolecules is desired [3-8]. Multiple studies have shown that the use of EVs for therapeutic purposes is feasible, and EVs have even already been applied in phase I clinical trials (reviewed in [9, 10]). However, EVs may also possess unfavorable characteristics which could limit their applicability as drug delivery systems. Their natural bioactive payloads may counteract the desired therapeutic effects and a lack of targeting specificity may result in uptake by non-targeted, healthy cells. Multiple reports have shown that EVs can be engineered to include specific cargo or express targeting ligands to improve their drug delivery potential [11-17]. Previously described targeting strategies have been mainly based on the fusion of targeting ligands with EV membrane proteins, such as Lamp2b [11, 15, 16]. Albeit effective in these cases, such strategies may have drawbacks. For example, the function of EV membrane proteins (e.g. fusion with cellular membranes or immune regulation [4, 18]) may be compromised upon fusion with targeting ligands, and some Lamp2b-fused targeting ligands have been described to undergo premature degradation instead of functional display on EVs [19]. To avoid such issues, multiple groups have explored strategies to functionalize EV surfaces after EV secretion, circumventing the need to modify EV producer cells [17, 20, 21]. For example, Smyth and coworkers grafted alkyne moieties onto isolated EVs to equip these vesicles with fluorescent probes using click chemistry [20]. Unfortunately, such modifications may also compromise the functionality of crucial EV components for EV-cell interactions and cargo delivery. In this work, we therefore propose an alternative strategy to efficiently decorate EVs with targeting proteins.

EVs have been described to be enriched in lipid raft-associated lipids, including sphingolipids and cholesterol, and proteins, including glycosylphosphatidylinositol (GPI)-anchored proteins [2, 22, 23]. In fact, the GPI-anchored protein decay-accelerating factor (DAF, also known as CD55) has been described to be selectively secreted in EVs during reticulocyte maturation [24]. We hypothesized that this phenomenon could be exploited for the expression of targeting moieties onto EVs. We therefore fused a human DAF-derived GPI-anchor signal peptide to nanobodies, which served as model targeting ligands. This GPI-anchor peptide has previously been employed to tether a variety of proteins to cell membranes [25-27]. Nanobodies are small (15 kD) single variable domains derived from heavy-chain antibodies from *Camelidae* species. They can be used as versatile targeting tools with binding capacity similar to antibodies. Nanobodies offer several advantages compared with their full-length counterparts, such as straightforward selection and recombinant production, and high chemical and thermal stability [28]. In this work, nanobodies were used to target the

epidermal growth factor receptor (EGFR), a well-studied oncogene against which a range of clinically approved inhibitors are directed for the treatment of solid tumors [29, 30]. Here, we investigated whether linkage of nanobodies to GPI-anchors is effective for the display of these proteins on EVs, and how this display influences EV characteristics and *in vitro* tumor targeting behavior. Furthermore, we studied the interactions of these EVs with tumor cells under flow conditions using a live-cell imaging perfusion setup.

Materials and methods

Materials

MicroBCA Protein Assay Kit and CellTracker Deep Red dye were obtained from Thermo Fisher Scientific (Waltham, USA). Sepharose CL-4B was ordered from Sigma-Aldrich (Steinheim, Germany). Sterile cell culture materials were purchased from Greiner Bio-One (Alphen aan de Rijn, The Netherlands). pET28a-EGa1 and pAX51-R2 vectors encoding EGa1 (PDB ID: 4KRN) and R2 (PDB ID: 1QD0) Myc-tagged nanobodies, respectively, were kindly provided by dr. S. Oliveira (Department of Biology, Utrecht University, Utrecht, The Netherlands).

Molecular cloning

EGa1 and R2 Myc-tagged nanobody sequences were PCR amplified from pET28a-EGa1 and pAX51-R2 vectors with primers designed to flank the nanobody sequences with Sfi and SalI restriction sites. Obtained inserts were Sfi/SalI digested and inserted into a pLNCX vector containing an N-terminal HA-tag, Sfi and SalI cloning sites, and a C-terminal $GGGGS_2$ linker sequence followed by 37 amino acids of human DAF under the control of a CMV promoter [25]. The resulting vectors (named pLNCX-DAF-R2 and pLNCX-DAF-EGa1) were sequenced using a BigDye® Terminator v3.1 Cycle Sequencing Kit (Thermo Fisher Scientific) according to the manufacturer's instructions to confirm in-frame insertion of the nanobody sequences.

Cell culture and generation of stable cell lines

All cells used in this study were maintained at 37°C and 5% CO_2, and were tested negative for mycoplasma. Neuro2A cells were cultured in Roswell Park Memorial Institute (RPMI, Gibco) 1640 medium supplemented with 10% FBS and 100 U/mL penicillin and 100 U/mL streptomycin. A431 and HeLa cells were grown in Dulbecco's Modified Eagle Medium (DMEM, Gibco) supplemented with 10% fetal bovine serum (FBS) and 100 U/mL penicillin and 100 U/mL streptomycin. To generate stable nanobody-DAF expressing cell lines, Neuro2A cells were transfected with pLNCX-DAF-R2 or pLNCX-DAF-EGa1 using TransIT 2020 transfection reagent (Mirius Bio, USA) according to the manufacturer's instructions, and selected for at least two weeks in medium containing 500 µg/mL G418 (Geneticin, Thermo Fisher Scientific) until cells regained normal growth and morphology. Cells were subsequently maintained in

medium containing 250 µg/mL G418.

EV isolation

For EV production, Neuro2A cells were seeded in T175 flasks and cultured for 24 hours in normal culture medium, after which medium was replaced by Opti-MEM Reduced Serum medium supplemented with GlutaMAX (Gibco, Thermo Fisher Scientific) and 100 U/mL penicillin, 100 U/mL streptomycin and 250 µg/mL G418 (for transfected cells). After 48 hours, when cells reached 90-95% confluency, EVs were isolated using a recently described ultrafiltration/size-exclusion liquid chromatography (UF-LC) method [31]. In brief, conditioned medium was centrifuged for 10 min at 300g and 2000g at 4°C to remove cells and debris, respectively. Medium was vacuum filtered through Steritop 0.22 µm filters (Merck Millipore) to remove large vesicles and debris, and concentrated to < 4 mL using Amicon Ultra-15 Centrifugal Filter Units with a 100 kD MWCO (Merck Millipore) at 4000g and 4°C. Concentrated medium samples were loaded onto a HiPrep 16/60 Sephacryl S-400 HR gel filtration column (GE Healthcare Life Sciences), which was equilibrated with phosphate buffered saline (PBS) and connected to an ÄKTA pure or ÄKTA start chromatography system (GE Healthcare, both maintained at 4°C). EVs were separated from non-vesicular material using PBS as eluent. EV containing fractions (determined by UV absorbance at 280 nm) were pooled and concentrated to < 500 µL samples using 100 kD MWCO Amicon Ultra-15 Centrifugal Filter Units. EV protein yields were determined using a MicroBCA Protein Assay according to manufacturer's instructions.

Western blot analysis

For analysis of protein content of cells, cells in culture flasks were washed once with PBS, trypsinized, and lysed in RIPA buffer (Alfa Aesar) supplemented with Protease Inhibitor Cocktail (Sigma-Aldrich). Cell lysates were centrifuged at 20 000g for 10 min at 4°C to remove insoluble material, and protein concentration was determined using a MicroBCA Protein Assay. EVs in PBS and cell lysates were mixed with sample buffer containing dithiothreitol (DTT), heated to 95˚C for 10 min and subjected to electrophoresis on 4-12% Bis-Tris polyacrylamide gels (Thermo Scientific). Proteins were blotted on Immobilon-FL polyvinylidene difluoride (PVDF) membranes (Millipore), after which membranes were blocked with 50% v/v Odyssey Blocking Buffer (LI-COR Biosciences) in Tris buffered saline (TBS). Subsequently membranes were probed overnight at 4°C with goat anti-HA (1:5000, A00168-100, Genscript), mouse anti-ALIX (1:1000, clone 3A9, Abcam), rabbit anti-TSG101 (1:1000, ab30871, Abcam), mouse anti-β-Actin (1:1000, clone 8H10D10, Cell Signaling Technology), rabbit anti-CD9 (1:2500, clone EPR2949, Abcam), or rabbit anti-EGFR (1:1000, clone D38B1, Cell Signaling Technology) antibodies in 50% v/v Odyssey Blocking Buffer in TBS with 0.1% Tween20 (TBS-T). Secondary antibodies included IRDye 800CW donkey anti-goat, IRDye 800CW donkey anti-mouse (LI-COR Biosciences), Alexa Fluor 680 goat anti-mouse, or Alexa Fluor 680 goat anti-rabbit (Thermo Fisher Scientific) and were applied at a 1:7500 dilution. Protein bands were visualized on an Odyssey Infrared Imager

(LI-COR Biosciences, Leusden, The Netherlands) at 700 and 800 nm.

Nanoparticle Tracking Analysis

EV size distribution and concentration was measured using a NanoSight NS500 system equipped with an LM14 405 nm violet laser unit (Malvern Instruments, Worcestershire, UK). Concentrated EV samples were diluted with PBS (confirmed to be particle-free when analyzed with the same settings) to appropriate dilutions for analysis (generally 1:1000-1:5000) and visualized at camera level 13 under control of a script, which included acquisition of five movies of 30 s at a fixed temperature of 22°C. Analysis was performed with NTA 3.1 software. Detection threshold was set at 9 and other settings were kept at default.

Transmission Electron Microscopy

EVs in PBS were adsorbed to carbon-coated formvar grids for 15 min at room temperature. Unbound EVs were removed by washing with PBS and grids were blocked with 1% BSA in PBS (PBSA) for 10 min. HA epitopes on the grids were immunolabeled with goat anti-HA antibody (1:200, A00168-100, Genscript) in PBSA for 30 min, followed by 10 min incubations with rabbit anti-goat IgG (1:250, RAG/IgG(Fc)/7S, Nordic-MUbio) and 10 nm Protein A gold (CMC, Utrecht, The Netherlands) in PBSA. Grids were thoroughly washed with PBS between incubations. Finally, grids were fixated in 1% glutaraldehyde in PBS for 10 min, counterstained with uranyl-oxalate and embedded in methyl cellulose uranyl-acetate [32]. Imaging was performed using a Tecnai T12 electron microscope (FEI, Eindhoven, The Netherlands).

EV labeling and purification

For functional assays, EVs were labeled with CellTracker Deep Red immediately after isolation. CellTracker Deep Red dye was dissolved at 2 mM concentration in DMSO, and mixed with fixed EV amounts (based on protein concentration) at a final dye concentration of 16 µM. EV/dye mixtures were incubated for 1 hour at 37°C and stored at 4°C until purification (maximally 16 hours). For removal of unincorporated label, Sepharose CL-4B (Sigma-Aldrich) was packed in a XK-16/20 column (GE Healthcare) according to the manufacturer's instructions. Column was connected to a refrigerated ÄKTA pure chromatography system, equilibrated with PBS, and EV/dye mixtures were injected. Pooled EV fractions were concentrated to 100-200 µL using Vivaspin ultrafiltration tubes with 100 kD cut-off (Sartorius, UK). To determine whether labeling efficiency differed among EV samples, protein concentrations were measured using a MicroBCA Protein Assay, and fluorescence of 60 µL samples in a black 96-well plate was determined using a SpectraMax M2e microplate reader (Molecular Devices) at 630 nm excitation and 650 nm emission. Relative labeling efficiency was defined as relative fluorescence intensity/µg EV protein, and deviations of < 10% between samples were considered acceptable before proceeding to cell association studies.

Cell binding assays

Neuro2A, HeLa or A431 cells were trypsinized and resuspended in ice-cold culture medium. Cell suspensions were transferred to round-bottom 96-well plates at a concentration of 40 000 cells/well on ice. CellTracker Deep Red-labeled EVs were added at a concentration of 5 µg/mL in triplicates and cells were incubated for 1 hour at 4°C to allow EV binding. Plates were centrifuged at 500g for 5 min, medium was removed, and cells were resuspended in ice-cold FACS buffer (0.3% BSA in PBS). This process was repeated twice for a total of three washes, and finally cells were resuspended in 0.2% formaldehyde in PBS. Mean fluorescence intensity (MFI) values were measured using a FACSCanto II flow cytometer (BD Biosciences, USA) and normalized to untreated cells.

Cell uptake assays

Neuro2A or A431 cells were cultured in normal culture medium in flat-bottom 96-well plates until a confluency of 80-90% was reached. CellTracker Deep Red-labeled EVs were added at a concentration of 5 µg/mL in triplicates and incubated for 1, 3 or 6 hours at 37°C. Medium was removed, cells were washed once with PBS, trypsinized, and transferred to round-bottom 96-well plates in normal culture medium. Cells were pelleted for 5 min at 500g and resuspended in FACS buffer. Subsequently, cells were washed once with acid wash buffer (0.5M NaCl, 0.2M acetic acid, pH 3) to remove cell-bound EVs and once more with FACS buffer. Finally, cells were resuspended in 0.2% formaldehyde in PBS and MFI values were determined by flow cytometry.

Perfusion experiments

Perfusion experiments were performed using perspex perfusion chambers containing a sample inlet, sample outlet connected to a syringe pump, and a connector for a vacuum pump (see Supplementary Figure 1). A silicone sheet with a thickness of 0.125 mm was placed on top of the perspex frame, thereby forming a flow channel of 2 x 30 mm between sample in- and outlets. A431 cells cultured on glass coverslips (24 x 50 mm) were placed over the silicone sheet, and vacuum was applied to the chamber to seal the flow channel. Cell-covered perfusion surfaces were prepared by placing sterilized glass coverslips in 4-well slide tray plates. Coverslips were covered with 0.9 mL of 1% gelatin for 20 min at 37°C. Subsequently, 1.8 mL of 0.5% glutaraldehyde was added and plates were incubated for 20 min at room temperature. Liquid was replaced with 1.8 mL of 1 M glycine and plates were incubated for 20 min at room temperature. Coverslips were washed with PBS and A431 cells were seeded in normal culture medium. When cells reached a confluency of 80-90%, medium was removed and cells were stained with DAPI (Sigma-Aldrich) in PBS for 5 min at room temperature. Coverslips were washed once with plain DMEM and assembled on the perfusion chamber which was pre-equilibrated with DMEM, preventing air from entering the flow channel. Perfusion chamber was mounted on an Axio Observer fluorescence microscope (Carl Zeiss,

Oberkochen, Germany) and cells were visualized using differential interference contrast (DIC) and DAPI channels with a 40x objective. A syringe was connected to the sample outlet of the perfusion chamber and liquid was slowly withdrawn by a Pump 22 Multiple Syringe Pump (Harvard Apparatus, USA) at 25 µL/min, corresponding with a shear rate of 82.5 s^{-1}. When flow rate stabilized, sample inlet was connected to a 2 µg/mL suspension of CellTracker Deep Red-labeled EVs in DMEM. EV perfusion was performed for 40 min, while pictures in DAPI, DIC and Cy5 fluorescence channels were taken with 10 s intervals. Cells were washed by perfusion with plain DMEM and fixated with 2% paraformaldehyde in PBS (PFA). Coverslips were removed and stored overnight in 1% PFA at 4°C. For semi-quantitative analysis, fixated coverslips were washed with PBS and mounted on microscopy slides using Vectashield HardSet Antifade mounting medium with DAPI (Vector Laboratories Inc.). Cell-associated EVs were imaged with a fluorescence microscope. Thirty to sixty images were randomly acquired across the entire area of the flow channel while focusing on the DAPI channel to avoid selection bias. The number of fluorescent EVs in each picture was analyzed by Zen 2 pro analysis software (Carl Zeiss), and normalized to the number of cells (DAPI-stained nuclei) in each picture.

Statistical analysis

When applicable, statistical analysis was performed using IBM SPSS Statistics, version 21. Multiple-group testing was performed using one-way ANOVA with Tukey post-hoc tests and comparisons between two groups were made using independent samples *t* tests. Differences with p values < 0.05 were considered statistically significant.

Results

Characterization of EVs derived from DAF-nanobody expressing cells

The EGa1 nanobody is a high-affinity ligand for EGFR which competitively inhibits binding of the natural ligand epidermal growth factor (EGF) and sterically prevents receptor activation [33, 34]. In contrast, the R2 nanobody, which was raised against the azo-dye Reactive Red (RR6) [35], was used as a control nanobody [36, 37]. It was hypothesized that nanobodies could be displayed on EVs via fusion to a C-terminal GPI signal peptide derived from human DAF. When expressed in cells, the DAF peptide is cleaved off by GPI transamidase enzymes, thereby driving nanobody attachment to GPI anchors [27]. This way, nanobodies would localize to GPI-rich lipid rafts in cell membranes [25, 38, 39] and possibly in EV membranes. To test this hypothesis, R2 or EGa1 sequences were cloned into pLNCX vectors designed to drive the expression of HA-tagged proteins fused to DAF peptides (schematically shown in Figure 1). The resulting constructs (pLNCX-DAF-R2 and pLNCX-DAF-EGa1) were stably transfected into Neuro2A cells to create DAF-R2 and DAF-EGa1 cells, respectively. EVs were isolated from these cells using a previously described "ultrafiltration followed by liquid chromatography" method [31]. EV yields

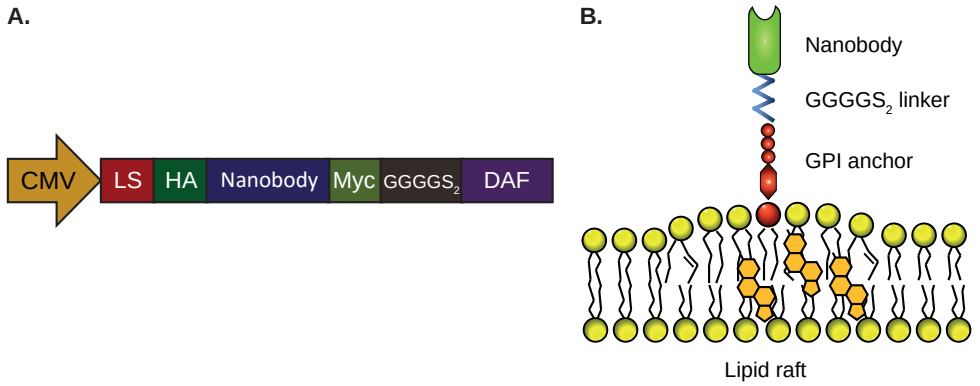

Figure 1: Schematic presentation of nanobody-DAF fusion proteins. Nanobody-DAF protein expression was driven by a CMV promoter in pLNCX vectors. Recombinant proteins comprise an Igκ leader sequence (LS), N-terminal HA tag (HA), nanobody sequence, Myc tag (Myc), $GGGGS_2$ linker, and a C-terminal GPI-anchor signal peptide (DAF) (A). Nanobodies fused to GPI-anchors were hypothesized to localize to lipid rafts in cellular membranes upon expression (B).

(as determined by protein quantification) typically ranged between 0.4 and 0.9 µg per mL of conditioned medium from Neuro2A and DAF-R2 cells, but were slightly lower for DAF-EGa1 cells (0.3 - 0.5 µg/mL of conditioned medium). Expression of GPI-anchored HA-tagged nanobodies in cells and EVs was analyzed by Western blotting (Figure 2A). DAF-R2 and DAF-EGa1 proteins were hardly detectable in cell lysates from their respective cell lines. Remarkably, both proteins were found to be highly enriched in EVs (termed EV-DAF-R2 and EV-DAF-EGa1) compared with their parent cells. Both showed bands of approximately 27 kD, which was slightly bigger than their calculated molecular weight (25.3 kD for DAF-R2 and 25.7 kD for DAF-EGa1), which may be explained by the successful attachment of GPI to the proteins. Commonly used EV markers ALIX, TSG101 and CD9 were also clearly detectable in all EV samples, and ALIX and CD9 were highly enriched compared with parent cells, in accordance with previous reports [6, 40, 41]. To investigate whether the expression of GPI-anchored nanobodies altered EV size, EVs were analyzed by Nanoparticle Tracking Analysis (NTA, Figure 2B). For both unmodified and DAF-nanobody EVs, a typical Neuro2A-derived EV size distribution was observed [31, 42], with a mode size of approximately 100 nm and a small population of EVs sizing around 150 - 250 nm (possibly suggesting that the latter mainly originate from the plasma membrane [1]). Of note, particle concentrations correlated well with protein concentrations among different EVs (typically one µg of EVs corresponded with 5-10 x 10^8 particles), indicating a similar protein load per particle. To assess the orientation of the nanobodies in the EV membranes and to assess whether expression of GPI-anchored nanobodies affected EV morphology, EVs were analyzed by whole-mount transmission electron microscopy (TEM) after immunogold labeling of HA tags (Figure 2C). Control EVs showed a 'cup-shaped' morphology, and were mostly unstained by anti-HA antibodies. EV-DAF-R2 and EV-DAF-EGa1 appeared

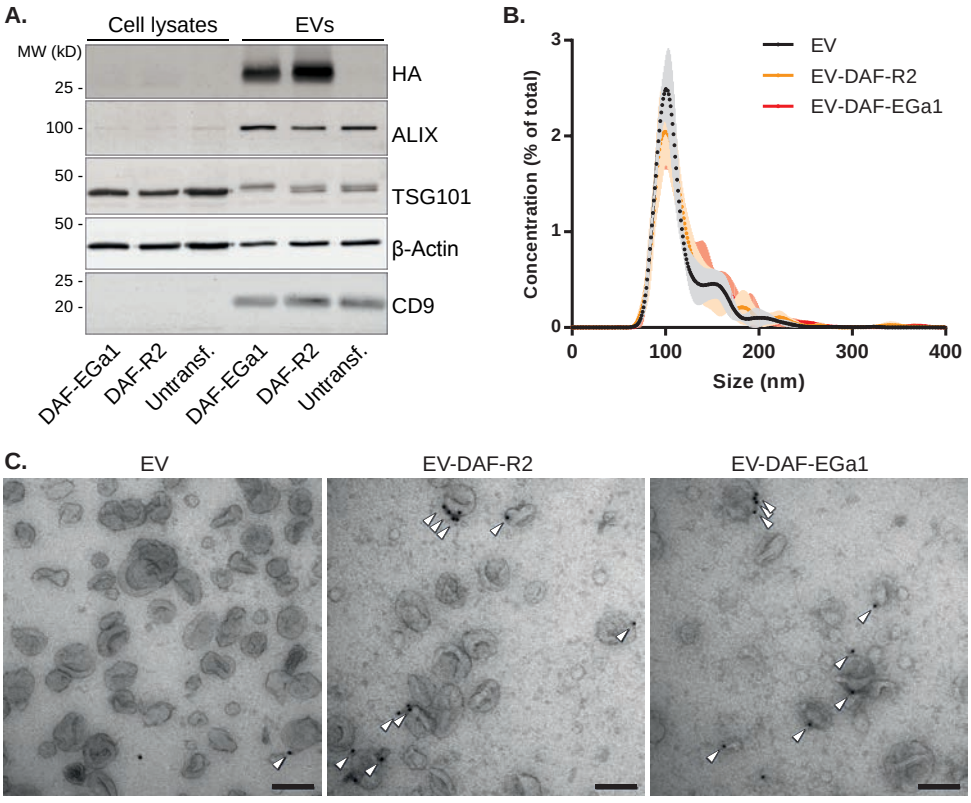

Figure 2: GPI-anchored nanobodies are enriched in EVs compared with parent cells, and are displayed on EV surfaces without affecting EV characteristics. A. Western blot analysis of Neuro2A cells after stable transfection with pLNCX-DAF-EGa1 (DAF-EGa1) and pLNCX-DAF-R2 (DAF-R2) vectors compared with untransfected controls and EVs secreted by these cell lines. HA-tag was used to detect nanobody expression, and ALIX, TSG101 and CD9 were used as EV markers. Equal amounts of protein were analyzed. Actin was included as a loading control. B. Size distribution of normal EVs and DAF-nanobody EVs as determined by Nanoparticle Tracking Analysis. Data are displayed as mean ± SD of 5 measurements. C. Transmission electron microscopy images of EVs and DAF-nanobody EVs after immunogold labeling with anti-HA antibodies (arrowheads indicate membrane-associated gold). Scale bars represent 100 nm.

similar to controls when comparing morphology and electron density, but a substantial amount of EV membranes stained positive for HA. Interestingly, some EVs showed patches of clustered gold particles on their membrane, possibly indicating the concentration of multiple GPI-anchored nanobodies in lipid rafts. Based on immunogold-TEM analysis, it was estimated that at least 15-25% of EVs displayed at least one nanobody, regardless of nanobody sequence. Taken together, these data show that GPI-anchors can be used to display nanobodies on EV surfaces, without affecting other EV characteristics (i.e. protein composition, size and morphology).

Cell association of targeted EVs

To investigate whether GPI-anchored nanobodies could influence the targeting behavior of EVs, a cell association assay was performed. For this assay, EVs were stained with the far-red fluorescent dye CellTracker Deep Red. Importantly, the labeling efficiency (defined as fluorescence intensity per µg of EVs) was determined for each batch of EVs prior to experiments. Higher EV protein concentration during labeling resulted in higher labeling efficiency, while increased EV storage time prior to labeling tended to decrease labeling efficiency (Supplementary Figure 2). To study cell association of nanobody-decorated EVs, labeled EVs were incubated with Neuro2A, HeLa or A431 cells for 1 hour at 4°C to allow binding, but inhibit EV uptake by these cells (Figure 3A) [14, 18, 43]. These cell types vary in EGFR expression level [36, 44], with undetectable expression in Neuro2A and clear overexpression in A431 (Western blot in Figure 3A). As shown in Figure 3A, EVs and EV-DAF-R2 associated to all three cell types with similar efficiency. In contrast, EV-DAF-EGa1 showed more than 10-fold higher association to A431 cells compared with controls. In addition, a small increase in binding to HeLa cells was observed, while binding to Neuro2A cells was similar compared with control EVs and EV-DAF-R2. Together, these data demonstrate that the GPI-anchored nanobodies are functional and facilitate EV binding to tumor cells in an EGFR-dependent manner. To investigate whether this altered binding behavior of EV-DAF-EGa1 also translated in altered uptake kinetics, uptake assays were performed in Neuro2A and A431 cells. EVs were incubated with cells for 1, 3 or 6 hours at 37°C and cells were acid washed prior to FACS analysis to remove surface-bound EVs. Surprisingly, uptake kinetics were similar between EV-DAF-EGa1, control EVs and EV-DAF-R2, and did not differ between EGFR-negative (Neuro2A) and EGFR-positive (A431) cells (Figure 3B). Moreover, these data suggest that, under these conditions, binding of EVs to cells does not result in the same degree of cellular uptake.

Cell association under flow conditions

We next reasoned that cell-specific binding of EVs under flow conditions could be of greater physiological relevance than binding under static conditions, given that EV-carrying liquids (e.g. blood and interstitial fluid) are constantly in motion. This is also the case in solid tumor tissue, given that high interstitial fluid pressure drives macromolecules and nanoparticles to the tumor periphery [45-47]. Efficient capture of EVs by tumor cells or tissues could greatly improve EV retention in such tissues and thereby facilitate targeted delivery of encapsulated cargo. To investigate whether the display of nanobodies on EVs could improve cell interaction under flow conditions, live-cell perfusion experiments were performed. A431 cells were grown on glass coverslips, which were subsequently mounted onto perspex perfusion chambers (see also Supplementary Figure 1). This setup allowed for controlled perfusion of EV-containing medium over the cells in a 2 x 30 mm flow channel, and real-time monitoring of EV cell association using a fluorescence microscope. For perfusion experiments, EVs were labeled with CellTracker Deep Red fluorescent dye and perfused over cells at a rate of 25 µL/min for

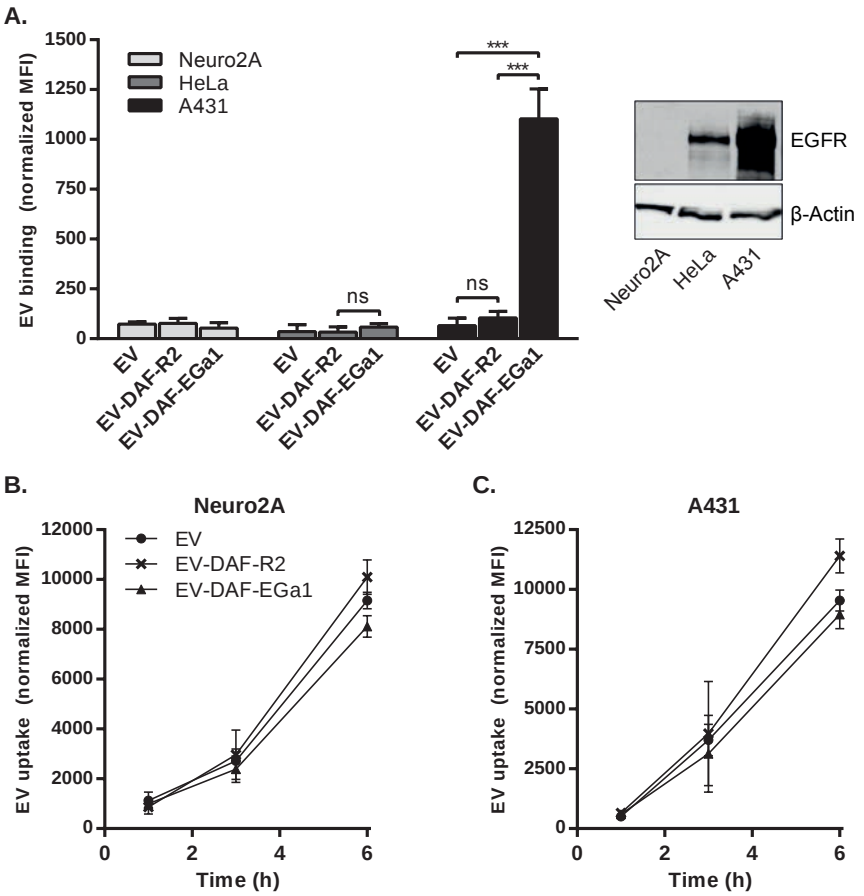

Figure 3: Display of GPI-anchored anti-EGFR nanobodies on EVs increases EV binding to EGFR-expressing tumor cells, but does not increase uptake by these cells. A. Binding of CellTracker Deep Red-labeled control EVs and EVs with GPI-anchored nanobodies to Neuro2A, HeLa and A431 cells for 1 hour at 4°C, as quantified by flow cytometry (left panel). EGFR expression in these cells was analyzed by Western Blot (right panel). B. Uptake of CellTracker Deep Red-labeled control EVs and EVs with GPI-anchored nanobodies by Neuro2A and A431 cells at 37°C for 1, 3 or 6 hours, as determined by flow cytometry. All data are displayed as mean ± SD and are representative of three independent experiments. ns = not significant and *** indicates $p < 0.001$ as determined by one-way ANOVA with Tukey post-hoc test.

40 min at room temperature. It was observed that control EVs and EV-DAF-R2 were not efficiently captured by the cells over the course of the experiment, while EV-DAF-EGa1 rapidly associated to cell surfaces (Figure 4A). To verify that this process occurred throughout the entire perfused area and not just in the recorded fields of view, cells were washed after perfusion, fixated and mounted on microscopy slides. EV-cell association was analyzed by acquiring fluorescence microscopy pictures at low magnification over the entire area of the perfusion channel

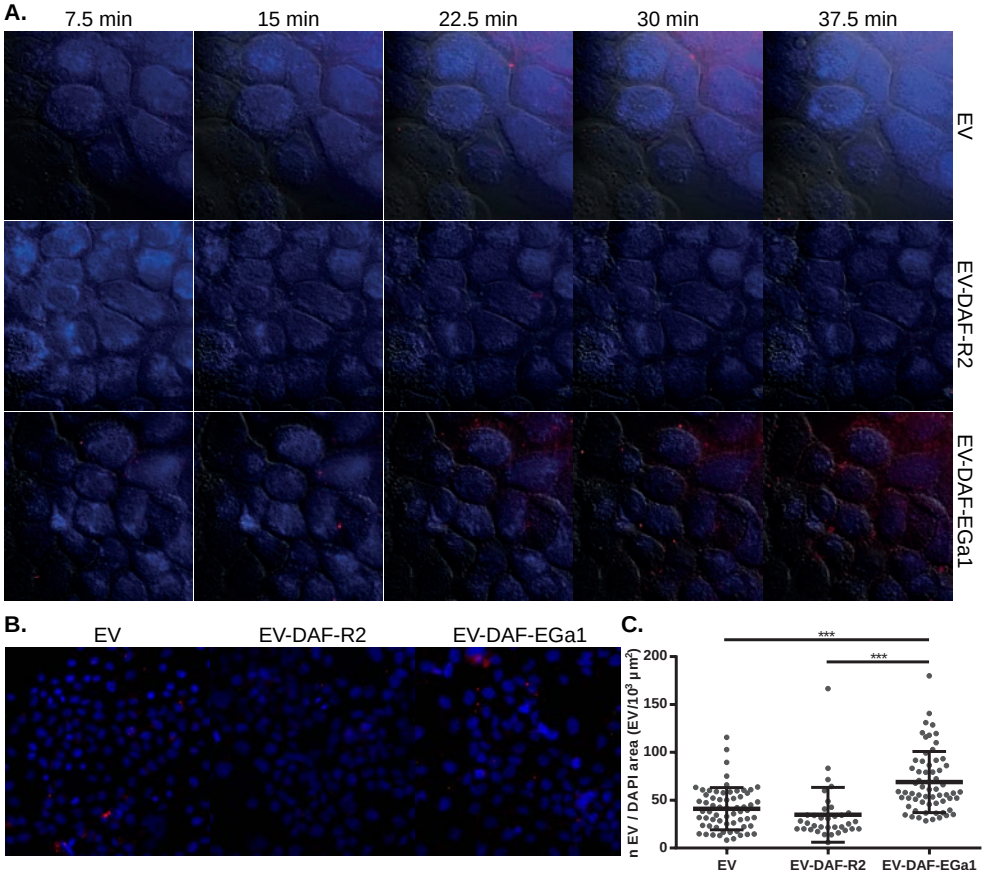

Figure 4: Display of GPI-anchored nanobodies on EVs increases association with tumor cells under flow conditions. A. Fluorescence microscopy pictures of DAPI (blue)-stained A431 cells perfused for 40 min with CellTracker Deep Red-labeled EVs (red) with and without GPI-anchored nanobodies. DIC overlays are shown in gray as a reference for cell boundaries. EVs were perfused over cells at a rate of 25 µL/min. After perfusion, cells in flow channels were washed, fixated and mounted on microscopy slides. Fluorescence microscopy pictures were randomly taken at low magnification across the entire area of the flow channel (35-60 pictures per channel). Representative CellTracker Deep Red/ DAPI overlay pictures are shown in B. The number of EVs (n EV) and the cell-covered area (DAPI area) in each picture were quantified with Zen 2 software and displayed in C. Results are shown as mean ± SD and *** indicates $p < 0.001$ as determined by one-way ANOVA with Tukey post-hoc test.

(Figure 4B). Again, it was evident that cell association was higher for EV-DAF-EGa1 than for control EVs and EV-DAF-R2, regardless of position in the channel. Quantification of the number of retained EVs in flow channels revealed that under these flow conditions, cell association of EGa1 was approximately 2-fold higher than cell association of EVs and EV-DAF-R2 (Figure 4C).

Discussion

EVs harbor favorable characteristics for the transfer of biological cargo to recipient cells, which increasingly highlights them as possible candidates for drug delivery. Unfortunately, engineering of EVs for targeted drug delivery is less straightforward than for synthetic systems (e.g. liposomes). While liposomes can be easily modified with targeting ligands and loaded with therapeutic cargoes, similar strategies are often not applicable to EVs due to their cellular origin [5]. Previously described EV targeting strategies are based on fusion of targeting ligands to EV membrane proteins, such as transmembrane domains of platelet derived growth factor (PDFG) [14, 48] and Lamp2b [11, 16]. Albeit various reports have demonstrated the feasibility of this approach, it remains unclear whether these strategies result in high-level expression (i.e. enrichment) of targeting ligands in EVs compared with parent cells. In this work, we present a novel method to display targeting ligands (i.e. nanobodies) on EV surfaces by linkage to GPI anchors. It was observed that nanobody expression was highly enriched in EVs compared with their parent cells, suggesting a selective secretion of GPI-anchored proteins in EVs. This finding is supported by previous reports, which showed efficient incorporation of GPI-anchored prion proteins in EVs [49] and selective release of GPI-anchored proteins in EVs during reticulocyte maturation [24]. Moreover, lipid raft microdomains, in which GPI-anchored proteins are highly enriched, are believed to be involved in EV biogenesis and have often been identified as abundant constituents of EV membranes [22, 23, 50-55]. Hence, GPI-anchoring of targeting ligands may be an appealing alternative to previously described targeting methods. Besides recombinant protein enrichment in EVs, this strategy may offer several advantages. The DAF GPI-anchoring signal peptide is relatively small (37 amino acids), highly soluble, and is not expected to interfere with proper recombinant protein folding, especially given that the peptide is cleaved off and replaced by a GPI anchor during post-translational modification of the protein [25-27]. This could be beneficial when expressing proteins with complex tertiary structures (e.g. antibodies or enzymes), which are expected to lose functionality when fused to membrane proteins. Furthermore, EV membrane proteins, such as tetraspanins, may be crucial for proper EV functioning, and influence binding, membrane fusion or signaling in recipient cells [4, 18]. Upon fusion with (targeting) proteins, the functionality of these natural EV constituents may be compromised. Such issues may be avoided when introducing new proteins onto EV membranes via GPI-anchors.

Furthermore, we showed in the present study that EV binding to EGFR-overexpressing cells dramatically increased upon display of GPI-anchored EGa1, both under static and flow conditions. We hypothesize that EV cell binding under flow conditions better represents in vivo physiology than cell binding under static conditions. *In vitro* experiments are often performed under static conditions, which potentially leads to improbable and non-specific interactions between EVs and cells. Such experiments may poorly translate to *in vivo* behavior of EVs, given that flow of EV-containing body fluids may significantly impact the exposure of EVs to their target tissue and affect their functionality. In this study EVs were perfused over

cells in a perfusion chamber with a shear rate of 82.5 s^{-1}, resembling a typical venous shear rate (20-200 s^{-1} [56]). EV association with A431 cells (visualized as immobilized EVs on cell surfaces) could be traced in real-time with a fluorescence microscope and quantified. It was observed that EV-DAF-EGa1 displayed enhanced association to EGFR-expressing cells under these conditions compared with control EVs and EV-DAF-R2, which could have major implications for their *in vivo* retention in tumor tissues.

Neuro2A EVs appeared to exert limited cell type specificity (illustrated by similar uptake kinetics for A431 and Neuro2A cells under static conditions), a phenomenon also reported for other EV types [57, 58]. Remarkably, under the conditions in our study, uptake of EGa1-displaying EVs by EGFR-overexpressing cells was unaltered compared with control EVs. These results indicate that EV binding to cells does not necessarily result in EV uptake. A possible explanation for this phenomenon could be that monovalent EGa1 nanobodies bind EGFR with high affinity, but do not trigger receptor clustering and internalization [59]. However, previous studies showed that when EGa1 nanobodies were grafted on the surface of liposomes, these liposomes promoted EGFR sequestration and were internalized by EGFR-expressing cells [37, 59]. Hence, it appears that uptake of EGa1-displaying nanoparticles is only triggered when the nanobody surface density is sufficient to promote receptor clustering. It could be that in our study, the achieved nanobody surface density was too low, resulting in cell binding, but not uptake. To further investigate this phenomenon, we decorated the surface of isolated EVs with nanobodies using a chemical linker. Using this procedure, nanobodies are expected to be non-reducibly conjugated to all EV proteins with accessible primary amine groups, resulting in a high nanobody surface density and a smear pattern as analyzed by Western blotting (Supplementary Figure 3A). When cell association experiments were performed with nanobody-conjugated EVs, both cell binding and cell uptake of EGa1-conjugated EVs were greatly increased when compared with untreated EVs and EVs conjugated to R2 nanobodies (Supplementary Figure 3B-C). Interestingly, EV conjugation with R2 nanobodies *decreased* cell binding and uptake, illustrating that EV proteins containing exposed primary amines - whose functionality is likely to be compromised upon chemical conjugation with nanobodies - play a major role in these processes. Furthermore, these results suggest that nanobody surface density may affect internalization of nanobody-decorated EVs after binding. This phenomenon has also been described for other targeted nanoparticulate systems [60, 61], and may be worth taking into account when designing a strategy to introduce targeting ligands in EVs. Additionally, it is important to note that EVs may be directed away from their natural uptake route (e.g. clathrin-, caveolin-, or lipid raft-mediated endocytosis, macropinocytosis or phagocytosis [18]) through the use of targeting ligands, which may alter functional delivery of cargo such as mRNA or miRNA. However, whether this is the case remains unclear, given that mechanisms through which natural EVs functionally transfer their cargo are yet to be elucidated.

It is possible that GPI-anchored proteins are not evenly distributed among secreted EVs, but concentrated in specific subpopulations. The basal uptake of 'blank' EVs may in this

case have masked any beneficial effects of EGa1 anchorage on EVs in cell uptake experiments. Using TEM analysis, we could only detect nanobodies on the surface of a minority of the secreted EVs. This may be explained by technical limitations of the TEM technique, but it is conceivable that lipid rafts (and associated proteins) are predominantly incorporated in a subset of EVs. Previous studies have shown that detergent-resistance and membrane lipid order differ between subpopulations of EVs, supporting the idea that lipid rafts (which exhibit high resistance to detergents [62]) are not evenly distributed among EV subsets [63, 64]. Interestingly, it was recently suggested that lipid rafts may be involved in RNA loading of EVs [65], implying that RNA may be specifically enriched in lipid-raft containing subpopulations of EVs. Hence, expression of GPI-anchored targeting proteins on EVs may open possibilities for co-purification of both targeted and RNA-enriched EVs (e.g. using an immunoprecipitation procedure).

In conclusion, we developed a novel approach to display targeting ligands on EV surfaces. Through fusion with GPI-anchors, nanobodies were strongly enriched in EVs compared with parent cells, dramatically improving EV-cell interactions under static and flow conditions. GPI-anchoring may potentially be used as a versatile tool to incorporate a variety of proteins on EVs, including antibodies, enzymes, reporter proteins and (immune-stimulatory) signaling molecules.

Acknowledgements

The authors declare no competing financial interests. The work of SAAK, CGA, PV and RMS on cell-derived membrane vesicles is supported by a European Research Council starting grant (260627) "MINDS" in the FP7 ideas program of the European Union. The work of SRR is supported by a grant from the Academia Sinica Research Program on Nanoscience and Nanotechnology. PV is supported by a VENI Fellowship (# 13667) from the Netherlands Organisation for Scientific Research (NWO).

References

1. M. Colombo, G. Raposo, C. Thery, Biogenesis, secretion, and intercellular interactions of exosomes and other extracellular vesicles, *Annu Rev Cell Dev Biol*, 30 (2014) 255-289.
2. M. Yanez-Mo, P.R. Siljander, Z. Andreu, A.B. Zavec, F.E. Borras, E.I. Buzas*, et al.*, Biological properties of extracellular vesicles and their physiological functions, *J Extracell Vesicles*, 4 (2015) 27066.
3. S.M. van Dommelen, P. Vader, S. Lakhal, S.A. Kooijmans, W.W. van Solinge, M.J. Wood*, et al.*, Microvesicles and exosomes: opportunities for cell-derived membrane vesicles in drug delivery, *J Control Release*, 161 (2012) 635-644.
4. S.A. Kooijmans, P. Vader, S.M. van Dommelen, W.W. van Solinge, R.M. Schiffelers, Exosome mimetics: a novel class of drug delivery systems, *Int J Nanomedicine*, 7 (2012) 1525-1541.
5. R. van der Meel, M.H. Fens, P. Vader, W.W. van Solinge, O. Eniola-Adefeso, R.M. Schiffelers, Extracellular vesicles as drug delivery systems: lessons from the liposome field, *J Control Release*, 195 (2014) 72-85.
6. S. El-Andaloussi, I. Mager, X.O. Breakefield, M.J. Wood, Extracellular vesicles: biology and emerging therapeutic opportunities, *Nat Rev Drug Discov*, 12 (2013) 347-357.
7. G. Fuhrmann, I.K. Herrmann, M.M. Stevens, Cell-derived vesicles for drug therapy and diagnostics: Opportunities and challenges, *Nano Today*, 10 (2015) 397-409.
8. E.V. Batrakova, M.S. Kim, Using exosomes, naturally-equipped nanocarriers, for drug delivery, *J Control Release*, 219 (2015) 396-405.
9. B. Gyorgy, M.E. Hung, X.O. Breakefield, J.N. Leonard, Therapeutic applications of extracellular vesicles: clinical promise and open questions, *Annu Rev Pharmacol Toxicol*, 55 (2015) 439-464.
10. T. Lener, M. Gimona, L. Aigner, V. Borger, E. Buzas, G. Camussi*, et al.*, Applying extracellular vesicles based therapeutics in clinical trials - an ISEV position paper, *J Extracell Vesicles*, 4 (2015) 30087.
11. L. Alvarez-Erviti, Y. Seow, H. Yin, C. Betts, S. Lakhal, M.J. Wood, Delivery of siRNA to the mouse brain by systemic injection of targeted exosomes, *Nat Biotechnol*, 29 (2011) 341-345.
12. K. Tang, Y. Zhang, H. Zhang, P. Xu, J. Liu, J. Ma*, et al.*, Delivery of chemotherapeutic drugs in tumour cell-derived microparticles, *Nat Commun*, 3 (2012) 1282.
13. V. Gujrati, S. Kim, S.H. Kim, J.J. Min, H.E. Choy, S.C. Kim*, et al.*, Bioengineered bacterial outer membrane vesicles as cell-specific drug-delivery vehicles for cancer therapy, *ACS Nano*, 8 (2014) 1525-1537.
14. S. Ohno, M. Takanashi, K. Sudo, S. Ueda, A. Ishikawa, N. Matsuyama*, et al.*, Systemically Injected Exosomes Targeted to EGFR Deliver Antitumor MicroRNA to Breast Cancer Cells, *Mol Ther*, 21 (2013) 185-191.
15. J.M. Cooper, P.B. Wiklander, J.Z. Nordin, R. Al-Shawi, M.J. Wood, M. Vithlani*, et al.*, Systemic exosomal siRNA delivery reduced alpha-synuclein aggregates in brains of transgenic mice, *Mov Disord*, 29 (2014) 1476-1485.
16. Y. Tian, S. Li, J. Song, T. Ji, M. Zhu, G.J. Anderson*, et al.*, A doxorubicin delivery platform using engineered natural membrane vesicle exosomes for targeted tumor therapy, *Biomaterials*, 35 (2014) 2383-2390.
17. S.A.A. Kooijmans, L.A.L. Fliervoet, R. van der Meel, M.H.A.M. Fens, H.F.G. Heijnen, P.M.P. van Bergen en Henegouwen*, et al.*, PEGylated and targeted extracellular vesicles display enhanced cell specificity and circulation time, *Journal of Controlled Release*, 224 (2016) 77-85.

18. L.A. Mulcahy, R.C. Pink, D.R. Carter, Routes and mechanisms of extracellular vesicle uptake, *J Extracell Vesicles*, 3 (2014) 24641.

19. M.E. Hung, J.N. Leonard, Stabilization of exosome-targeting peptides via engineered glycosylation, *J Biol Chem*, 290 (2015) 8166-8172.

20. T. Smyth, K. Petrova, N.M. Payton, I. Persaud, J.S. Redzic, M.W. Graner, *et al.*, Surface functionalization of exosomes using click chemistry, *Bioconjug Chem*, 25 (2014) 1777-1784.

21. M. Wang, S. Altinoglu, Y.S. Takeda, Q. Xu, Integrating Protein Engineering and Bioorthogonal Click Conjugation for Extracellular Vesicle Modulation and Intracellular Delivery, *PLoS One*, 10 (2015) e0141860.

22. R. Wubbolts, R.S. Leckie, P.T. Veenhuizen, G. Schwarzmann, W. Mobius, J. Hoernschemeyer, *et al.*, Proteomic and biochemical analyses of human B cell-derived exosomes. Potential implications for their function and multivesicular body formation, *J Biol Chem*, 278 (2003) 10963-10972.

23. A. de Gassart, C. Geminard, B. Fevrier, G. Raposo, M. Vidal, Lipid raft-associated protein sorting in exosomes, *Blood*, 102 (2003) 4336-4344.

24. H. Rabesandratana, J.P. Toutant, H. Reggio, M. Vidal, Decay-accelerating factor (CD55) and membrane inhibitor of reactive lysis (CD59) are released within exosomes during In vitro maturation of reticulocytes, *Blood*, 91 (1998) 2573-2580.

25. C.P. Chen, Y.T. Hsieh, Z.M. Prijovich, H.Y. Chuang, K.C. Chen, W.C. Lu, *et al.*, ECSTASY, an adjustable membrane-tethered/soluble protein expression system for the directed evolution of mammalian proteins, *Protein Eng Des Sel*, 25 (2012) 367-375.

26. W.C. Chou, K.W. Liao, Y.C. Lo, S.Y. Jiang, M.Y. Yeh, S.R. Roffler, Expression of chimeric monomer and dimer proteins on the plasma membrane of mammalian cells, *Biotechnol Bioeng*, 65 (1999) 160-169.

27. T.L. Cheng, S. Roffler, Membrane-tethered proteins for basic research, imaging, and therapy, *Med Res Rev*, 28 (2008) 885-928.

28. H. Revets, P. De Baetselier, S. Muyldermans, Nanobodies as novel agents for cancer therapy, *Expert Opin Biol Ther*, 5 (2005) 111-124.

29. F. Ciardiello, G. Tortora, EGFR antagonists in cancer treatment, *N Engl J Med*, 358 (2008) 1160-1174.

30. N. Tebbutt, M.W. Pedersen, T.G. Johns, Targeting the ERBB family in cancer: couples therapy, *Nat Rev Cancer*, 13 (2013) 663-673.

31. J.Z. Nordin, Y. Lee, P. Vader, I. Mager, H.J. Johansson, W. Heusermann, *et al.*, Ultrafiltration with size-exclusion liquid chromatography for high yield isolation of extracellular vesicles preserving intact biophysical and functional properties, *Nanomedicine*, 11 (2015) 879-883.

32. H.F. Heijnen, A.E. Schiel, R. Fijnheer, H.J. Geuze, J.J. Sixma, Activated platelets release two types of membrane vesicles: microvesicles by surface shedding and exosomes derived from exocytosis of multivesicular bodies and alpha-granules, *Blood*, 94 (1999) 3791-3799.

33. E.G. Hofman, M.O. Ruonala, A.N. Bader, D. van den Heuvel, J. Voortman, R.C. Roovers, *et al.*, EGF induces coalescence of different lipid rafts, *J Cell Sci*, 121 (2008) 2519-2528.

34. K.R. Schmitz, A. Bagchi, R.C. Roovers, P.M. van Bergen en Henegouwen, K.M. Ferguson, Structural evaluation of EGFR inhibition mechanisms for nanobodies/VHH domains, *Structure*, 21 (2013) 1214-1224.

35. L.G. Frenken, R.H. van der Linden, P.W. Hermans, J.W. Bos, R.C. Ruuls, B. de Geus, *et al.*, Isolation of antigen specific llama VHH antibody fragments and their high level secretion by Saccharomyces cerevisiae, *J Biotechnol*, 78 (2000) 11-21.

36. S. Oliveira, G.A. van Dongen, M. Stigter-van Walsum, R.C. Roovers, J.C. Stam, W. Mali*, et al.*, Rapid visualization of human tumor xenografts through optical imaging with a near-infrared fluorescent anti-epidermal growth factor receptor nanobody, *Mol Imaging*, 11 (2012) 33-46.

37. R. van der Meel, S. Oliveira, I. Altintas, R. Haselberg, J. van der Veeken, R.C. Roovers*, et al.*, Tumor-targeted Nanobullets: Anti-EGFR nanobody-liposomes loaded with anti-IGF-1R kinase inhibitor for cancer treatment, *J Control Release*, 159 (2012) 281-289.

38. S. Udenfriend, K. Kodukula, How glycosylphosphatidylinositol-anchored membrane proteins are made, *Annu Rev Biochem*, 64 (1995) 563-591.

39. I. Levental, M. Grzybek, K. Simons, Greasing their way: lipid modifications determine protein association with membrane rafts, *Biochemistry*, 49 (2010) 6305-6316.

40. C. Thery, S. Amigorena, G. Raposo, A. Clayton, Isolation and characterization of exosomes from cell culture supernatants and biological fluids, *Curr Protoc Cell Biol*, Chapter 3 (2006) Unit 3.22.

41. C. Thery, M. Ostrowski, E. Segura, Membrane vesicles as conveyors of immune responses, *Nat Rev Immunol*, 9 (2009) 581-593.

42. J. Li, Y. Lee, H.J. Johansson, I. Mager, P. Vader, J.Z. Nordin*, et al.*, Serum-free culture alters the quantity and protein composition of neuroblastoma-derived extracellular vesicles, *J Extracell Vesicles*, 4 (2015) 26883.

43. A. Montecalvo, A.T. Larregina, W.J. Shufesky, D. Beer Stolz, M.L. Sullivan, J.M. Karlsson*, et al.*, Mechanism of transfer of functional microRNAs between mouse dendritic cells via exosomes, *Blood*, 119 (2012) 756-766.

44. F. Zhang, S. Wang, L. Yin, Y. Yang, Y. Guan, W. Wang*, et al.*, Quantification of epidermal growth factor receptor expression level and binding kinetics on cell surfaces by surface plasmon resonance imaging, *Anal Chem*, 87 (2015) 9960-9965.

45. R.K. Jain, Barriers to drug delivery in solid tumors, *Sci Am*, 271 (1994) 58-65.

46. R.K. Jain, R.T. Tong, L.L. Munn, Effect of vascular normalization by antiangiogenic therapy on interstitial hypertension, peritumor edema, and lymphatic metastasis: insights from a mathematical model, *Cancer Res*, 67 (2007) 2729-2735.

47. D. Ozturk, S. Yonucu, D. Yilmaz, M.B. Unlu, Influence of vascular normalization on interstitial flow and delivery of liposomes in tumors, *Phys Med Biol*, 60 (2015) 1477-1496.

48. C.P. Lai, O. Mardini, M. Ericsson, S. Prabhakar, C.A. Maguire, J.W. Chen*, et al.*, Dynamic biodistribution of extracellular vesicles in vivo using a multimodal imaging reporter, *ACS Nano*, 8 (2014) 483-494.

49. B. Fevrier, D. Vilette, F. Archer, D. Loew, W. Faigle, M. Vidal*, et al.*, Cells release prions in association with exosomes, *Proc Natl Acad Sci U S A*, 101 (2004) 9683-9688.

50. I. Del Conde, C.N. Shrimpton, P. Thiagarajan, J.A. Lopez, Tissue-factor-bearing microvesicles arise from lipid rafts and fuse with activated platelets to initiate coagulation, *Blood*, 106 (2005) 1604-1611.

51. S. Staubach, H. Razawi, F.G. Hanisch, Proteomics of MUC1-containing lipid rafts from plasma membranes and exosomes of human breast carcinoma cells MCF-7, *Proteomics*, 9 (2009) 2820-2835.

52. K. Laulagnier, C. Motta, S. Hamdi, S. Roy, F. Fauvelle, J.F. Pageaux*, et al.*, Mast cell- and dendritic cell-derived exosomes display a specific lipid composition and an unusual membrane organization, *Biochem J*, 380 (2004) 161-171.

53. S.S. Tan, Y. Yin, T. Lee, R.C. Lai, R.W. Yeo, B. Zhang*, et al.*, Therapeutic MSC exosomes are derived from lipid raft microdomains in the plasma membrane, *J Extracell Vesicles*, 2 (2013).

54. K. Trajkovic, C. Hsu, S. Chiantia, L. Rajendran, D. Wenzel, F. Wieland, *et al.*, Ceramide triggers budding of exosome vesicles into multivesicular endosomes, *Science*, 319 (2008) 1244-1247.

55. C. Thery, A. Regnault, J. Garin, J. Wolfers, L. Zitvogel, P. Ricciardi-Castagnoli, *et al.*, Molecular characterization of dendritic cell-derived exosomes. Selective accumulation of the heat shock protein hsc73, *J Cell Biol*, 147 (1999) 599-610.

56. M.H. Kroll, J.D. Hellums, L.V. McIntire, A.I. Schafer, J.L. Moake, Platelets and shear stress, *Blood*, 88 (1996) 1525-1541.

57. D. Zech, S. Rana, M.W. Buchler, M. Zoller, Tumor-exosomes and leukocyte activation: an ambivalent crosstalk, *Cell Commun Signal*, 10 (2012) 37.

58. K.J. Svensson, H.C. Christianson, A. Wittrup, E. Bourseau-Guilmain, E. Lindqvist, L.M. Svensson, *et al.*, Exosome uptake depends on ERK1/2-heat shock protein 27 signaling and lipid Raft-mediated endocytosis negatively regulated by caveolin-1, *J Biol Chem*, 288 (2013) 17713-17724.

59. S. Oliveira, R.M. Schiffelers, J. van der Veeken, R. van der Meel, R. Vongpromek, P.M. van Bergen En Henegouwen, *et al.*, Downregulation of EGFR by a novel multivalent nanobody-liposome platform, *J Control Release*, 145 (2010) 165-175.

60. Y. Zhong, F. Meng, C. Deng, Z. Zhong, Ligand-directed active tumor-targeting polymeric nanoparticles for cancer chemotherapy, *Biomacromolecules*, 15 (2014) 1955-1969.

61. K.G. Reuter, J.L. Perry, D. Kim, J.C. Luft, R. Liu, J.M. DeSimone, Targeted PRINT Hydrogels: The Role of Nanoparticle Size and Ligand Density on Cell Association, Biodistribution, and Tumor Accumulation, *Nano Lett*, 15 (2015) 6371-6378.

62. D.A. Brown, E. London, Functions of lipid rafts in biological membranes, *Annu Rev Cell Dev Biol*, 14 (1998) 111-136.

63. X. Osteikoetxea, B. Sodar, A. Nemeth, K. Szabo-Taylor, K. Paloczi, K.V. Vukman, *et al.*, Differential detergent sensitivity of extracellular vesicle subpopulations, *Org Biomol Chem*, 13 (2015) 9775-9782.

64. X. Osteikoetxea, A. Balogh, K. Szabo-Taylor, A. Nemeth, T.G. Szabo, K. Paloczi, *et al.*, Improved characterization of EV preparations based on protein to lipid ratio and lipid properties, *PLoS One*, 10 (2015) e0121184.

65. T. Janas, M.M. Janas, K. Sapon, Mechanisms of RNA loading into exosomes, *FEBS Lett*, 589 (2015) 1391-1398.

Supplementary Methods

Chemical conjugation of nanobodies with EVs

EGa1 and R2 Myc-tagged nanobodies were expressed in BL21 Star (DE3)pLysS chemically competent E. Coli (Invitrogen) and purified as described elsewhere [17]. Protected sulfhydryl groups were introduced in nanobodies by reaction with SATA as previously described [17, 37]. EVs were isolated from Neuro2A cells using a differential centrifugation protocol. Cells were seeded in medium depleted from EVs by overnight centrifugation at 100 000g, and allowed to secrete EVs for 72 hours. Conditioned medium was centrifuged at 300g and 2000g for 10 min at 4°C to remove cells and debris, respectively, and filtered through 0.22 µm Steritop filters (Merck Millipore) to remove large vesicles and debris. EVs were pelleted at 100 000g for 70 min at 4°C, resuspended in PBS, and pelleted again at 100 000g for 70 min. EVs were resuspended in 100-200 µL PBS, and EV aggregates were removed by centrifugation at 1000g for 10 min. For cell association studies, EVs were labeled with 0.125 µg/µL Calcein AM (Molecular Probes) in 0.5% DMSO for 1.5 hours at 37°C, or with 3.75 µM PKH26 (Sigma-Aldrich) in 50% Diluent C for 5 min at room temperature. Immediately after labeling, EVs were purified from unbound label by Sepharose CL-4B size exclusion chromatography and concentrated on 100 kD Vivaspin ultrafiltration tubes. EV protein concentrations were quantified by MicroBCA Protein Assay, and EVs were decorated with nanobodies using sulfo-EMCS (Thermo Fisher Scientific) as a chemical linker. This linker contains an NHS-ester and a maleimide reactive group, allowing it to react with accessible primary amines in EV proteins and with the sulfhydryl groups on the nanobodies. For reaction of the linker with EVs, sulfo-EMCS was dissolved in PBS, immediately mixed with EVs at a final linker concentration of 0.5 mg/mL and incubated for 30 min at room temperature. Simultaneously, SATA-modified nanobodies were deacetylated with deacetylation buffer (50 mM hydroxylamine, 2.5 mM EDTA, 50 mM HEPES, pH 7) for 60 min at room temperature. Nanobodies and EVs were purified from unconjugated sulfo-EMCS and deacetylation buffer using 0.5 mL Zeba Spin Desalting columns with a 7 kD MWCO (Thermo Fisher Scientific) according to the manufacturer's instructions. EVs and nanobodies were eluted in PBS, mixed in a nanobody:EV ratio of 1:75 (nmol:µg), and allowed to react for 30 min at room temperature. EVs were purified from unconjugated nanobodies by size exclusion chromatography and concentrated on 100 kD Vivaspin ultrafiltration tubes. The presence of nanobodies on the EVs was confirmed by Western Blot analysis using mouse anti-Myc antibodies (1:4000, clone 9E10, Sigma-Aldrich).

Supplementary Figures

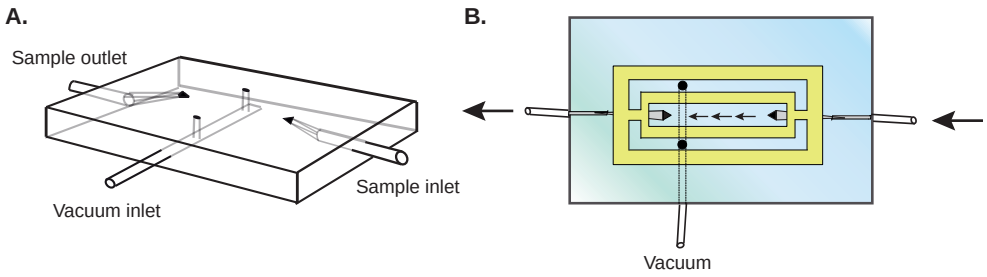

Supplementary Figure 1: Schematic presentation of perfusion chamber used in perfusion experiments. A. Perspex frame containing in- and outlets for samples (e.g. medium with EVs), and an inlet for a vacuum pump. B. Top view of perfusion chamber during perfusion experiments. A silicon sheet (yellow) with a thickness of 0.125 mm is mounted on the perspex frame, creating a flow channel of 2 x 30 mm (W x L) between sample in- and outlets. A glass coverslip with a near-confluent monolayer of cells is placed on top of the sheet and sealed by applying a vacuum over the vacuum inlet. The entire perfusion chamber is mounted on a fluorescence microscope for imaging and the sample outlet is connected to a syringe pump to generate flow in the direction of the arrows.

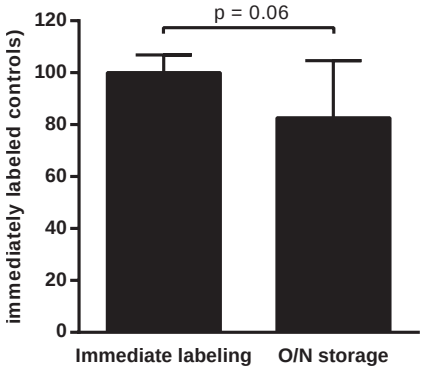

Supplementary Figure 2: Efficiency of EV labeling with CellTracker Deep Red dye tends to decrease with increased EV storage time prior to labeling. N2A EVs were labeled with CellTracker Deep Red dye immediately after isolation or after O/N storage (16 hours) at 4°C, and labeling efficiency was determined. Data are displayed as mean ± SD from 4 replicate experiments, and differences between groups were analyzed using an independent samples t test.

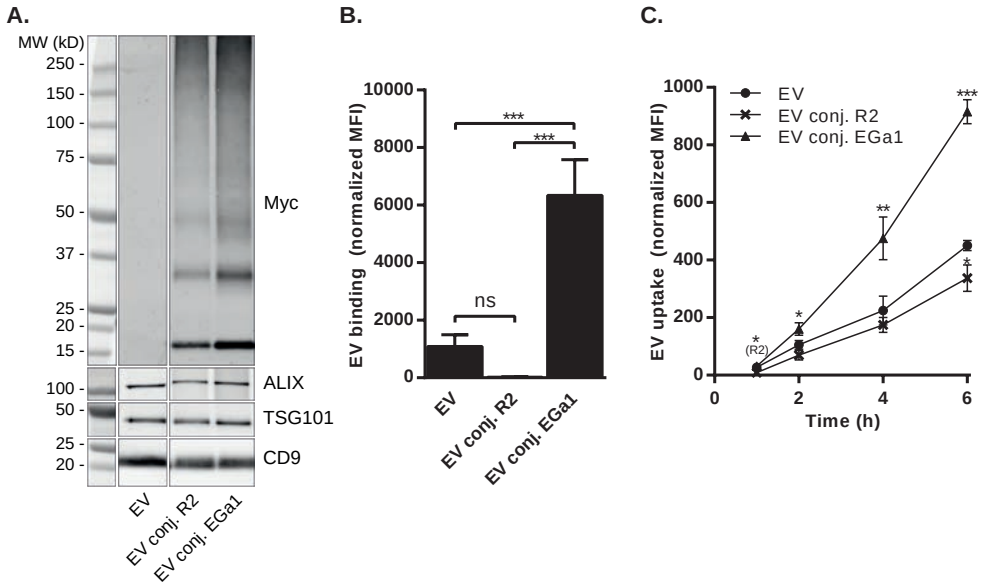

Supplementary Figure 3: Chemical conjugation of nanobodies to EVs strongly increases EV binding and uptake by A431 cells. R2 or EGa1 nanobodies were non-specifically conjugated to surface proteins of EVs using a chemical linker (EV conj. R2 and EV conj. EGa1, respectively) to generate EVs with a high nanobody surface density. A. Western blot analysis of nanobody density and EV markers in nanobody-conjugated EVs. Nanobodies (17 kD) contain a Myc tag and were visualized by anti-Myc antibodies. A smear pattern is observed after nanobody conjugation due to the formation of stable, non-reducible bonds between nanobodies and EV surface proteins with accessible reactive groups across a range of molecular weights. Binding of nanobody-conjugated calcein AM-labeled EVs to A431 cells for 1 hour at 4°C, as determined by flow cytometry. C. Uptake of PKH26-labeled nanobody-conjugated EVs by A431 cells for 1-6 hours at 37°C, as determined by flow cytometry. Data are displayed as mean ± SD and are representative of at least two replicate experiments. ns = not significant, * indicates $p < 0.05$, ** $p < 0.01$, and *** $p < 0.001$ compared with EV control (unless indicated otherwise) as determined by one-way ANOVA with Tukey post-hoc test.

CHAPTER 5

PEGylated and targeted extracellular vesicles display enhanced cell specificity and circulation time

S.A.A. Kooijmans[1], L.A.L. Fliervoet[2], R. van der Meel[1,3], M.H.A.M. Fens[1], H.F.G. Heijnen[1], P.M.P. van Bergen en Henegouwen[4], P. Vader[1], R.M. Schiffelers[1]

[1]Department of Clinical Chemistry and Haematology, University Medical Center Utrecht, Utrecht, The Netherlands; [2]Department of Pharmaceutics, Utrecht Institute for Pharmaceutical Sciences, University of Utrecht, Utrecht, The Netherlands ; [3]Department of Biochemistry and Molecular Biology, The University of British Columbia, Vancouver, British Columbia, Canada V6T 1Z3; [4]Division of Cell Biology, Department of Biology, Utrecht University, Utrecht, The Netherlands.

Journal of Controlled Release, 2016. 224, 77-85

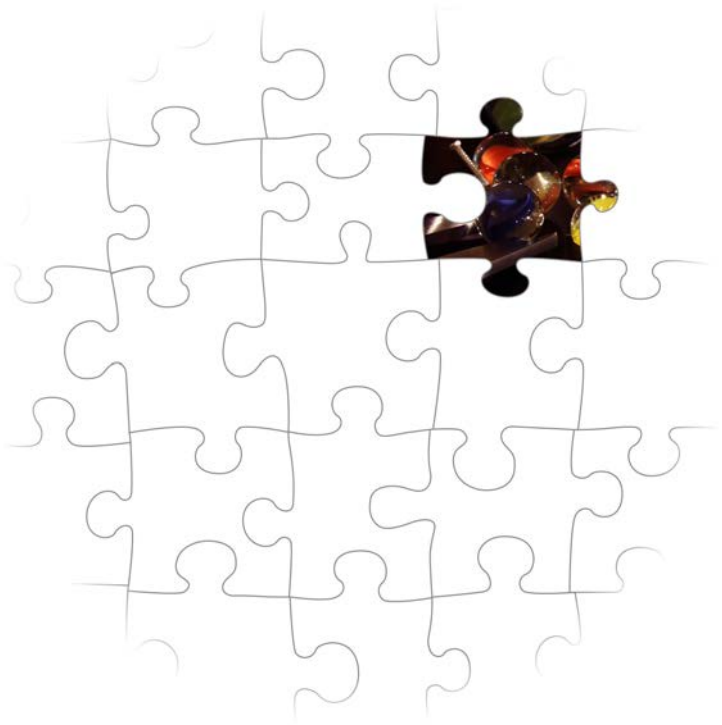

Abstract

Extracellular vesicles (EVs) are increasingly being recognized as candidate drug delivery systems due to their ability to functionally transfer biological cargo between cells. However, the therapeutic applicability of EVs may be limited due to a lack of cell-targeting specificity and rapid clearance of exogenous EVs from the circulation. In order to improve EV characteristics for drug delivery to tumor cells, we have developed a novel method for decorating EVs with targeting ligands conjugated to polyethylene glycol (PEG). Nanobodies specific for the epidermal growth factor receptor (EGFR) were conjugated to phospholipid (DMPE)-PEG derivatives to prepare nanobody-PEG-micelles. When micelles were mixed with EVs derived from Neuro2A cells or platelets, a temperature-dependent transfer of nanobody-PEG-lipids to the EV membranes was observed, indicative of a 'post-insertion' mechanism. This process did not affect EV morphology, size distribution, or protein composition. After introduction of PEG-conjugated control nanobodies to EVs, cellular binding was compromised due to the shielding properties of PEG. However, specific binding to EGFR-overexpressing tumor cells was dramatically increased when EGFR-specific nanobodies were employed. Moreover, whereas unmodified EVs were rapidly cleared from the circulation within 10 min after intravenous injection in mice, EVs modified with nanobody-PEG-lipids were still detectable in plasma for longer than 60 min post-injection. In conclusion, we propose post-insertion as a novel technique to confer targeting capacity to isolated EVs, circumventing the requirement to modify EV-secreting cells. Importantly, insertion of ligand-conjugated PEG-derivatized phospholipids in EV membranes equips EVs with improved cell specificity and prolonged circulation times, potentially increasing EV accumulation in targeted tissues and improving cargo delivery.

Introduction

Over the past decade extracellular vesicles (EVs) have increasingly gained attention as candidate drug delivery systems due to their unique properties. As extensively reviewed elsewhere [1-4], EVs are lipid bilayer-surrounded vesicles released by many, if not all, cell types in the body. They are heterogeneous in terms of protein, nucleic acid and lipid composition, with sizes ranging from 30 to 1000 nm. EVs can be subdivided in different classes based on intracellular origin, e.g. microvesicles (or ectosomes) are released through direct budding of the plasma membrane, while exosomes are released from endosomal compartments upon fusion with the plasma membrane [5, 6]. EVs have been implicated in intercellular communication, and are believed to be capable of functionally transferring condensed packages of biological cargo (e.g. miRNA, mRNA and proteins) to target cells and tissues [1, 7]. These characteristics make EVs ideal candidate delivery systems for therapeutic nucleic acids (e.g. siRNA and miRNA). Hence, it is not surprising that therapeutic applications of EVs are a topic of intense investigation, and the first clinical trials with EVs are emerging [8].

Although EVs harbor potential advantages for drug delivery over conventional drug delivery systems, such as biological tolerability and the ability to induce phenotypical changes in recipient cells [1, 9], major challenges for their therapeutic applicability remain. Due to their highly complex and variable composition, cell specificity and biological effects of EVs can be unpredictable [10]. These could manifest as off-target effects when EVs are employed as drug carriers. To limit such effects and promote therapeutic efficacy, EVs may be equipped with targeting ligands and appropriate cargos. Such modifications have been explored in several studies, which showed successful targeted drug delivery using EVs and underlined their therapeutic potential [11-16].

A popular strategy to decorate EVs with targeting ligands is the transfection of EV-producing cells to drive expression of targeting moieties fused with EV membrane proteins, such as Lamp2b [11, 17, 18]. Although effective, such strategies are hampered by the requirement to modify producer cells, which often is time-consuming and challenging, especially when using primary cells. In addition, some targeting ligands are prone to improper expression and degradation, which limits their functional display on EVs [17]. Moreover, while decoration of EVs with targeting ligands usually improves target cell interactions, it does not necessarily prevent interactions with other, non-target cells, allowing nonspecific uptake and related off-target effects. To overcome such issues, we here propose a novel method to provide stealth as well as tumor cell-targeting characteristics to pre-isolated EVs, based on the 'post-insertion' method previously applied to functionalize liposomes [19]. The hydrophilic polymer polyethylene glycol (PEG) is well known to shield nanoparticles from interactions with plasma proteins and improve circulation time [20, 21]. We hypothesized that these features would be beneficial for EV-based drug delivery systems, given that exogenously administered EVs have been described to be rapidly cleared from the circulation by the reticulo-endothelial system (RES) [22], limiting their accumulation in target tissue. Furthermore, we employed nanobodies

against the epidermal growth factor receptor (EGFR) as model targeting ligands. This receptor is overexpressed in a range of solid tumors and is an established target for cancer therapy with several inhibitors used in the clinic [23, 24]. Nanobodies are single variable domains derived from the heavy chains (VH) of *Camelidae* heavy (H) chain antibodies, and are therefore also termed VHHs or single-domain antibodies (sdAbs) [25]. These 15 kD fragments possess the full antigen-binding capacity of the original antibody, and have other favorable characteristics compared with conventional antibodies, such as high solubility and resistance to extreme thermal and chemical conditions [26, 27]. Here, we evaluated how introduction of polyethylene glycol (PEG)-conjugated nanobodies onto EVs *via* post-insertion affects EV characteristics, *in vitro* interactions with tumor cells, and *in vivo* circulation time and tissue distribution in tumor-bearing mice.

Materials and methods

Materials

1,2-Distearoyl-sn-glycero-3-phosphoethanolamine (DSPE)-PEG, MW 2000 and 1,2-Dimyristoyl-sn-glycero-3-phosphoethanolamine (DMPE)-PEG-maleimide, MW 3400 were purchased from Nanocs Inc. (New York, USA). 1,1″-dioctadecyl-3,3, 3″,3″-tetramethylindotricarbocyanine iodide (DiR), MicroBCA Protein Assay Kit, *N*-succinimidyl S-acetylthioacetate (SATA) and CellTracker Deep Red dye were obtained from Thermo Fisher Scientific (Waltham, USA). Sepharose CL-4B was ordered from Sigma-Aldrich (Steinheim, Germany). Sterile cell culture materials were purchased from Greiner Bio-One (Alphen aan de Rijn, The Netherlands). pET28a vectors encoding EGa1 and R2 Myc-tagged nanobodies were kindly provided by Dr. S. Oliveira (Department of Biology, Utrecht University, Utrecht, The Netherlands).

Nanobody production

R2 and EGa1 nanobodies were expressed and purified as described previously [28], with minor modifications. pET28a expression vectors, containing a pelB leader sequence followed by a nanobody sequence with C-terminal c-Myc- and His_6-tags for detection and purification, respectively, were introduced in BL21 Star (DE3)pLysS chemically competent E. coli (Thermo Fisher Scientific). Cells were grown overnight in shaking cultures at 37°C in 2xYT medium supplemented with 2% (w/v) glucose and selection antibiotics. A 5L Bioflo 115 fermentor (Eppendorf, Germany) with ZYP-5052 auto induction medium (described in [29]) was inoculated with the overnight culture and cells were grown for several hours at 37°C until log phase was observed. The culture was incubated for 22 hours at 22°C, and protein was extracted from the periplasmic space with lysis buffer (25 mM HEPES, 0.5M NaCl, 1µg/mL DNase I, 10 mM $MgCl_2$, pH 7.8) in three freeze-thaw cycles using liquid nitrogen. After removal of insoluble material by centrifugation at 10 000g and 4°C for 1 hour, nanobodies were extracted overnight

at 4°C with TALON Superflow IMAC resin (Clontech Laboratories, Inc). Nanobodies were eluted from the resin with elution buffer (25 mM HEPES, 0.5M NaCl, 500 mM imidazole) and further purified in HEPES-buffered saline (HBS) on an ÄKTA FPLC system (GE Healthcare Europe GmbH, Germany) coupled to a HiLoad 26/60 Superdex gel filtration column (GE Healthcare). Protein concentrations were measured by spectrophotometry at 280 nm, using molar extinction coefficients calculated via the online ProtParam tool (web.expasy.org/protparam/). Purity of the nanobodies was verified by PageBlue staining after SDS-PAGE.

Preparation of nanobody-PEG micelles

Reactive sulfhydryl groups were introduced to the nanobodies with SATA as described elsewhere [30]. Unconjugated SATA was removed using Zeba Spin desalting columns with a 7 kD MWCO (Thermo Fisher Scientific). DMPE-PEG-maleimide and DSPE-PEG were dissolved in a 1:1 molar ratio in HEPES buffer (10 mM HEPES, 135 mM NaCl, pH 7.4) for 15 min at 60°C to form micelles. After deprotection of the sulfhydryl groups, nanobodies were conjugated to the micelles in a 8.6:1000 molar ratio of nanobody:DMPE-PEG-maleimide overnight at 4°C. Unreacted maleimide groups were quenched by addition of a 20-fold molar excess of β-mercaptoethanol, and free nanobodies were removed by four washing steps on 100 kD MWCO Vivaspin tubes (Sartorius, UK). Traces of β-mercaptoethanol were removed by overnight dialysis against excess HBS in 10 kD Slide-A-Lyzer cassettes (Thermo Scientific). Micelles were redissolved at 60°C for 10 min, followed by sonication with 10 µm amplitude for 2x 5 sec in a Soniprep 150 sonicator (MSE, UK) to reduce micelle size and facilitate upstream separation from EVs. Concentration of nanobodies on the micelles was estimated using a MicroBCA Protein Assay according to the manufacturer's instructions. Micelles were stored at 4°C and used within 2 weeks.

Cell culture and EV isolation

Human epidermoid carcinoma cells (A431, ATCC, Manassas, USA) were cultured at 37˚C and 5% CO_2 in Dulbecco's Modified Eagle Medium (DMEM) supplemented with 10% fetal bovine serum (FBS) and 100 U/mL penicillin and 100 U/mL streptomycin. Mouse neuroblastoma cells (Neuro2A, ATCC) were maintained under the same conditions in Roswell Park Memorial Institute (RPMI) 1640 medium supplemented with 10% FBS and antibiotics. For EV production, Neuro2A cells were seeded at an appropriate density in EV-depleted medium (which contained FBS depleted from EVs by overnight centrifugation at 100 000g at 4°C). Cells were allowed to produce EVs and after 72h, when cells reached 90-95% confluency, EVs were isolated with a differential (ultra)centrifugation method as previously described [31]. The washed EV pellet after the final 100 000g step was resuspended in phosphate-buffered saline (PBS). EV aggregates resulting from ultracentrifugation were removed by centrifugation at 1000g for 10 min at 4°C. EV protein concentration was determined with a MicroBCA Protein Assay.

Introduction of nanobody-PEG-lipids on EVs using post-insertion

EVs were mixed with nanobody-PEG micelles in a 1:1 ratio (µg protein:µg protein) in a total volume of 100-150 µL and incubated in a GeneAmp PCR System 9700 thermocycler with heated lid for 2 hours at 40°C (unless stated otherwise). EV-micelle mixtures were cooled to 4°C and EVs were immediately purified from free micelles by size-exclusion chromatography.

Purification of EVs by size-exclusion chromatography

For purification of EVs from free nanobody-PEG micelles, Sepharose CL-4B (Sigma-Aldrich) was packed in a XK-26/40 column (GE Healthcare) according to manufacturer's instructions. A smaller column (XK-16/20) was employed for purification of EVs from fluorescent dyes. Column was connected to an ÄKTA pure system (GE Healthcare) which was maintained at 4°C and equilibrated with PBS. EV suspensions were injected and eluted fractions containing EVs (identified by UV absorbance at 280 nm) were pooled and concentrated using 100 kD MWCO Vivaspin tubes (Sartorius).

Western blot analysis

EV samples were mixed with sample buffer containing dithiothreitol (DTT), heated to 95˚C for 10 min and separated on 4-12% Bis-Tris polyacrylamide gels (Thermo Scientific). Proteins were electrotransferred to Immobilon-FL polyvinylidene difluoride (PVDF) membranes (Millipore). Membranes were blocked with 50% v/v Odyssey Blocking Buffer (LI-COR Biosciences) in Tris buffered saline (TBS). All immunolabeling was performed with 50% v/v Odyssey Blocking Buffer in TBS containing 0.1% Tween 20 (TBS-T). Primary antibodies were used overnight at 4°C and included rabbit anti-CD9 antibody (Abcam, clone EPR2949, 1:2500 dilution), rabbit anti-TSG101 (Abcam, ab30871, 1:1000 dilution), mouse anti-Alix (Abcam, clone 3A9, 1:1000 dilution), rabbit anti-EGFR (Cell Signaling Technology, clone D38B1, 1:1000 dilution) mouse anti-β-actin (Cell Signaling Technology, clone 8H10D10, 1:1000 dilution), and mouse anti-Myc (9E10 from MYC 1-9E10.2 hybridoma, ATCC, 1:4000). Secondary antibodies included Alexa Fluor 680-conjugated anti-rabbit antibodies (Thermo Fisher Scientific, A-21076, 1:7500 dilution) or IRDye 800CW anti-mouse antibodies (LI-COR Biosciences, 926-32212, 1:7500 dilution). Imaging was performed on an Odyssey Infrared Imager (LI-COR Biosciences, Leusden, the Netherlands) at 700 and 800 nm, respectively.

Immuno-electron microscopy

EVs in PBS were adsorbed to carbon-coated formvar grids, fixated in a mixture of 2% paraformaldehyde and 0.2% glutaraldehyde in 0.1 M phosphate buffer, and immunolabeled with mouse anti-Myc antibody (9E10, 1:100), followed by rabbit-anti-mouse IgG (Rockland, 610-4120, 1:250) and 10 nm Protein A gold (CMC, Utrecht, The Netherlands). Grids were counterstained with uranyl-oxalate and embedded in methyl cellulose uranyl-acetate [6]. Imaging was performed using a Tecnai T12 electron microscope (FEI, Eindhoven, The

Netherlands).

Nanoparticle tracking analysis

EV size distribution and concentration was determined with nanoparticle tracking analysis (NTA) using a Nanosight LM10-HS (NanoSight, UK). Before measurements, EVs were diluted to an appropriate dilution with sterile PBS (confirmed to be particle-free). Of each sample, 5 movies of 30 seconds were recorded using camera level 13, while temperature was maintained at 22°C. Data was analyzed with NTA Analytical Software suite version 2.3.

Cell binding assays

To evaluate the binding of EVs to EGFR-expressing cells, EVs were mixed with 10 µM CellTracker Deep Red dye (dissolved at 2 mM in dimethyl sulfoxide (DMSO)) and incubated for 1 hour at 37°C. EVs were purified from free dye using size-exclusion chromatography. If applicable, post-insertion was performed, followed by size-exclusion chromatography and determination of protein concentration. To determine whether differences in labeling efficiency existed among samples, fluorescence of all samples was analyzed in a black 96-well plate in a Spectramax M2 microplate reader (Molecular Devices, UK) at excitation 630 nm and emission 660 nm, and compared with corresponding protein concentrations. For binding assays, A431 and Neuro2A cells were trypsinized, resuspended in ice-cold culture medium and seeded in round-bottom 96-well plates at a density of 3×10^4 cells/well. EVs were mixed with the cells at a concentration of 8 µg/mL while cells were kept on ice to inhibit cellular uptake. After 1 hour, cells were collected by centrifugation at 500g and 4°C for 5 min. Medium was removed and cells were resuspended in ice-cold PBS with 0.3% bovine serum albumin (PBSA). This washing procedure was repeated twice and cells were resuspended in 0.2% formaldehyde in PBS. Mean fluorescence intensity of the cells was analyzed in a FACSCanto II flow cytometer (BD Biosciences, USA) and corrected for the autofluorescence of untreated cells.

In vivo circulation time and biodistribution

All animal experiments were performed with approval from the Utrecht Animal Welfare Body of the UMC Utrecht, and animal care was according to established guidelines. Sixty female Crl:NU-Foxn1^{nu} mice (20-25g) were obtained from Charles River International Laboratories, Inc. (Germany) with free access to water and a chlorophyll-reducing chow (2016S, Harlan Laboratories, The Netherlands) to reduce organ autofluorescence. To establish human tumor xenografts, A431 cells were trypsinized, counted and suspended in ice-cold PBS. Mice were subcutaneously injected with 100 µL containing 1×10^6 cells in the right flank. Tumor growth was monitored during approximately two weeks, using a caliper to measure tumor size. Tumor volume was calculated with the formula $V = (\pi/6)LS^2$, where L and S are the largest and smallest superficial diameters, respectively. When tumors reached a volume of 200-300 mm^3, mice were injected intravenously in the tail vein with 2.5 µg DiR-labeled EVs in

100 µL PBS. EVs were labeled by mixing EV suspension with 5 µM DiR (using a DiR stock of 1 mM in DMSO), followed by incubation for 1 hour at 22°C. EVs were purified from free DiR with size-exclusion chromatography, modified with post-insertion, and purified again. To exclude the presence of aggregates, EVs were filtered through 0.45 µm syringe filters (Millipore). EV protein concentration and number was quantified with MicroBCA Protein Assay and NTA, respectively, before administration to mice. Blood samples were collected in EDTA anti-coagulated tubes by submandibular vein punctures at 1, 10, 20 and 30 min post-injection (n = 3 per time point). Mice were sacrificed 60 and 240 min post-injection by cervical dislocation, and additional blood samples were collected via heart puncture. Blood samples were centrifuged for 10 min at 2000g and 4°C and platelet-poor plasma was collected and stored at -80°C. For analysis of circulation times, 35 µL of each plasma sample was transferred to a clear 384-well plate and analyzed by an Odyssey Infrared Imager at 800 nm. Quantification of fluorescent signals was performed using Odyssey software (LI-COR Biosciences). EV plasma concentrations were calculated using a standard curve of corresponding EVs spiked in normal mouse plasma. To evaluate EV biodistribution, mouse organs were collected 60 and 240 min post-injection and imaged using a Pearl Impulse Imager (LI-COR Biosciences) at the 800 nm channel. Images were analyzed by Pearl Cam software.

Statistical data analysis

When applicable, statistical data analysis was performed using IBM SPSS Statistics, version 21. Multiple-group comparisons were performed using one-way ANOVA with Tukey post-hoc tests.

Results

Introduction of nanobody-PEG-lipids onto extracellular vesicles via post-insertion

The nanobody EGa1 has previously been described as a high-affinity ligand for EGFR, without activating the receptor [32]. R2 is a nanobody raised against the azo-dye Reactive Red (RR6), which has been used as a non-targeting control nanobody in previous reports [28, 33]. In this work, we investigated whether these nanobodies could be conjugated to PEG-phospholipid micelles, and subsequently introduced onto EVs using a post-insertion procedure (Figure 1). Nanobodies were first chemically modified with SATA reagent using a previously described method, to introduce sulfhydryl groups [30]. With this method, up to 8 SATA molecules (4-5 molecules on average) have been shown to be conjugated to a single nanobody molecule, without loss of affinity for the antigen [28]. The sulfhydryl groups allow nanobody conjugation to PEG-phospholipids (i.e. DMPE-PEG), which are functionalized with maleimide groups at the distal end of the PEG chains. Prior to conjugation, DMPE-PEG-maleimide was mixed with (non-reactive) DSPE-PEG at a 1:1 molar ratio and dissolved in an aqueous buffer to form micelles.

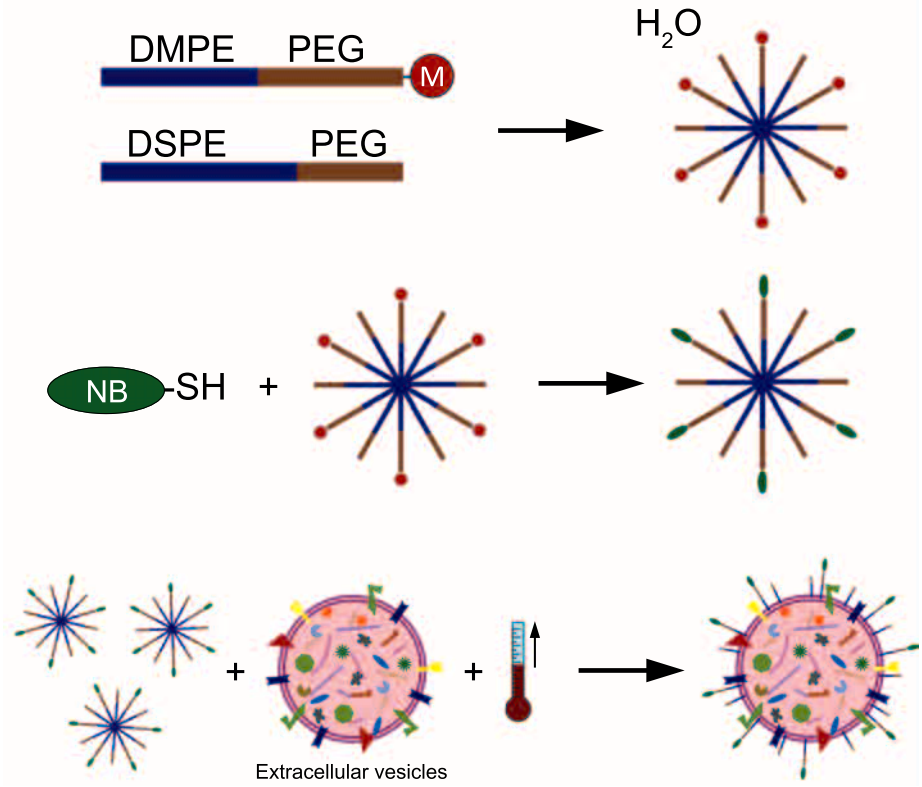

Figure 1: Schematic representation of the protocol by which isolated extracellular vesicles are decorated with nanobodies via PEG-micellar post-insertion. Firstly, micelles are formed by dissolving phospholipid (DMPE and DSPE)-PEG derivatives in an aqueous buffer. DMPE-PEG is functionalized with a maleimide group (M). Secondly, nanobodies (NB) which are modified with sulfhydryl groups (-SH) are conjugated to the micelles via stable thioether bonds. Thirdly, nanobody-PEG micelles are mixed with isolated EVs and incubated at elevated temperatures (i.e. 40°C), resulting in incorporation of nanobody-PEG-lipid into the vesicles. Picture is not drawn to scale.

Upon addition of nanobodies, stable non-reducible thioether bonds between nanobodies and the micelles are formed, increasing the molecular weight of the nanobodies as shown by Western Blotting (Figure 2A). Unmodified nanobodies typically displayed a single band at their molecular weight of 15-16 kD, which changed to a ladder-like pattern after conjugation to PEG-phospholipids. This pattern may be explained by the conjugation of one, two or multiple PEG-phospholipids (3.4 kD per unit) to each nanobody which alters their SDS-PAGE migration rate, and corresponds to previous reports in which nanobodies were attached to PEGylated liposomes [28, 30]. Band intensities suggested that most nanobodies were conjugated to one or two PEG-phospholipid chains, and this modification pattern was similar for R2 and EGa1 nanobodies. The attachment of DMPE-PEG-maleimide to these nanobodies is not expected to

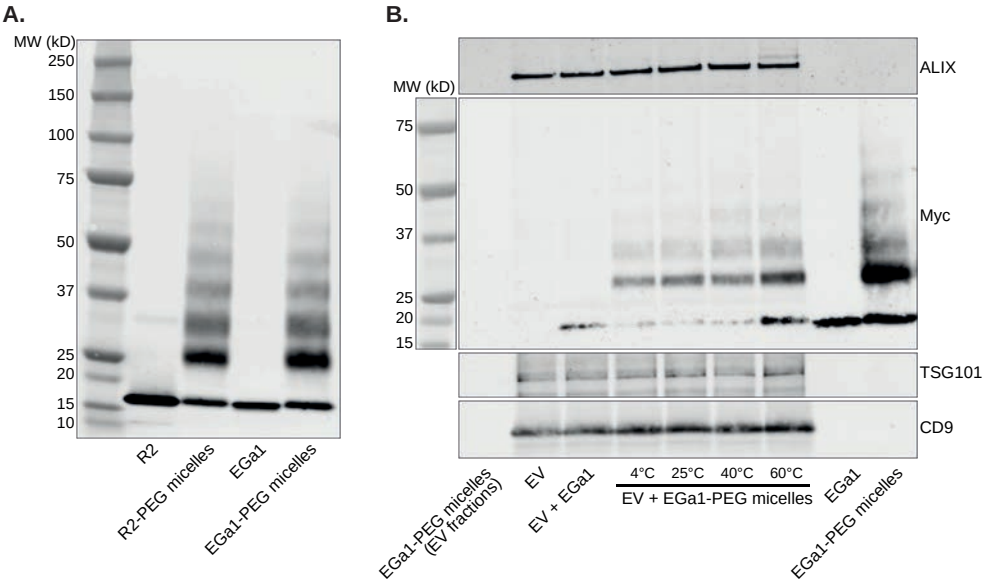
A.
MW (kD)
250
150
100
75
50
37
25
20
15
10
R2
R2-PEG micelles
EGa1
EGa1-PEG micelles
B.
MW (kD)
75
50
37
25
20
15
ALIX
Myc
TSG101
CD9
EGa1-PEG micelles (EV fractions)
EV
EV + EGa1
4°C
25°C
40°C
60°C
EV + EGa1-PEG micelles
EGa1
EGa1-PEG micelles

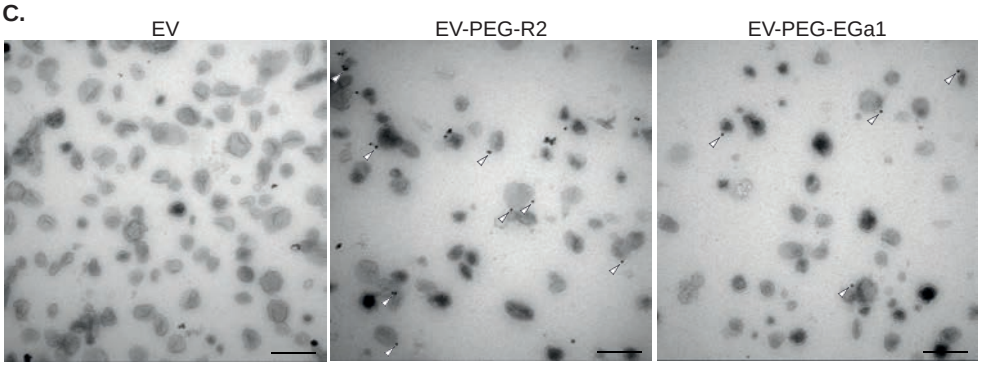
C.
EV
EV-PEG-R2
EV-PEG-EGa1

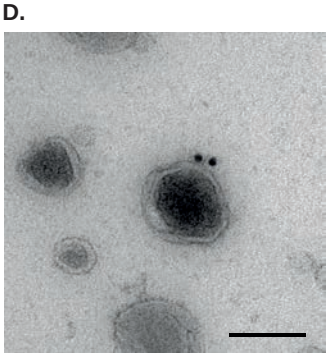
D.

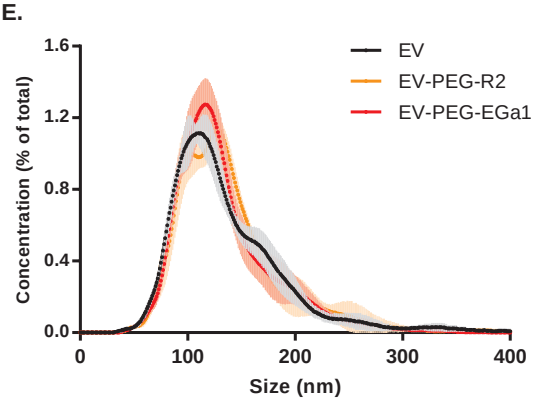
E.
1.6
1.2
0.8
0.4
0.0
Concentration (% of total)
0
100
200
300
400
Size (nm)
EV
EV-PEG-R2
EV-PEG-EGa1

Figure 2: EVs can be decorated with nanobodies using PEG-micellar post-insertion in a temperature dependent manner without loss of EV characteristics. A. Western blot analysis of Myc-tagged R2 and EGa1 nanobodies after coupling to DMPE-PEG-maleimide : DSPE-PEG (1:1) micelles. B. Western blot analysis of EV markers and nanobodies on Neuro2A EVs after post-insertion of EGa1-PEG micelles at various temperatures, and after purification with size-exclusion chromatography (SEC). Controls include concentrates of EV-fractions after SEC purification of EGa1-PEG micelles (first lane), untreated EVs (second lane), and EVs after incubation with EGa1 at 40°C (third lane). EGa1 and EGa1-PEG micelles were loaded as a reference. C. Transmission electron microscopy images of EVs before and after post-insertion with R2-PEG and EGa1-PEG micelles. Grids were immunogold labeled with anti-Myc antibodies (arrowheads indicate membrane-associated gold). Scale bars represent 200 nm. D. High-magnification transmission electron microscopy image of EVs after post-insertion with EGa1-PEG micelles. Scale bar represents 100 nm. E. Size distribution of EVs before and after post-insertion, as analyzed by Nanoparticle Tracking Analysis. Data is shown as mean ± SD of 5 replicate measurements.

compromise the interactions of the nanobodies with EGFR [28, 30]. We then studied whether these micelles could be used to decorate the surface of EVs with nanobodies *via* post-insertion. Post-insertion of PEG-lipids into liposomes has been shown to be a temperature-dependent process, in which the efficiency of lipid incorporation improves with increasing temperature [34-37]. To test whether this mechanism would also apply to EVs, EVs derived from Neuro2A cells were mixed with nanobody-PEG micelles and incubated for 2 hours at temperatures ranging from 4°C to 60°C. After incubation, EVs were purified from free micelles by size-exclusion chromatography (SEC) performed at 4°C. Nanobody incorporation was assessed by Western blotting (Figure 2B). When nanobody-PEG micelles in the absence of EVs were loaded onto the SEC column and typical EV fractions were analyzed, no nanobodies could be detected, indicating that the SEC method was suitable for complete separation of EVs from micelles (first lane in Figure 2B). When untreated EVs were applied to the column, the same fractions showed the presence of commonly used EV marker proteins ALIX, TSG101 and CD9 [1] (second lane in Figure 2B). Simple mixing of EVs with EGa1 nanobody resulted in a faint nanobody band in the EV sample, possibly due to co-elution of small nanobody aggregates. However, when EVs were incubated with EGa1-PEG micelles, nanobody incorporation was dramatically increased. The efficiency of nanobody incorporation improved with increasing temperature, indicative of a post-insertion mechanism. In addition, incorporation of nanobodies conjugated to multiple lipid-PEG chains seemed to be increased at higher temperatures. Incubation at 60°C, a common temperature for efficient post-insertion of PEG-lipids into liposomes [36, 38], resulted in the highest association of nanobodies with EVs. However, as could be expected at this temperature, EV proteins showed signs of aggregation (illustrated by the appearance of a double ALIX band in Figure 2B), and EV integrity and morphology were severely compromised as observed by electron microscopy (data not shown). Therefore, post-insertion at 40°C was found to be optimal for nanobody incorporation while preserving EV characteristics. To further evaluate the degree of nanobody incorporation at this temperature, EVs modified with R2-

PEG or EGa1-PEG micelles (EV-PEG-R2 and EV-PEG-EGa1, respectively) were analyzed by transmission electron microscopy (TEM) after immunogold labeling of the Myc-tags on the nanobodies (Figure 2C). Unmodified EVs showed a typical cup-shaped morphology as seen in negative stain EM and were negative for immunogold labeling, while clear labeling of the EV surface was observed after post-insertion. Based on TEM images it was estimated that using these labeling conditions at least 7-14% of EVs contained one or more nanobodies, with both R2 and EGa1 nanobodies being incorporated at similar efficiencies. Furthermore, based on analysis of immuno-TEM images and Western blot band intensities, it was estimated that PEGylated EVs contained on average 0.4-4 nanobodies per EV. This theoretically corresponds with approximately 50-500 DMPE-PEG molecules per EV, assuming that micellar nanobody-conjugated DMPE-PEG inserted at similar efficiency into EVs as unconjugated DMPE-PEG. In addition, morphology and electron density of EVs after post-insertion were similar to untreated EVs, suggesting that insertion of PEG-lipids in EVs did not compromise EV integrity (Figure 2D). This observation was supported by NTA data showing that EV size distribution was unaltered after post-insertion (Figure 2E).

We hypothesized that the principle of post-insertion could also be applicable to EVs from other sources. To test this, EVs were isolated from platelets from healthy donors and subjected to post-insertion with EGa1-PEG micelles at different temperatures. A similar temperature-dependent nanobody-PEG-lipid incorporation was observed for platelet EVs (with optimal incorporation at 40°C), while EV integrity was maintained (Supplementary Figure 1). These data illustrate that EVs with distinct characteristics (e.g. origin, size, morphology) can be decorated with nanobody-conjugated PEG-lipids using the post-insertion method.

In vitro cell association of EVs after post-insertion with nanobody-PEG-lipids

To study whether post-insertion of nanobody-PEG-lipids affects EV-target cell interactions, Neuro2A-derived fluorescently labeled EVs were post-inserted with R2-PEG or EGa1-PEG micelles at various temperatures and incubated with A431 and Neuro2A cells. A431 cells overexpress EGFR, while Neuro2A cells lack EGFR expression (Figure 3A). When post-insertion temperature was increased (improving nanobody-PEG-lipid incorporation), association of EVs with Neuro2A cells decreased, regardless of the nanobody used (Figure 3B). When post-insertion was performed at 60°C, cell binding was severely compromised, which is in line with previous observations showing loss of EV integrity after post-insertion at this temperature. In contrast, binding of EVs to A431 cells was significantly increased after post-insertion with EGa1-PEG micelles, while insertion with R2-PEG micelles slightly decreased cell association when compared with unmodified EVs. The increase in cell binding after post-insertion with EGa1-PEG micelles correlated with EGa1 incorporation efficiency at different post-insertion temperatures. In this assay, it was confirmed that insertion at 40°C was most efficient for optimal binding to A431 cells and this condition was therefore used in further experiments. Importantly, when EVs were incubated with EGa1 at 40°C in the absence of lipid-PEG anchors,

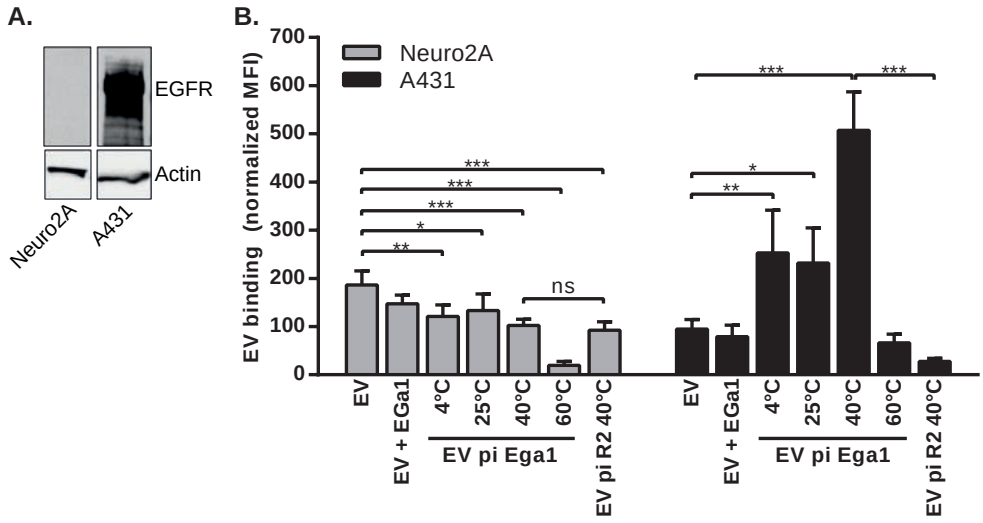

Figure 3: Post-insertion of EVs with R2-PEG micelles decreases EV binding to Neuro2A and A431 cells, while post-insertion with EGa1-PEG micelles specifically increases binding to EGFR-overexpressing A431 cells. A. Western blot analysis of EGFR expression in Neuro2A and A431 cells. Actin is shown as a loading control. B. Binding of CellTracker Deep Red-labeled Neuro2A EVs to Neuro2A and A431 cells, after post-insertion (pi) with R2-PEG or EGa1-PEG micelles at various temperatures, determined by flow cytometry. A control in which EVs were incubated with unconjugated EGa1 at 40°C and purified by size-exclusion chromatography was included (EV + Ega1). Representative data of at least three replicate experiments are shown, and data are displayed as mean ± SD. ns = not significant, * represents $p < 0.05$, ** $p < 0.01$, and *** $p < 0.001$ using one-way ANOVA with Tukey post-hoc test.

A431 cell binding was unaltered compared with unmodified controls. These data demonstrate that conjugation to lipid-PEG micelles is crucial for proper and functional anchoring of nanobodies to the surface of EVs.

In vivo circulation times and biodistribution of EVs after post-insertion with nanobody-PEG-lipids

Tissue distribution and related therapeutic efficacy of nanoparticles is largely determined by their circulation time [39]. PEGylation has been extensively applied to different types of nanoparticles in order to decrease deposition of plasma proteins on the particle surface, evade uptake by the RES and increase circulation time to boost their delivery potency [40, 41]. We hypothesized that the introduction of PEG chains *via* post-insertion in EVs could have a similar effect on the circulation time of these particles. Multiple studies have shown that the circulation time of intravenously administered EVs is short compared with PEGylated liposomes (which can display circulation half-lives of up to several days [20]), with the majority of EVs being cleared within 60 min post-injection [22, 42-45].

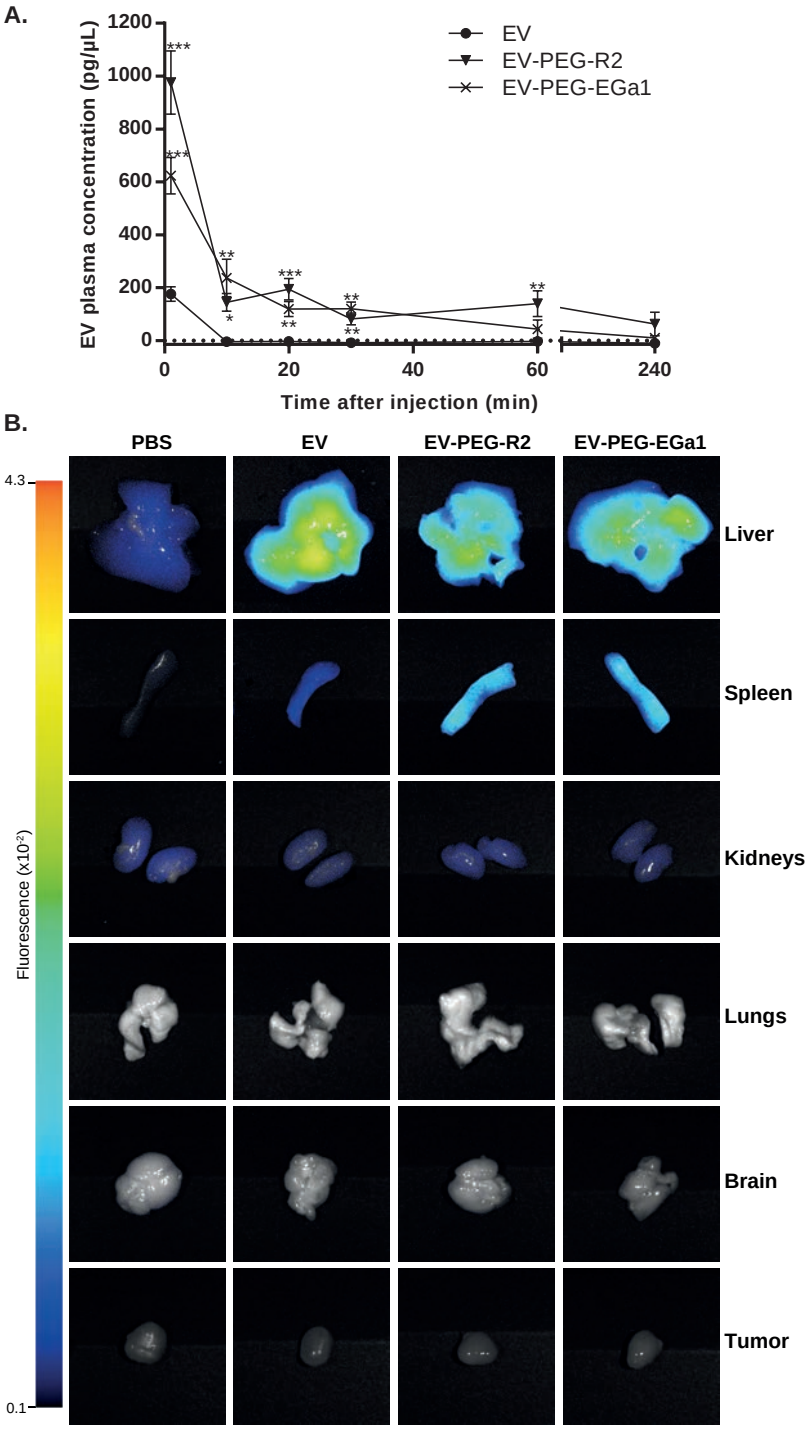
A.
EV plasma concentration (pg/µL)
1200
1000
800
600
400
200
0
0
20
40
60
240
Time after injection (min)
EV
EV-PEG-R2
EV-PEG-EGa1
B.
PBS
EV
EV-PEG-R2
EV-PEG-EGa1
Liver
Spleen
Kidneys
Lungs
Brain
Tumor
Fluorescence (x10⁻²)
4.3
0.1

Figure 4: Post-insertion with nanobody-PEG micelles increases EV circulation time and does not affect general biodistribution. A. Plasma concentration of DiR-labeled Neuro2A EVs before and after post-insertion with nanobody-PEG micelles, measured at several time points after i.v. injection of 2.5 µg of EVs in tail veins of Crl:NU-Foxn1^{nu} mice. Dotted line indicates lower detection threshold. B. Representative fluorescence/white field overlay Pearl Impulse images of organs from mice injected i.v. with 6 µg of DiR-labeled Neuro2A EVs, harvested 4 hours post-injection. Results in A are expressed as mean ± SEM, n=3-6. * represents $p < 0.05$, ** $p < 0.01$, and *** $p < 0.001$ compared with EV group at the same time point using one-way ANOVA with Tukey post-hoc test.

Neuro2A EVs were labeled with the lipophilic near-infrared dye DiR, purified, and subjected to post-insertion with R2-PEG and EGa1-PEG micelles. After removal of non-inserted DiR and micelles, 2.5 µg of EVs were intravenously administered to A431 tumor-bearing immunocompromised mice, and plasma samples were obtained at fixed time points after injection. It should be noted that the number of injected particles was comparable among EV samples, given that protein concentrations correlated well with particle concentrations as analyzed by NTA, regardless of the presence of PEG and nanobodies (2.5 µg of protein corresponded to approximately $2*10^{10}$ particles). To evaluate EV circulation time, DiR fluorescence signals in plasma were compared with a calibration curve of known concentrations of the injected batch of DiR-labeled EVs spiked in blank plasma. As expected, unmodified EVs were rapidly removed from blood plasma, and were below detection threshold 10 min post-injection (Figure 4A). In contrast, when EVs were PEGylated *via* post-insertion with R2-PEG or EGa1-PEG micelles, circulation time was significantly increased. Modified EVs were still detectable in plasma of all mice 60 min post-injection, and some mice even showed plasma DiR signal at 240 min post-injection. These kinetics were similar when a higher dose (i.e. 6 µg of EVs) was administered (Supplementary Figure 2). Such an increase in circulation time could have important implications for tumor accumulation. Organs of tumor-bearing mice intravenously injected with DiR-labeled EV were harvested and analyzed 4 hours post-injection (Figure 4B). EVs showed a typical nanoparticle-like biodistribution pattern, with the vast majority of the signal partitioning to the major RES organs liver and spleen. For other organs (kidneys, lungs, brain and tumor), DiR signals from EVs were below the detection limit. When organs were analyzed 1 hour post-injection, a similar pattern was observed (data not shown). This is in correspondence with previous reports on EV biodistribution [22, 46]. After post-insertion of the EVs with nanobody-PEG micelles, organ distribution was unaltered compared with unmodified EVs. A small increase in spleen compared with liver accumulation was observed, which may be due to increased exposure of the PEGylated EVs to circulating monocytes and macrophages [47].

Discussion

In this study we show that nanobodies can be introduced onto EVs from two distinct sources (Neuro2A tumor cells and platelets) using a PEG-micellar post-insertion strategy. While EVs

maintained their morphologic and biophysical characteristics, the insertion of nanobody-coupled PEG chains had important implications for *in vitro* and *in vivo* interactions of EVs with their environment. We found that EV-cell interactions *in vitro* were strongly reduced by PEG, but could be specifically recovered or even enhanced for EGFR-expressing cells when EGFR-binding nanobodies (EGa1) were attached to the distal end of PEG chains. This effect has also been described for synthetic PEGylated particles in previous studies [48, 49]. These data suggest that EVs were specifically redirected to EGFR-expressing tumor cells, while evading interactions with other cells. Given that EVs are reported to be readily taken up by a variety of cell types, and targeting specificity appears to be only subtle or unpredictable [10, 50, 51], combined PEGylation and targeting could be a valuable advancement towards the use of EVs as cell- or tissue-specific drug carriers. Evasion of uptake by non-targeted cells could minimize the occurrence of off-target effects and promote therapeutic efficacy. However, PEGylation has been described to impede the escape of nanoparticles from endosomal compartments after internalization, resulting in lysosomal degradation instead of functional delivery of the cargo (e.g. therapeutic nucleic acids) [52-54]. Furthermore, PEGylated EVs, targeted with EGa1 nanobodies, would be expected to be taken up via EGFR-dependent endocytosis [30], while their natural counterparts may be taken up via other routes (e.g. lipid-raft mediated endocytosis or macropinocytosis [10]). On the other hand, the present study shows that the post-insertion procedure is relatively mild, and does not noticeably affect EV integrity or protein composition. It is therefore conceivable that the potency of EVs to functionally deliver their cargo is retained to some extent after PEGylation. This is an important advantage of EVs compared with their synthetic counterparts (i.e. liposomes), which are often characterized by poor intracellular delivery efficiency, which further declines upon PEGylation [39, 55, 56]. Whether PEGylated and retargeted EVs can still promote functional cargo delivery through their unique composition remains to be elucidated and may be a subject for further studies.

The RES has been shown to be responsible for the clearance of the majority of nanoparticulate systems [20, 57, 58], and has also been implicated in the clearance of exogenously administered EVs [42]. We show that PEGylation of EVs results in a significant increase in circulation time in mice, suggesting that PEGylated EVs avoided plasma protein opsonization and phagocytosis by cells from the RES. We expected that this would result in an increased passive accumulation of these EVs in tumor tissue due to extravasation through leaky tumor vasculature (commonly known as the enhanced-permeability-and-retention (EPR) effect [20, 39, 59]). After successful migration into the tumor tissue, the presence of EGFR-specific nanobodies was hypothesized to promote retention of the EVs in the tumor tissue and facilitate entry into tumor cells. Unfortunately, EV PEGylation did not result in a detectable increase in tumor accumulation. This may be explained by technical detection limitations in this study. Stringent EV purification protocols in our study limited the EV dose that could be administered to 2-5*10^{10} particles/mouse, which is approximately 10-fold lower than reported in similar studies [46]. This, together with the fact that we assessed tumor accumulation at an

earlier time point (4h versus 24h after injection [46]), may have prevented any accumulated EV signal from reaching the detection threshold. The use of a reporter system with higher sensitivity than DiR, such as the recently described *Gaussia* luciferase-based reporter [22], may aid to better evaluate the effect of EV PEGylation on tumor accumulation.

It was roughly estimated that PEGylated EVs contained on average 50-500 PEG-DMPE molecules per EV. This is similar to the calculated amount of exterior-facing PEG chains in 100 nm unilamellar liposomes formulated with 0.5-1 mol% of PEG-lipids, assuming that these liposomes contain on average 80 000 lipids per vesicle. Despite this substantial PEG grafting density, which has been shown to confer shielding properties to liposomes [60, 61], EV plasma concentrations still steeply declined by > 80% within 10 min after injection. This could correspond with the observation that after post-insertion only a minority of all EVs contained nanobodies (and therefore PEG) as estimated using TEM. It could also be that only subtypes of EVs with a specific protein/lipid composition are amenable to post-insertion, that post-inserted lipids gradually partitioned out of the EV membranes, or that the insertion protocol needs further optimization. In this study, DMPE-PEG(3400) phospholipids were employed. The advantage of phospholipids with such short acyl chains (14 carbon atoms) is their ability to readily transfer to lipid bilayer membranes at temperatures compatible with biological systems [62]. This is crucial in order to maintain EV integrity, given that EV integrity was severely compromised upon incubation at elevated temperatures (60°C). Unfortunately, post-inserted short-chain phospholipids have also been described to readily partition out of liposomes, especially in the presence of serum proteins [62, 63]. This may have resulted in a gradual loss of 'stealth' properties *in vivo* and consequently affected circulation half-life. The plasma stability of post-inserted DMPE-PEG in EV membranes was not investigated in the current study, however it is conceivable that the stability of exogenously introduced lipids is different in EV membranes compared with liposomes due to their unique membrane composition [39]. EVs are typically enriched in membrane-stabilizing lipids, such as cholesterol, sphingomyelin and ganglioside GM3 [2, 64], which may improve retention of inserted PEG-lipids [63, 65]. To possibly increase PEG stability in the EV membrane, PEGylated phospholipids with longer acyl chains (e.g. 16 or 18 carbon atoms, DPPE or DSPE, respectively) could be used for post-insertion. These have been described to show improved anchoring properties compared with DMPE when employed in liposomes, however at the cost of post-insertion efficiency at physiological temperatures [62, 63, 66]. These mechanisms are also likely to apply to EVs, given that in preliminary experiments post-insertion with DSPE-PEG was less efficient than post-insertion with DMPE-PEG (data not shown). Hence, a trade-off between PEG grafting density and anchor stability may exist. Furthermore, the efficiency of post-insertion is also determined by the length of the PEG chains, with shorter PEG chains being inserted in liposomes with higher efficiency than longer PEG chains [66], while longer PEG chains have been described to better shield particles from clearance by the RES [20]. In addition, optimization of the number of PEG chains and targeting ligands per particle may be crucial to balance proper cell entry

with sufficient shielding properties [67, 68]. These parameters could be considered as starting points to further improve the stable and functional insertion of PEGylated targeting ligands in EVs.

Given that the described post-insertion strategy may be used to target EVs to specific cell types while avoiding interactions with others and also increasing circulation time, our data highlight possibilities for future research. PEGylated EVs could be employed to increase accumulation at sites of inflammation in other pathologies, such as rheumatoid arthritis and inflammatory bowel diseases, which are characterized by localized increased vascular permeability [69]. In addition, the ease of ligand coupling to functionalized PEG-phospholipids allows for application of a range of targeting ligands (e.g. well-studied RGD peptides to target angiogenic endothelial cells [70] or clinically approved antibodies against established tumor targets [71]). Taken together, decoration of EVs with PEG-coupled targeting ligands *via* post-insertion is a promising new tool to improve the potential of EVs for drug delivery.

Acknowledgements

The work of SAAK, LALF, PV and RMS on cell-derived membrane vesicles is supported by a European Research Council starting grant (260627) "MINDS" in the FP7 ideas program of the European Union. PV is supported by a VENI Fellowship (# 13667) from the Netherlands Organisation for Scientific Research (NWO). RvdM is supported by funding from the European Union's Horizon 2020 research and innovation programme under the Marie Skłodowska-Curie grant agreement No 660426. C.W. Seinen is gratefully acknowledged for technical assistance in electron microscopy experiments.

References

1. S. El-Andaloussi, I. Mager, X.O. Breakefield, M.J. Wood, Extracellular vesicles: biology and emerging therapeutic opportunities, *Nat Rev Drug Discov*, 12 (2013) 347-357.
2. S.A. Kooijmans, P. Vader, S.M. van Dommelen, W.W. van Solinge, R.M. Schiffelers, Exosome mimetics: a novel class of drug delivery systems, *Int J Nanomedicine*, 7 (2012) 1525-1541.
3. S.M. van Dommelen, P. Vader, S. Lakhal, S.A. Kooijmans, W.W. van Solinge, M.J. Wood*, et al.*, Microvesicles and exosomes: opportunities for cell-derived membrane vesicles in drug delivery, *J Control Release*, 161 (2012) 635-644.
4. P. Vader, X.O. Breakefield, M.J. Wood, Extracellular vesicles: emerging targets for cancer therapy, *Trends Mol Med*, 20 (2014) 385-393.
5. C. Thery, M. Ostrowski, E. Segura, Membrane vesicles as conveyors of immune responses, *Nat Rev Immunol*, 9 (2009) 581-593.
6. H.F. Heijnen, A.E. Schiel, R. Fijnheer, H.J. Geuze, J.J. Sixma, Activated platelets release two types of membrane vesicles: microvesicles by surface shedding and exosomes derived from exocytosis of multivesicular bodies and alpha-granules, *Blood*, 94 (1999) 3791-3799.
7. K. Denzer, M.J. Kleijmeer, H.F. Heijnen, W. Stoorvogel, H.J. Geuze, Exosome: from internal vesicle of the multivesicular body to intercellular signaling device, *J Cell Sci*, 113 Pt 19 (2000) 3365-3374.
8. B. Gyorgy, M.E. Hung, X.O. Breakefield, J.N. Leonard, Therapeutic applications of extracellular vesicles: clinical promise and open questions, *Annu Rev Pharmacol Toxicol*, 55 (2015) 439-464.
9. J.G. van den Boorn, M. Schlee, C. Coch, G. Hartmann, SiRNA delivery with exosome nanoparticles, *Nat Biotechnol*, 29 (2011) 325-326.
10. L.A. Mulcahy, R.C. Pink, D.R. Carter, Routes and mechanisms of extracellular vesicle uptake, *J Extracell Vesicles*, 3 (2014) 24641.
11. L. Alvarez-Erviti, Y. Seow, H. Yin, C. Betts, S. Lakhal, M.J. Wood, Delivery of siRNA to the mouse brain by systemic injection of targeted exosomes, *Nat Biotechnol*, 29 (2011) 341-345.
12. J. Wahlgren, L.K.T. De, M. Brisslert, F. Vaziri Sani, E. Telemo, P. Sunnerhagen*, et al.*, Plasma exosomes can deliver exogenous short interfering RNA to monocytes and lymphocytes, *Nucleic Acids Res*, 40 (2012) e130.
13. S. Ohno, M. Takanashi, K. Sudo, S. Ueda, A. Ishikawa, N. Matsuyama*, et al.*, Systemically Injected Exosomes Targeted to EGFR Deliver Antitumor MicroRNA to Breast Cancer Cells, *Mol Ther*, 21 (2013) 185-191.
14. V. Gujrati, S. Kim, S.H. Kim, J.J. Min, H.E. Choy, S.C. Kim*, et al.*, Bioengineered bacterial outer membrane vesicles as cell-specific drug-delivery vehicles for cancer therapy, *ACS Nano*, 8 (2014) 1525-1537.
15. K. Tang, Y. Zhang, H. Zhang, P. Xu, J. Liu, J. Ma*, et al.*, Delivery of chemotherapeutic drugs in tumour cell-derived microparticles, *Nat Commun*, 3 (2012) 1282.
16. S.C. Jang, O.Y. Kim, C.M. Yoon, D.S. Choi, T.Y. Roh, J. Park*, et al.*, Bioinspired exosome-mimetic nanovesicles for targeted delivery of chemotherapeutics to malignant tumors, *ACS Nano*, 7 (2013) 7698-7710.
17. M.E. Hung, J.N. Leonard, Stabilization of exosome-targeting peptides via engineered glycosylation, *J Biol Chem*, 290 (2015) 8166-8172.
18. Y. Tian, S. Li, J. Song, T. Ji, M. Zhu, G.J. Anderson*, et al.*, A doxorubicin delivery platform using engineered natural membrane vesicle exosomes for targeted tumor therapy, *Biomaterials*, 35 (2014) 2383-2390.

19. T.M. Allen, P. Sapra, E. Moase, Use of the post-insertion method for the formation of ligand-coupled liposomes, *Cell Mol Biol Lett*, 7 (2002) 889-894.

20. J.S. Suk, Q. Xu, N. Kim, J. Hanes, L.M. Ensign, PEGylation as a strategy for improving nanoparticle-based drug and gene delivery, *Adv Drug Deliv Rev*, (2015).

21. J.V. Jokerst, T. Lobovkina, R.N. Zare, S.S. Gambhir, Nanoparticle PEGylation for imaging and therapy, *Nanomedicine (Lond)*, 6 (2011) 715-728.

22. C.P. Lai, O. Mardini, M. Ericsson, S. Prabhakar, C.A. Maguire, J.W. Chen*, et al.*, Dynamic biodistribution of extracellular vesicles in vivo using a multimodal imaging reporter, *ACS Nano*, 8 (2014) 483-494.

23. F. Ciardiello, G. Tortora, EGFR antagonists in cancer treatment, *N Engl J Med*, 358 (2008) 1160-1174.

24. N. Tebbutt, M.W. Pedersen, T.G. Johns, Targeting the ERBB family in cancer: couples therapy, *Nat Rev Cancer*, 13 (2013) 663-673.

25. H. Revets, P. De Baetselier, S. Muyldermans, Nanobodies as novel agents for cancer therapy, *Expert Opin Biol Ther*, 5 (2005) 111-124.

26. S. Ewert, C. Cambillau, K. Conrath, A. Pluckthun, Biophysical properties of camelid V(HH) domains compared to those of human V(H)3 domains, *Biochemistry*, 41 (2002) 3628-3636.

27. E. Dolk, C. van Vliet, J.M. Perez, G. Vriend, H. Darbon, G. Ferrat*, et al.*, Induced refolding of a temperature denatured llama heavy-chain antibody fragment by its antigen, *Proteins*, 59 (2005) 555-564.

28. R. van der Meel, S. Oliveira, I. Altintas, R. Haselberg, J. van der Veeken, R.C. Roovers*, et al.*, Tumor-targeted Nanobullets: Anti-EGFR nanobody-liposomes loaded with anti-IGF-1R kinase inhibitor for cancer treatment, *J Control Release*, 159 (2012) 281-289.

29. F.W. Studier, Protein production by auto-induction in high density shaking cultures, *Protein Expr Purif*, 41 (2005) 207-234.

30. S. Oliveira, R.M. Schiffelers, J. van der Veeken, R. van der Meel, R. Vongpromek, P.M. van Bergen En Henegouwen*, et al.*, Downregulation of EGFR by a novel multivalent nanobody-liposome platform, *J Control Release*, 145 (2010) 165-175.

31. S.A. Kooijmans, S. Stremersch, K. Braeckmans, S.C. de Smedt, A. Hendrix, M.J. Wood*, et al.*, Electroporation-induced siRNA precipitation obscures the efficiency of siRNA loading into extracellular vesicles, *J Control Release*, 172 (2013) 229-238.

32. E.G. Hofman, M.O. Ruonala, A.N. Bader, D. van den Heuvel, J. Voortman, R.C. Roovers*, et al.*, EGF induces coalescence of different lipid rafts, *J Cell Sci*, 121 (2008) 2519-2528.

33. S. Oliveira, G.A. van Dongen, M. Stigter-van Walsum, R.C. Roovers, J.C. Stam, W. Mali*, et al.*, Rapid visualization of human tumor xenografts through optical imaging with a near-infrared fluorescent anti-epidermal growth factor receptor nanobody, *Mol Imaging*, 11 (2012) 33-46.

34. T. Perrier, P. Saulnier, F. Fouchet, N. Lautram, J.P. Benoit, Post-insertion into Lipid NanoCapsules (LNCs): From experimental aspects to mechanisms, *Int J Pharm*, 396 (2010) 204-209.

35. P.S. Uster, T.M. Allen, B.E. Daniel, C.J. Mendez, M.S. Newman, G.Z. Zhu, Insertion of poly(ethylene glycol) derivatized phospholipid into pre-formed liposomes results in prolonged in vivo circulation time, *FEBS Lett*, 386 (1996) 243-246.

36. T. Ishida, D.L. Iden, T.M. Allen, A combinatorial approach to producing sterically stabilized (Stealth) immunoliposomal drugs, *FEBS Lett*, 460 (1999) 129-133.

37. K. Nakamura, K. Yamashita, Y. Itoh, K. Yoshino, S. Nozawa, H. Kasukawa, Comparative studies of polyethylene glycol-modified liposomes prepared using different PEG-modification methods, *Biochim Biophys Acta*, 1818 (2012) 2801-2807.

38. J.N. Moreira, T. Ishida, R. Gaspar, T.M. Allen, Use of the post-insertion technique to insert peptide ligands into pre-formed stealth liposomes with retention of binding activity and cytotoxicity, *Pharm Res*, 19 (2002) 265-269.

39. R. van der Meel, M.H. Fens, P. Vader, W.W. van Solinge, O. Eniola-Adefeso, R.M. Schiffelers, Extracellular vesicles as drug delivery systems: lessons from the liposome field, *J Control Release*, 195 (2014) 72-85.

40. A. Puri, K. Loomis, B. Smith, J.H. Lee, A. Yavlovich, E. Heldman, *et al.*, Lipid-based nanoparticles as pharmaceutical drug carriers: from concepts to clinic, *Crit Rev Ther Drug Carrier Syst*, 26 (2009) 523-580.

41. L. Zhang, F.X. Gu, J.M. Chan, A.Z. Wang, R.S. Langer, O.C. Farokhzad, Nanoparticles in medicine: therapeutic applications and developments, *Clin Pharmacol Ther*, 83 (2008) 761-769.

42. T. Imai, Y. Takahashi, M. Nishikawa, K. Kato, M. Morishita, T. Yamashita, *et al.*, Macrophage-dependent clearance of systemically administered B16BL6-derived exosomes from the blood circulation in mice, *J Extracell Vesicles*, 4 (2015) 26238.

43. S.C. Saunderson, A.C. Dunn, P.R. Crocker, A.D. McLellan, CD169 mediates the capture of exosomes in spleen and lymph node, *Blood*, 123 (2014) 208-216.

44. M. Morishita, Y. Takahashi, M. Nishikawa, K. Sano, K. Kato, T. Yamashita, *et al.*, Quantitative analysis of tissue distribution of the B16BL6-derived exosomes using a streptavidin-lactadherin fusion protein and iodine-125-labeled biotin derivative after intravenous injection in mice, *J Pharm Sci*, 104 (2015) 705-713.

45. Y. Takahashi, M. Nishikawa, H. Shinotsuka, Y. Matsui, S. Ohara, T. Imai, *et al.*, Visualization and in vivo tracking of the exosomes of murine melanoma B16-BL6 cells in mice after intravenous injection, *J Biotechnol*, 165 (2013) 77-84.

46. O.P. Wiklander, J.Z. Nordin, A. O'Loughlin, Y. Gustafsson, G. Corso, I. Mager, *et al.*, Extracellular vesicle in vivo biodistribution is determined by cell source, route of administration and targeting, *J Extracell Vesicles*, 4 (2015) 26316.

47. S.W. Jones, R.A. Roberts, G.R. Robbins, J.L. Perry, M.P. Kai, K. Chen, *et al.*, Nanoparticle clearance is governed by Th1/Th2 immunity and strain background, *J Clin Invest*, 123 (2013) 3061-3073.

48. P. Vader, B.J. Crielaard, S.M. van Dommelen, R. van der Meel, G. Storm, R.M. Schiffelers, Targeted delivery of small interfering RNA to angiogenic endothelial cells with liposome-polycation-DNA particles, *J Control Release*, 160 (2012) 211-216.

49. S.D. Li, L. Huang, Targeted delivery of antisense oligodeoxynucleotide and small interference RNA into lung cancer cells, *Mol Pharm*, 3 (2006) 579-588.

50. D. Zech, S. Rana, M.W. Buchler, M. Zoller, Tumor-exosomes and leukocyte activation: an ambivalent crosstalk, *Cell Commun Signal*, 10 (2012) 37.

51. K.J. Svensson, H.C. Christianson, A. Wittrup, E. Bourseau-Guilmain, E. Lindqvist, L.M. Svensson, *et al.*, Exosome uptake depends on ERK1/2-heat shock protein 27 signaling and lipid Raft-mediated endocytosis negatively regulated by caveolin-1, *J Biol Chem*, 288 (2013) 17713-17724.

52. K. Remaut, B. Lucas, K. Braeckmans, J. Demeester, S.C. De Smedt, Pegylation of liposomes favours the endosomal degradation of the delivered phosphodiester oligonucleotides, *J Control Release*, 117 (2007) 256-266.

53. R.N. Majzoub, C.L. Chan, K.K. Ewert, B.F. Silva, K.S. Liang, E.L. Jacovetty, *et al.*, Uptake and transfection efficiency of PEGylated cationic liposome-DNA complexes with and without RGD-tagging, *Biomaterials*, 35 (2014) 4996-5005.

54. N.N. Sanders, L. Peeters, I. Lentacker, J. Demeester, S.C. De Smedt, Wanted and unwanted properties of surface PEGylated nucleic acid nanoparticles in ocular gene transfer, *J Control Release*, 122 (2007) 226-235.

55. N. Arraud, R. Linares, S. Tan, C. Gounou, J.M. Pasquet, S. Mornet, *et al.*, Extracellular vesicles from blood plasma: determination of their morphology, size, phenotype and concentration, *J Thromb Haemost*, 12 (2014) 614-627.

56. T.M. Allen, P.R. Cullis, Liposomal drug delivery systems: from concept to clinical applications, *Adv Drug Deliv Rev*, 65 (2013) 36-48.

57. D.E. Owens, 3rd, N.A. Peppas, Opsonization, biodistribution, and pharmacokinetics of polymeric nanoparticles, *Int J Pharm*, 307 (2006) 93-102.

58. R. van der Meel, L.J. Vehmeijer, R.J. Kok, G. Storm, E.V. van Gaal, Ligand-targeted particulate nanomedicines undergoing clinical evaluation: current status, *Adv Drug Deliv Rev*, 65 (2013) 1284-1298.

59. S.D. Li, L. Huang, Nanoparticles evading the reticuloendothelial system: role of the supported bilayer, *Biochim Biophys Acta*, 1788 (2009) 2259-2266.

60. R.M. Schiffelers, I.A. Bakker-Woudenberg, G. Storm, Localization of sterically stabilized liposomes in experimental rat Klebsiella pneumoniae pneumonia: dependence on circulation kinetics and presence of poly(ethylene)glycol coating, *Biochim Biophys Acta*, 1468 (2000) 253-261.

61. N. Dos Santos, C. Allen, A.M. Doppen, M. Anantha, K.A. Cox, R.C. Gallagher, *et al.*, Influence of poly(ethylene glycol) grafting density and polymer length on liposomes: relating plasma circulation lifetimes to protein binding, *Biochim Biophys Acta*, 1768 (2007) 1367-1377.

62. W.M. Li, L. Xue, L.D. Mayer, M.B. Bally, Intermembrane transfer of polyethylene glycol-modified phosphatidylethanolamine as a means to reveal surface-associated binding ligands on liposomes, *Biochim Biophys Acta*, 1513 (2001) 193-206.

63. G.N. Chiu, M.B. Bally, L.D. Mayer, Effects of phosphatidylserine on membrane incorporation and surface protection properties of exchangeable poly(ethylene glycol)-conjugated lipids, *Biochim Biophys Acta*, 1560 (2002) 37-50.

64. Y.J. Yoon, O.Y. Kim, Y.S. Gho, Extracellular vesicles as emerging intercellular communicasomes, *BMB Rep*, 47 (2014) 531-539.

65. N. Golkar, A.M. Tamaddon, S.M. Samani, Effect of lipid composition on incorporation of trastuzumab-PEG-lipid into nanoliposomes by post-insertion method: physicochemical and cellular characterization, *J Liposome Res*, (2015) 1-13.

66. K. Shimada, S. Matsuo, Y. Sadzuka, A. Miyagishima, Y. Nozawa, S. Hirota, *et al.*, Determination of incorporated amounts of poly(ethylene glycol)-derivatized lipids in liposomes for the physicochemical characterization of stealth liposomes, *Int J Pharm*, 203 (2000) 255-263.

67. J.M. Saul, A. Annapragada, J.V. Natarajan, R.V. Bellamkonda, Controlled targeting of liposomal doxorubicin via the folate receptor in vitro, *J Control Release*, 92 (2003) 49-67.

68. M. Rabenhold, F. Steiniger, A. Fahr, R.E. Kontermann, R. Ruger, Bispecific single-chain diabody-immunoliposomes targeting endoglin (CD105) and fibroblast activation protein (FAP) simultaneously, *J Control Release*, 201 (2015) 56-67.

69. H. Nehoff, N.N. Parayath, L. Domanovitch, S. Taurin, K. Greish, Nanomedicine for drug targeting: strategies beyond the enhanced permeability and retention effect, *Int J Nanomedicine*, 9 (2014) 2539-2555.

70. K. Temming, R.M. Schiffelers, G. Molema, R.J. Kok, RGD-based strategies for selective delivery of therapeutics and imaging agents to the tumour vasculature, *Drug Resist Updat*, 8 (2005) 381-402.

71. P.M. Glassman, J.P. Balthasar, Mechanistic considerations for the use of monoclonal antibodies for cancer therapy, *Cancer Biol Med*, 11 (2014) 20-33.

Supplementary Methods

Isolation of platelet EVs

Blood was obtained from healthy volunteers who had not received platelet-suppressive therapy (e.g. anticoagulants) for at least 10 days before blood withdrawal. Blood samples were anticoagulated with 3.2% w/v trisodium citrate. Withdrawal of blood samples was approved by the University Medical Centre Utrecht (UMCU) Ethics Committee. Platelets were isolated according to methods described elsewhere [72]. Platelet concentration was determined using a CellDyn1800 (Abbott, Hoofddorp, The Netherlands) and set at 200 000/µL. Washed platelets were incubated for 30 min at room temperature, and then activated with 1 µM thapsigargin (Sigma-Aldrich) and 0.5 U/mL thrombin (Enzyme Research Laboratories, IN) in the presence of 1 mM $CaCl_2$ for 40 min at 22°C. Activation was stopped by addition of 20 mM EDTA, and platelets were removed by centrifugation at 3200g for 10 min at 4°C. This was repeated once to remove residual platelets and debris. Large vesicles were pelleted for 30 min at 10 000g and 4°C, and EVs were recovered from the supernatant by centrifugation at 100 000g and 4°C for 70 min. EV pellet was washed once with PBS at 100 000g for 70 min and resuspended in PBS. EV aggregates were removed by a final centrifugation step for 10 min at 1000g and 4°C.

Dynamic light scattering measurements

To assess whether post-insertion affected EV size and potentially caused EV aggregation, EV sizes were measured with dynamic light scattering using a CGS-3 multiangle goniometer with a 632 nm JDS Uniphase 22 mW He-Ne laser (Malvern Instruments Ltd, UK) at a 90° angle. Autocorrelation functions were used to calculate the mean size and polydispersity index (PDI) of the analyzed samples.

72. S.J. Korporaal, M. Van Eck, J. Adelmeijer, M. Ijsseldijk, R. Out, T. Lisman, P.J. Lenting, T.J. Van Berkel, J.W. Akkerman, Platelet activation by oxidized low density lipoprotein is mediated by CD36 and scavenger receptor-A, Arterioscler Thromb Vasc Biol, 27 (2007) 2476-2483.

SUPPLEMENTARY FIGURES

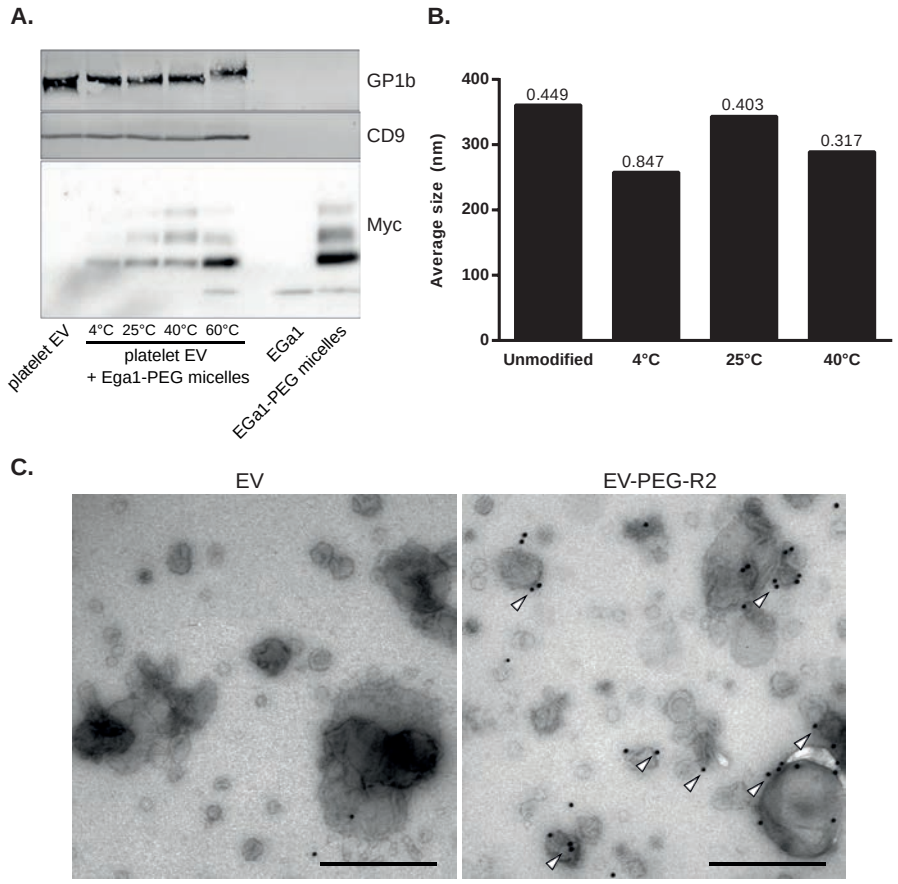

Supplementary Figure 1: Platelet EVs can be decorated with nanobodies using post-insertion in a temperature dependent manner without loss of EV characteristics. A. Western blot analysis of EV markers and nanobodies on platelet EVs after post-insertion with EGa1-PEG micelles at various temperatures, and after purification with size-exclusion chromatography (SEC). Incubation at 60°C resulted in severe loss of EV integrity and aggregation of EV proteins, such as the platelet-specific marker glycoprotein 1b (GP1b). To evaluate whether the size of platelet-derived EVs had changed due to post-insertion, or whether EV aggregation had occurred, EVs were analyzed by Dynamic Light Scattering (DLS). When the temperature of post-insertion was increased, leading to higher nanobody incorporation, size of the EVs did not increase compared with unmodified EVs (B). Numbers above bars indicate polydispersity indices (PDI). Given that in DLS analysis particle sizes are readily overestimated in the presence of only a few large EV/micelle aggregates, it was concluded that such aggregates were not formed during post-insertion. TEM analysis of EVs after post-insertion with R2-micelles revealed that EV morphology was unaltered compared with unmodified controls, and that nanobodies appeared to be almost exclusively associated with EV membranes (C). Immunogold labelling was performed with anti-Myc antibodies (arrowheads indicate membrane-associated gold). Scale bars represent 500 nm.

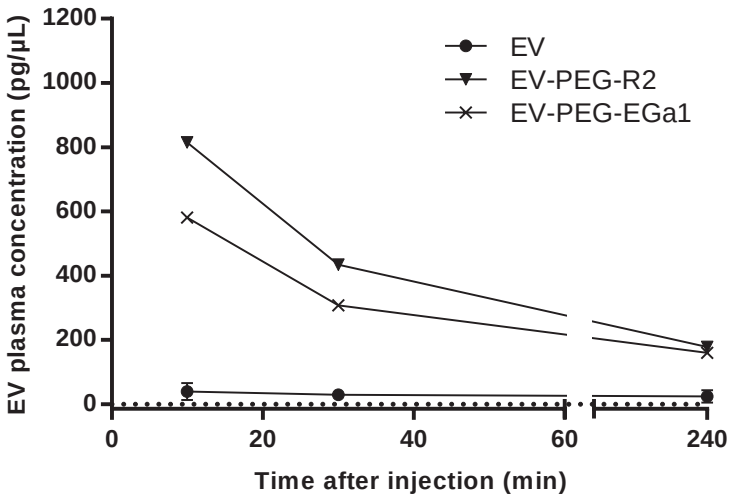

Supplementary Figure 2: Post-insertion with nanobody-PEG micelles increases circulation time of Neuro2A EVs when administered at higher doses. Plasma concentration of DiR-labelled Neuro2A EVs before and after post-insertion with nanobody-PEG micelles, measured at several time points after i.v. injection of 6 µg of EVs in tail veins of tumor-bearing Crl:NU-Foxn1^{nu} mice. Dotted line indicates lower detection threshold. Results are expressed as mean ± SEM, n=1-3.

CHAPTER 6

Recombinant phosphatidylserine-binding nanobodies for targeting of extracellular vesicles to tumor cells: A plug-and-play approach

S.A.A. Kooijmans[1], J.J.J.M. Gitz-Francois[1], P. Vader[1], R.M. Schiffelers[1]

[1]Department of Clinical Chemistry and Haematology, University Medical Center Utrecht, Utrecht, The Netherlands

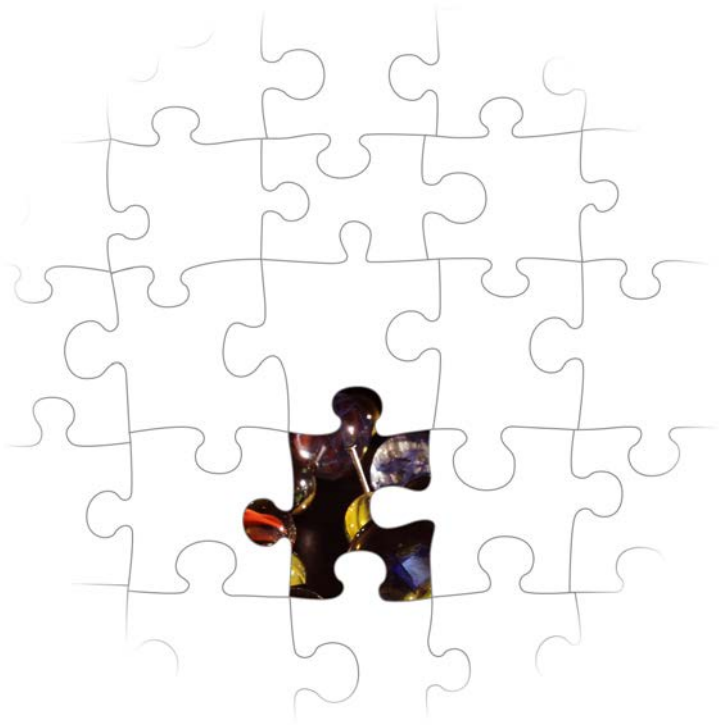

Abstract

Extracellular vesicles (EVs) are increasingly being recognized as candidate drug delivery systems due to their ability to functionally transfer biological cargo between cells. However, manipulation of targeting properties of EVs by engineering of the producer cell can be challenging and time-consuming. As a novel approach to confer tumor targeting properties to isolated EVs, we generated recombinant fusion proteins of nanobodies against the epidermal growth factor receptor (EGFR) fused to phosphatidylserine (PS)-binding domains of lactadherin (C1C2) and evaluated their effects on EV tumor cell targeting. C1C2-nanobody fusion proteins were expressed in HEK293 cells and isolated from culture medium with near-complete purity as determined by SDS-PAGE. Fusion proteins specifically bound PS and showed no affinity for other common EV membrane lipids. Furthermore, C1C2 fused to anti-EGFR nanobodies (EGa1-C1C2) bound EGFR with high affinity and competed with binding of its natural ligand EGF, as opposed to C1C2 fused to non-targeting control nanobodies (R2-C1C2). Both proteins readily self-associated onto membranes of EVs derived from erythrocytes and Neuro2A cells without affecting EV size and integrity. EV-bound R2-C1C2 did not influence EV-cell interactions, while EV-bound EGa1-C1C2 dose-dependently enhanced specific binding and uptake of EVs by EGFR-overexpressing tumor cells. In conclusion, we developed a novel strategy to efficiently and universally confer tumor targeting properties to PS-exposing EVs after their isolation without affecting EV characteristics, circumventing the need to modify EV-secreting cells. This strategy may also be employed to decorate EVs with other moieties, including imaging probes or therapeutic proteins.

Introduction

In the past decade, the view that extracellular vesicles (EVs) may be exploited as drug delivery systems has gained increasing support in the scientific community. EVs are naturally occurring lipid membrane-enclosed vesicles with sizes ranging from 50 to 1000 nm, which are either shed from plasma membranes or released from intracellular compartments of virtually all cells in the body. The former class of (plasma membrane-derived) EVs is often referred to as microvesicles (or ectosomes) and the latter class is usually termed exosomes, but in practice these show overlapping characteristics [1]. They are believed to play a role in intercellular communication by transporting their cargo, which consists of bioactive lipids, proteins and nucleic acids (e.g. miRNA and mRNA) from one cell to another via bodily fluids [2]. EVs can transfer these macromolecules to recipient cells and thereby induce pronounced phenotypical changes [3-6]. This phenomenon has created excitement in the drug delivery field, where efficient, biocompatible and targeted transfer of such cargo is often desired [7-10], and has already resulted in the first clinical trials using EVs for therapeutic purposes [11].

However, the biological nature of EVs presents not only opportunities, but also challenges for their application as drug delivery systems. EVs may be 'pre-programmed' with selected cargoes and cell-specific targeting moieties, which may not necessarily overlap with their intended therapeutic application. To overcome these challenges, various strategies have been employed to manipulate EV content. For example, the EV membrane protein Lamp2b has been successfully fused to brain- or angiogenic endothelium specific targeting ligands to target EVs to these respective tissues [12, 13]. In addition, the platelet-derived growth factor receptor was used as an anchor to express tumor targeting ligands on EV surfaces [14]. Although such strategies were shown to result in efficient targeting of EVs to specific cell types, their general applicability may be limited by the need to engineer EV-secreting cells, which can be particularly challenging in primary cells. Furthermore, targeting ligands expressed in such a manner may be displayed with an insufficient density for proper targeting, or even directed to intracellular degradation pathways resulting in minimal display on EVs [15].

In this study, we present a novel approach to confer targeting properties to EVs after their isolation, without the need to modify EV secreting cells and with broad applicability for EVs from multiple cell sources. It has recurrently been described that EVs are enriched in the negatively charged phospholipid phosphatidylserine (PS) [2, 16, 17]. This phospholipid is normally exclusively located in the inner leaflet of the plasma membrane and this asymmetrical membrane distribution is actively maintained by flippase enzymes [18]. However, during EV formation this lipid asymmetry can be lost, resulting in PS-exposure on EVs [1, 19, 20]. Hence, it is not surprising that in proteomic studies EVs are often found to be associated with the opsonin lactadherin (also named MFG-E8) [21-26], which contains two PS-binding C-domains (C1 and C2, together referred to as C1C2) that share homology with the corresponding domains in coagulation factor V and VIII [27, 28]. Due to its localization on EV membranes, the C1C2 domain of lactadherin has been exploited as an EV membrane anchor for recombinant

proteins [29-32]. In these reports, C1C2-fusion protein encoding vectors were transfected into EV producer cells to obtain EVs exposing the desired proteins. We reasoned that, given that lactadherin is a soluble protein, the C1C2-fusion strategy could be employed to equip EVs with tumor cell targeting properties after isolation in a 'plug-and-play' fashion. We fused C1C2 domains with nanobodies raised against the well-studied oncogene epidermal growth factor receptor (EGFR), which is the main target of a range of inhibitors used for cancer treatment in the clinic [33, 34]. Nanobodies (also termed single-domain antibodies, sdAbs or VHHs) are single variable domains of the heavy-chain only antibodies found in *Camelidae* species [35]. These antibody fragments typically possess antigen-binding capacity similar to that of the full length antibody, but are generally more resistant to extreme chemical and thermal conditions [36, 37]. Furthermore, their size of approximately 15 kD, ease of production and high solubility allows nanobodies to be employed as versatile targeting ligands. Here, we describe the purification of C1C2-nanobodies from cell culture supernatants, and characterized the specificity of these proteins for PS and EGFR. Furthermore, we evaluated whether these proteins could be employed as tools to confer tumor cell targeting properties to isolated EVs from distinct sources, including red blood cells (RBCs) and Neuro2A cells.

Materials and methods

Materials

MicroBCA Protein Assay Kit and AlexaFluor 488 NHS ester and the pcDNA3.1 vector with Neomycin resistance were purchased from Thermo Fisher Scientific (Waltham, USA). Sepharose CL-4B and cholesterol were obtained from Sigma-Aldrich (Steinheim, Germany) and TALON Superflow Metal Affinity Resin was from Clontech Laboratories, Inc. (Saint-Germain-en-Laye, France). Phospholipids were purchased from Avanti Polar Lipids (Birmingham, USA), except egg phosphatidylcholine, which was obtained from Lipoid AG (Steinhausen, Switzerland). Sterile cell culture flasks were obtained from Greiner Bio-One (Alphen aan de Rijn, The Netherlands). pET28a-EGa1 and pAX51-R2 vectors encoding EGa1 (PDB ID: 4KRN) and R2 (PDB ID: 1QD0) Myc-tagged nanobodies, respectively, were kindly provided by Dr. S. Oliveira (Department of Biology, Utrecht University, Utrecht, The Netherlands).

Molecular cloning

Mouse splenic dendritic cells (D1) were cultured as described [38], and RNA was isolated using TRIzol Reagent (Thermo Fisher Scientific) according to the manufacturer's instructions. cDNA synthesis was performed using iScript cDNA Synthesis Kit (Bio-Rad Laboratories, Veenendaal, The Netherlands) according to the manufacturer's protocol. The C1C2 region of MFG-E8 was PCR amplified using forward primer Fw_C1C2 and reverse primer Rv_C1C2 (see Supplementary Table 1). These primers were designed to flank the C1C2 sequence with a 5' NotI restriction

site and 2xGGGGS linker sequence, and a 3' Tobacco Etch Virus (TEV) cleavage site and EagI restriction site. After NotI/EagI digestion, C1C2 sequence was inserted into pET28-EGa1 at the NotI site. The resulting EGa1-C1C2-Myc-His cassette was PCR amplified, flanked with NheI and XbaI sites and inserted in pcDNA3.1. Subsequently, an Igκ leader sequence (see Supplementary Table 1) was inserted in-frame at the NheI site to generate pcDNA3.1-EGa1-C1C2. For the pcDNA3.1-R2-C1C2 vector, the R2 sequence was PCR amplified from pAX51-R2 and flanked with NheI and NotI sites. The EGa1 sequence was excised from pcDNA3.1-EGa1-C1C2 using the same restriction enzymes and replaced with the R2 sequence. All obtained vectors were sequenced using a BigDye® Terminator v3.1 Cycle Sequencing Kit (Thermo Fisher Scientific) according to the manufacturer's instructions.

Generation of cell lines and cell culture

All used cell lines were maintained at 37˚C and 5% CO_2. Human epidermoid carcinoma cells (A431, ATCC, Manassas, USA) and human embryonic kidney cells (HEK293, ATCC) were cultured in Dulbecco's Modified Eagle Medium (DMEM) supplemented with 10% fetal bovine serum (FBS), 100 U/mL penicillin and 100 U/mL streptomycin. Mouse neuroblastoma cells (Neuro2A, ATCC) were grown in Roswell Park Memorial Institute (RPMI) 1640 medium supplemented with 10% FBS, 100 U/mL penicillin and 100 U/mL streptomycin. To generate cell lines stably expressing R2-C1C2 or EGa1-C1C2 proteins, HEK293 cells were transfected overnight with pcDNA3.1-R2-C1C2 or pcDNA3.1-EGa1-C1C2 using Lipofectamine 2000 (Thermo Fisher Scientific) according to the manufacturer's instructions. Cells were selected for at least 2 weeks using 500 µg/mL G418 (Thermo Fisher Scientific) selection antibiotic, until normal morphology and growth was regained.

Large-scale purification of recombinant phosphatidylserine-binding proteins

HEK293 cells expressing R2-C1C2 or EGa1-C1C2 were seeded at 50% confluency in 10-layer HYPERflask M cell culture vessels (Corning Life Sciences B.V., Amsterdam, The Netherlands) in normal growth medium. After 72h, medium was replaced with production medium, consisting of Opti-MEM Reduced Serum medium supplemented with GlutaMAX (Gibco, Thermo Fisher Scientific), 0.5% v/v Ultroser G serum substitute (Pall Corporation, Washington, USA), 250 µg/mL G418 and penicillin/streptomycin. Cells were cultured for 48h, after which conditioned medium was harvested and replaced with fresh production medium. Conditioned medium was mixed with 0.2 mM benzamidine HCl, depleted of cells and debris by centrifugation at 5000g for 15 min at 4°C and stored at -20°C until processing. When 5-10L of conditioned medium was collected, medium was thawed and concentrated to ± 120 mL using a 10 kD MWCO hollow fiber cartridge mounted on a Quixstand benchtop system (GE Healthcare, Eindhoven, The Netherlands). Concentrate was mixed with 0.5% v/v Triton X-100 to disrupt interactions of recombinant proteins with HEK293 EVs. Talon Superflow Metal Affinity Resin beads were washed with HEPES buffer (500 mM NaCl, 25 mM HEPES, pH 7.8) according

to the manufacturer's instructions and incubated overnight at 4°C with medium concentrate. Beads were pelleted at 500g and 4°C for 5 min and washed three times with optimized stabilizing buffer (OSB, 18 mM L-Arginine, 3.5 mM L-Leucine, 5.7 mM L-Glutamic acid, 0.009% (w/v) fatty acid free bovine serum albumin (BSA), 8% glycerol, 500 mM NaCl, 25 mM HEPES, pH 7.4). Beads were packed in a Tricorn 10/50 column (GE Healthcare) connected to a refrigerated ÄKTA Pure chromatography system according to the manufacturer's instructions and washed with at least 10 column volumes of OSB, Wash Buffer (2 mM imidazole and 0.7% v/v Triton X-100 in OSB) and once more with OSB. Proteins were stripped from the resin with Elution Buffer (250 mM imidazole and 100 mM EDTA in OSB), concentrated on 3 kD MWCO Vivaspin tubes (Sartorius, UK) and dialyzed overnight in 10 kD MWCO Slide-A-Lyzer dialysis cassettes (Thermo Fisher Scientific) against excess OSB. Subsequently, protein concentrates were loaded onto a 26/600 Hiload Superdex 200 pg gel filtration column (GE Healthcare), connected to an refrigerated ÄKTA Pure chromatography system and equilibrated with OSB. After elution in OSB, protein containing fractions (as determined by Western blotting) were pooled and protein concentrations were determined using absorbance at 280 nm and calculated molar extinction coefficients of both proteins. Finally, proteins were concentrated on 3 kD MWCO Vivaspin tubes, and stored in aliquots at -20°C.

SDS-PAGE and Western blot analysis

Samples were mixed with reducing sample buffer containing dithiothreitol (DTT), heated to 95 ˚C for 10 min and electrophoresed over 4-12% Bis-Tris polyacrylamide gels (Thermo Fisher Scientific). Gels were stained with PageBlue Protein Staining Solution (Thermo Fisher Scientific) according to manufacturer's instructions. Alternatively, proteins were blotted on Immobilon-FL polyvinylidene difluoride (PVDF) membranes (Merck Millipore, Amsterdam, The Netherlands), which were blocked with 50% v/v Odyssey Blocking Buffer (LI-COR Biosciences, Leusden, The Netherlands) in Tris buffered saline (TBS). Antibody incubations were performed in 50% v/v Odyssey Blocking Buffer in TBS containing 0.1% v/v Tween 20 (TBS-T). Primary antibodies included mouse anti-Myc (9E10 from MYC 1-9E10.2 hybridoma, ATCC, 1:4000), mouse anti-β-actin (Cell Signaling Technology, clone 8H10D10, 1:1000), rabbit anti-alpha 1 spectrin (Abcam, clone EPR9300, 1:1000). Secondary antibodies included Alexa Fluor 680-conjugated anti-rabbit antibodies (Thermo Fisher Scientific, A-21076, 1:7500 dilution) or IRDye 800CW anti-mouse antibodies (LI-COR Biosciences, 926-32212, 1:7500 dilution). Imaging was performed on an Odyssey Infrared Imager (LI-COR Biosciences, Leusden, the Netherlands) at 700 and 800 nm.

Protein-lipid overlay assay

Protein-lipid overlay assay was performed as described elsewhere [39], with minor modifications. Phospholipids (16:0-18:1 phosphatidylserine (PS), egg phosphatidylglycerol (PG), cholesterol (CHL), milk ganglioside GM3 (GM3), milk sphingomyelin (SM), egg- or soy-derived phosphatidylcholine (PC^{egg} and PC^{soy}, respectively) and egg phosphatidylethanolamine

(PE) were dissolved in 1:1 chloroform:methanol (except GM3, which was dissolved in water) and diluted to 500 µM with a mixture of chloroform:methanol:water (2:1:0.8). Of each phospholipid, 1 µL was spotted on an Immobilon-FL PVDF membrane and dried for 1 hour at room temperature. Membrane was blocked with 50% v/v Odyssey Blocking Buffer in TBS for 2 hours at room temperature, followed by overnight incubation at 4°C with 45 nM of R2-C1C2 or EGa1-C1C2 in 50% v/v Odyssey Blocking Buffer in TBS-T. Blots were washed 5 times with TBS-T and probed with primary antibodies (mouse anti-Myc) and Alexa Fluor 680-conjugated secondary antibodies as described under "*SDS-PAGE and Western blot analysis*". Protein-lipid binding was visualized using an Odyssey Infrared Imager at 700 nm.

Enzyme-linked immunosorbent assay (ELISA)

Extracellular domains of EGFR fused with Fc domains of human antibodies (EGFR-Fc, R&D Systems, Inc, USA) were coated overnight at 4°C onto maxisorp plates at 2 µg/mL. Wells were washed three times with PBS and blocked with 2% skimmed milk in phosphate buffered saline (PBS) for 1 hour. Wells were emptied and incubated with C1C2-nanobodies diluted in 2% skimmed milk for 1 hour. Plates were washed three times with PBS containing 0.05 % v/v Tween20 (PBS-T) and incubated with mouse anti-Myc antibodies (9E10, 1:2000) for 1 hour. After washing with PBS-T, plates were incubated with rabbit-anti-mouse HRP (DAKO, P0260, 1:1000) for 1 hour. All protein and antibody incubations were performed in triplicates in 2% skimmed milk in PBS at room temperature while shaking. Plates were washed with PBS-T and stained with 100 µL TMB substrate solution (Thermo Fisher Scientific). Reactions were quenched by addition of 50 µL 1 M H_2SO_4, and absorbance at 450 nm was measured using a SpectraMax M2e microplate reader (Molecular Devices, UK). Absorbance values were normalized to control wells to which no C1C2 nanobodies were added. Data was plotted in Graphpad Prism 6 software (Graphpad Software, Inc, USA) and non-linear regression was performed using the 'one site-specific binding' option to calculate dissociation constants (Kd).

EGF competition ELISA

Maxisorp plates were coated overnight at 4°C with goat anti-human antibodies (Thermo Fisher Scientific, PA1-85606, 1:1000) in PBS. Plates were washed three times with PBS, and incubated with EGFR-Fc (2 µg/mL in PBS) for 1 hour. After washing with PBS, plates were blocked with 2% fatty acid free BSA in PBS (2% PBSA) for 1 hour, and subsequently incubated with six replicate samples of C1C2 nanobodies mixed with 40 nM EGF-IRDye 800CW optical probe (LI-COR Biosciences) in 2% PBSA for 1 hour. All incubations were performed at room temperature while shaking. Finally, plates were washed three times with PBS and analyzed using an Odyssey Infrared Imager at 800 nm. Fluorescence intensity values of the wells were quantified using Odyssey software (V3.0, LI-COR Biosciences) and normalized to control wells to which no EGFR-Fc was added.

Isolation and stimulation of red blood cells

Blood was obtained from healthy volunteers and anticoagulated with sodium heparin. Withdrawal of blood samples was approved by the University Medical Centre Utrecht (UMCU) Ethics Committee. RBCs were isolated using α-cellulose columns and resuspended in Ringer's buffer (125 mM NaCl, 5 mM KCl, 1.6 mM $CaCl_2$, 5 mM glucose, 10 mM HEPES, pH 7.4) at 40% haematocrit as measured using a CellDyn1800 (Abbott, Hoofddorp, The Netherlands). RBCs were stimulated overnight at room temperature with 4 μM of Ca^{2+}-ionophore A23187 (Sigma-Aldrich) in a tube rotator to induce EV secretion.

Isolation of EVs

After overnight stimulation, RBCs were centrifuged twice at 2000g for 10 min to remove cells and debris. Supernatant centrifuged 10 000g for 10 min to remove large vesicles and debris. Subsequently, supernatant was centrifuged at 100 000g for 70 min using a fixed-angle rotor (Type 50.2 Ti, *k*-factor 206.3, Beckman Coulter) to pellet EVs. EV pellet was resuspended in PBS and centrifuged again at 100 000g for 70 min. All centrifugation steps were performed at 4°C. Washed EV pellet was resuspended in a small volume of PBS (< 1 mL). EV protein concentration was measured using a MicroBCA Protein Assay Kit according to the manufacturer's instructions.

EV decoration and purification by size-exclusion chromatography

EVs were mixed with R2-C1C2 or EGa1-C1C2 or equal volumes of OSB, and incubated at room temperature for 30 min. To remove unbound proteins, Sepharose CL-4B was packed in a XK-16/20 column (GE Healthcare) according to the manufacturer's instructions, connected to a refrigerated ÄKTA Pure chromatography system, and equilibrated on PBS. EV/protein mixtures were injected, eluted with PBS, and EV containing fractions (visualized by UV absorbance at 280 nm) were pooled. EV samples were concentrated to 100-200 μL using Vivaspin ultrafiltration tubes with 100 kD MWCO (Sartorius, UK).

Nanoparticle Tracking Analysis

Concentrated EV samples were diluted with PBS to appropriate dilutions for analysis and automatically injected into a NanoSight NS500 system equipped with an LM14 405 nm violet laser unit (Malvern Instruments, Worcestershire, UK). Five movies of 30 seconds were recorded at camera level 13 and at a fixed temperature of 22°C. Data was analyzed using NTA 3.1 software, with detection threshold 9 and other settings kept at default. PBS used for dilution was confirmed to be particle-free with these settings.

Immuno-electron microscopy

EVs in PBS were adsorbed to carbon-coated formvar grids for 15 min at room temperature, washed, and fixated in 2% paraformaldehyde and 0.2% glutaraldehyde in 0.1 M phosphate buffer. Immunolabeling was performed with mouse anti-Myc antibody (9E10, 1:100), followed

by rabbit-anti-mouse IgG (Rockland, 610-4120, 1:250) and 10 nm Protein A gold (CMC, Utrecht, The Netherlands). Grids were embedded in methyl cellulose uranyl-acetate after counterstaining with uranyl-oxalate [40]. Grids were imaged using a Tecnai T12 transmission electron microscope (FEI, Eindhoven, The Netherlands).

Cell association assays

For *in vitro* cell association and uptake assays, EVs were labeled with the fluorescent dye AlexaFluor 488 NHS ester. Lyophilized dye was dissolved at a concentration of 10 mg/mL in dimethyl sulfoxide (DMSO). EVs were mixed with 100 mM sodium bicarbonate and 1% v/v AlexaFluor 488 NHS ester, and incubated for 1 hour at 22°C in a shaker incubator at 1400 rpm. Unbound label was removed using size exclusion chromatography with a Sepharose CL-4B column as described above. Labeled EVs were decorated with PS-binding proteins and purified again using size exclusion chromatography. To exclude the possibility of labeling biases among samples, EV protein concentrations were measured using a MicroBCA Protein Assay, and fluorescence of 60 µL EV samples in a black 96-well plate was determined using a SpectraMax M2e microplate reader at 488 nm excitation and 530 nm emission. Differences in labeling efficiency (expressed as fluorescence intensity per µg of EV protein) of less than 10% were considered acceptable before proceeding with cell association or uptake assays.

For cell association assays, Neuro2A or A431 cells were trypsinized and resuspended in ice-cold culture medium at a concentration of 300 000 cells/mL. Cells were transferred to round bottom 96-well plates (100 µL/well) on ice and mixed with 3.8 µg of EVs per well. EV-cell mixtures were incubated for 1 hour at 4°C to allow EV binding. Plates were centrifuged for 5 min at 500g and 4°C to pellet cells. Cells were resuspended in ice-cold FACS buffer (PBS containing 0.3% BSA), and this procedure was repeated twice for a total of three washes. Finally, cells were resuspended in 0.2% formaldehyde in PBS and analyzed using a FACSCanto II flow cytometer (BD Biosciences, USA). Mean fluorescence intensity (MFI) values of treated cells were normalized to untreated cells.

Cell uptake assays

Neuro2A or A431 were cultured in flat-bottom 96-well plates in normal growth medium. When a confluency of 80-90% was reached, 3.8 µg of AlexaFluor 488 NHS ester-labeled EVs were added and cells were incubated for 4 hours at 37°C to allow EV uptake. Cells were washed once with PBS, trypsinized, resuspended in culture medium and transferred to round-bottom 96-well plates. Cells were washed once with FACS buffer, once with an acid wash buffer (0.5 M NaCl, 0.2 M acetic acid, pH 3) to remove cell-bound EVs, and once more with FACS buffer as described under *Cell association assays*. Cells were resuspended in 0.2% formaldehyde in PBS and MFI values were determined using flow cytometry.

Statistical data analysis

When applicable, statistical analysis was performed using IBM SPSS Statistics, version 21. Differences between two groups were analyzed using independent samples *t* tests, and multiple-group comparisons were made using one-way ANOVA with Tukey post-hoc tests. Differences with $p < 0.05$ were considered statistically significant.

RESULTS

Design and purification of C1C2-nanobody fusion proteins

In this work, we investigated whether isolated, PS-exposing EVs can be equipped with nanobodies to improve their targeting specificity. The EGa1 nanobody was used as a targeting ligand for EGFR-expressing tumor cells. This nanobody has been described to bind EGFR with high affinity, without triggering its activation [41]. The R2 nanobody, which was raised against the azo-dye Reactive Red (RR6) [42], served as a negative control nanobody as it showed negligible affinity for EGFR in previous reports [43, 44]. DNA sequences of these nanobodies were cloned into pcDNA3.1 vectors with a CMV-promoter, and fused to PS-binding C1C2 domains of MFG-E8 via a $GGGS_2$ linker sequence (Figure 1A). In addition, an Igκ leader sequence was inserted to induce protein secretion, and C-terminal c-Myc- and His_6 tags were inserted for detection and purification, respectively. It was hypothesized that the resulting fusion proteins could self-associate with PS in EV membranes, resulting in nanobody display on the membrane (Figure 1B).

To test this hypothesis, vectors encoding C1C2-fused to R2 or EGa1 (R2-C1C2 and EGa1-C1C2, respectively) were stably transfected into HEK293 cells. Both proteins were successfully expressed in these cells, and appeared as bands at their calculated molecular weights of 56.9 kD (R2-C1C2) and 57.4 kD (EGa1-C1C2) as analyzed by Western blotting (Figure 2A). Expression of R2-C1C2 was lower than expression of EGa1-C1C2, possibly due to differences in transfection or selection efficiency. Both proteins were secreted into the culture medium and showed two bands on Western blot. This could be explained by partial cleavage of the Igκ leader sequence (2.4 kD) from the proteins during secretion. To purify the C1C2-nanobodies from cell culture supernatants, proteins were adsorbed to immobilized metal affinity chromatography (IMAC) resins and thoroughly washed with detergents to remove any protein-bound EVs and phospholipids from HEK293 cells. After elution from the resins, proteins were purified to near complete purity using gel filtration, as analyzed by Western blotting and SDS-PAGE (Figures 2B and 2C, respectively). Importantly, it was observed that the C1C2-nanobodies readily and irreversibly precipitated from solutions when dissolved in commonly used aqueous solutions (e.g. PBS). To prevent this issue, proteins were formulated in an optimized stabilizing buffer (based on studies with recombinant factor VIII [45]), in which this buffer was found to prevent protein precipitation even after three freeze-thaw cycles (data not shown). This formulation

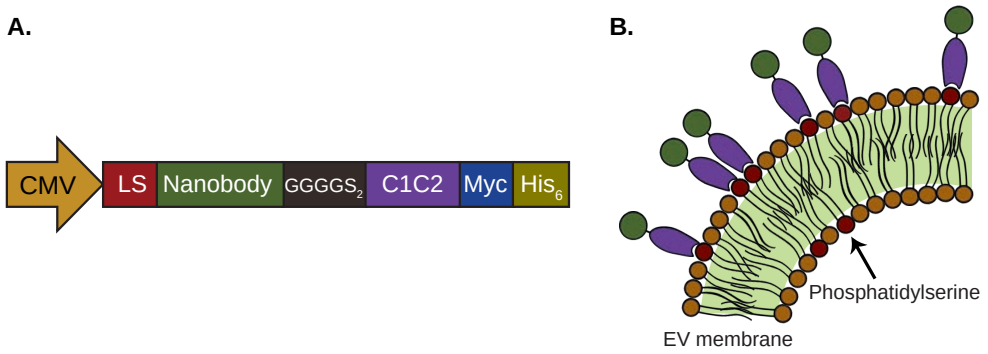

Figure 1: Schematic presentation of C1C2-nanobody fusion proteins. A. Protein expression cassette as cloned in the pcDNA3.1 vector. Expression is driven by a CMV-promoter. Recombinant proteins comprise an Igκ leader sequence (LS), nanobody sequence, $GGGGS_2$ linker sequence, C1 and C2 domains of mouse MFG-E8 (C1C2), and Myc and His_6 tags for detection and purification, respectively. B. C1C2 domains (purple) of the targeting proteins are expected to self-associate with PS in the outer leaflets of EV membranes, resulting in display of nanobodies (green).

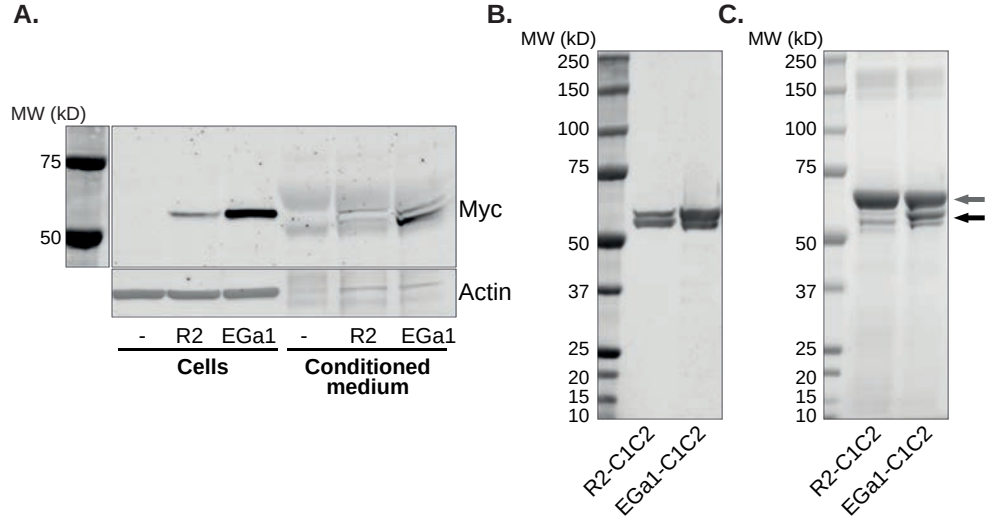

Figure 2: C1C2-proteins are expressed and secreted by HEK293 cells and can be purified from conditioned medium. A. Western blot of HEK293 cells after stable transfection with pcDNA3.1-R2-C1C2 (R2) or pcDNA3.1-EGa1-C1C2 (EGa1) vectors and corresponding conditioned medium. Myc tags were used to detect C1C2-nanobody expression, and actin was included as a loading control. B. Western blot of R2-C1C2 and EGa1-C1C2 after purification from conditioned medium, stained with anti-Myc antibodies. C. SDS-PAGE of purified R2-C1C2 and EGa1-C1C2. Arrows indicate bands of BSA (gray) and C1C2-nanobodies (black).

contains BSA, which appeared as a 66 kD band when proteins were analyzed by SDS-PAGE (Figure 2C).

C1C2-nanobody association with PS and EGFR

To investigate whether the C1C2 domains of the recombinant proteins could promote association with PS, a protein-lipid overlay assay was employed. In this assay, a variety of common EV membrane lipids, including phosphatidylethanolamine (PE), phosphatidylcholine (PC), sphingomyelin (SM), ganglioside GM3 and PS [46], were spotted onto a PVDF membrane and incubated with equimolar concentrations of R2-C1C2 or EGa1-C1C2. Both proteins bound exclusively to PS in a concentration dependent manner, even when spotted in a 100-fold lower concentration compared with the other lipids (Figure 3A). Importantly, both proteins showed no binding to phosphatidylglycerol (PG), a phospholipid also bearing a negative charge like PS, but lacking the recognition motif for C1C2, indicating that protein binding is not solely based on simple electrostatic interactions.

To determine whether the nanobody domains of the PS-binding proteins showed affinity for EGFR, an anti-EGFR ELISA was performed. Extracellular domains of EGFR were captured on 96-well plates and incubated with R2-C1C2 or EGa1-C1C2 (Figure 3B). As expected, EGa1-C1C2 bound EGFR with high affinity (Kd = 39.3 ± 2.7 nM). In contrast, R2-C1C2 showed no affinity for EGFR, confirming that these proteins could serve as non-binding controls for EGa1-C1C2. EGa1 has been described to not only bind EGFR, but also compete with its natural ligand epidermal growth factor (EGF) and thereby prevent EGF-induced receptor phosphorylation [41, 43, 44].

To investigate whether EGa1-C1C2 also competed with EGF, a competition ELISA was employed in which C1C2-nanobodies were mixed with EGF conjugated to a near-infrared fluorophore (EGF-IR) and allowed to bind immobilized extracellular domains of EGFR. EGa1-C1C2 competed with IR-EGF for binding to EGFR, while no IR-EGF competition was observed for R2-C1C2 (Figure 3C).

Association of C1C2-nanobodies with RBC EVs

We next investigated whether these PS-binding properties allowed the C1C2-nanobodies to bind to EV surfaces. RBCs were isolated from blood from healthy volunteers and stimulated with Ca^{2+}-ionophore. This procedure has been described to stimulate secretion of EVs which are predominantly PS-positive [47, 48]. EVs were isolated using a differential (ultra)centrifugation method, with typical EV protein yields of 0.25-0.35 mg per mL of RBCs (at 40% hematocrit), corresponding with $7*10^{11}$ - $9.8*10^{11}$ particles per mL of RBCs as determined by Nanoparticle Tracking Analysis (NTA). Isolated EVs were incubated with R2-C1C2 and EGa1-C1C2 to allow protein binding to EV surfaces. Unbound proteins were removed by size-exclusion chromatography (SEC), and EVs were analyzed by Western blotting. The amount of R2-C1C2 and EGa1-C1C2 that co-eluted with EVs increased in a concentration dependent manner (Figure 4A). Importantly, when high concentrations of R2-C1C2 and EGa1-C1C2 without EVs were loaded onto the SEC column, no proteins were detected in the typical EV fractions (last two lanes in Figure 4A), indicating that the purification method was suitable to completely

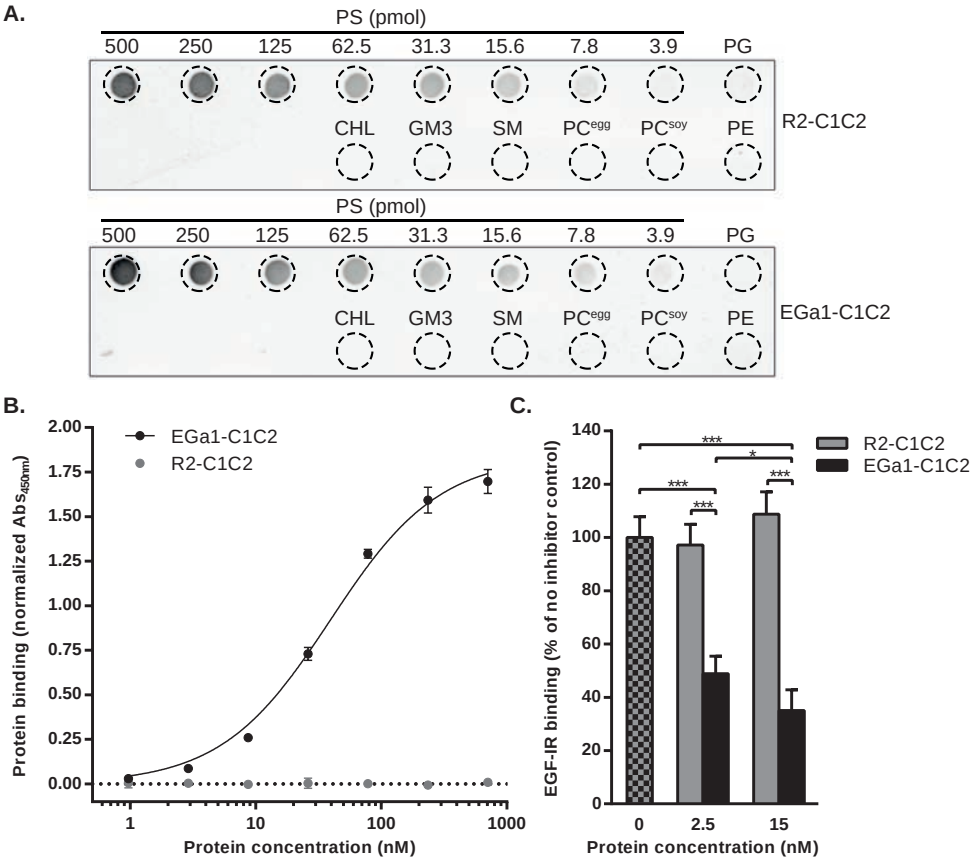

Figure 3: Purified C1C2-nanobodies bind to PS and EGFR with high affinity and compete with binding of EGF. A. Protein-lipid overlay assay in which a PVDF membrane was spotted with 500 pmol of phosphatidylglycerol (PG), cholesterol (CHL), ganglioside GM3 (GM3), sphingomyelin (SM), egg- and soy-derived phosphatidylcholine (PC^{egg} and PC^{soy}, respectively), phosphatidylethanolamine (PE), and decreasing quantities of PS. Binding of R2-C1C2 and EGa1-C1C2 was detected with anti-Myc antibodies. B. ELISA showing binding of R2-C1C2 and EGa1-C1C2 at increasing concentrations to immobilized extracellular domains of EGFR. C1C2-nanobody binding was quantified using anti-Myc antibodies with peroxidase detection. C. Competition ELISA in which C1C2-nanobodies were mixed with 40 nM EGF-IRDye800 (EGF-IR) and incubated with plate-captured extracellular domains of EGFR. EGF-IR binding was analyzed using an Odyssey imager. All data are displayed as mean ± SD and are representative of at least two replicate experiments. * indicates $p < 0.05$ and ***$p < 0.001$ using one-way ANOVA with Tukey post-hoc test.

separate EVs from unbound protein. Decoration of EVs with R2-C1C2 or EGa1-C1C2 did not affect EV size distribution as determined by NTA (Figure 4B). EVs typically showed a heterogeneous size distribution with a mean size of ± 160 nm. To investigate whether decoration with C1C2-nanobodies affected EV integrity or morphology, EVs were analyzed by

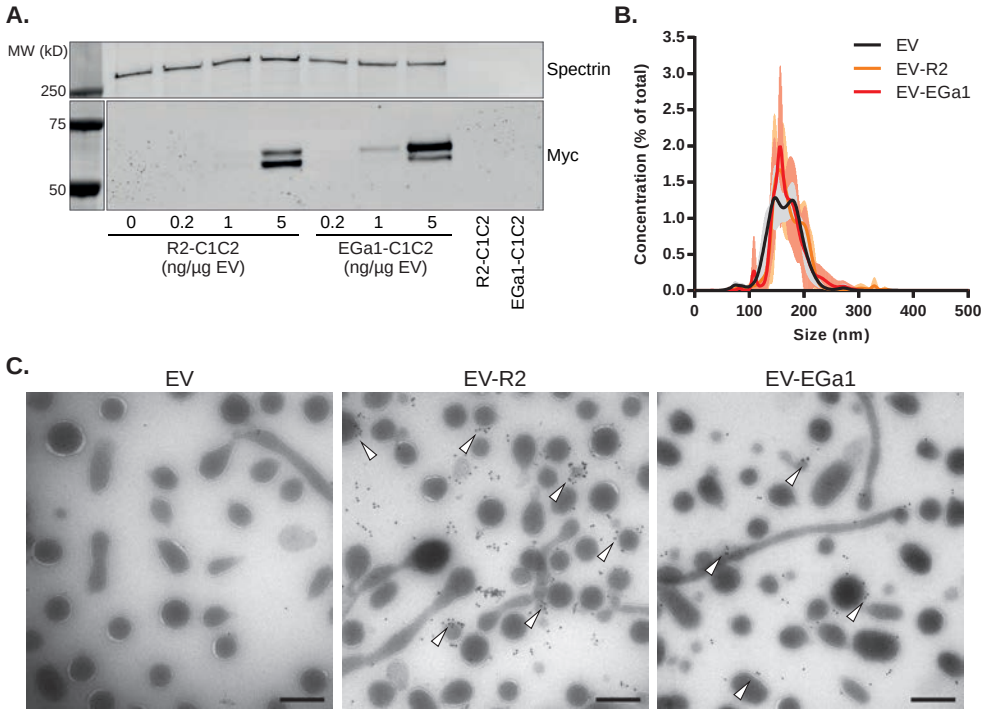

Figure 4: C1C2-nanobodies self-associate with RBC EVs in a dose-dependent manner without affecting EV size and integrity. A. Western blot of RBC EVs after decoration with increasing amounts of R2-C1C2 and EGa1-C1C2 and after SEC purification. C1C2-nanobodies were detected with anti-Myc antibodies and alpha-1-spectrin was used as a loading control for EVs. Last two lanes show typical EV fractions after loading of high concentrations of R2-C1C2 or EGa1-C1C2 (corresponding with concentrations used in lanes 4 and 7) onto the SEC column. B. Size distribution of RBC EVs after decoration with C1C2-nanobodies (40 ng/µg EV), determined by Nanoparticle Tracking Analysis. Data is displayed as mean ± SD of 5 replicate measurements. C. Transmission Electron Microscopy pictures of SEC-purified RBC EVs after decoration with R2-C1C2 (EV-R2) or EGa1-C1C2 (EV-EGa1) at a concentration of 40 ng/µg EV. Immunogold labeling was performed with anti-Myc antibodies and arrowheads indicate examples of membrane-associated gold. Scale bars represent 200 nm.

Transmission Electron Microscopy (TEM). Immunogold labeling was performed on Myc tags to analyze recombinant protein localization. EVs appeared as heterogeneous spherical structures and displayed variable electron density (Figure 4C). Furthermore, EV samples contained elongated tubular structures with lengths of up to several micrometers, which is consistent with findings in previous morphological studies [49, 50]. Control RBC EV membranes were mostly gold-negative, whereas gold clearly associated with EV membranes after EV incubations with R2-C1C2 or EGa1-C1C2. However, under these conditions also non-associated gold was observed, which might be the result of protein dissociation from EV membranes during, or

before EM sample processing. The presence of C1C2-nanobodies did not affect EV size, morphology or electron density. Interestingly, both proteins were not homogenously distributed over all EVs in the sample, but appeared to be concentrated on specific EV subpopulations instead. These subpopulations could not be characterized by particular features (e.g. low electron density or tubular/spherical size).

Effects of EV decoration with C1C2-nanobodies on EV interactions with tumor cells

To study whether decoration with C1C2-nanobodies altered the targeting specificity of RBC EVs, cell association and cell uptake assays with EGFR-negative Neuro2A cells and EGFR-overexpressing A431 cells [51] were performed. For cell association assays, cells in suspension were incubated with AlexaFluor 488 fluorescently labeled EVs for 1 hour at 4°C. The low temperature allows association, but prevents uptake of the EVs by the cells. When EVs were decorated in C1C2-nanobody/EV ratios of 2 or 10 ng/µg, association with Neuro2A cells did not change, regardless of nanobody type (Figure 5A, left panel). Remarkably, Neuro2A cell association increased slightly when EVs were decorated at a C1C2-nanobody/EV ratio of 50 ng/µg, and this effect was similar for R2-C1C2 and EGa1-C1C2. When R2-C1C2 decorated EVs were incubated with A431 cells, the same behavior was observed (Figure 5A, right panel). However, when EVs were decorated with EGa1-C1C2, association with A431 cells dramatically increased. This effect was dependent on the EGa1-C1C2/EV ratio, and reached statistical significance when EGa1-C1C2/EV ratios were ≥ 10 ng/µg. To evaluate whether this improvement in cell association translated into improved EV *uptake* by these cells, uptake assays were performed in which the same fluorescently labeled EVs were incubated with cells for 4 hours at 37°C. After incubation, cells were acid washed to remove any cell-bound material and analyzed by flow cytometry. Interestingly, under these incubation conditions, untreated EVs were barely taken up by both cell types (Figure 5B). Decoration with either R2-C1C2 or EGa1-C1C2 had no effect on EV uptake by Neuro2A cells, even when a high C1C2-nanobody/EV ratio was applied. In contrast, decoration of EVs with small amounts of EGa1-C1C2 resulted in a significantly increased EV uptake by A431 cells compared with untreated EVs or R2-C1C2 decorated EVs. Again, EV uptake was dependent on the EGa1-C1C2/EV ratio, whereas decoration with R2-C1C2 (even in a high R2-C1C2/EV ratio) did not affect EV uptake by these cells.

We next hypothesized that C1C2-nanobodies could also equip PS-exposing EVs from other cellular sources than RBCs with tumor cell targeting properties. This was tested in preliminary experiments, in which EVs were isolated from Neuro2A cells and mixed with R2-C1C2 and EGa1-C1C2. Indeed, C1C2-nanobodies dose-dependently self-associated with these EVs, whereas EV marker expression remained unaltered (Supplementary Figure 1A). Moreover, similar to RBC EVs, EGa1-C1C2 specifically enhanced binding and uptake of Neuro2A EVs by A431 cells, while binding and uptake by Neuro2A cells was unaffected or even slightly decreased (Supplementary Figure 1B and 1C, respectively).

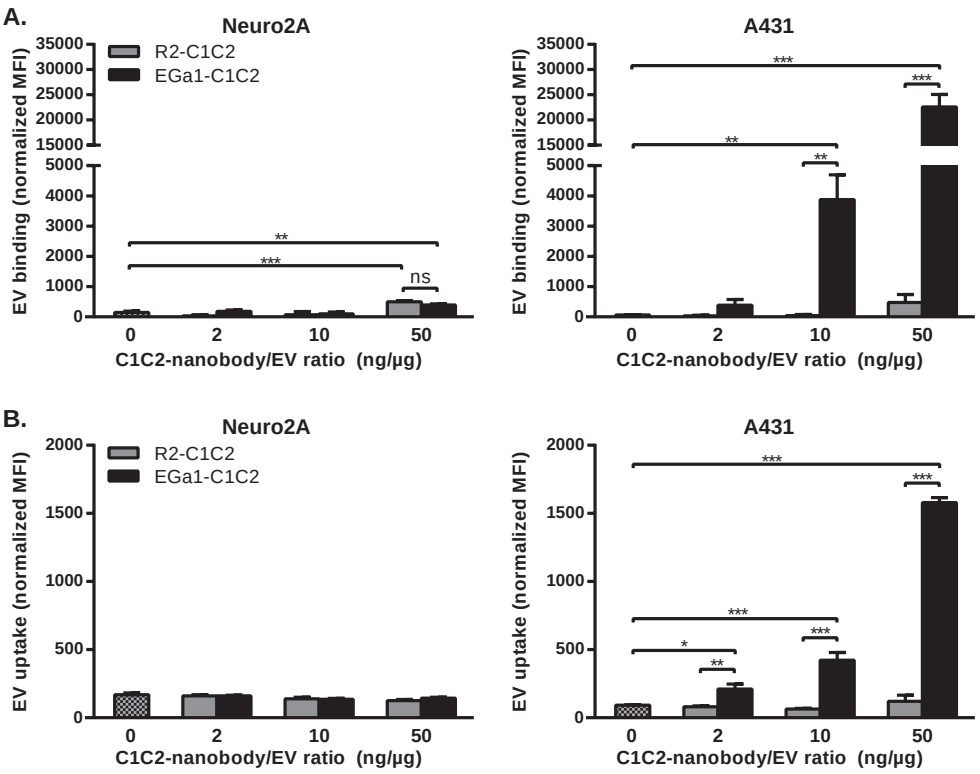

Figure 5: Decoration of RBC EVs with EGa1-C1C2 dose-dependently increases EV binding and uptake specifically by EGFR-overexpressing A431 cells. A. Binding of AlexaFluor488-labeled RBC EVs decorated with increasing amounts of C1C2-nanobodies to Neuro2A cells (left panel) and A431 cells (right panel) for 1 hour at 4°C, determined by flow cytometry. B. Uptake of AlexaFluor488-labeled RBC EVs decorated with increasing amounts of C1C2-nanobodies by Neuro2A cells (left panel) and A431 cells (right panel) for 4 hours at 37°C, determined by flow cytometry. Representative data of at least 2 replicate experiments are shown and data are displayed as mean ± SD. ns = not significant, * represents $p < 0.05$, ** $p < 0.01$, and *** $p < 0.001$ using one-way ANOVA with Tukey post-hoc test.

Discussion

In this study, we show for the first time that C1C2 domains of lactadherin can be successfully fused to nanobodies and purified from cell culture supernatants of mammalian cells, and that these can be used to improve target cell-specific binding and uptake of EVs. It has been described that the C2 domain of lactadherin, which shares homology with the C2 domains of coagulation factors V and VIII, is mainly responsible for PS-binding [28, 52]. However, the C1 domain can further improve PS-association of the C2 domain, especially when the lipid is incorporated in membranes of lipid vesicles (e.g. EVs) [29, 53, 54]. Together, C1C2 domains are therefore attractive anchoring moieties for the attachment of targeting ligands to PS-exposing EVs, given that these domains (1) show high affinity for PS (Kd = ~ 4 nM [28]),

(2) bind PS in a calcium-independent fashion [55, 56], (3) their binding to PS increases with increasing membrane curvature and hence would be expected to favor EVs over larger PS-exposing surfaces in circulation (e.g. of apoptotic cells) [56, 57], (4) may shield PS on EVs from recognition by plasma components, such as coagulation factors V and VIII [55], which may reduce their thrombogenic potential, and (5) may shield PS on EVs from direct or lactadherin-mediated PS-recognition by phagocytes in the reticulo-endothelial system (RES), which may prevent premature clearance [58, 59]. Despite these beneficial features, the use of purified C1C2 domains for the decoration of EV surfaces is limited to a single report. Delcayre and coworkers showed that these domains could be used to decorate dendritic cell-derived exosomes with cytokine sequences to elicit immune responses [29]. This work was followed-up by others who showed that cells transfected with C1C2-fusion proteins secreted EVs displaying these proteins, including tumor antigens [30-32] and reporter proteins [60, 61], on their membrane. However, these proteins were not purified, restricting their use to the transfected parent cells and corresponding EVs. Such strategies are therefore less suitable for hard-to-transfect cells, such as primary cells. The applicability of C1C2-fusion proteins can be significantly expanded by purification of these proteins. However, this process is be hampered by technical challenges, given that C1C2 domains are hydrophobic and tend to irreversibly precipitate in aqueous solutions when not associated with lipid membranes. Indeed, when the C1C2-nanobodies described here were initially expressed in *E. coli* cells, pronounced protein accumulation in inclusion bodies was observed (data not shown). Protein precipitation was slightly reduced when a mammalian expression system was employed, possibly due to post-translational modifications. Nonetheless, significant irreversible C1C2-nanobody precipitation was observed during purification of these proteins with affinity chromatography (data not shown). To overcome these issues, a stabilizing formulation was developed, which contained a mixture of neutral, positively and negatively charged amino acids, and a low concentration of BSA. This formulation significantly facilitated purification of these proteins and prevented their precipitation, even after several freeze-thaw cycles. As a result, both the N-terminal nanobody domains and the C-terminal C1C2 domains retained their functionality.

We showed that the C1C2 domains of the C1C2-nanobodies could direct specific protein association with PS, but not with other membrane lipids, including phospholipids with negatively charged head groups. As expected, this resulted in rapid association of the C1C2 nanobodies with EVs derived from Ca^{2+}-ionophore stimulated RBCs, which have been described to be predominantly PS-positive [20, 47]. Furthermore, C1C2-nanobodies self-associated with EVs from Neuro2A cells, illustrating that a substantial percentage of these EVs also expose PS. These data show that C1C2-nanobodies may be applied to equip EVs from a variety of cell types, such as circulating cells in the blood stream, which have been described to secrete large quantities of PS-positive EVs, with targeting moieties [49, 50]. Nevertheless, it should be noted that a subset of EVs may be PS-negative and hence would not be receptive to C1C2-based decoration with targeting ligands. This is in line with our TEM observations , where

C1C2-nanobodies' distribution over EVs was heterogeneous. In fact, the current dogma states that EVs which originate from direct blebbing of the plasma membrane (i.e. microvesicles or ectosomes) are PS-positive, while EVs released via fusion of multivesicular bodies with the plasma membrane (i.e. exosomes) are predominantly PS-negative [20, 40, 62]. However, in lipidomic studies even exosomes are often found to be enriched in PS compared with their parent cells [2, 16, 17]. Furthermore, exosomes typically do not contain flippase (the enzyme that actively maintains the assymetrical lipid distribution in cellular membranes). This may result in gradual PS-exposure [1] and possibly also makes exosomes amenable for C1C2 binding.

Association of C1C2-nanobodies with EVs resulted in major changes of EV-cell interactions. Whereas 'naked' RBC EVs typically showed only little binding and uptake by tumor cells, these processes were dramatically enhanced upon decoration with EGa1-C1C2, suggesting that the tropism of EVs was shifted towards EGFR-overexpressing cells. This was also the case for Neuro2A EVs, which typically already show a higher basal association and uptake by these cells. It should be noted however, that the intracellular fates of C1C2-decorated EVs remain to be investigated. Proper delivery of EV-carried nucleic acids and other molecules may require fusion of EV membranes with endosomal or plasma membranes [7]. These processes may be inhibited when EVs are directed towards an EGFR-dependent uptake mechanism. Still, given the biocompatible nature of EV manipulation using C1C2 fusion proteins (which are partly derived from naturally occurring lactadherin), it is well conceivable that EVs retain their capacity to transfer their cargo to targeted cells.

Besides these beneficial effects on EV targeting, EV decoration with C1C2-nanobodies may provide additional advantages for EVs as drug delivery systems. PS on EVs may serve as an 'eat-me' signal, signaling phagocytic cells for EV engulfment and clearance [63]. The PS-binding protein Annexin V has been described to inhibit this process, possibly due to shielding of PS recognition by phagocytes [64]. C1C2-nanobodies could fulfill a similar role, thereby prolonging the circulation time of EVs, which is typically short compared with synthetic drug delivery systems [51, 65]. To test whether this could be the case, in a small pilot experiment immunocompromised mice received intravenous administrations of DiR-labeled RBC EVs after decoration with R2-C1C2. Unfortunately, EVs were as rapidly cleared as controls and could not be detected in plasma after 20 min post-injection. EV plasma concentrations at 1 min post-injection did not differ between EVs decorated with vehicle and R2-C1C2 (Supplementary Figure 2). This may be explained by the low ratio of C1C2-nanobody to EVs, which might not have been sufficient for complete masking of all PS residues on EV surfaces. This is supported by the observation that RBC EV binding and internalization by A431 cells after decoration with EGa1-C1C2 was dependent on the C1C2-nanobody/EV ratio, but did not appear to reach a plateau, even at the highest ratio tested (50 ng C1C2-nanobody per µg EV, corresponding to approximately 200 C1C2-nanobody molecules per vesicle).

In addition to its EGFR targeting properties, EGa1-C1C2 may serve as an inhibitor of

EGFR signaling. Our data showed that EGa1-C1C2 competed with EGF for its receptor, even at a 16-fold lower molar concentration than EGF. This is in agreement with previously published data on EGa1 [41]. Furthermore, EGa1-exposing liposomes have been described to induce EGFR downregulation and inhibit proliferation of tumor cells [43, 44]. Whether this antitumor effect is also conferred to EVs after decoration with EGa1-C1C2 remains to be investigated.

In conclusion, we show that C1C2-domains can be fused to nanobodies, and purified to near-complete purity while avoiding protein precipitation. These proteins confer remarkable tumor targeting properties to EVs from RBCs and Neuro2A cells without affecting EV integrity, and could possibly be used as 'plug-and-play' EV tumor targeting tools. Furthermore, the generation of recombinant C1C2-fused proteins may be an appealing strategy to decorate EVs with other moieties, such as therapeutic proteins and imaging reporters. Future research will be focused on the delivery of EV cargo to further boost their therapeutic potential.

Acknowledgements

The work of SAAK, JJJG, PV and RMS on cell-derived membrane vesicles is supported by a European Research Council starting grant (260627) "MINDS" in the FP7 ideas program of the European Union. PV is supported by a VENI Fellowship (# 13667) from the Netherlands Organisation for Scientific Research (NWO). Dr. M.H.A.M. Fens is gratefully acknowledged for technical assistance in animal experiments.

References

1. M. Colombo, G. Raposo, C. Thery, Biogenesis, secretion, and intercellular interactions of exosomes and other extracellular vesicles, *Annu Rev Cell Dev Biol*, 30 (2014) 255-289.
2. M. Yanez-Mo, P.R. Siljander, Z. Andreu, A.B. Zavec, F.E. Borras, E.I. Buzas*, et al.*, Biological properties of extracellular vesicles and their physiological functions, *J Extracell Vesicles*, 4 (2015) 27066.
3. H. Valadi, K. Ekstrom, A. Bossios, M. Sjostrand, J.J. Lee, J.O. Lotvall, Exosome-mediated transfer of mRNAs and microRNAs is a novel mechanism of genetic exchange between cells, *Nat Cell Biol*, 9 (2007) 654-659.
4. A. Zomer, C. Maynard, F.J. Verweij, A. Kamermans, R. Schafer, E. Beerling*, et al.*, In Vivo imaging reveals extracellular vesicle-mediated phenocopying of metastatic behavior, *Cell*, 161 (2015) 1046-1057.
5. C. Thery, M. Ostrowski, E. Segura, Membrane vesicles as conveyors of immune responses, *Nat Rev Immunol*, 9 (2009) 581-593.
6. B. Costa-Silva, N.M. Aiello, A.J. Ocean, S. Singh, H. Zhang, B.K. Thakur*, et al.*, Pancreatic cancer exosomes initiate pre-metastatic niche formation in the liver, *Nat Cell Biol*, 17 (2015) 816-826.
7. S. El-Andaloussi, I. Mager, X.O. Breakefield, M.J. Wood, Extracellular vesicles: biology and emerging therapeutic opportunities, *Nat Rev Drug Discov*, 12 (2013) 347-357.
8. S.A. Kooijmans, P. Vader, S.M. van Dommelen, W.W. van Solinge, R.M. Schiffelers, Exosome mimetics: a novel class of drug delivery systems, *Int J Nanomedicine*, 7 (2012) 1525-1541.
9. S.M. van Dommelen, P. Vader, S. Lakhal, S.A. Kooijmans, W.W. van Solinge, M.J. Wood*, et al.*, Microvesicles and exosomes: opportunities for cell-derived membrane vesicles in drug delivery, *J Control Release*, 161 (2012) 635-644.
10. R. van der Meel, M.H. Fens, P. Vader, W.W. van Solinge, O. Eniola-Adefeso, R.M. Schiffelers, Extracellular vesicles as drug delivery systems: lessons from the liposome field, *J Control Release*, 195 (2014) 72-85.
11. B. Gyorgy, M.E. Hung, X.O. Breakefield, J.N. Leonard, Therapeutic applications of extracellular vesicles: clinical promise and open questions, *Annu Rev Pharmacol Toxicol*, 55 (2015) 439-464.
12. L. Alvarez-Erviti, Y. Seow, H. Yin, C. Betts, S. Lakhal, M.J. Wood, Delivery of siRNA to the mouse brain by systemic injection of targeted exosomes, *Nat Biotechnol*, 29 (2011) 341-345.
13. Y. Tian, S. Li, J. Song, T. Ji, M. Zhu, G.J. Anderson*, et al.*, A doxorubicin delivery platform using engineered natural membrane vesicle exosomes for targeted tumor therapy, *Biomaterials*, 35 (2014) 2383-2390.
14. S. Ohno, M. Takanashi, K. Sudo, S. Ueda, A. Ishikawa, N. Matsuyama*, et al.*, Systemically Injected Exosomes Targeted to EGFR Deliver Antitumor MicroRNA to Breast Cancer Cells, *Mol Ther*, 21 (2013) 185-191.
15. M.E. Hung, J.N. Leonard, Stabilization of exosome-targeting peptides via engineered glycosylation, *J Biol Chem*, 290 (2015) 8166-8172.
16. A. Llorente, T. Skotland, T. Sylvanne, D. Kauhanen, T. Rog, A. Orlowski*, et al.*, Molecular lipidomics of exosomes released by PC-3 prostate cancer cells, *Biochim Biophys Acta*, 1831 (2013) 1302-1309.
17. M. Record, K. Carayon, M. Poirot, S. Silvente-Poirot, Exosomes as new vesicular lipid transporters involved in cell-cell communication and various pathophysiologies, *Biochim Biophys Acta*, 1841 (2014) 108-120.

18. K. Segawa, S. Nagata, An Apoptotic 'Eat Me' Signal: Phosphatidylserine Exposure, *Trends Cell Biol*, 25 (2015) 639-650.

19. B. Hugel, M.C. Martinez, C. Kunzelmann, J.M. Freyssinet, Membrane microparticles: two sides of the coin, *Physiology (Bethesda)*, 20 (2005) 22-27.

20. A. Piccin, W.G. Murphy, O.P. Smith, Circulating microparticles: pathophysiology and clinical implications, *Blood Rev*, 21 (2007) 157-171.

21. C. Thery, A. Regnault, J. Garin, J. Wolfers, L. Zitvogel, P. Ricciardi-Castagnoli*, et al.*, Molecular characterization of dendritic cell-derived exosomes. Selective accumulation of the heat shock protein hsc73, *J Cell Biol*, 147 (1999) 599-610.

22. V. Luga, L. Zhang, A.M. Viloria-Petit, A.A. Ogunjimi, M.R. Inanlou, E. Chiu*, et al.*, Exosomes mediate stromal mobilization of autocrine Wnt-PCP signaling in breast cancer cell migration, *Cell*, 151 (2012) 1542-1556.

23. K. Hassani, M. Olivier, Immunomodulatory impact of leishmania-induced macrophage exosomes: a comparative proteomic and functional analysis, *PLoS Negl Trop Dis*, 7 (2013) e2185.

24. B. Fevrier, D. Vilette, F. Archer, D. Loew, W. Faigle, M. Vidal*, et al.*, Cells release prions in association with exosomes, *Proc Natl Acad Sci U S A*, 101 (2004) 9683-9688.

25. R.J. Simpson, S.S. Jensen, J.W. Lim, Proteomic profiling of exosomes: current perspectives, *Proteomics*, 8 (2008) 4083-4099.

26. P. Veron, E. Segura, G. Sugano, S. Amigorena, C. Thery, Accumulation of MFG-E8/lactadherin on exosomes from immature dendritic cells, *Blood Cells Mol Dis*, 35 (2005) 81-88.

27. J.D. Stubbs, C. Lekutis, K.L. Singer, A. Bui, D. Yuzuki, U. Srinivasan*, et al.*, cDNA cloning of a mouse mammary epithelial cell surface protein reveals the existence of epidermal growth factor-like domains linked to factor VIII-like sequences, *Proc Natl Acad Sci U S A*, 87 (1990) 8417-8421.

28. M.H. Andersen, H. Graversen, S.N. Fedosov, T.E. Petersen, J.T. Rasmussen, Functional analyses of two cellular binding domains of bovine lactadherin, *Biochemistry*, 39 (2000) 6200-6206.

29. A. Delcayre, A. Estelles, J. Sperinde, T. Roulon, P. Paz, B. Aguilar*, et al.*, Exosome Display technology: applications to the development of new diagnostics and therapeutics, *Blood Cells Mol Dis*, 35 (2005) 158-168.

30. Z.C. Hartman, J. Wei, O.K. Glass, H. Guo, G. Lei, X.Y. Yang*, et al.*, Increasing vaccine potency through exosome antigen targeting, *Vaccine*, 29 (2011) 9361-9367.

31. R.B. Rountree, S.J. Mandl, J.M. Nachtwey, K. Dalpozzo, L. Do, J.R. Lombardo*, et al.*, Exosome targeting of tumor antigens expressed by cancer vaccines can improve antigen immunogenicity and therapeutic efficacy, *Cancer Res*, 71 (2011) 5235-5244.

32. I.S. Zeelenberg, M. Ostrowski, S. Krumeich, A. Bobrie, C. Jancic, A. Boissonnas*, et al.*, Targeting tumor antigens to secreted membrane vesicles in vivo induces efficient antitumor immune responses, *Cancer Res*, 68 (2008) 1228-1235.

33. F. Ciardiello, G. Tortora, EGFR antagonists in cancer treatment, *N Engl J Med*, 358 (2008) 1160-1174.

34. N. Tebbutt, M.W. Pedersen, T.G. Johns, Targeting the ERBB family in cancer: couples therapy, *Nat Rev Cancer*, 13 (2013) 663-673.

35. H. Revets, P. De Baetselier, S. Muyldermans, Nanobodies as novel agents for cancer therapy, *Expert Opin Biol Ther*, 5 (2005) 111-124.

36. S. Ewert, C. Cambillau, K. Conrath, A. Pluckthun, Biophysical properties of camelid V(HH) domains compared to those of human V(H)3 domains, *Biochemistry*, 41 (2002) 3628-3636.

37. E. Dolk, C. van Vliet, J.M. Perez, G. Vriend, H. Darbon, G. Ferrat*, et al.*, Induced refolding of a temperature denatured llama heavy-chain antibody fragment by its antigen, *Proteins*, 59 (2005) 555-564.

38. C. Winzler, P. Rovere, M. Rescigno, F. Granucci, G. Penna, L. Adorini*, et al.*, Maturation stages of mouse dendritic cells in growth factor-dependent long-term cultures, *J Exp Med*, 185 (1997) 317-328.

39. M. Miyanishi, K. Tada, M. Koike, Y. Uchiyama, T. Kitamura, S. Nagata, Identification of Tim4 as a phosphatidylserine receptor, *Nature*, 450 (2007) 435-439.

40. H.F. Heijnen, A.E. Schiel, R. Fijnheer, H.J. Geuze, J.J. Sixma, Activated platelets release two types of membrane vesicles: microvesicles by surface shedding and exosomes derived from exocytosis of multivesicular bodies and alpha-granules, *Blood*, 94 (1999) 3791-3799.

41. E.G. Hofman, M.O. Ruonala, A.N. Bader, D. van den Heuvel, J. Voortman, R.C. Roovers*, et al.*, EGF induces coalescence of different lipid rafts, *J Cell Sci*, 121 (2008) 2519-2528.

42. L.G. Frenken, R.H. van der Linden, P.W. Hermans, J.W. Bos, R.C. Ruuls, B. de Geus*, et al.*, Isolation of antigen specific llama VHH antibody fragments and their high level secretion by Saccharomyces cerevisiae, *J Biotechnol*, 78 (2000) 11-21.

43. S. Oliveira, R.M. Schiffelers, J. van der Veeken, R. van der Meel, R. Vongpromek, P.M. van Bergen En Henegouwen*, et al.*, Downregulation of EGFR by a novel multivalent nanobody-liposome platform, *J Control Release*, 145 (2010) 165-175.

44. R. van der Meel, S. Oliveira, I. Altintas, R. Haselberg, J. van der Veeken, R.C. Roovers*, et al.*, Tumor-targeted Nanobullets: Anti-EGFR nanobody-liposomes loaded with anti-IGF-1R kinase inhibitor for cancer treatment, *J Control Release*, 159 (2012) 281-289.

45. S.H. Paik, Y.J. Kim, S.K. Han, J.M. Kim, J.W. Huh, Y.I. Park, Mixture of three amino acids as stabilizers replacing albumin in lyophilization of new third generation recombinant factor VIII GreenGene F, *Biotechnol Prog*, 28 (2012) 1517-1525.

46. C. Subra, K. Laulagnier, B. Perret, M. Record, Exosome lipidomics unravels lipid sorting at the level of multivesicular bodies, *Biochimie*, 89 (2007) 205-212.

47. R.L. Koshiar, S. Somajo, E. Norstrom, B. Dahlback, Erythrocyte-derived microparticles supporting activated protein C-mediated regulation of blood coagulation, *PLoS One*, 9 (2014) e104200.

48. P.E. Van Der Meijden, M. Van Schilfgaarde, R. Van Oerle, T. Renne, H. ten Cate, H.M. Spronk, Platelet- and erythrocyte-derived microparticles trigger thrombin generation via factor XIIa, *J Thromb Haemost*, 10 (2012) 1355-1362.

49. N. Arraud, C. Gounou, R. Linares, A.R. Brisson, A simple flow cytometry method improves the detection of phosphatidylserine-exposing extracellular vesicles, *J Thromb Haemost*, 13 (2015) 237-247.

50. N. Arraud, R. Linares, S. Tan, C. Gounou, J.M. Pasquet, S. Mornet*, et al.*, Extracellular vesicles from blood plasma: determination of their morphology, size, phenotype and concentration, *J Thromb Haemost*, 12 (2014) 614-627.

51. S.A.A. Kooijmans, L.A.L. Fliervoet, R. van der Meel, M.H.A.M. Fens, H.F.G. Heijnen, P.M.P. van Bergen en Henegouwen*, et al.*, PEGylated and targeted extracellular vesicles display enhanced cell specificity and circulation time, *Journal of Controlled Release*, 224 (2016) 77-85.

52. C. Shao, V.A. Novakovic, J.F. Head, B.A. Seaton, G.E. Gilbert, Crystal structure of lactadherin C2 domain at 1.7A resolution with mutational and computational analyses of its membrane-binding motif, *J Biol Chem*, 283 (2008) 7230-7241.

53. H. Wakabayashi, A.E. Griffiths, P.J. Fay, Factor VIII lacking the C2 domain retains cofactor activity in vitro, *J Biol Chem*, 285 (2010) 25176-25184.

54. K. Oshima, N. Aoki, T. Kato, K. Kitajima, T. Matsuda, Secretion of a peripheral membrane protein, MFG-E8, as a complex with membrane vesicles, *Eur J Biochem*, 269 (2002) 1209-1218.

55. J. Shi, G.E. Gilbert, Lactadherin inhibits enzyme complexes of blood coagulation by competing for phospholipid-binding sites, *Blood*, 101 (2003) 2628-2636.

56. D.E. Otzen, K. Blans, H. Wang, G.E. Gilbert, J.T. Rasmussen, Lactadherin binds to phosphatidylserine-containing vesicles in a two-step mechanism sensitive to vesicle size and composition, *Biochim Biophys Acta*, 1818 (2012) 1019-1027.

57. J. Shi, C.W. Heegaard, J.T. Rasmussen, G.E. Gilbert, Lactadherin binds selectively to membranes containing phosphatidyl-L-serine and increased curvature, *Biochim Biophys Acta*, 1667 (2004) 82-90.

58. K.S. Ravichandran, Beginnings of a good apoptotic meal: the find-me and eat-me signaling pathways, *Immunity*, 35 (2011) 445-455.

59. S.K. Dasgupta, H. Abdel-Monem, P. Niravath, A. Le, R.V. Bellera, K. Langlois, *et al.*, Lactadherin and clearance of platelet-derived microvesicles, *Blood*, 113 (2009) 1332-1339.

60. Y. Takahashi, M. Nishikawa, H. Shinotsuka, Y. Matsui, S. Ohara, T. Imai, *et al.*, Visualization and in vivo tracking of the exosomes of murine melanoma B16-BL6 cells in mice after intravenous injection, *J Biotechnol*, 165 (2013) 77-84.

61. M. Morishita, Y. Takahashi, M. Nishikawa, K. Sano, K. Kato, T. Yamashita, *et al.*, Quantitative analysis of tissue distribution of the B16BL6-derived exosomes using a streptavidin-lactadherin fusion protein and iodine-125-labeled biotin derivative after intravenous injection in mice, *J Pharm Sci*, 104 (2015) 705-713.

62. M. Kanada, M.H. Bachmann, J.W. Hardy, D.O. Frimannson, L. Bronsart, A. Wang, *et al.*, Differential fates of biomolecules delivered to target cells via extracellular vesicles, *Proc Natl Acad Sci U S A*, 112 (2015) E1433-1442.

63. L.A. Mulcahy, R.C. Pink, D.R. Carter, Routes and mechanisms of extracellular vesicle uptake, *J Extracell Vesicles*, 3 (2014) 24641.

64. K. Yuyama, H. Sun, S. Mitsutake, Y. Igarashi, Sphingolipid-modulated exosome secretion promotes clearance of amyloid-beta by microglia, *J Biol Chem*, 287 (2012) 10977-10989.

65. C.P. Lai, O. Mardini, M. Ericsson, S. Prabhakar, C.A. Maguire, J.W. Chen, *et al.*, Dynamic biodistribution of extracellular vesicles in vivo using a multimodal imaging reporter, *ACS Nano*, 8 (2014) 483-494.

66. J.Z. Nordin, Y. Lee, P. Vader, I. Mager, H.J. Johansson, W. Heusermann, *et al.*, Ultrafiltration with size-exclusion liquid chromatography for high yield isolation of extracellular vesicles preserving intact biophysical and functional properties, *Nanomedicine*, 11 (2015) 879-883.

Supplementary Methods

Isolation and labeling of Neuro2A EVs

Neuro2A cells were seeded in T175 flasks and cultured for 24 hours, after which medium was replaced by Opti-MEM Reduced Serum medium supplemented with GlutaMAX (Gibco, Thermo Fisher Scientific) and 100 U/mL penicillin, 100 U/mL streptomycin. Cells were allowed to produce EVs for 48 hours. EVs were isolated according to a previously described 'ultrafiltration followed by liquid-chromatography' method (UF-LC [66]). In brief, conditioned medium was cleared of cells and debris by centrifugation at 300g and 2000g for 10 min at 4°C, followed by vacuum driven filtration through 0.22 µm Steritop filters (Merck Millipore). Medium was concentrated to < 4 mL using Amicon Ultra-15 Centrifugal Filter Units with a 100 kD MWCO (Merck Millipore) at 4000g and 4°C, and loaded onto a HiPrep 16/60 Sephacryl S-400 HR gel filtration column (GE Healthcare Life Sciences), which was equilibrated with phosphate buffered saline (PBS) and connected to a refrigerated ÄKTA pure chromatography system. EVs were eluted at 0.6 mL/min, and EV containing fractions (as visualized by UV absorbance at 280 nm) were again concentrated on 100 kD MWCO Amicon Ultra-15 Centrifugal Filter Units. Immediately after isolation, EVs were mixed with 10 µM CellTracker Deep Red fluorescent dye (Thermo Fisher Scientific, diluted from 2 mM stock in DMSO) and incubated for 1 hour at 37°C. EVs were purified from unbound dye using Sepharose CL-4B SEC and concentrated on 100 kD Vivaspin tubes. Protein concentrations were determined using a MicroBCA Protein Assay Kit.

Western blot analysis of Neuro2A EVs

Western blot analysis was performed as described under "Methods". Additional primary antibodies included mouse anti-ALIX (1:1000, clone 3A9, Abcam), rabbit anti-TSG101 (1:1000, ab30871, Abcam) and rabbit anti-CD9 (1:2500, clone EPR2949, Abcam).

In vivo circulation time of RBC EVs

All animal experiments were performed with approval from the Utrecht Animal Welfare Body of the UMC Utrecht, and animal care was according to established guidelines. Six female Crl:NU-Foxn1nu mice (25-30g) from Charles River International Laboratories, Inc. (Germany) were provided with free access to water and a chlorophyll-reducing chow (2016S, Harlan Laboratories, The Netherlands) to reduce organ autofluorescence. RBC EVs were labeled with 5 µM DiR (diluted from a 1 mM DiR stock in DMSO) for 1 hour at room temperature, and purified using Sepharose CL-4B SEC. Protein concentrations were determined, EVs were decorated with either 85 ng R2-C1C2 per µg of EVs or an equal volume of OSB, and EVs were purified again using SEC. To exclude the presence of aggregates, EVs were filtered through 0.45 µm syringe filters (Millipore). Protein and particle concentrations were measured using MicroBCA Protein Assay Kit and NTA, respectively. Mice were injected intravenously in the tail vein with 50 µg DiR-labeled EVs (corresponding to approximately $1.6*10^{11}$ particles) in 100 µL PBS. Blood samples

were collected in EDTA anti-coagulated tubes by submandibular vein punctures at 1, 20 min post-injection (n = 3 per time point). 60 min post-injection, mice were sacrificed by cervical dislocation, and additional blood samples were collected via heart puncture. Blood samples were centrifuged for 10 min at 2000g and 4°C and platelet-poor plasma was collected and stored at -80°C. DiR fluorescence in plasma samples was determined using an Odyssey Infrared Imager at 800 nm, and plasma concentrations were calculated using a calibration curve of DiR-labeled EVs in mouse plasma as previously described [51].

Supplementary Figures

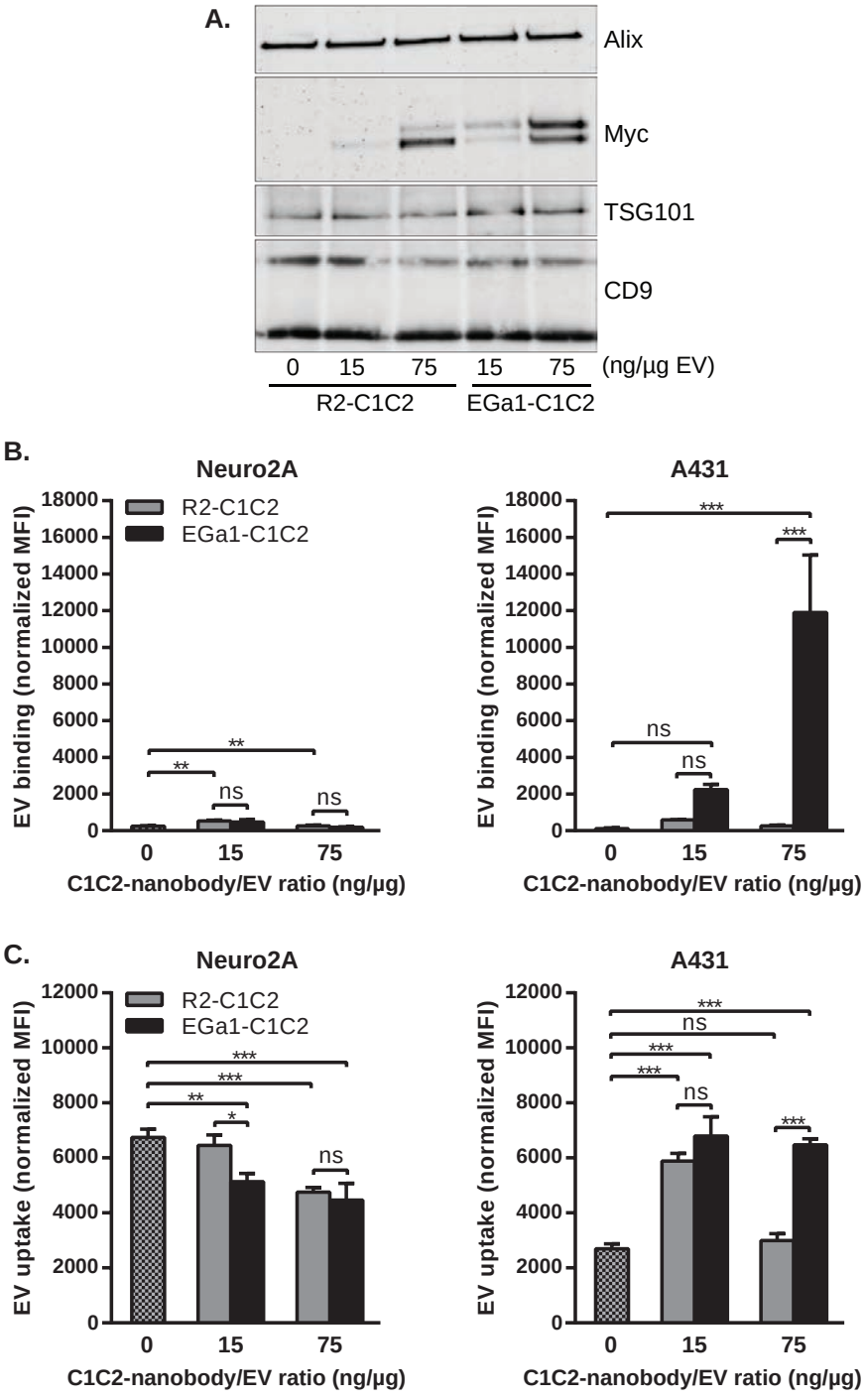

Supplementary Figure 1: C1C2-nanobodies dose-dependently bind to Neuro2A EVs and enhance EGFR-dependent EV binding and uptake by tumor cells. A. Western blot of Neuro2A EVs after decoration with increasing amounts of R2-C1C2 and EGa1-C1C2 and after SEC purification. C1C2-nanobodies were detected with anti-Myc antibodies and EV markers Alix, TSG101 and CD9 were used as loading controls. B. Binding of CellTracker Deep Red-labeled Neuro2A EVs decorated with increasing amounts of C1C2-nanobodies to Neuro2A cells (left panel) and A431 cells (right panel) for 1 hour at 4°C, determined by flow cytometry. B. Uptake of CellTracker Deep Red-labeled Neuro2A EVs decorated with increasing amounts of C1C2-nanobodies by Neuro2A cells (left panel) and A431 cells (right panel) for 4 hours at 37°C, determined by flow cytometry. Data are displayed as mean ± SD. ns = not significant, ** represents $p < 0.01$ and *** $p < 0.001$ using one-way ANOVA with Tukey post-hoc test.

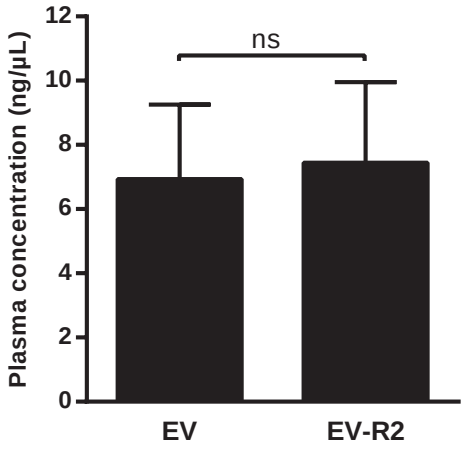

Supplementary Figure 2: Decoration of RBC EVs with R2-C1C2 does not increase EV circulation time. EVs were labeled with DiR, decorated with 85 ng R2-C1C2 per µg of EVs, and 50 µg of EVs was intravenously administered to immunodeficient mice. Plasma concentration was measured 1 min after injection. Data are displayed as mean ± SD (n=3). ns = not significant using independent samples t test.

Supplementary Table

Supplementary Table 1: Sequences of used primers and oligonucleotides.

Name	Sequence (5'-3')
Fw_C1C2	ATTGCGGCCGCAGGCGGTGGAGGCAGCGGTGGCGGGGGTAGCTGTTCTACA CAGCTGGGC
Rv_C1C2	AATCGGCCGAGCCCTGAAAATACAGGTTTTCCTTAAGACAGCCCAGCAGCTC
Igκ chain leader sequence	ATGGAGACAGACACACTCCTGCTATGGGTACTGCTGCTCTGGGTTCCAGGTTC CACTGGTGAC

CHAPTER 7

Exosome mimetics: a novel class of drug delivery systems

Sander A.A. Kooijmans[1], Pieter Vader[1], Susan M. van Dommelen[1], Wouter W. van Solinge[1], Raymond M. Schiffelers[1]

[1]Department of Clinical Chemistry and Haematology, University Medical Center Utrecht, Utrecht, The Netherlands

International Journal of Nanomedicine, 2012. 7, 1525-41

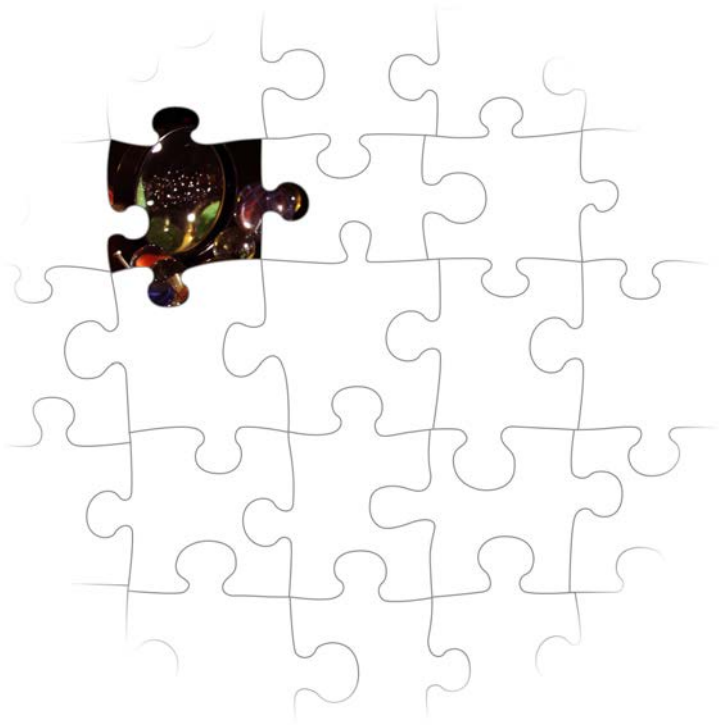

Abstract

The identification of extracellular phospholipid vesicles as conveyors of cellular information has created excitement in the field of drug delivery. Biological therapeutics, including siRNA and recombinant proteins, are prone to degradation, have limited ability to cross biological membranes and may elicit immune responses. Therefore, delivery systems for such drugs are under intensive investigation. Exploiting extracellular vesicles as carriers for biological therapeutics is a promising strategy to overcome these issues and to achieve efficient delivery to the cytosol of target cells. Exosomes are a well-studied class of extracellular vesicles known to carry proteins and nucleic acids, making them especially suitable for such strategies. However, the considerable complexity and the related high chance of off-target effects of these carriers are major barriers for translation to the clinic. Given that it is well possible that not all components of exosomes are required for their proper functioning, an alternative strategy would be to synthetically mimic these vesicles. By assembly of liposomes harboring only crucial components of natural exosomes, functional exosome mimetics (EMs) may be created. The low complexity and the use of well-characterized components strongly increase the pharmaceutical acceptability of such systems. However, exosomal components that would be required for the assembly of functional EMs remain to be identified. This review provides insights on the composition and functional properties of exosomes, and focuses on components which could be used to enhance the drug delivery properties of EMs.

Introduction

Cells are well known to communicate via soluble mediators or cell-cell contact, but in the last decades also intercellular communication through extracellular vesicles has increasingly gained attention. The first notion of such vesicles arose when Wolf described the formation of 'platelet dust' upon storage of blood platelets [1]. These phospholipid-rich particles were shown to exert coagulant activity and were later determined to be actively shed membrane-derived vesicles [2]. Since then our knowledge about such vesicles has expanded dramatically, and vesicle secretion is now widely accepted to occur in most, if not all, cell types. Characterization studies identified three main populations of extracellular vesicles, which are commonly classified based on their intracellular origin. Cells that undergo apoptosis fractionate their cellular content into subcellular apoptotic bodies (ABs) in order to prevent leakage of possibly toxic or immunogenic cellular contents into the extracellular matrix (Figure 1, left panel) [3]. ABs appear as a heterogeneous group of vesicles with sizes ranging from 50 nm to 5 µm and a buoyant density of 1.16-1.28 g/mL [4-7]. They contain a variety of cellular contents, including DNA, RNA and histones, and display 'eat-me' signaling molecules, causing them to be rapidly cleared by macrophages [8, 9]. Due to their specific cellular content and high density, they may be distinguished from two other major vesicle populations, which show considerably more overlap.

One of these populations originates from budding and fission from the plasma membrane into the extracellular space (Figure 1, middle panel) and contains vesicles of about 50 - 1000 nm in size. Such vesicles are interchangingly referred to as microvesicles [10], ectosomes [11], shedding vesicles [12], microparticles [13, 14], plasma membrane-derived vesicles [15] or even exovesicles [16]. In order to avoid confusion and promote standardization of nomenclature, in this review the term 'microvesicles' (MVs) will be used to denote this vesicle population. The buoyant density of MVs is still not well defined [7] and also the intracellular mechanisms for vesicle release remain unclear. MV secretion may take place in resting cells, but the vesicle shedding rate increases dramatically upon stimulation. The stimuli and intensity of stimuli required for vesicle formation can vary among cell types. As a common principle, increasing intracellular levels of Ca^{2+} result in increased secretion of MVs [17, 18]. For example, erythrocytes can be stimulated with high levels of extracellular Ca^{2+} in combination with a suitable ionophore [19, 20]. In various human tumor cell lines MV production was increased at extracellular Ca^{2+} concentrations up to 25 mM, however concentrations of higher than 10 mM also decreased cell viability [21]. Other common stimulators for MV release include lipopolysaccharide (LPS) for monocytes [22], and activation of the $P2X_7$ receptor with ATP for macrophages and other myeloid cells [23, 24].

The last population of secreted membrane vesicles comprises exosomes, which differ from MVs mainly in their intracellular origin. Whereas MVs are supposedly generated from the budding from the plasma membrane, exosomes appear to be formed by tightly controlled inward budding into large multivesicular bodies (MVBs) in the cytosol. These MVBs are able

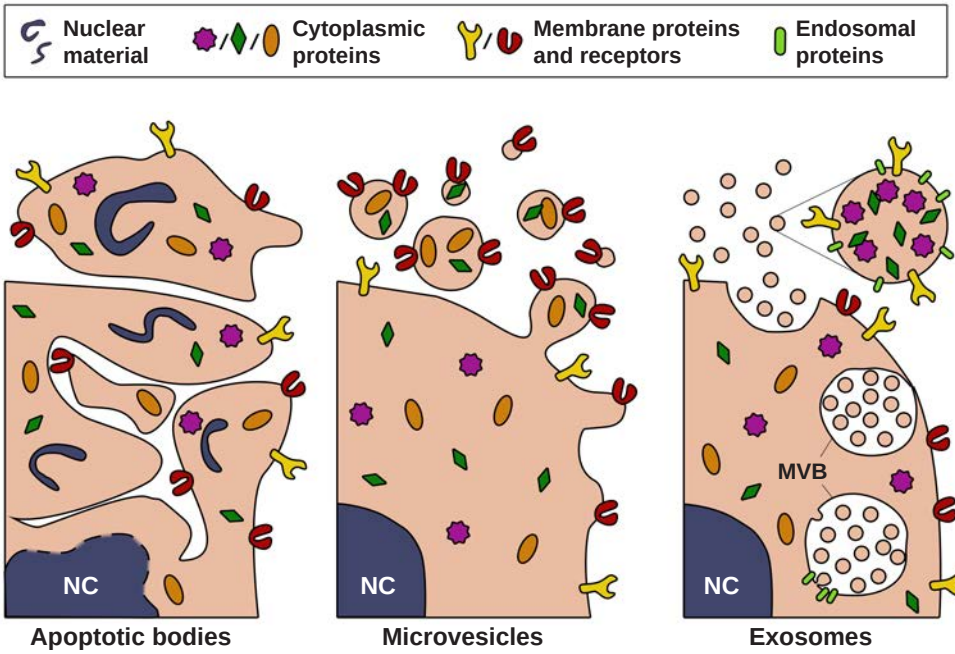

Figure 1: Schematic presentation of the biogenesis and composition of the three main classes of extracellular vesicles. Apoptotic bodies (left panel) are formed when cells enter apoptosis, and may contain nuclear material such as histones and DNA. They are heterogenous in size (50 – 5000 nm), irregularly shaped and harbor a variety of cellular proteins. Microvesicles (middle panel) are formed by budding and subsequent fission of the plasma membrane. Selective incorporation of membrane proteins and cytosolic proteins takes place during formation, resulting in vesicles which may be enriched in specific proteins and lipids compared to the parent cell. Microvesicles are thought to be smaller than apoptotic bodies (50-1000 nm) and more homogenously shaped. Selective enrichment of cellular content also occurs during the formation of exosomes (right panel), however exosomes originate from budding into the limiting membrane of large endosomal structures named multivesicular bodies (denoted with MVB). This process is facilitated by endosomal proteins. Subsequent fusion of MVBs with the plasma membrane results in release of the exosomes. Exosomes are small (< 100 nm), relatively homogenous in size, and may contain (endosomal) proteins involved in their assembly, such as CD9, Alix and TSG101. NC: nucleus.

to fuse with the plasma membrane, causing the release of exosomes into the extracellular space (Figure 1, right panel) [25]. In theory exosomes and MVs are clearly distinguishable by their origin, however in practice such a distinction is seldom possible. Therefore attempts are made to characterize and separate both populations based on phenotypical features, such as buoyant density, size, morphology and protein and lipid composition. Exosomes typically share characteristics with the vesicles inside MVBs. They are commonly 40 -100 nm in size [26]. although somewhat larger diameters have been reported [27]. When analysed with electron microscopy, exosomes show a typical cup-shaped morphology [28], however in biological

fluids they are likely to exist as spherical structures [29]. In addition to being more homogenous in size than MVs, they are believed to be more dense and float on a sucrose density gradient at heights of 1.13-1.19 g/mL [26]. Furthermore, exosomes often contain specific proteins which are incorporated during the formation process in MVBs, such as Alix, TSG101 and tetraspanins (CD9, CD63) [7, 30], which are frequently used as markers for their identification.

Exosomes and MVs are involved in a large variety of body processes. They are concentrated carriers of genetic and proteomic information, and thus they are believed to play important roles in intercellular communication. Secreted vesicles can transfer their messages in different ways. Firstly, they may activate target cells via ligands expressed on their surface. For example, it has been demonstrated that antigen presenting exosomes derived from dendritic cells provoke T-cell mediated immune responses *in vivo* [31]. In addition to eliciting immune responses, ligand-receptor signaling via exosomes can also play a role in other regulatory processes, such as angiogenesis [32], hemostasis [33] and cancer progression [34]. Secondly, secreted vesicles may transfer surface receptors from one cell to another by budding and subsequent fusion with plasma membranes of target cells [35, 36]. This mechanism may be exploited by the human immunodeficiency virus, increasing the susceptibility of infection by transferring CD4 receptors from infected cells to non-infected cells [37]. Additionally, the shedding of MVs has been proposed to be a mechanism by which cells protect themselves from potentially harmful substances [12]. A third mechanism of action is based on the horizontal transfer of proteins and genetic material, such as micro RNAs (miRNA), between cells. Cytosolic content of a donor cell can be transferred directly to the recipient cell following fusion or internalization of MVs and exosomes [38, 39]. This results in the release of cargo in the cytosol of the target cell and subsequent intracellular signaling. An example of protein transfer between cells has recently been presented by Sarkar *et al.*, who elegantly demonstrated that the intracellular apoptotic protein caspase-1 was transferred between monocytes and vascular smooth muscle cells via MVs, inducing apoptosis in the latter [40]. The encapsulation of caspase-1 in MVs was shown to be necessary for the apoptotic effect of the enzyme.

First evidence of exosome-mediated transfer of mRNAs and miRNAs was recently presented by Valadi *et al.*, who showed that exosomes from mouse mast cells contained substantial amounts of RNA [41]. Many of the miRNAs were enriched compared to the parent cells, indicative of a selective incorporation process. Furthermore, mouse exosomes containing mRNA could be taken up by human mast cells, which resulted in the expression of mouse proteins in these cells. Additional evidence of functional miRNA transfer by exosomes was provided by Montecalvo *et al.*, who showed that exosomes released from dendritic cells contained a variety of miRNAs.[42] These exosomes were taken up by acceptor dendritic cells and effectively repressed target mRNA expression. Thus, while it has been suggested that only a minority of all circulating miRNA is confined within exosomes [43, 44], exosomal miRNA may potently regulate gene expression in target cells *in vivo*. In addition to mRNA and miRNA, also mitochondrial DNA (mtDNA) has been found in exosomes of astrocytes, myoblasts

and glioblastoma cells [45, 46]. Given that horizontal transfer of RNA by exosomes or MVs is important for cellular communication, vesicle-associated RNA may also serve as a diagnostic tool in disease. Disease states may cause specific miRNAs to be enriched in extracellular vesicles compared to healthy controls. For example, extracellular vesicles from patients with prostate cancer were selectively enriched in miR-141 compared to healthy controls [47], and EGFRvIII mRNA in circulating MVs was associated with clinically distinct subtypes of glioblastoma [48]. Viral infections may also be detected by analysis of exosomal RNA content [49].

Exosomes and MVs are naturally adapted for the transport and intracellular delivery of proteins and nucleic acids. This makes them particularly attractive for the delivery of pharmaceutical proteins and nucleic acids, such as short interfering RNA (siRNA). Intracellular delivery of siRNA is a challenging task, given that (i) naked siRNAs are rapidly degraded in the circulation, (ii) their large size and negative charge limits membrane passage and cellular uptake, (iii) some siRNA sequence motifs may elicit undesired immune responses, and (iv) targeting to specific tissues and cells is required to reduce adverse effects caused by off-target silencing [50, 51]. Encapsulation of nucleic acid-based therapeutics in endogenous transporting vesicles is a promising novel strategy to overcome most of these delivery issues. Exosomes may be most suitable for such strategies, as they are small (40-100 nm), relatively homogenous in size, and well studied. Their size <100 nm is advantageous for their use as drug delivery systems, as this allows them to evade rapid clearance by the mononuclear phagocyte system and enhances passage through fenestrations in the vessel wall as might occur during inflammation [52].

Exosome-based drug delivery systems: biotechnological versus synthetic approaches

The successful use of exosomes for the targeted delivery of siRNA has been recently demonstrated by Alvarez-Erviti *et al.* [53]. They harvested dendritic cells from mice and transfected them to express the neuronal targeting ligand RVG coupled to the exosomal membrane protein Lamp2b. This protein was expressed by the cells and incorporated in secreted exosomes. The exosomes were harvested, purified and loaded with siRNA against an important protein in Alzheimer pathogenesis (BACE1) by electroporation. When the modified exosomes were intravenously injected in wild-type mice, a 60% decrease of *BACE1* mRNA in the brain cortex was observed after three days. This ultimately resulted in a decrease (55%) of the harmful β-amyloid 1-42 protein in the brain. Moreover, no increase in IL-6, IP-10, TNF-α and IFN-α serum concentrations was observed after injection of the exosomes, suggesting that the modified exosomes were immunologically inert. However, immunological responses to repeated administration of exosomes were not evaluated, albeit repeated administration of exosomes loaded with siRNA against *GAPDH* did not result in a loss in silencing efficiency.

The biotechnological approach to create exosome-based delivery systems used by Alvarez-Erviti *et al.* was the first demonstration of an exosome-based drug delivery system

which showed efficient *in vivo* delivery of siRNA [53]. Other strategies to exploit exosomes for therapeutic purposes have also been reported. In 2005, Delcayre *et al.* described an 'exosome display technology' in which various antigens were fused to the C1C2 domain of lactadherin [54]. This protein domain binds to the lipid phosphatidylserine exposed by exosomes [55], resulting in the presentation of the fused antigen to the immune system. When CHO cells were transfected with fusion constructs of C1C2 and interleukin-2 (IL-2) or granulocyte/monocyte colony-stimulating factor (GM-CSF), the exosomes derived from these cells were significantly enriched with the recombinant cytokines compared to the parent cells. Moreover, the recombinant exosomes were able to induce proliferative responses in IL-2 and GM-CSF dependent cell lines, respectively [54]. The therapeutic potential of C1C2-coupled antigen display by exosomes was further explored in subsequent studies. These showed that tumors secreting exosome-bound ovalbumin grew slower than tumors secreting soluble ovalbumin, due to an enhanced immune stimulatory effect of the former [56]. Furthermore, the tumor-associated antigens carcinoembryonic antigen (CEA) and HER2 elicited potent anti-tumor immune responses when recombinantly coupled to exosomes [57]. Anti-tumor potential of this approach was also demonstrated in two prostate cancer models, in which tumor growth was severely attenuated by vaccination with exosomes displaying the tumor antigens prostate-specific antigen (PSA) or prostatic acid phosphatase (PAP) [58]. The feasibility of anti-tumor therapy based on immune stimulatory exosomes was evaluated in two phase I trials [59, 60]. In these trials, dendritic cells of patients with stage III/IV melanoma were isolated and pulsed with MAGE3 tumor antigens. Exosomes presenting MAGE3 were isolated and re-administered to melanoma patients. Therapy appeared to be well tolerated by all patients and induced the desired immune effects in some patients, showing clinical feasibility for exosome-based therapeutics.

In addition to C1C2-coupling, therapeutics may also be non-specifically bound to exosomes. This was recently demonstrated by Sun *et al.*, who showed that mixing curcumin with exosomes enhanced its bioavailability, stability and solubility and improved its anti-inflammatory activity in an *in vivo* LPS-induced septic shock model compared to curcumin alone [61]. Furthermore, intranasally administered mouse lymphoma exosomes facilitated curcumin and stat3 inhibitor delivery to brain microglia, inducing anti-inflammatory and anti-tumor effects, respectively [62].

The examples mentioned above all use endogenous exosomes in their full complexity (or with only minimal modifications to their natural content) to deliver therapeutic cargo. This may offer a range of advantages over conventional drug delivery systems, such as viral or synthetic (non-viral) nanoparticles. Virus-based drug delivery systems have some of the advantages of natural viruses, including their excellent capacity to invade host cells and incorporate their viral load into the host genome [63]. However, their potential of insertional mutagenesis or oncogenesis, high production costs and risk of immunogenicity limit their clinical use [64]. Non-viral drug delivery vehicles, such as cationic polyplexes and lipoplexes,

are generally considered to be less immunogenic and mutagenic, however cytotoxicity and low transfection efficiencies *in vivo* are still major challenges to overcome [64, 65].

Exosome-based drug delivery systems may provide unique advantages over other systems, including (i) limited or no undesired immunogenicity when self-derived exosomes are used, (ii) greater stability in the blood due to evasion of complement and coagulation factors [66], (iii) efficient delivery of cargo into the cytosol of the target cell, and (iv) possibly less off-target effects due to the natural tendency of exosomes to act on specific target cells.

Despite these advantages, there are still some major obstacles and challenges to overcome before endogenous exosomes may be used in a clinical setting. Naturally derived exosomes are complex structures which are difficult to pharmaceutically characterize. In addition, they have complicated roles in health and disease, which are still poorly understood [27, 67, 68]. They may therefore induce adverse effects when used in pharmaceutical preparations. Thorough characterization of exosome content and function is required to avoid such issues. Furthermore, biological fluids contain a mixture of extracellular vesicle populations from various cell types. The purification of single populations of cell-specific vesicles (e.g. cancer cell-derived exosomes) still provides a barrier which hinders translation to the clinic. Highly purified populations of exosomes may be obtained from exosome-secreting cell lines, however such exosomes may lack 'self'-signals and elicit undesired immune responses. In addition, nanotechnological approaches for scalable production and efficient loading of exosomes are lacking, and remain an area of investigation [69].

A viable alternative for biotechnologically tailored exosome-based drug delivery systems are synthetic exosome mimetics (EMs). It is well possible that not all components in natural exosomes are required for specific and efficient delivery of cargo to the target cell. By extensive characterization of lipid, protein and nucleic acid content of exosomes, only functional components could be used for selective incorporation in EMs. Given that natural exosomes exist as spherical lipid bilayer structures, liposomes would provide a logical basis for the generation of EMs. Similar to exosomes, liposomes are bilayered phospholipid structures with (adjustable) diameters around 100 nm, which can be loaded with a variety of proteins, nucleic acids, or drug molecules [70, 71]. Liposomes have been shown to be valuable tools in drug delivery; several liposome-based drug delivery systems are currently in preclinical development and clinical trials, while others have been approved for clinical development (for review see [71]). The tailoring of liposomes to mimic exosomes could therefore provide a springboard for a novel class of non-viral drug delivery systems. Such drug delivery systems would have the benefits of endogenous exosomes (e.g. limited immunogenicity, efficient cargo delivery, enhanced stability in body fluids), but could diminish some of the anticipated problems with biotechnologically engineered exosomes. Production of EMs is more easily scalable for use in preclinical or clinical settings. In addition, the assembly process of EMs is controllable and results in the formation of 'clean', well characterized drug delivery systems with high pharmaceutical acceptability. Moreover, the use of EMs allows us to study the effect

of each component separately. However, the components which are likely to be required for proper functioning of EMs as drug delivery systems are yet not well defined in literature. Therefore this review aims to describe potential candidate components for the assembly of functional EMs.

Lipids

In 2009 an initiative was taken by Mathivanan and Simpson to create an online database of all studies on exosomal protein and nucleic acid content, named ExoCarta [72]. This allows scientists to catalogue exosome-specific proteomic and genomic data and make them available to other scientists in the field. ExoCarta has grown steadily since its development, and now contains 134 studies covering data of 4,049 proteins, 1,639 mRNAs and 764 miRNAs. As it is increasingly understood that not only proteins and nucleic acids contribute to exosomal function, recently also the feature to include data on exosomal lipids in the database has been added [73]. At this moment, only a handful of lipids has been registered in Exocarta, including four prostaglandins (E_2, F_2, J_2 and D_2) and the conical lipid lysobisphosphatidic acid (LBPA). Exosome-bound prostaglandins are involved in specific intracellular signaling pathways of the target cells [74] and thus do not appear to be essential for exosomal stability and delivery. Likewise, it is unlikely that LBPA plays a functional role in circulating exosomes. Exosomes derived from rat mast cells, human dendritic cells and B cells have been found to contain only minor amounts of this lipid compared to their parent cells [75, 76]. Rather, the lipid may be involved in exosome biogenesis at the MVB limiting membrane, where its abundant presence has been shown [77, 78]. It has been postulated that LBPA could contribute to vesicle budding at this membrane, without being incorporated in the newly formed exosomes itself [79]. In addition, the lipid may be involved in fusion of endocytosed vesicles with LBPA-containing endosomal membranes. It has been demonstrated that some infectious particles, including vesicular stomatitis and dengue viruses, fuse with late endosomes through interactions with LBPA, resulting in the release their contents into the cytosol of the target cell [80-82]. Thus, the activity of LBPA appears to be limited to intracellular fusion and budding processes.

The lipid bilayer of circulating exosomes appears to be mainly constituted of plasma membrane lipids, including sphingomyelin (SM), phosphatidylcholine (PC), phosphatidylethanolamine (PE), phosphatidylserine (PS), ganglioside GM3 and phosphatidylinositol (PI) [79]. The ratios of these lipids vary among exosomes from different cell types. For instance, almost half of the lipids in exosomes derived from reticulocytes constitute PC [83], whereas this lipid forms less than one third of total lipid content of mast cell- and dendritic cell-derived exosomes [75]. In general, exosomes appear to be enriched in SM, cholesterol, GM3 and PS compared to their parent cells [79]. These lipids are not commonly used in liposomal drug delivery systems, however their incorporation can be advantageous. SM and cholesterol are thought to form hydrogen bonds, resulting in tight packing of SM/cholesterol bilayers and low water permeability [84, 85]. In addition, they provide detergent resistance [86].

Therefore, incorporation of these lipids in EMs may increase their rigidity and stability. Indeed, liposomes containing SM/cholesterol have longer circulation times and showed decreased insertion of plasma proteins into their membrane [87]. Liposomes containing SM/cholesterol and loaded with vincristine have shown promising results in phase II clinical trials: they were tolerated at twice the dose of non-encapsulated vincristine in patients with aggressive Non-Hodgkin Lymphoma and showed a favorable side effect profile [88, 89].

Also GM3 may act as a stabilizer of the exosomal wall and may shield the vesicle from interactions with blood components. Gangliosides, SM and cholesterol were demonstrated to act synergistically to decrease uptake of liposomes by the reticuloendothelial system both *in vitro* and *in vivo* [90, 91]. However, Yokoyama and colleagues demonstrated with DPPG/GM3 liposomes that high molar concentrations (> 15 mol%) of GM3 may induce membrane segregation and leakage from vesicles [92]. Therefore, GM3 may be beneficial in EMs when used in low concentrations only.

The structural function of PS in biological membranes is less well studied, however it is known to play a role as a signaling molecule in a large variety of biological processes. The biological role of PS may differ among vesicle populations and cellular sources. For instance, circulating erythrocytes gradually externalize PS during aging, providing an 'eat-me' signal for the reticuloendothelial system [93]. Allen *et al.* showed that low concentrations of PS (> 2 mol%) in the membrane of erythrocyte-resembling liposomes were sufficient to dramatically induce clearance by this system, without affecting membrane lipid organization [94]. The 'eat-me' signaling function of PS is nature's way of clearing PS-exposing apoptotic cells by phagocytosis, reducing leakage of cellular content to the extracellular matrix [95]. The lipid may also serve as a docking station for factors of the coagulation cascade [96] and has been suggested to play roles in other physiological processes, such as muscle formation and anti-inflammatory responses [97, 98].

Whilst these characteristics appear to be unfavorable for EMs for which longer circulation times are often desired, incorporation of PS in EMs may be beneficial nonetheless. The natural conical shape of PS may aid in the assembly of the curved EM membrane [99]. In addition, conically shaped lipids facilitate fusion and fission of biological membranes [100-102]. PS could thus enhance fusion of EMs with target cell membranes and promote intracellular release of cargo. Indeed, it has been shown in a number of studies that inhibition of PS on MV-membranes by Annexin-V or Diannexin reduced fusion of MVs with plasma membranes of their target cells [36, 38, 103, 104], evidencing that PS is an important mediator of vesicle fusion. Moreover, it has been postulated that the negatively charged PS enhances the stability of cell membranes by electrostatic interactions with (cationic) skeletal proteins [105]. This effect may be exploited in EMs loaded with cationic compounds, increasing the retention of encapsulated cargo. However, given that PS displayed on the outer layer of EMs may dramatically decrease their circulation time, incorporation of the lipid in EMs has to be carried out with caution.

Regardless of the exact lipid composition of extracellular vesicles, the lipid bilayer of exosomes appears to be adapted to their target environment. Extracellular pH may differ among target tissues, and rigidity of the vesicle needs to be maintained in these environments to assure optimal function. Parolini *et al.* showed that exosomes released in an acidic microenvironment contained higher concentrations of SM and GM3 compared with exosomes from the same cellular origin but released in a buffered environment [106]. These lipids were suggested to increase exosomal rigidity upon interaction with cholesterol [107]. Moreover, they demonstrated enhanced fusion of acidic exosomes with target cells compared with exosomes secreted in buffered conditions. Given that the target cells (metastatic melanoma) are surrounded by an acidic extracellular matrix under physiological conditions [106], this suggests that the lipid composition of exosomes may be tailored to their target microenvironment. The influence of extravesicular pH on exosome behavior was also demonstrated by Laulagnier *et al.*, who showed that exosomal rigidity increased from pH 5 to 7, a common transition during release of exosomes from acidic MVBs [75]. The rigid bilayer at physiological pH may enhance membrane fusion with target cells, but this was not investigated in this study.

Proteins

Although lipids are increasingly accepted to play important roles in exosomal function, exosome-associated proteins are indispensable. Such proteins can actively participate in regulatory processes and trigger cellular responses, but are also irrefutably involved in functional aspects of exosomes, such as assembly, (preventing) interaction with the extracellular matrix and binding and fusion with target cells. For instance, it was demonstrated that cross-linking of proteins on exosomes by paraformaldehyde decreased exosomal fusion with parental cells by ~20% [106]. Furthermore, when these exosomes were solubilized with octylglucoside and reconstructed by dialysis (removing membrane proteins), they showed a dramatically reduced ability to fuse with target cells compared with untreated exosomes. The fusion efficiency of the protein-depleted exosomes was comparable with the fusion efficiency of large unilamellar vesicles (LUVs) with a similar lipid composition as the natural exosomes, confirming the importance of exosomal proteins in fusion events [106].

According to a variety of proteomic studies (catalogued in Exocarta), a number of proteins and protein families are abundantly detected in exosomes [30]. Many of these, such as heat shock proteins, annexins and proteins of the Rab family are mainly involved in intracellular assembly and trafficking of exosomes and may not be required anymore once the vesicles are secreted. Thus, the inclusion of such proteins in EMs would probably not be beneficial for drug delivery purposes. However, several other exosomal proteins or protein families may be exploited to enhance the delivery properties of EMs. It should be noted that incorporation of proteins in EMs is still a challenging task, especially when simultaneous incorporation of multiple components is desired. However, work in this area is progressing and has yielded promising results [108-112]. For instance, recently the functional reconstitution of a voltage-

gated potassium channel and $\alpha_{bII}\beta_3$ integrin in giant unilamellar vesicles (GUVs) was described [108, 110]. The potential advantages of the incorporation of several exosomal proteins in EMs are discussed below.

Tetraspanins

Tetraspanins are a family of transmembrane proteins commonly detected in exosomes. Among them are CD9, CD63, CD81 and CD82, which are often used as exosome markers [30, 113]. Some tetraspanins are selectively enriched in exosomes compared to their parent cells. An example is CD9, which was found to be more than 10-fold enriched in dendritic cell-derived exosomes [114]. CD37, CD63, CD81 and CD82 were abundantly detected in exosomes derived from B-lymphocytes [115]. Atay *et al.* demonstrated that CD81 was selectively enriched in exosomes from trophoblast cells, but could not detect CD63 (considered to be a canonical exosomal protein) on both parent cells and exosomes [116]. Tetraspanin enrichment patterns in exosomes thus vary among parent cells.

Tetraspanins have been relatively understudied due to their limited ligand-receptor interaction and their small size, which in some cases may prevent biochemical or immunological detection [117]. However, their functions as mediators of fusion, cell migration, cell-cell adhesion and signaling events designate them as interesting targets in the field of drug discovery [118]. Moreover, their functions in exosomes (albeit largely unknown) may be exploited to enhance the properties of EMs as drug delivery systems.

The tetraspanin CD9 has been shown to mediate fusion processes in a variety of cell types. Miyado *et al.* demonstrated that egg cells from CD9 knockout mice ($CD9^{-/-}$) failed to fuse with sperm cells from wild-type males, although binding between the two cell types was unaltered. Normal fusion events were observed between sperm cells and $CD^{+/+}$ eggs, suggestive of an involvement of CD9 in the fusion process. Moreover, when CD9 on eggs was blocked with anti-CD9 antibodies, fusion was significantly inhibited [119]. A role of CD9 in fusion processes was also evidenced by Tachibana *et al.*, who showed that blocking CD9 and CD81 on myoblast cells inhibited cell fusion to syncytia, and upregulation of the two tetraspanins resulted in enhanced cell fusion [120]. It has been suggested that tetraspanin-mediated cell fusion is exploited by various viruses, allowing them to spread while avoiding exposure to the humoral immune system [121, 122]. However, the fusogenic properties of CD9 and CD81 were contradicted by studies to the fusion behavior of mononuclear phagocytes. Incubation of these cells with antibodies against CD9 and CD81 resulted in an *enhanced* formation of multinucleated giant cells (MCGs), and $CD9^{-/-}$ and $CD81^{-/-}$ alveolar macrophages formed three- to fourfold more MCGs than wild-type cells [123]. These results were supported by Parasathy and coworkers, who additionally showed that in contrast to CD9 and CD81, CD63 in fact promoted monocyte fusion [124]. Thus, the fusogenic properties of tetraspanins appear to be cell-type dependent.

Interestingly, the tetraspanins which are often found to be enriched in exosomes (CD9,

CD63, CD81 and CD82 [30, 113]) have been shown to be involved in the migration of dendritic cells. In a chemotaxis assay, antibodies against the single tetraspanins increased migration of these cells by 50-70%, while a 100% increased migration was observed when these antibodies were combined [125]. The increase in migration was attributed to a decreased binding of the cells to integrins expressed in the extracellular matrix. These results suggest that tetraspanins in exosomal membranes may effectuate their binding to target cells.

Although fusogenic and matrix-binding properties of tetraspanins in cell membranes have been described, not much is known about the functions of tetraspanins in exosomes. However, tetraspanins Tspan8, CD49d and CD106 appeared to be involved in binding and uptake of pancreatic adenocarninoma-derived exosomes by fibroblasts and endothelial cells [126]. It has also been suggested that CD9 is involved in fusion of exosomes with their target cells [52], indicating that tetraspanins may have similar functions in exosomes and cell membranes.

It is important to consider that tetraspanins probably exert most of their functions in unison with other membrane proteins. In cell membranes, tetraspanins are laterally organized in tetraspanin-enriched microdomains (TEMs), which are resistant to mild detergent conditions. TEMs generally contain integrins, signaling molecules and other tetraspanins and are involved in a variety of cell fusion, cell adhesion strengthening and signaling events (as excellently reviewed in [117, 118, 127, 128]). The effects of single tetraspanins, particularly in extracellular vesicles, are yet poorly understood. Incorporation of tetraspanins in EMs may therefore not only enhance EM functioning (i.e. binding and uptake in target cells), but may also provide important clues on tetraspanin functioning in exosomes.

Adhesion molecules

According to the Exocarta database, integrins are among the most abundant proteins detected in exosomes derived from cancer and immune cells [129]. Integrins are membrane-spanning proteins which exist as heterodimers of α and β subunits. A total of 24 different heterodimers have been identified in vertebrates, of which β_1, β_2 and α_v integrins comprise the largest group. They function primarily as adhesion molecules and establish cell-binding to the extracellular matrix, although other functions have been described (reviewed in [130, 131]). In exosomes, integrins are most likely involved in addressing the vesicles to their target cells [31]. Therefore, incorporation of integrins in EMs may potentiate their interactions with the extracellular matrix, increasing their delivery potential.

Given that integrins are abundantly detected in a range of exosomal preparations (especially those derived from cancer cells [132, 133]), it is surprising that only a limited number of studies have addressed the functional role of these adhesion molecules in exosomes. In seminal work of Rieu *et al.*, it was shown that integrin $\alpha_4\beta_1$ is present on the surface of young reticulocytes and its surface levels decrease during maturation [134]. The adhesion molecules of mature reticulocytes were detected in the exosomal fraction, suggesting that the cells use

exosomes to dispose of integrins. Functional examination of the exosomes showed that $\alpha_4\beta_1$ integrin mediated binding of the exosomes to fibronectin. This binding was dependent on divalent cations (Mg^{2+}, Mn^{2+}) and was significantly inhibited by the $\alpha_4\beta_1$-binding domain of fibronectin and anti-α_4 antibodies. In a similar work, it was found that exosomes from fibroblasts and epithelial cells contained β_1 integrins and that exosomes from human B-cells expressed both β_1 and β_2 integrins [135]. B-cell derived exosomes bound collagen-I and fibronectin in a cation-dependent manner and binding was inhibited by antibodies against α_4 and β_1 integrins. Moreover, it was shown that these exosomes strongly adhered to TNF-α stimulated fibroblasts through integrin-ICAM-1 interaction. Integrin β_1 and CD9 were also detected on the surface of retroviral particles, and it was suggested that these contribute to adhesion of viruses to host cells [136]. Taken together, these results suggest that exosomal integrins play a crucial role in establishing exosomal adhesion to the extracellular matrix. Given that binding to target cells is the first step in intracellular drug delivery, incorporation of integrins in EMs may thus greatly enhance their drug delivery potential. This strategy has not been implemented in drug delivery systems yet, however integrin-ligand interactions have been successfully exploited. For instance, the fibronectin-derived RGD peptide is commonly used to target drug delivery systems to $\alpha_v\beta_3$ integrin, which is overexpressed in tumor vasculature [137]. Integrin incorporation in EMs may work in a similar fashion to deliver therapeutics to specific tissues. It has been shown that integrin $\alpha_{IIb}\beta_3$ can be incorporated in liposomal membranes without losing its ability to bind to its ligands [109, 138]. However, the affinity of this integrin for its ligand cyclo(RGDfV) was higher in cell membranes than in liposomes [139], suggesting that other endogenous membrane molecules (e.g. tetraspanins, lipids) contribute to integrin-mediated adhesion. Indeed, such a synergistic effect was demonstrated in a study of Zheng *et al.* [111], who incorporated integrin $\alpha_5\beta_1$ in PC/cholesterol liposomes containing increasing concentrations of ganglioside GM3 (0-10 nmol/55 μg PC). The binding of the liposomes to fibronectin-coated plates differed significantly among varying concentrations of GM3, and was optimal at GM3 concentrations of 0.2-0.4 nmol(0.22-0.44 μg)/55 μg PC. In addition, mammary carcinoma cells mutated to contain high concentrations of GM3 bound better to these plates than their parent cells, further evidencing the synergistic effect of other membrane components to integrin function [111]. Given that the membranes of EMs resemble those of endogenous exosomes, integrin incorporation may be a powerful strategy to enhance the adhesive properties of EMs.

In addition to integrins, other adhesion molecules which may be potentially exploited in EMs have been identified in exosomes. Comprehensive proteomic studies have identified thrombospondin-1 in exosomes in urine, plasma and saliva of healthy volunteers [140-143]. In addition, thrombospondin-1 and thrombospondin-2 were detected in exosomes from patients diagnosed with various types of cancer, and in exosomes derived from a colon cancer cell line [144, 145]. Thrombospondin-1 contains a variety of adhesive domains, including an RGD sequence that binds $\alpha_v\beta_3$ integrins [146]. Nucera *et al.* demonstrated that the protein

plays an important role in cancer metastasis [147]. They showed that knockdown of the thrombospondin-1 gene in papillary thyroid carcinoma cells decreased their adhesion and migration *in vitro* and *in vivo*, and that treatment with a thrombospondin-1 inhibitor decreased metastasis and tumor growth in an orthotopic mouse model. In an attempt to use the adhesive properties of thrombospondins for targeted drug delivery, Rivera-Fillat *et al.* developed aspartimide analogs of thrombospondin-1 and 2 and conjugated them to liposomes loaded with doxorubicin [148]. Both peptides adhered to endothelial cells and colon carcinoma cells *in vitro*. In addition, it was demonstrated that the thrombospondin-1 analog enhanced the anti-tumor effect of doxorubicin loaded liposomes in mice bearing a human colon carcinoma; tumor growth was inhibited and mouse survival was prolonged compared to the untargeted doxorubicin liposomes. This effect was most likely due to enhanced delivery of doxorubicin to their target cells, given that targeted liposomes without doxorubicin did not exert anti-tumoral activity. In addition to conferring adhesion properties, thrombospondins also serve as signaling molecules with anti-angiogenic and anti-tumoral effects. Therefore, they may have therapeutic potential on their own (for reviews see [149, 150]). Thrombospondins may thus be valuable tools in tumor-targeted EMs; they may promote adhesion to target cells and induce anti-angiogenic signaling pathways.

A third interesting class of adhesion molecules found associated with exosomes is the family of intercellular adhesion molecules (ICAMs). ICAM-1 and ICAM-3 have been detected in immune cell-derived exosomes [41, 115, 151-153] and may function as important mediators in immune responses. ICAM-1 is a ligand for integrin $\alpha_L\beta_2$ (LFA-1) and Mac-1 and promotes leukocyte adhesion [154], while ICAM-3 binds DC-SIGN on dendritic cells [155]. Their functions in exosomes are still under investigation, although some interesting results have been published. Segura *et al.* showed that exosomes from mature dendritic cells contained markedly more ICAM-1 compared to those from immature dendritic cells [156]. Mature exosomes induced T-cell activation and proliferation *in vitro*, and enhanced T-cell activation and skin graft rejection *in vivo* compared to immature exosomes. The authors showed that ICAM-1 expression was an important contributor to this process, and suggested that ICAM-1 mediates exosome adhesion to target antigen presenting cells, thereby inducing the immune response [156]. In a follow-up study, the group showed that ICAM-1-exposing exosomes induced significantly stronger T-cell responses than ICAM-$1^{-/-}$ exosomes *in vitro* and *in vivo*, and that this effect was due to loss of exosome-cell adhesion mediated by ICAM-1 and LFA-1 [157]. These results demonstrate the importance of ICAM-1 in the adhesion of exosomes to LFA-1 expressing immune cells. When targeting the immune system (e.g. in vaccine preparations), the incorporation of ICAM-1 in EMs may be considered.

Other membrane proteins

Apart from tetraspanins and adhesion molecules, also other proteins which have the potential to enhance the drug delivery properties of EMs have been identified in exosomes.

Two of these, CD55 and CD59, have been found in exosomes derived from various sources, including B-cells, dendritic cells, colorectal cancer cells, saliva and bronchial epithelial cells [66, 141, 145, 153, 158, 159]. Both factors protect cells from complement-mediated lysis: CD55 accelerates the decay of autologous complement factors [160], whereas CD59 prevents the activation of the membrane attack complex by inhibition of C9 incorporation in C5b-9 [161]. In an interesting study of Clayton *et al.*, it was demonstrated that inhibition of exosomal CD55 resulted in increased membrane disposition of C3b and exosome lysis [66]. Blockade of CD59 also enhanced complement-mediated exosome lysis, and inhibition of both CD55 and CD59 increased lysis even further. These proteins thus appear to protect exosomes from complement-mediated lysis. Given that liposomes are prone to lysis mediated by complement factors [162, 163], CD55 and CD59 may be used to improve the stability and circulation time of EMs.

Another exosomal protein with possible therapeutic applications is lactadherin (also known as EGF-factor VIII or MFG-E8) [114]. This protein is commonly found in exosomes derived from immune cells [114, 164, 165] and fibroblasts.[166] Lactadherin consists of two EGF-like domains and two lectin type C domains (C1 and C2) with high homology to coagulation factors V and VIII [167]. The EGF-like domains mediate binding to integrins $\alpha_v\beta_3$ and $\alpha_v\beta_5$ via an RGD motif, while the C2 domain promotes binding to PS in biological membranes [168]. Thus, it acts as a scaffold protein between the surface of PS-exposing apoptotic cells or exosomes and target cells. It has been reported that lactadherin promotes adhesion and uptake of exosomes by dendritic cells [169], but also interactions with other phagocytotic cells expressing integrins $\alpha_v\beta_{3/5}$, such as macrophages and endothelial cells, are likely [114]. To demonstrate that angiogenic endothelial cells are capable of phagocytosis, Fens *et al.* prepared PS-exposing liposomes and opsonised them with lactadherin [170]. Marked uptake of the opsonized liposomes in human umbilical vein endothelial cells (HUVECs) was observed, whereas uptake was several-fold lower in the absence of lactadherin. Moreover, membrane vesicles containing egg phosphatidyl glycerol (EPG), which is a negatively charged phospholipid that lacks a lactadherin binding site, were barely taken up by HUVECs in the presence of the opsonin. These results show that lactadherin may be used to target EMs to specific integrin expressing cells, such as angiogenic endothelial cells and dendritic cells.

Furthermore, it has been shown that fusion proteins containing the lactadherin C1C2 domain can be exploited to induce immune responses to tumor antigens [56-58]. In such strategies, the PS-binding domain of the opsonin is used to coat exosomes and exploit the excellent delivery potential of these vesicles to deliver the antigen to antigen-presenting cells, resulting in immune responses. These studies illustrate the versatility of the lactadherin protein and its application in EM-mediated drug delivery. An advantage of lactadherin is that it does not need to be incorporated in the membrane of EMs. Rather, it is possible to recombinantly produce the protein [171] and attach it to PS-exposing EMs after vesicle formation. Additionally, fusion proteins of lactadherin and functional domains of other proteins can be

engineered, conferring unique properties to EMs coated with these constructs. For instance, by fusing the C1C2 domain of lactadherin to targeting ligands, EMs may be targeted to specific organs and cell types. An additional advantage of lactadherin coating of PS-exposing EMs is that recognition of the lipid by PS-receptors may be blocked. This way the 'eat-me' signaling function of PS would be inhibited, resulting in prolonged circulation time of the vesicles.

Decoration of EMs with specific proteins may also be achieved by the use of exosomal membrane anchors. In contrast to lactadherin that is coated on the surface of EMs, such anchors may be plugged into the EM membrane during EM assembly and provide a stable scaffold for fused proteins. An example is Lamp2b, which was used by Alvarez-Erviti *et al.* to anchor the neuron-specific RVG peptide to the exosomal membrane [53]. Although this study exploited the endogenous exosomal pathway to incorporate the anchor into exosomes, it may be possible to reconstitute the protein into an artificial membrane (i.e. EM membrane). Thus, EM linkage of proteins which are not naturally expressed in exosomes may be achieved, circumventing possible expression issues in biotechnologically engineered exosomes. Such issues were clearly demonstrated by Shen *et al.*, who attempted to target a highly oligomeric cytoplasmic protein (TyA-GFP) to secreted vesicles by fusing the protein to a variety of exosomal membrane proteins, including CD4, CD38, CD43, CD69 and CD83 [172]. After transfection of Jurkat T-cells with expression vectors encoding the fusion proteins, only CD43-TyA-GFP could be weakly detected in the secreted vesicles. The authors suggested that endoplasmic reticulum (ER)-associated degradation could be responsible for the undetectable exosomal expression of some of the other constructs. A small number of constructs was degraded nor secreted, but was found to be retained in the ER instead. In this regard the synthetic construction of EMs can offer a solution. A promising novel technique to incorporate membrane proteins in liposomes is the cell-free expression of such proteins in the presence of liposomes (reviewed in [173-175]). Using this technique, integral membrane proteins are inserted into the liposomal membrane during their expression, resulting in functional and stable protein incorporation. Successful cell-free expression in liposomes has been demonstrated for a number of membrane proteins, such as membrane channel proteins [175-177].

Therapeutic cargo

EMs provide an opportunity to deliver therapeutic cargo directly into the cytoplasm of target cells. It is possible to load EMs with synthetic drugs, as is commonly done in other liposomal formulations [178, 179], but the unique exosome-resembling characteristics of EMs allow them to excel in the delivery of therapeutic proteins and nucleic acids. An interesting class of molecules which could benefit from EM-mediated delivery, are miRNAs. These short non-coding endogenous RNA molecules recruit cellular proteins and bind to target mRNA sequences via Watson-Crick base-pairing, resulting in cleavage or translation repression of the target strand (RNA interference). This way, they regulate protein expression and cellular functioning [180]. Since the discovery that miRNAs are not only involved in the regulation of

cellular processes in the miRNA-producing cell, but that they also regulate processes in other cells by exosomal transfer [41], the therapeutic applications of miRNAs have gained increasing attention.

Intracellular levels of miRNAs have been extensively mapped in a number of diseases. Among the most studied diseases in this regard is cancer, in which specific miRNAs are often over- or underexpressed compared to healthy cells [181]. Low levels of cancer-associated miRNAs can be compensated by miRNA-based therapeutics (so-called miRNA restoration or replacement), resulting in improvement of the disease outcomes. Successful restoration of miRNA to treat various types of cancer has been described in a number of recent studies (reviewed by Henry *et al.* [182]). For instance, in 2009 Kota *et al.* showed that the expression of the miRNA miR-26a in liver tumors was markedly decreased compared to healthy liver tissue [183]. To test whether restoration of miR-26a could have anti-tumorigenic effects, an adeno-associated virus (AAV) vector packed with miR-26a was intravenously administered to liver tumor-bearing mice. Three weeks after treatment disease progression was dramatically decreased, cancer cell proliferation was inhibited, and tumor cell-specific apoptosis was increased compared to mice treated with empty vectors. The therapeutic effect of miRNA restoration was also shown for miR-34a, which was found to be underexpressed in prostate cancer cells [184]. Upon repetitive intravenous administration of miR-34a complexed with a lipid-based delivery agent to xenograft prostate cancer mice, tumor growth and metastasis were inhibited and mouse survival was elongated. These effects were likely due to miR-34a-mediated downregulation of the adhesion molecule CD44 in tumor cells [184].

While some miRNAs appear to be downregulated in various disease states, other miRNAs have been shown to be overexpressed. This phenomenon has supported the emergence of anti-miRNA-based therapeutics (reviewed in [185]). These are antisense oligonucleotides with sequences complementary to those of the targeted miRNA, which disrupt miRNA biogenesis and functioning at multiple fronts (e.g. miRNA processing and interactions with the target mRNA) [186]. Several interesting studies have effectively employed anti-miRNA strategies to induce cancer cell death and inhibit disease progression [187-191].

These exciting results illustrate the potential of miRNAs and anti-miRNAs as a novel class of endogenous therapeutics. However, the intracellular delivery of (anti-)miRNAs is generally poor, and multiple (intratumoral) injections are often required for an effect [192, 193]. Given that exosomes are natural carriers for miRNAs, EMs would be excellent delivery systems for such molecules. As their membrane resembles that of natural exosomes, the stability of encapsulated miRNAs could be increased. Furthermore, EMs may allow for non-toxic and non-immunogenic delivery of their cargo to target cells, strongly potentiating the effects of (anti-) miRNAs.

Although miRNAs are promising therapeutic targets, it is important to note that they do not require full (100%) binding to their target mRNA sequences for inhibiting effects [194]. This allows them to act synergistically on various targets within signaling pathways,

but also increases their chance for off-target effects. These can be minimized by extensive characterization of possible target sequences and optimization of the administered miRNA doses. Alternatively, siRNA, which is known for its excellent sequence specificity [195], may be used to silence the expression of specific target genes. Similar to miRNA, the properties of siRNA (e.g. their anionic charge, size and rapid clearance) call for packaging in adequate delivery systems. Given that biotechnically engineered exosomes have previously been successfully applied for delivery of siRNA [53], EMs hold great potential for siRNA-delivery.

Concluding remarks and perspectives

The safe and effective delivery of drug molecules to their target site is a field which has increasingly gained attention in drug design and development. In the last decades, the focus has shifted from synthetic drug compounds to the delivery of biological drugs (i.e. proteins and nucleic acids), which are very prone to immune effects and degradation. In this regard EMs are promising candidate delivery vehicles, given that they mimic nature's delivery vehicles of biologicals, but are not as complex as their biological counterparts. These characteristics may allow them to deliver biologicals in an effective and safe manner, with high pharmaceutical acceptability due to their well characterized components. However, before the full potential of EMs can be exploited, a number of challenges still needs to be overcome. The assembly of liposomes with varying sizes and lipid compositions is commonly performed and well understood, but the incorporation of functional proteins and nucleic acids with reasonable efficiency is a field on its own. Membrane proteins have been successfully incorporated in liposomes without losing their functionality [108-112], however the incorporation of multiple proteins is a time-consuming and complicated process. Their membrane localization may require a specific lipid composition and chaperone proteins. Moreover, the (recombinant) production of membrane proteins is a challenging task due to their high hydrophobicity and cytotoxicity, tendency to form aggregates and low expression levels. The use of promising cell-free expression systems may aid to overcome these production issues [173-175].

For assembly of functional EMs it is also important to take into account the structural and biological functions of the lipids to be incorporated. Lipids come in various sizes and shapes, which influence the behavior of the liposome in biological environments (e.g. fusion and stability). In this regard it may be wise to borrow a leaf from natures book and mimic the lipid composition of exosomes in the intended target environment for optimal functionality. Increasingly powerful analytical methods in the field of lipidomics may aid in elucidating both function and composition of lipids in natural exosomes. These may provide valuable clues for drug delivery with EMs.

An additional challenge governing the assembly of functional EMs is the loading of therapeutic cargo. Although work is progressing in this area, high-efficiency loading of siRNA (and likewise miRNA) in lipid vesicles is still rarely achieved [196, 197]. Given that exosomes are loaded with multiple components that probably contribute to the outstanding delivery

capacities of these vesicles, efficient loading of a combination of nucleic acids and proteins in EMs merits investigation. Furthermore, it is important to note that crucial components of exosomes are still largely unknown, and probably differ among exosomes with varying functions and target cells. The rapidly expanding field of *exosomics* allows us to increase our understanding of the composition and function of these intriguing vesicles, but is still in its infancy. Extensive proteomic studies have identified > 4,000 proteins and > 1,500 miRNAs in exosomes from various sources, but integrative studies are required to elucidate the biological functions of these components. The answer to "What makes natural exosomes such effective delivery vehicles?", is the first step towards the design and assembly of functional EMs.

Acknowledgements

The work of SAAK, PV, SMvD and RMS on cell-derived membrane vesicles is supported by ERC Starting Grant 260627 'MINDS' in the FP7 Ideas program of the EU.

References

1. P. Wolf, The nature and significance of platelet products in human plasma, *Br J Haematol*, 13 (1967) 269-288.
2. N. Crawford, The presence of contractile proteins in platelet microparticles isolated from human and animal platelet-free plasma, *Br J Haematol*, 21 (1971) 53-69.
3. F. Doonan, T.G. Cotter, Morphological assessment of apoptosis, *Methods*, 44 (2008) 200-204.
4. M. Hristov, W. Erl, S. Linder, P.C. Weber, Apoptotic bodies from endothelial cells enhance the number and initiate the differentiation of human endothelial progenitor cells in vitro, *Blood*, 104 (2004) 2761-2766.
5. Y. Xie, O. Bai, J. Yuan, R. Chibbar, K. Slattery, Y. Wei, *et al.*, Tumor apoptotic bodies inhibit CTL responses and antitumor immunity via membrane-bound transforming growth factor-beta1 inducing CD8+ T-cell anergy and CD4+ Tr1 cell responses, *Cancer Res*, 69 (2009) 7756-7766.
6. A.M. Cline, M.Z. Radic, Apoptosis, subcellular particles, and autoimmunity, *Clin Immunol*, 112 (2004) 175-182.
7. C. Thery, M. Ostrowski, E. Segura, Membrane vesicles as conveyors of immune responses, *Nat Rev Immunol*, 9 (2009) 581-593.
8. M. Schiller, I. Bekeredjian-Ding, P. Heyder, N. Blank, A.D. Ho, H.M. Lorenz, Autoantigens are translocated into small apoptotic bodies during early stages of apoptosis, *Cell Death Differ*, 15 (2008) 183-191.
9. C.D. Gregory, J.D. Pound, Microenvironmental influences of apoptosis in vivo and in vitro, *Apoptosis*, 15 (2010) 1029-1049.
10. V. Muralidharan-Chari, J.W. Clancy, A. Sedgwick, C. D'Souza-Schorey, Microvesicles: mediators of extracellular communication during cancer progression, *J Cell Sci*, 123 (2010) 1603-1611.
11. D. Pilzer, O. Gasser, O. Moskovich, J.A. Schifferli, Z. Fishelson, Emission of membrane vesicles: roles in complement resistance, immunity and cancer, *Springer Semin Immunopathol*, 27 (2005) 375-387.

12. K. Shedden, X.T. Xie, P. Chandaroy, Y.T. Chang, G.R. Rosania, Expulsion of small molecules in vesicles shed by cancer cells: association with gene expression and chemosensitivity profiles, *Cancer Res*, 63 (2003) 4331-4337.

13. M. Sekula, G. Janawa, E. Stankiewicz, E. Stepien, Endothelial microparticle formation in moderate concentrations of homocysteine and methionine in vitro, *Cell Mol Biol Lett*, 16 (2011) 69-78.

14. E. Shantsila, P.W. Kamphuisen, G.Y. Lip, Circulating microparticles in cardiovascular disease: implications for atherogenesis and atherothrombosis, *J Thromb Haemost*, 8 (2010) 2358-2368.

15. S. Antwi-Baffour, S. Kholia, Y.K. Aryee, E.A. Ansa-Addo, D. Stratton, S. Lange, *et al.*, Human plasma membrane-derived vesicles inhibit the phagocytosis of apoptotic cells--possible role in SLE, *Biochem Biophys Res Commun*, 398 (2010) 278-283.

16. C. Obregon, B. Rothen-Rutishauser, S.K. Gitahi, P. Gehr, L.P. Nicod, Exovesicles from human activated dendritic cells fuse with resting dendritic cells, allowing them to present alloantigens, *Am J Pathol*, 169 (2006) 2127-2136.

17. B. Hugel, M.C. Martinez, C. Kunzelmann, J.M. Freyssinet, Membrane microparticles: two sides of the coin, *Physiology (Bethesda)*, 20 (2005) 22-27.

18. R. Bucki, C. Bachelot-Loza, A. Zachowski, F. Giraud, J.C. Sulpice, Calcium induces phospholipid redistribution and microvesicle release in human erythrocyte membranes by independent pathways, *Biochemistry*, 37 (1998) 15383-15391.

19. L.J. Gonzalez, E. Gibbons, R.W. Bailey, J. Fairbourn, T. Nguyen, S.K. Smith, *et al.*, The influence of membrane physical properties on microvesicle release in human erythrocytes, *PMC Biophys*, 2 (2009) 7.

20. U. Salzer, P. Hinterdorfer, U. Hunger, C. Borken, R. Prohaska, Ca(++)-dependent vesicle release from erythrocytes involves stomatin-specific lipid rafts, synexin (annexin VII), and sorcin, *Blood*, 99 (2002) 2569-2577.

21. S. Crawford, D. Diamond, L. Brustolon, R. Penarreta, Effect of increased extracellular ca on microvesicle production and tumor spheroid formation, *Cancer Microenviron*, 4 (2010) 93-103.

22. A. Aharon, T. Tamari, B. Brenner, Monocyte-derived microparticles and exosomes induce procoagulant and apoptotic effects on endothelial cells, *Thromb Haemost*, 100 (2008) 878-885.

23. L.M. Thomas, R.D. Salter, Activation of macrophages by P2X7-induced microvesicles from myeloid cells is mediated by phospholipids and is partially dependent on TLR4, *J Immunol*, 185 (2010) 3740-3749.

24. J.S. Wiley, R. Sluyter, B.J. Gu, L. Stokes, S.J. Fuller, The human P2X7 receptor and its role in innate immunity, *Tissue Antigens*, 78 (2011) 321-332.

25. M. Record, C. Subra, S. Silvente-Poirot, M. Poirot, Exosomes as intercellular signalosomes and pharmacological effectors, *Biochem Pharmacol*, 81 (2011) 1171-1182.

26. M. Simons, G. Raposo, Exosomes--vesicular carriers for intercellular communication, *Curr Opin Cell Biol*, 21 (2009) 575-581.

27. D.D. Taylor, C. Gercel-Taylor, Exosomes/microvesicles: mediators of cancer-associated immunosuppressive microenvironments, *Semin Immunopathol*, 33 (2011) 441-454.

28. S. Sahoo, E. Klychko, T. Thorne, S. Misener, K.M. Schultz, M. Millay, *et al.*, Exosomes from human CD34(+) stem cells mediate their proangiogenic paracrine activity, *Circ Res*, 109 (2011) 724-728.

29. V. Sokolova, A.K. Ludwig, S. Hornung, O. Rotan, P.A. Horn, M. Epple, *et al.*, Characterisation of exosomes derived from human cells by nanoparticle tracking analysis and scanning electron microscopy, *Colloids Surf B Biointerfaces*, 87 (2011) 146-150.

30. R.J. Simpson, S.S. Jensen, J.W. Lim, Proteomic profiling of exosomes: current perspectives, *Proteomics*, 8 (2008) 4083-4099.

31. C. Thery, L. Duban, E. Segura, P. Veron, O. Lantz, S. Amigorena, Indirect activation of naive CD4+ T cells by dendritic cell-derived exosomes, *Nat Immunol*, 3 (2002) 1156-1162.

32. M.C. Martinez, R. Andriantsitohaina, Microparticles in angiogenesis: therapeutic potential, *Circ Res*, 109 (2011) 110-119.

33. A. Aharon, B. Brenner, Microparticles, thrombosis and cancer, *Best Pract Res Clin Haematol*, 22 (2009) 61-69.

34. J.A. Cho, H. Park, E.H. Lim, K.H. Kim, J.S. Choi, J.H. Lee*, et al.*, Exosomes from ovarian cancer cells induce adipose tissue-derived mesenchymal stem cells to acquire the physical and functional characteristics of tumor-supporting myofibroblasts, *Gynecol Oncol*, 123 (2011) 379-386.

35. M. Baj-Krzyworzeka, M. Majka, D. Pratico, J. Ratajczak, G. Vilaire, J. Kijowski*, et al.*, Platelet-derived microparticles stimulate proliferation, survival, adhesion, and chemotaxis of hematopoietic cells, *Exp Hematol*, 30 (2002) 450-459.

36. K. Al-Nedawi, B. Meehan, R.S. Kerbel, A.C. Allison, J. Rak, Endothelial expression of autocrine VEGF upon the uptake of tumor-derived microvesicles containing oncogenic EGFR, *Proc Natl Acad Sci U S A*, 106 (2009) 3794-3799.

37. J. Ratajczak, M. Wysoczynski, F. Hayek, A. Janowska-Wieczorek, M.Z. Ratajczak, Membrane-derived microvesicles: important and underappreciated mediators of cell-to-cell communication, *Leukemia*, 20 (2006) 1487-1495.

38. I. Del Conde, C.N. Shrimpton, P. Thiagarajan, J.A. Lopez, Tissue-factor-bearing microvesicles arise from lipid rafts and fuse with activated platelets to initiate coagulation, *Blood*, 106 (2005) 1604-1611.

39. T. Tian, Y. Wang, H. Wang, Z. Zhu, Z. Xiao, Visualizing of the cellular uptake and intracellular trafficking of exosomes by live-cell microscopy, *J Cell Biochem*, 111 (2010) 488-496.

40. A. Sarkar, S. Mitra, S. Mehta, R. Raices, M.D. Wewers, Monocyte derived microvesicles deliver a cell death message via encapsulated caspase-1, *PLoS One*, 4 (2009) e7140.

41. H. Valadi, K. Ekstrom, A. Bossios, M. Sjostrand, J.J. Lee, J.O. Lotvall, Exosome-mediated transfer of mRNAs and microRNAs is a novel mechanism of genetic exchange between cells, *Nat Cell Biol*, 9 (2007) 654-659.

42. A. Montecalvo, A.T. Larregina, W.J. Shufesky, D. Beer Stolz, M.L. Sullivan, J.M. Karlsson*, et al.*, Mechanism of transfer of functional microRNAs between mouse dendritic cells via exosomes, *Blood*, 119 (2012) 756-766.

43. J.D. Arroyo, J.R. Chevillet, E.M. Kroh, I.K. Ruf, C.C. Pritchard, D.F. Gibson*, et al.*, Argonaute2 complexes carry a population of circulating microRNAs independent of vesicles in human plasma, *Proc Natl Acad Sci U S A*, 108 (2011) 5003-5008.

44. A. Turchinovich, L. Weiz, A. Langheinz, B. Burwinkel, Characterization of extracellular circulating microRNA, *Nucleic Acids Res*, 39 (2011) 7223-7233.

45. M. Guescini, S. Genedani, V. Stocchi, L.F. Agnati, Astrocytes and Glioblastoma cells release exosomes carrying mtDNA, *J Neural Transm*, 117 (2010) 1-4.

46. M. Guescini, D. Guidolin, L. Vallorani, L. Casadei, A.M. Gioacchini, P. Tibollo*, et al.*, C2C12 myoblasts release micro-vesicles containing mtDNA and proteins involved in signal transduction, *Exp Cell Res*, 316 (2010) 1977-1984.

47. P.S. Mitchell, R.K. Parkin, E.M. Kroh, B.R. Fritz, S.K. Wyman, E.L. Pogosova-Agadjanyan*, et al.*, Circulating microRNAs as stable blood-based markers for cancer detection, *Proc Natl Acad Sci U S A*,105 (2008) 10513-10518.

48. J. Skog, T. Wurdinger, S. van Rijn, D.H. Meijer, L. Gainche, M. Sena-Esteves*, et al.*, Glioblastoma microvesicles transport RNA and proteins that promote tumour growth and provide diagnostic biomarkers, *Nat Cell Biol*, 10 (2008) 1470-1476.

49. D.M. Pegtel, K. Cosmopoulos, D.A. Thorley-Lawson, M.A. van Eijndhoven, E.S. Hopmans, J.L. Lindenberg*, et al.*, Functional delivery of viral miRNAs via exosomes, *Proc Natl Acad Sci U S A*, 107 (2010) 6328-6333.

50. D. Castanotto, J.J. Rossi, The promises and pitfalls of RNA-interference-based therapeutics, *Nature*, 457 (2009) 426-433.

51. H. Baigude, T.M. Rana, Delivery of therapeutic RNAi by nanovehicles, *Chembiochem*, 10 (2009) 2449-2454.

52. J.G. van den Boorn, M. Schlee, C. Coch, G. Hartmann, SiRNA delivery with exosome nanoparticles, *Nat Biotechnol*, 29 (2011) 325-326.

53. L. Alvarez-Erviti, Y. Seow, H. Yin, C. Betts, S. Lakhal, M.J. Wood, Delivery of siRNA to the mouse brain by systemic injection of targeted exosomes, *Nat Biotechnol*, 29 (2011) 341-345.

54. A. Delcayre, A. Estelles, J. Sperinde, T. Roulon, P. Paz, B. Aguilar*, et al.*, Exosome Display technology: applications to the development of new diagnostics and therapeutics, *Blood Cells Mol Dis*, 35 (2005) 158-168.

55. D.E. Otzen, K. Blans, H. Wang, G.E. Gilbert, J.T. Rasmussen, Lactadherin binds to phosphatidylserine-containing vesicles in a two-step mechanism sensitive to vesicle size and composition, *Biochim Biophys Acta*, (Epub 2011 Sep 2).

56. I.S. Zeelenberg, M. Ostrowski, S. Krumeich, A. Bobrie, C. Jancic, A. Boissonnas*, et al.*, Targeting tumor antigens to secreted membrane vesicles in vivo induces efficient antitumor immune responses, *Cancer Res*, 68 (2008) 1228-1235.

57. Z.C. Hartman, J. Wei, O.K. Glass, H. Guo, G. Lei, X.Y. Yang*, et al.*, Increasing vaccine potency through exosome antigen targeting, *Vaccine*, (Epub 2011 Oct 12).

58. R.B. Rountree, S.J. Mandl, J.M. Nachtwey, K. Dalpozzo, L. Do, J.R. Lombardo*, et al.*, Exosome targeting of tumor antigens expressed by cancer vaccines can improve antigen immunogenicity and therapeutic efficacy, *Cancer Res*, 71 (2011) 5235-5244.

59. B. Escudier, T. Dorval, N. Chaput, F. Andre, M.P. Caby, S. Novault*, et al.*, Vaccination of metastatic melanoma patients with autologous dendritic cell (DC) derived-exosomes: results of the first phase I clinical trial, *J Transl Med*, 3 (2005) 10.

60. M.A. Morse, J. Garst, T. Osada, S. Khan, A. Hobeika, T.M. Clay*, et al.*, A phase I study of dexosome immunotherapy in patients with advanced non-small cell lung cancer, *J Transl Med*, 3 (2005) 9.

61. D. Sun, X. Zhuang, X. Xiang, Y. Liu, S. Zhang, C. Liu*, et al.*, A novel nanoparticle drug delivery system: the anti-inflammatory activity of curcumin is enhanced when encapsulated in exosomes, *Mol Ther*, 18 (2010) 1606-1614.

62. X. Zhuang, X. Xiang, W. Grizzle, D. Sun, S. Zhang, R.C. Axtell*, et al.*, Treatment of brain inflammatory diseases by delivering exosome encapsulated anti-inflammatory drugs from the nasal region to the brain, *Mol Ther*, 19 (2011) 1769-1779.

63. K. Ogawara, M.G. Rots, R.J. Kok, H.E. Moorlag, A.M. Van Loenen, D.K. Meijer, *et al.*, A novel strategy to modify adenovirus tropism and enhance transgene delivery to activated vascular endothelial cells in vitro and in vivo, *Hum Gene Ther*, 15 (2004) 433-443.

64. W.J. Kim, S.W. Kim, Efficient siRNA delivery with non-viral polymeric vehicles, *Pharm Res*, 26 (2009) 657-666.

65. K. Singha, R. Namgung, W.J. Kim, Polymers in small-interfering RNA delivery, *Nucleic Acid Ther*, 21 (2011) 133-147.

66. A. Clayton, C.L. Harris, J. Court, M.D. Mason, B.P. Morgan, Antigen-presenting cell exosomes are protected from complement-mediated lysis by expression of CD55 and CD59, *Eur J Immunol*, 33 (2003) 522-531.

67. D.G. Meckes, Jr., N. Raab-Traub, Microvesicles and Viral Infection, *J Virol*, (Epub 2011 Oct 5).

68. G. Camussi, M.C. Deregibus, S. Bruno, C. Grange, V. Fonsato, C. Tetta, Exosome/microvesicle-mediated epigenetic reprogramming of cells, *Am J Cancer Res*, 1 (2011) 98-110.

69. T.S. Chen, F. Arslan, Y. Yin, S.S. Tan, R.C. Lai, A.B. Choo, *et al.*, Enabling a robust scalable manufacturing process for therapeutic exosomes through oncogenic immortalization of human ESC-derived MSCs, *J Transl Med*, 9 (2011) 47.

70. A. Puri, K. Loomis, B. Smith, J.H. Lee, A. Yavlovich, E. Heldman, *et al.*, Lipid-based nanoparticles as pharmaceutical drug carriers: from concepts to clinic, *Crit Rev Ther Drug Carrier Syst*, 26 (2009) 523-580.

71. D.B. Fenske, P.R. Cullis, Liposomal nanomedicines, *Expert Opin Drug Deliv*, 5 (2008) 25-44.

72. S. Mathivanan, R.J. Simpson, ExoCarta: A compendium of exosomal proteins and RNA, *Proteomics*, 9 (2009) 4997-5000.

73. S. Mathivanan, C.J. Fahner, G.E. Reid, R.J. Simpson, ExoCarta 2012: database of exosomal proteins, RNA and lipids, *Nucleic Acids Res*, (Epub 2011 Oct 11).

74. C. Subra, D. Grand, K. Laulagnier, A. Stella, G. Lambeau, M. Paillasse, *et al.*, Exosomes account for vesicle-mediated transcellular transport of activatable phospholipases and prostaglandins, *J Lipid Res*, 51 (2010) 2105-2120.

75. K. Laulagnier, C. Motta, S. Hamdi, S. Roy, F. Fauvelle, J.F. Pageaux, *et al.*, Mast cell- and dendritic cell-derived exosomes display a specific lipid composition and an unusual membrane organization, *Biochem J*, 380 (2004) 161-171.

76. R. Wubbolts, R.S. Leckie, P.T. Veenhuizen, G. Schwarzmann, W. Mobius, J. Hoernschemeyer, *et al.*, Proteomic and biochemical analyses of human B cell-derived exosomes. Potential implications for their function and multivesicular body formation, *J Biol Chem*, 278 (2003) 10963-10972.

77. R. Alonso, C. Mazzeo, M.C. Rodriguez, M. Marsh, A. Fraile-Ramos, V. Calvo, *et al.*, Diacylglycerol kinase alpha regulates the formation and polarisation of mature multivesicular bodies involved in the secretion of Fas ligand-containing exosomes in T lymphocytes, *Cell Death Differ*, 18 (2011) 1161-1173.

78. I.J. White, L.M. Bailey, M.R. Aghakhani, S.E. Moss, C.E. Futter, EGF stimulates annexin 1-dependent inward vesiculation in a multivesicular endosome subpopulation, *EMBO J*, 25 (2006) 1-12.

79. C. Subra, K. Laulagnier, B. Perret, M. Record, Exosome lipidomics unravels lipid sorting at the level of multivesicular bodies, *Biochimie*, 89 (2007) 205-212.

80. S.L. Roth, G.R. Whittaker, Promotion of vesicular stomatitis virus fusion by the endosome-specific phospholipid bis(monoacylglycero)phosphate (BMP), *FEBS Lett*, 585 (2011) 865-869.

81. E. Zaitseva, S.T. Yang, K. Melikov, S. Pourmal, L.V. Chernomordik, Dengue virus ensures its fusion in late endosomes using compartment-specific lipids, *PLoS Pathog*, 6 (2010) e1001131.

82. I. Le Blanc, P.P. Luyet, V. Pons, C. Ferguson, N. Emans, A. Petiot*, et al.*, Endosome-to-cytosol transport of viral nucleocapsids, *Nat Cell Biol*, 7 (2005) 653-664.

83. M. Vidal, J. Sainte-Marie, J.R. Philippot, A. Bienvenue, Asymmetric distribution of phospholipids in the membrane of vesicles released during in vitro maturation of guinea pig reticulocytes: evidence precluding a role for "aminophospholipid translocase", *J Cell Physiol*, 140 (1989) 455-462.

84. D. Needham, R.S. Nunn, Elastic deformation and failure of lipid bilayer membranes containing cholesterol, *Biophys J*, 58 (1990) 997-1009.

85. B. Ramstedt, J.P. Slotte, Membrane properties of sphingomyelins, *FEBS Lett*, 531 (2002) 33-37.

86. G. Abi-Rizk, F. Besson, Interactions of Triton X-100 with sphingomyelin and phosphatidylcholine monolayers: influence of the cholesterol content, *Colloids Surf B Biointerfaces*, 66 (2008) 163-167.

87. D.C. Drummond, O. Meyer, K. Hong, D.B. Kirpotin, D. Papahadjopoulos, Optimizing liposomes for delivery of chemotherapeutic agents to solid tumors, *Pharmacol Rev*, 51 (1999) 691-743.

88. M.A. Rodriguez, R. Pytlik, T. Kozak, M. Chhanabhai, R. Gascoyne, B. Lu*, et al.*, Vincristine sulfate liposomes injection (Marqibo) in heavily pretreated patients with refractory aggressive non-Hodgkin lymphoma: report of the pivotal phase 2 study, *Cancer*, 115 (2009) 3475-3482.

89. L. Boehlke, J.N. Winter, Sphingomyelin/cholesterol liposomal vincristine: a new formulation for an old drug, *Expert Opin Biol Ther*, 6 (2006) 409-415.

90. T.M. Allen, G.A. Austin, A. Chonn, L. Lin, K.C. Lee, Uptake of liposomes by cultured mouse bone marrow macrophages: influence of liposome composition and size, *Biochim Biophys Acta*, 1061 (1991) 56-64.

91. T.M. Allen, A. Chonn, Large unilamellar liposomes with low uptake into the reticuloendothelial system, *FEBS Lett*, 223 (1987) 42-46.

92. S. Yokoyama, T. Takeda, T. Tsunoda, Y. Ohta, T. Imura, M. Abe, Membrane properties of mixed dipalmitoylphosphatidylglycerol/ganglioside GM3 liposomes in the presence of bovine serum albumin, *Colloids and Surfaces B: Biointerfaces*, 27 (2003) 141-146.

93. K. Schutters, C. Reutelingsperger, Phosphatidylserine targeting for diagnosis and treatment of human diseases, *Apoptosis*, 15 (2010) 1072-1082.

94. T.M. Allen, P. Williamson, R.A. Schlegel, Phosphatidylserine as a determinant of reticuloendothelial recognition of liposome models of the erythrocyte surface, *Proc Natl Acad Sci U S A*, 85 (1988) 8067-8071.

95. V. Pittoni, G. Valesini, The clearance of apoptotic cells: implications for autoimmunity, *Autoimmun Rev*, 1 (2002) 154-161.

96. O. Morel, L. Jesel, J.M. Freyssinet, F. Toti, Cellular mechanisms underlying the formation of circulating microparticles, *Arterioscler Thromb Vasc Biol*, 31 (2011) 15-26.

97. J. Jeong, I.M. Conboy, Phosphatidylserine directly and positively regulates fusion of myoblasts into myotubes, *Biochem Biophys Res Commun*, 414 (2011) 9-13.

98. Z. Wu, H. Nakanishi, Phosphatidylserine-containing liposomes: potential pharmacological interventions against inflammatory and immune diseases through the production of prostaglandin E(2) after uptake by myeloid derived phagocytes, *Arch Immunol Ther Exp (Warsz)*, 59 (2011) 195-201.

99. F.R. Maxfield, T.E. McGraw, Endocytic recycling, *Nat Rev Mol Cell Biol*, 5 (2004) 121-132.

100. L.V. Chernomordik, M.M. Kozlov, Protein-lipid interplay in fusion and fission of biological membranes, *Annu Rev Biochem*, 72 (2003) 175-207.

101. D. Papahadjopoulos, S. Nir, N. Duzgunes, Molecular mechanisms of calcium-induced membrane fusion, *J Bioenerg Biomembr*, 22 (1990) 157-179.

102. I.M. Hafez, P.R. Cullis, Roles of lipid polymorphism in intracellular delivery, *Adv Drug Deliv Rev*, 47 (2001) 139-148.

103. K. Al-Nedawi, B. Meehan, J. Micallef, V. Lhotak, L. May, A. Guha*, et al.*, Intercellular transfer of the oncogenic receptor EGFRvIII by microvesicles derived from tumour cells, *Nat Cell Biol*, 10 (2008) 619-624.

104. D.G. Meckes, Jr., K.H. Shair, A.R. Marquitz, C.P. Kung, R.H. Edwards, N. Raab-Traub, Human tumor virus utilizes exosomes for intercellular communication, *Proc Natl Acad Sci U S A*, 107 (2010) 20370-20375.

105. S. Manno, Y. Takakuwa, N. Mohandas, Identification of a functional role for lipid asymmetry in biological membranes: Phosphatidylserine-skeletal protein interactions modulate membrane stability, *Proc Natl Acad Sci U S A*, 99 (2002) 1943-1948.

106. I. Parolini, C. Federici, C. Raggi, L. Lugini, S. Palleschi, A. De Milito*, et al.*, Microenvironmental pH is a key factor for exosome traffic in tumor cells, *J Biol Chem*, 284 (2009) 34211-34222.

107. P.S. Niemela, S. Ollila, M.T. Hyvonen, M. Karttunen, I. Vattulainen, Assessing the nature of lipid raft membranes, *PLoS Comput Biol*, 3 (2007) e34.

108. S. Aimon, J. Manzi, D. Schmidt, J.A. Poveda Larrosa, P. Bassereau, G.E. Toombes, Functional reconstitution of a voltage-gated potassium channel in giant unilamellar vesicles, *PLoS One*, 6 (2011) e25529.

109. E.M. Erb, K. Tangemann, B. Bohrmann, B. Muller, J. Engel, Integrin alphaIIb beta3 reconstituted into lipid bilayers is nonclustered in its activated state but clusters after fibrinogen binding, *Biochemistry*, 36 (1997) 7395-7402.

110. P. Streicher, P. Nassoy, M. Barmann, A. Dif, V. Marchi-Artzner, F. Brochard-Wyart*, et al.*, Integrin reconstituted in GUVs: a biomimetic system to study initial steps of cell spreading, *Biochim Biophys Acta*, 1788 (2009) 2291-2300.

111. M. Zheng, H. Fang, T. Tsuruoka, T. Tsuji, T. Sasaki, S. Hakomori, Regulatory role of GM3 ganglioside in alpha 5 beta 1 integrin receptor for fibronectin-mediated adhesion of FUA169 cells, *J Biol Chem*, 268 (1993) 2217-2222.

112. A. Varnier, F. Kermarrec, I. Blesneac, C. Moreau, L. Liguori, J.L. Lenormand*, et al.*, A simple method for the reconstitution of membrane proteins into giant unilamellar vesicles, *J Membr Biol*, 233 (2010) 85-92.

113. F. Raimondo, L. Morosi, C. Chinello, F. Magni, M. Pitto, Advances in membranous vesicle and exosome proteomics improving biological understanding and biomarker discovery, *Proteomics*, 11 (2011) 709-720.

114. C. Thery, A. Regnault, J. Garin, J. Wolfers, L. Zitvogel, P. Ricciardi-Castagnoli*, et al.*, Molecular characterization of dendritic cell-derived exosomes. Selective accumulation of the heat shock protein hsc73, *J Cell Biol*, 147 (1999) 599-610.

115. J.M. Escola, M.J. Kleijmeer, W. Stoorvogel, J.M. Griffith, O. Yoshie, H.J. Geuze, Selective enrichment of tetraspan proteins on the internal vesicles of multivesicular endosomes and on exosomes secreted by human B-lymphocytes, *J Biol Chem*, 273 (1998) 20121-20127.

116. S. Atay, C. Gercel-Taylor, M. Kesimer, D.D. Taylor, Morphologic and proteomic characterization of exosomes released by cultured extravillous trophoblast cells, *Exp Cell Res*, 317 (2011) 1192-1202.

117. M.E. Hemler, Tetraspanin functions and associated microdomains, *Nat Rev Mol Cell Biol*, 6 (2005) 801-811.

118. M.E. Hemler, Targeting of tetraspanin proteins--potential benefits and strategies, *Nat Rev Drug Discov*, 7 (2008) 747-758.

119. K. Miyado, G. Yamada, S. Yamada, H. Hasuwa, Y. Nakamura, F. Ryu*, et al.*, Requirement of CD9 on the egg plasma membrane for fertilization, *Science*, 287 (2000) 321-324.

120. I. Tachibana, M.E. Hemler, Role of transmembrane 4 superfamily (TM4SF) proteins CD9 and CD81 in muscle cell fusion and myotube maintenance, *J Cell Biol*, 146 (1999) 893-904.

121. F. Martin, D.M. Roth, D.A. Jans, C.W. Pouton, L.J. Partridge, P.N. Monk*, et al.*, Tetraspanins in viral infections: a fundamental role in viral biology?, *J Virol*, 79 (2005) 10839-10851.

122. M. Gordon-Alonso, M. Yanez-Mo, O. Barreiro, S. Alvarez, M.A. Munoz-Fernandez, A. Valenzuela-Fernandez*, et al.*, Tetraspanins CD9 and CD81 modulate HIV-1-induced membrane fusion, *J Immunol*, 177 (2006) 5129-5137.

123. Y. Takeda, I. Tachibana, K. Miyado, M. Kobayashi, T. Miyazaki, T. Funakoshi*, et al.*, Tetraspanins CD9 and CD81 function to prevent the fusion of mononuclear phagocytes, *J Cell Biol*, 161 (2003) 945-956.

124. V. Parthasarathy, F. Martin, A. Higginbottom, H. Murray, G.W. Moseley, R.C. Read*, et al.*, Distinct roles for tetraspanins CD9, CD63 and CD81 in the formation of multinucleated giant cells, *Immunology*, 127 (2009) 237-248.

125. A.R. Mantegazza, M.M. Barrio, S. Moutel, L. Bover, M. Weck, P. Brossart*, et al.*, CD63 tetraspanin slows down cell migration and translocates to the endosomal-lysosomal-MIICs route after extracellular stimuli in human immature dendritic cells, *Blood*, 104 (2004) 1183-1190.

126. I. Nazarenko, S. Rana, A. Baumann, J. McAlear, A. Hellwig, M. Trendelenburg*, et al.*, Cell surface tetraspanin Tspan8 contributes to molecular pathways of exosome-induced endothelial cell activation, *Cancer Res*, 70 (2010) 1668-1678.

127. M.E. Hemler, Tetraspanin proteins mediate cellular penetration, invasion, and fusion events and define a novel type of membrane microdomain, *Annu Rev Cell Dev Biol*, 19 (2003) 397-422.

128. M. Zoller, Tetraspanins: push and pull in suppressing and promoting metastasis, *Nat Rev Cancer*, 9 (2009) 40-55.

129. S.M. van Dommelen, P. Vader, S. Lakhal, S.A. Kooijmans, W.W. van Solinge, M.J. Wood*, et al.*, Microvesicles and exosomes: opportunities for cell-derived membrane vesicles in drug delivery, *J Control Release*, 161 (2012) 635-644.

130. M. Barczyk, S. Carracedo, D. Gullberg, Integrins, *Cell Tissue Res*, 339 (2010) 269-280.

131. I.D. Campbell, M.J. Humphries, Integrin structure, activation, and interactions, *Cold Spring Harb Perspect Biol*, 3 (2011) a004994.

132. J. Hakulinen, L. Sankkila, N. Sugiyama, K. Lehti, J. Keski-Oja, Secretion of active membrane type 1 matrix metalloproteinase (MMP-14) into extracellular space in microvesicular exosomes, *J Cell Biochem*, 105 (2008) 1211-1218.

133. J.L. Welton, S. Khanna, P.J. Giles, P. Brennan, I.A. Brewis, J. Staffurth*, et al.*, Proteomics analysis of bladder cancer exosomes, *Mol Cell Proteomics*, 9 (2010) 1324-1338.

134. S. Rieu, C. Geminard, H. Rabesandratana, J. Sainte-Marie, M. Vidal, Exosomes released during reticulocyte maturation bind to fibronectin via integrin alpha4beta1, *Eur J Biochem*, 267 (2000) 583-590.

135. A. Clayton, A. Turkes, S. Dewitt, R. Steadman, M.D. Mason, M.B. Hallett, Adhesion and signaling by B cell-derived exosomes: the role of integrins, *FASEB J*, 18 (2004) 977-979.

136. M.M. Segura, A. Garnier, M.R. Di Falco, G. Whissell, A. Meneses-Acosta, N. Arcand*, et al.*, Identification of host proteins associated with retroviral vector particles by proteomic analysis of highly purified vector preparations, *J Virol*, 82 (2008) 1107-1117.

137. K. Temming, R.M. Schiffelers, G. Molema, R.J. Kok, RGD-based strategies for selective delivery of therapeutics and imaging agents to the tumour vasculature, *Drug Resist Updat*, 8 (2005) 381-402.

138. R. Meinecke, B. Meyer, Determination of the binding specificity of an integral membrane protein by saturation transfer difference NMR: RGD peptide ligands binding to integrin alphaIIbbeta3, *J Med Chem*, 44 (2001) 3059-3065.

139. B. Claasen, M. Axmann, R. Meinecke, B. Meyer, Direct observation of ligand binding to membrane proteins in living cells by a saturation transfer double difference (STDD) NMR spectroscopy method shows a significantly higher affinity of integrin alpha(IIb)beta3 in native platelets than in liposomes, *J Am Chem Soc*, 127 (2005) 916-919.

140. P.A. Gonzales, T. Pisitkun, J.D. Hoffert, D. Tchapyjnikov, R.A. Star, R. Kleta*, et al.*, Large-scale proteomics and phosphoproteomics of urinary exosomes, *J Am Soc Nephrol*, 20 (2009) 363-379.

141. M. Gonzalez-Begne, B. Lu, X. Han, F.K. Hagen, A.R. Hand, J.E. Melvin*, et al.*, Proteomic analysis of human parotid gland exosomes by multidimensional protein identification technology (MudPIT), *J Proteome Res*, 8 (2009) 1304-1314.

142. T. Pisitkun, R.F. Shen, M.A. Knepper, Identification and proteomic profiling of exosomes in human urine, *Proc Natl Acad Sci U S A*, 101 (2004) 13368-13373.

143. C. Looze, D. Yui, L. Leung, M. Ingham, M. Kaler, X. Yao*, et al.*, Proteomic profiling of human plasma exosomes identifies PPARgamma as an exosome-associated protein, *Biochem Biophys Res Commun*, 378 (2009) 433-438.

144. M.P. Bard, J.P. Hegmans, A. Hemmes, T.M. Luider, R. Willemsen, L.A. Severijnen*, et al.*, Proteomic analysis of exosomes isolated from human malignant pleural effusions, *Am J Respir Cell Mol Biol*, 31 (2004) 114-121.

145. S. Mathivanan, J.W. Lim, B.J. Tauro, H. Ji, R.L. Moritz, R.J. Simpson, Proteomics analysis of A33 immunoaffinity-purified exosomes released from the human colon tumor cell line LIM1215 reveals a tissue-specific protein signature, *Mol Cell Proteomics*, 9 (2010) 197-208.

146. A.S. John, V.L. Rothman, G.P. Tuszynski, Thrombospondin-1 (TSP-1) Stimulates Expression of Integrin alpha6 in Human Breast Carcinoma Cells: A Downstream Modulator of TSP-1-Induced Cellular Adhesion, *J Oncol*, 2010 (2010) 645376.

147. C. Nucera, A. Porrello, Z.A. Antonello, M. Mekel, M.A. Nehs, T.J. Giordano*, et al.*, B-Raf(V600E) and thrombospondin-1 promote thyroid cancer progression, *Proc Natl Acad Sci U S A*, 107 (2010) 10649-10654.

148. M.P. Rivera-Fillat, F. Reig, E.M. Martinez, M.R. Grau-Oliete, Improved therapeutic responses for liposomal doxorubicin targeted via thrombospondin peptidomimetics versus untargeted doxorubicin, *J Pept Sci*, 16 (2010) 315-321.

149. S. Kazerounian, K.O. Yee, J. Lawler, Thrombospondins in cancer, *Cell Mol Life Sci*, 65 (2008) 700-712.

150. X. Zhang, J. Lawler, Thrombospondin-based antiangiogenic therapy, *Microvasc Res*, 74 (2007) 90-99.

151. D. Skokos, S. Le Panse, I. Villa, J.C. Rousselle, R. Peronet, B. David*, et al.*, Mast cell-dependent B and T lymphocyte activation is mediated by the secretion of immunologically active exosomes, *J Immunol*, 166 (2001) 868-876.

152. D. Skokos, S. Le Panse, I. Villa, J.C. Rousselle, R. Peronet, A. Namane*, et al.*, Nonspecific B and T cell-stimulatory activity mediated by mast cells is associated with exosomes, *Int Arch Allergy Immunol*, 124 (2001) 133-136.

153. S.I. Buschow, B.W. van Balkom, M. Aalberts, A.J. Heck, M. Wauben, W. Stoorvogel, MHC class II-associated proteins in B-cell exosomes and potential functional implications for exosome biogenesis, *Immunol Cell Biol*, 88 (2010) 851-856.

154. E.O. Long, ICAM-1: getting a grip on leukocyte adhesion, *J Immunol*, 186 (2011) 5021-5023.

155. U. Svajger, M. Anderluh, M. Jeras, N. Obermajer, C-type lectin DC-SIGN: an adhesion, signalling and antigen-uptake molecule that guides dendritic cells in immunity, *Cell Signal*, 22 (2010) 1397-1405.

156. E. Segura, C. Nicco, B. Lombard, P. Veron, G. Raposo, F. Batteux*, et al.*, ICAM-1 on exosomes from mature dendritic cells is critical for efficient naive T-cell priming, *Blood*, 106 (2005) 216-223.

157. E. Segura, C. Guerin, N. Hogg, S. Amigorena, C. Thery, CD8+ dendritic cells use LFA-1 to capture MHC-peptide complexes from exosomes in vivo, *J Immunol*, 179 (2007) 1489-1496.

158. D.S. Choi, J.M. Lee, G.W. Park, H.W. Lim, J.Y. Bang, Y.K. Kim*, et al.*, Proteomic analysis of microvesicles derived from human colorectal cancer cells, *J Proteome Res*, 6 (2007) 4646-4655.

159. M. Kesimer, M. Scull, B. Brighton, G. DeMaria, K. Burns, W. O'Neal*, et al.*, Characterization of exosome-like vesicles released from human tracheobronchial ciliated epithelium: a possible role in innate defense, *FASEB J*, 23 (2009) 1858-1868.

160. W.G. Brodbeck, C. Mold, J.P. Atkinson, M.E. Medof, Cooperation between decay-accelerating factor and membrane cofactor protein in protecting cells from autologous complement attack, *J Immunol*, 165 (2000) 3999-4006.

161. S.A. Rollins, P.J. Sims, The complement-inhibitory activity of CD59 resides in its capacity to block incorporation of C9 into membrane C5b-9, *J Immunol*, 144 (1990) 3478-3483.

162. S. Liu, T. Ishida, H. Kiwada, Characterization of bovine serum factor triggering the lysis of liposomes via complement activation, *Biol Pharm Bull*, 21 (1998) 390-397.

163. A.J. Bradley, D.V. Devine, S.M. Ansell, J. Janzen, D.E. Brooks, Inhibition of liposome-induced complement activation by incorporated poly(ethylene glycol)-lipids, *Arch Biochem Biophys*, 357 (1998) 185-194.

164. B. Fevrier, D. Vilette, F. Archer, D. Loew, W. Faigle, M. Vidal*, et al.*, Cells release prions in association with exosomes, *Proc Natl Acad Sci U S A*, 101 (2004) 9683-9688.

165. I. Potolicchio, G.J. Carven, X. Xu, C. Stipp, R.J. Riese, L.J. Stern*, et al.*, Proteomic analysis of microglia-derived exosomes: metabolic role of the aminopeptidase CD13 in neuropeptide catabolism, *J Immunol*, 175 (2005) 2237-2243.

166. H. Ji, N. Erfani, B.J. Tauro, E.A. Kapp, H.J. Zhu, R.L. Moritz*, et al.*, Difference gel electrophoresis analysis of Ras-transformed fibroblast cell-derived exosomes, *Electrophoresis*, 29 (2008) 2660-2671.

167. M.H. Andersen, H. Graversen, S.N. Fedosov, T.E. Petersen, J.T. Rasmussen, Functional analyses of two cellular binding domains of bovine lactadherin, *Biochemistry*, 39 (2000) 6200-6206.

168. L. Lin, Q. Huai, M. Huang, B. Furie, B.C. Furie, Crystal structure of the bovine lactadherin C2 domain, a membrane binding motif, shows similarity to the C2 domains of factor V and factor VIII, *J Mol Biol*, 371 (2007) 717-724.

169. A.E. Morelli, A.T. Larregina, W.J. Shufesky, M.L. Sullivan, D.B. Stolz, G.D. Papworth*, et al.*, Endocytosis, intracellular sorting, and processing of exosomes by dendritic cells, *Blood*, 104 (2004) 3257-3266.

170. M.H. Fens, E. Mastrobattista, A.M. de Graaff, F.M. Flesch, A. Ultee, J.T. Rasmussen*, et al.*, Angiogenic endothelium shows lactadherin-dependent phagocytosis of aged erythrocytes and apoptotic cells, *Blood*, 111 (2008) 4542-4550.

171. X. Qiang, J. Li, R. Wu, Y. Ji, W. Chaung, W. Dong*, et al.*, Expression and characterization of recombinant human milk fat globule-EGF factor VIII, *Int J Mol Med*, 28 (2011) 1071-1076.

172. B. Shen, N. Wu, J.M. Yang, S.J. Gould, Protein targeting to exosomes/microvesicles by plasma membrane anchors, *J Biol Chem*, 286 (2011) 14383-14395.

173. C. Klammt, D. Schwarz, F. Lohr, B. Schneider, V. Dotsch, F. Bernhard, Cell-free expression as an emerging technique for the large scale production of integral membrane protein, *FEBS J*, 273 (2006) 4141-4153.

174. S. Reckel, S. Sobhanifar, F. Durst, F. Lohr, V.A. Shirokov, V. Dotsch*, et al.*, Strategies for the cell-free expression of membrane proteins, *Methods Mol Biol*, 607 (2010) 187-212.

175. D. Schwarz, V. Dotsch, F. Bernhard, Production of membrane proteins using cell-free expression systems, *Proteomics*, 8 (2008) 3933-3946.

176. N.T. Hovijitra, J.J. Wuu, B. Peaker, J.R. Swartz, Cell-free synthesis of functional aquaporin Z in synthetic liposomes, *Biotechnol Bioeng*, 104 (2009) 40-49.

177. M. Kaneda, S.M. Nomura, S. Ichinose, S. Kondo, K. Nakahama, K. Akiyoshi*, et al.*, Direct formation of proteo-liposomes by in vitro synthesis and cellular cytosolic delivery with connexin-expressing liposomes, *Biomaterials*, 30 (2009) 3971-3977.

178. Y. Malam, M. Loizidou, A.M. Seifalian, Liposomes and nanoparticles: nanosized vehicles for drug delivery in cancer, *Trends Pharmacol Sci*, 30 (2009) 592-599.

179. Y.S. Tarahovsky, "Smart" liposomal nanocontainers in biology and medicine, *Biochemistry (Mosc)*, 75 (2010) 811-824.

180. H.X. Wang, T.V. Kolesnikova, C. Denison, S.P. Gygi, M.E. Hemler, The C-terminal tail of tetraspanin protein CD9 contributes to its function and molecular organization, *J Cell Sci*, 124 (2011) 2702-2710.

181. C.L. Bartels, G.J. Tsongalis, MicroRNAs: novel biomarkers for human cancer, *Clin Chem*, 55 (2009) 623-631.

182. J.C. Henry, A.C. Azevedo-Pouly, T.D. Schmittgen, microRNA Replacement Therapy for Cancer, *Pharm Res*, 28 (2011) 3030-3042.

183. J. Kota, R.R. Chivukula, K.A. O'Donnell, E.A. Wentzel, C.L. Montgomery, H.W. Hwang*, et al.*, Therapeutic microRNA delivery suppresses tumorigenesis in a murine liver cancer model, *Cell*, 137 (2009) 1005-1017.

184. C. Liu, K. Kelnar, B. Liu, X. Chen, T. Calhoun-Davis, H. Li*, et al.*, The microRNA miR-34a inhibits prostate cancer stem cells and metastasis by directly repressing CD44, *Nat Med*, 17 (2011) 211-215.

185. R. Gambari, E. Fabbri, M. Borgatti, I. Lampronti, A. Finotti, E. Brognara*, et al.*, Targeting microRNAs involved in human diseases: a novel approach for modification of gene expression and drug development, *Biochem Pharmacol*, 82 (2011) 1416-1429.

186. S.K. Kota, S. Balasubramanian, Cancer therapy via modulation of micro RNA levels: a promising future, *Drug Discov Today*, 15 (2010) 733-740.

187. H. Matsubara, T. Takeuchi, E. Nishikawa, K. Yanagisawa, Y. Hayashita, H. Ebi*, et al.*, Apoptosis induction by antisense oligonucleotides against miR-17-5p and miR-20a in lung cancers overexpressing miR-17-92, *Oncogene*, 26 (2007) 6099-6105.

188. M.F. Segura, D. Hanniford, S. Menendez, L. Reavie, X. Zou, S. Alvarez-Diaz*, et al.*, Aberrant miR-182 expression promotes melanoma metastasis by repressing FOXO3 and microphthalmia-associated transcription factor, *Proc Natl Acad Sci U S A*, 106 (2009) 1814-1819.

189. M.L. Si, S. Zhu, H. Wu, Z. Lu, F. Wu, Y.Y. Mo, miR-21-mediated tumor growth, *Oncogene*, 26 (2007) 2799-2803.

190. Y. Sylvestre, V. De Guire, E. Querido, U.K. Mukhopadhyay, V. Bourdeau, F. Major*, et al.*, An E2F/miR-20a autoregulatory feedback loop, *J Biol Chem*, 282 (2007) 2135-2143.

191. Y. Lu, S. Roy, G. Nuovo, B. Ramaswamy, T. Miller, C. Shapiro*, et al.*, Anti-microRNA-222 (Anti-miR-222) and -181B Suppress Growth of Tamoxifen-resistant Xenografts in Mouse by Targeting TIMP3 Protein and Modulating Mitogenic Signal, *J Biol Chem*, 286 (2011) 42292-42302.

192. Y.P. Yang, Y. Chien, G.Y. Chiou, J.Y. Cherng, M.L. Wang, W.L. Lo*, et al.*, Inhibition of cancer stem cell-like properties and reduced chemoradioresistance of glioblastoma using microRNA145 with cationic polyurethane-short branch PEI, *Biomaterials*, (Epub 2011 Nov 17).

193. D. Xu, F. Takeshita, Y. Hino, S. Fukunaga, Y. Kudo, A. Tamaki*, et al.*, miR-22 represses cancer progression by inducing cellular senescence, *J Cell Biol*, 193 (2011) 409-424.

194. D.H. Kim, J.J. Rossi, Strategies for silencing human disease using RNA interference, *Nat Rev Genet*, 8 (2007) 173-184.

195. P. Guo, O. Coban, N.M. Snead, J. Trebley, S. Hoeprich, S. Guo*, et al.*, Engineering RNA for targeted siRNA delivery and medical application, *Adv Drug Deliv Rev*, 62 (2010) 650-666.

196. F. Szoka, Molecular biology. The art of assembly, *Science*, 319 (2008) 578-579.

197. S. Lakhal, M.J. Wood, Exosome nanotechnology: an emerging paradigm shift in drug delivery: exploitation of exosome nanovesicles for systemic in vivo delivery of RNAi heralds new horizons for drug delivery across biological barriers, *Bioessays*, 33 (2011) 737-741.

CHAPTER 8

Summarizing discussion and perspectives

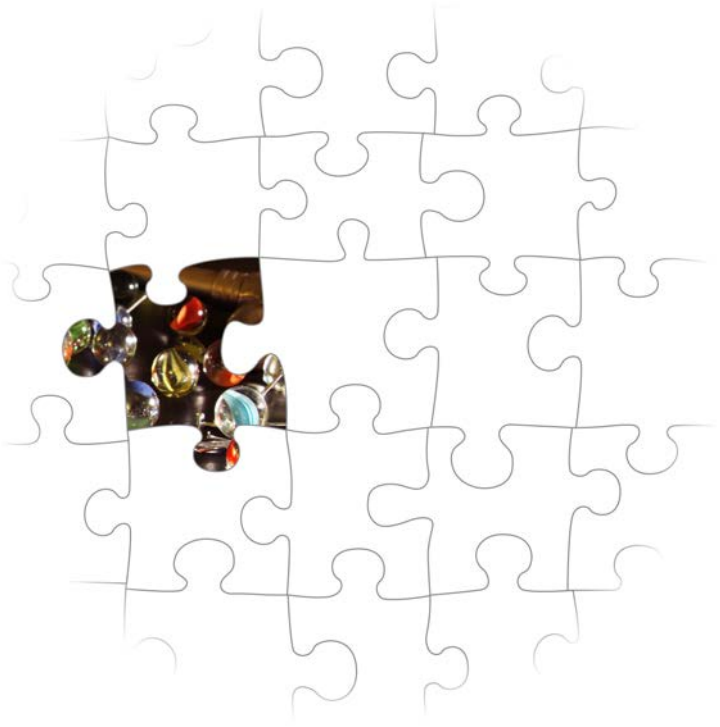

Extracellular vesicles as candidate drug delivery systems

For many diseases, the clinical effectiveness of state-of-the-art therapy could be improved by packaging of therapeutic molecules into synthetic nanoparticles, like liposomes and polymeric micelles. Nanoparticles for drug delivery are typically designed to (1) protect encapsulated cargo (e.g. siRNA) against degradation by plasma components, (2) have a size of < 200 nm, allowing passive extravasation in inflamed tissues and limiting premature renal clearance [1], and (3) provide a customizable surface, which can be tailored towards the desired application (e.g. by incorporation of targeting ligands or shielding moieties to improve pharmacokinetic profiles)[2]. However, despite intensive research over the past decades, the number of approved nanoparticulate drug delivery systems in the clinic is still limited [3-6]. There are multiple reasons for the fact that the overwhelming numbers of publications and citations on this topic have resulted in such limited clinical success. For example, the large-scale and reproducible production of nanoparticulate drug delivery systems is generally costly, and their multi-component composition compared with small molecule drugs complicates approval by regulatory agencies [5, 7-9]. However, perhaps the most striking phenomenon encountered by synthetic drug delivery systems is that in early research stages they show promising characteristics for drug delivery, but often fail to transition to clinical development due to toxicity, immunogenicity, undesired interactions with blood components, and off-target tissue distribution [8-10].

Despite the many challenges, attempts are continuously being made to convey therapeutic messages to diseased cells using synthetic systems. Strikingly, similar messages are sent back and forth between cells in our body by one of nature's own intercellular communication nanosystems: extracellular vesicles (EVs). The finding that EVs can transfer bioactive cargo (proteins, lipids and nucleic acids) to recipient cells and thereby initiate phenotypical changes in those cells [11], has – quite justifiably – created excitement in the field of drug delivery. Why start with *de novo* synthesis of drug delivery systems, if the blueprint for successful drug delivery systems, harnessed by EVs, is already available? The idea that EVs could potentially be exploited for targeted and biocompatible delivery of therapeutic cargo formed the basis for the research described in this thesis.

The word 'blueprint' employed in the previous paragraph suggests that EVs cannot be considered as fully developed drug delivery systems yet. In order to employ EVs for therapeutic purposes, some intrinsic characteristics of naturally occurring EVs may need to be manipulated or improved. In this thesis, we explored engineering of two aspects of EVs to improve their therapeutic value: their cargo and their targeting specificity towards tumor cells.

Loading of therapeutic cargo into extracellular vesicles

Multiple reports have shown that EVs carry small RNAs (e.g. miRNA) and mRNAs, and that these can be functionally transferred to recipient cells [12-18]. Hence, EVs are hypothesized to be highly suitable for the delivery of therapeutic nucleic acids, including siRNA (whose structure

resembles that of miRNA) to target cells. Although siRNA has great therapeutic value due to its ability to specifically silence virtually any gene, its physicochemical characteristics (high molecular weight and net negative charge) prevent entry into the cellular cytosol, where it exerts its effects. Incorporation of siRNA into 'Trojan horse' EVs could greatly facilitate its intracellular delivery efficiency. However, given that the fact that EVs share characteristics with their parent cells, including a bilayer membrane bearing a negative charge, passive diffusion of exogenous nucleic acids into EVs is efficiently prevented. Hence, simple mixing of EVs with siRNAs does not typically result in siRNA-loaded EVs (although remarkable cases of successful miRNA loading into EVs using this approach have been described [19, 20]). Therefore, in the past decade, alternative approaches for siRNA loading into EVs have been gradually explored. The first report of successful loading of siRNA into EVs was published in 2011 by the Wood lab [21]. In this exceptional study, electroporation of a mixture of EVs and siRNA resulted in highly efficient association of the siRNA with EVs after pelleting, supposedly due to temporary formation of pores into the EV membrane, allowing trapping of siRNA in the EV lumen. Subsequently, the siRNA could be functionally delivered to the brains of mice after intravenous administration of the EVs. Hence, electroporation quickly became accepted as an efficient method to incorporate small RNAs into EVs, and was adopted by others [22-28]. However, the mechanism of the efficient incorporation of siRNA using this approach remained unclear.

To elucidate this mechanism and in an attempt to further optimize the electroporation protocol, we performed the study described in **Chapter 2**. To our surprise, electroporation of siRNA according to the previously established protocols resulted in pronounced siRNA precipitation, regardless of the presence of EVs in the electroporation mixture. In addition, our results showed that the amount of siRNA retained by the EVs after electroporation was negligible. siRNA precipitation resulted from the release of metal ions from the cuvette electrodes into the electroporation buffer upon electroporation. These ions formed insoluble complexes with hydroxide ions and siRNA, and these complexes showed sizes overlapping those of EVs. Hence, these complexes could not be separated from EVs by commonly used ultracentrifugation protocols, suggesting that previously reported siRNA loading efficiencies after electroporation were severely overestimated [21, 23]. In an attempt to reduce siRNA precipitation during electroporation and thereby improve its retention in EVs, protocols in which metal ions were either absent or removed by chelators were investigated. Unfortunately, despite the successful removal of siRNA precipitates using these protocols, loading of siRNA into EVs using electroporation could not be demonstrated.

Our study thus demonstrates that loading of siRNA into isolated EVs using electroporation is less straightforward than previously anticipated. However, the electroporation technique theoretically has important potential advantages over other loading procedures, including independence of nucleic acid sequence and EV type, controllability, and high-throughput scalability, which merits further optimization of this technique. Recently it was shown that addition of the disaccharide trehalose to the electroporation medium can

inhibit precipitate formation and promote colloidal stability of the EVs during electroporation when aluminum electrodes are used [29, 30]. Interestingly, the authors claimed that 5 nm superparamagnetic iron oxide particles could be loaded into EVs using this electroporation medium, although solid evidence for this outcome was not presented [29]. Nevertheless, such advances may ultimately lead to the development of suitable electroporation methods for loading of exogenous cargoes into EVs with retained colloidal stability and integrity.

To pursue such goals, it is important to identify what loading efficiency would at least be required for the desired therapeutic effects. The theoretical maximal siRNA capacity of EVs can be estimated to be approximately 17 500 copies per EV, assuming that EVs are perfect spherical empty structures with an average diameter of 100 nm, and assuming that a single siRNA molecule has a diameter of 2 nm and a length of 7.5 nm [31]. However, in practice, this number is likely to be considerably lower, given that EVs are not empty, but rather dense structures that already carry protein and nucleic acid cargo, which limits the space for exogenously introduced cargo. Still, given that a few hundred siRNA molecules delivered to the cytoplasm of a cell is sufficient for adequate gene silencing [32, 33], the loading of as much as one siRNA molecule per EV (corresponding to a luminal siRNA concentration of ~ 3 μM) could prove to be valuable if the loaded EVs truly efficiently transfer this cargo to the cytoplasm of recipient cells. In fact, stoichiometric analyses have shown that EVs by nature contain similar low levels of regulatory miRNAs [34, 35], which nevertheless seems sufficient to influence target gene expression in recipient cells [35].

Besides electroporation, other strategies have been described to load EVs with exogenous cargoes after their isolation through temporary disruption of the EV membrane, including extrusion, sonication, freeze/thawing, hypotonic dialysis and detergent permeabilization [36-38]. However, the majority of these methods (i.e. extrusion, sonication, freeze/thawing and saponin permeabilization) result in severe loss of EV morphology and integrity [36, 38], which likely compromises their potential to functionally deliver biological cargoes such as siRNA. However, for small molecule drug cargoes, delivery into the cytoplasm of recipient cells is not always required for eliciting therapeutic effects. In these scenarios, subtle membrane disruption methods, such as electroporation and permeabilization with low concentrations of detergents, may facilitate the loading of hydrophilic molecules into EVs, which may boost intracellular drug uptake due to co-internalization with EVs by recipient cells [37, 39]. However, detrimental membrane disruption during loading may result in compromised EV stability in circulation and rapid drug release. For hydrophobic compounds, such loading methods may not be required, as simple co-incubation of drug molecules with EVs is often sufficient for drug incorporation into the hydrophobic EV membrane [37, 40-42]. However, it is conceivable that these molecules are also rapidly extracted from EVs in plasma, possibly resulting in undesirable (burst release) pharmacokinetics and impaired delivery to target cells.

Despite the current lack of robust protocols for loading of biological cargoes into *isolated*

EVs, methods for EV enrichment with such molecules via cellular engineering are relatively well established. In fact, the involvement of cells in the loading process may be essential to load RNAs into EVs in such a way that they can be functionally transferred to recipient cells. Recent studies suggest that miRNA effector molecules (e.g. Ago2) in EV producer cells play a role in sorting and stabilization of miRNAs into EVs, and promote the functionality of these miRNAs in recipient cells [43-45].

Cellular engineering for (small) RNA loading into EVs is briefly reviewed in **Chapter 3,** and can be achieved using two engineering approaches. In the first approach, EV-producing cells are transfected or transduced with vectors designed to drive overexpression of the RNA of interest. It is commonly observed that this results in higher levels of the selected RNA in EVs, possibly due to non-specific sorting of cellular RNA into EVs [13, 15, 46-51]. In the second approach, cells are transfected directly with synthetic (small) RNAs, resulting in increased cellular RNA levels and improved secretion of the transfected RNAs into EVs [52-58]. This method provides the additional advantage that the synthetic RNAs can be modified (e.g. with fluorophores, radioisotopes or stabilizing modifications) and traced in downstream applications [54, 58]. Unfortunately, cellular engineering strategies also have disadvantages compared with post-secretion loading strategies. Firstly, RNA partitioning into EVs is believed to occur with some sequence specificity, however it is unclear how this process is regulated, especially for small RNAs. It is conceivable that RNA sequences and/or secondary structures determine localization into EVs [59-65], and in some scenarios these cannot be altered to increase incorporation into EVs (e.g. siRNA will lose target specificity and activity when its sequence is mutated). As a consequence, therapeutic RNAs may be preferentially retained by cells instead of sorted into EVs. Secondly, EVs could possibly be 'contaminated' with transfection reagents used to modify their parent cells, which could bias their performance in reporter assays. Thirdly, overexpressed RNA sequences can be preferentially secreted by cells through other mechanisms besides via EVs, such as via chaperone proteins. In fact, it is increasingly being recognized that the vast majority of RNAs secreted in plasma from various cell sources (> 99%) is *not* incorporated in EVs [66-68], although lower percentages have been reported for other bodily fluids [69, 70]. Taken together, despite the multitude of reports describing successful loading of RNA into EVs using engineered cells, underlying cellular RNA sorting machineries need to be unraveled first to further exploit this strategy for the reproducible generation of siRNA-loaded EVs.

An overview of currently employed strategies to load EVs with (small) RNAs, either through cell engineering or isolated EV engineering, is shown in Table 1.

TARGETING OF EXTRACELLULAR VESICLES

The question whether EVs are naturally programmed to selectively interact with specific cell types or tissues is still subject to debate. While some combinations of EVs and cells appear to result in higher uptake than others, suggestive of cell specificity [71-73], other reports indicate that such specificity may be lacking [74, 75] and that 'cell-specific' EV uptake is predominantly

Table 1: Overview of advantages and disadvantages of EV RNA-loading strategies discussed in this thesis.

Loading strategy	Advantages	Disadvantages
Cell engineering		
Producer cell modification with RNA-expressing vectors	• Incorporation of RNAs in the EV lumen, protected from degradation • Magnitude of RNA incorporation often reflects cellular expression levels • EV characteristics remain likely unaltered compared to native EVs	• Necessity to modify producer cells • Sequence-specific secretion of RNA may limit incorporation of desired RNAs into EVs • Regulatory effects and undesired translation of RNAs in producer cells may disrupt cell function and compromise secretion of RNA-loaded EVs • Time-consuming
Producer cell transfection with synthetic RNAs	• Incorporation of RNAs in the EV lumen, protected from degradation • Magnitude of RNA incorporation may correlate with RNA doses used to modify producer cells • Allows loading of EVs with labeled RNAs for downstream tracing	• Necessity to modify producer cells • Sequence-specific secretion of RNA may limit incorporation of desired RNAs into EVs • Regulatory effects and undesired translation of RNAs in producer cells may disrupt cell function and compromise secretion of RNA-loaded EVs • Presence of traces of transfection reagent in/ on EVs may bias delivery performance in downstream assays. • Expensive (transfection reagents, oligonucleotides), especially when performed at scales required for *in vivo* application
Isolated EV engineering		
Electroporation	• Rapid procedure • Scalable to high-throughput application • Sequence-independent incorporation • Producer cells not required, potentially suitable for plasma-derived EVs	• Possible aggregation, precipitation and integrity loss of EVs • RNAs may not be fully incorporated in the EV lumen, allowing for degradation and loss of function • Extremely low incorporation efficiency, validated protocols are still lacking

Isolated EV engineering (continued)		
Other chemical and phyisical membrane disruption methods: 1. Detergent solubilization 2. Sonication 3. Extrusion 4. Hypotonic dialysis 5. Freeze/thawing	• Sequence-independent incorporation • Producer cells not required, potentially suitable for plasma-derived EVs	• Small increases in EV size (for 1, 2 and 4), severe EV aggregation/loss of integrity (for 2, 3 and 5), loss of functionality (for 4 and 5), and loss of zeta potential (for 3) have been reported [36-38] • RNAs may not be fully incorporated in the EV lumen, allowing for degradation and loss of function • Hard-to-remove traces of detergent may affect EV functioning (for 1) • Low loading efficiencies reported (for 3). • Not yet demonstrated for RNA cargo

determined by the phagocytic activity of the recipient cells [76]. Nevertheless, for drug delivery purposes, these targeting characteristics may need to be manipulated to improve the target cell-specific uptake of EVs and reduce their uptake by other, non-targeted cells. For synthetic particulate delivery systems this is traditionally achieved through the introduction of targeting ligands on the particle surface. However, given that the composition of EVs is dictated by their producing cells, surface modifications are less straightforward for EVs than for synthetic systems.

The challenge to introduce targeting ligands onto EVs was first tackled by the Wood lab, who described the generation of fusion constructs of neuron-specific targeting peptides fused to the external N-terminus of the EV membrane protein Lamp2b [21]. After transfection of immature dendritic cells with these vectors, these cells secreted EVs which displayed the targeting peptides on their surface, resulting in improved cargo delivery to neuronal cells. In follow-up studies, this seemingly simple yet effective engineering technique was also applied to other targeting ligands [21, 39], for another EV surface receptor [53], and for EV incorporation of tags and reporter proteins [77, 78]. However, a recent report demonstrated that, instead of sorting into EVs, degradation of fusion proteins may occur when this approach is employed [77]. Furthermore, fusion of recombinant proteins to EV membrane proteins may impair the functionality of these membrane proteins, possibly affecting delivery performance. Hence, here we investigated alternative strategies to introduce targeting ligands onto EVs in an efficient manner.

In this thesis, four novel EV targeting strategies have been described (summarized in Table 2). All targeting strategies were performed using high-affinity anti-epidermal growth factor receptor (EGFR) nanobodies as targeting ligands, which facilitates comparison between

these methods.

In **Chapter 4** we explored the use of glycosylphosphatidylinositol (GPI)-anchoring peptides to display nanobodies onto EVs. Herein, nanobody DNA sequences were fused to GPI-anchor peptide sequences and stably expressed in Neuro2A cells. The GPI-anchor peptides are cleaved from the nanobodies during intracellular processing and drive attachment of GPI to the C-terminus of the nanobodies. As a consequence, the nanobodies were shown to be inserted onto cellular and EV membranes. Moreover, given that EVs are typically enriched in tightly packed, specialized membrane microdomains which contain high concentrations of GPI (lipid rafts), GPI-fused nanobodies were highly enriched in EVs compared with their parent cells. Through this modification, EV association with EGFR-expressing tumor cells was greatly enhanced, while interactions with other (EGFR-negative) cells were unaltered, suggestive of increased EV cell targeting specificity. Interestingly, these improved binding characteristics were maintained in a perfusion model, in which EV-tumor cell interactions were challenged with shear forces. While this system was not fully representative for *in vivo* tumor physiology, it clearly confirmed that decoration of EVs with targeting moieties efficiently altered interactions with their environment. In future studies, this model may be employed to investigate EV interactions with extracellular matrix proteins and the vessel wall, to increase our understanding of EV behavior in circulation and further improve tissue-specific EV targeting.

While GPI-anchoring is an efficient strategy to display nanobodies on EVs, its time-consuming protocol and the necessity to modify and culture producer cells may limit its widespread application for the generation of targeted EVs. In addition, when screening for appropriate (combinations of) targeting ligands and/or EV sources for the intended application, cell engineering strategies are seldom preferable. Instead, direct surface engineering of EVs *after secretion* would possibly allow for controllable, high-density ligand incorporation regardless of ligand type, while cellular ligand expression issues are avoided. However, robust and biocompatible protocols for the grafting of targeting ligands onto isolated EVs are currently lacking.

In an attempt to devise such protocols, in Chapter 4 we also employed the stable conjugation of targeting ligands to the surface of isolated EVs using chemical linkers. Herein, NHS ester reactive groups on EVs, mostly comprising available N-termini and lysine residues of membrane proteins, are stably linked to targeting ligands under biocompatible reaction conditions. This reaction mechanism has been previously employed to efficiently decorate EVs with reactive alkyne moieties [79]. Using this method, we efficiently decorated EVs with anti-EGFR nanobodies at a high surface density, dramatically altering EV binding and internalization by EGFR-overexpressing tumor cells. However, when non-targeting control nanobodies were employed, it was observed that EV-cell interactions were severely compromised compared with unmodified EVs. These data indicate that this conjugation strategy can be considered as a 'brute force' strategy, which non-selectively replaces the natural functions of EV membrane proteins (possibly required for cell association, intracellular processing and cargo delivery)

with specific receptor-binding properties. The question remains whether this EV surface functionalization - despite enhancing internalization by target cells - also improves cargo delivery to these cells, or whether it rather drives EV accumulation into lysosomes of target cells and/or cargo degradation. It is anticipated that careful fine-tuning of nanobody/EV ratios is required in order to preserve functionality of crucial EV proteins, while introducing sufficient amounts of targeting ligands to improve cell specificity.

As an alternative strategy to equip isolated EVs with targeting ligands, in **Chapter 5** we investigated whether the 'post-insertion' technique, well-studied in the liposome field, could also be applied to EVs, which - given their shape, size and lipid bilayer membrane - may be considered as complex liposomes. According to this technique, anti-EGFR nanobodies were fused to the distal ends of polyethylene glycol (PEG)-coupled phospholipids, which formed micelles in aqueous solutions. Subsequently, these micelles were mixed with EVs derived from Neuro2A cells, and incubated at elevated temperatures to promote micelle disintegration and spontaneous incorporation of the nanobody-PEG-lipids onto the EV membrane. To our surprise, nanobody-PEG-lipids readily transferred to EV membranes in a temperature-dependent manner. Interestingly, some lipid transfer was even observed at low temperatures (4°C). Hence, the efficiency of this transfer appeared to be similar to, or perhaps even higher than that reported for liposomes [80, 81]. Furthermore, this strategy appears to be applicable to EVs from other sources, given that similar nanobody-PEG-lipid transfer to platelet-derived EVs was observed, which widens its general applicability. The incorporation of nanobodies on Neuro2A EVs through post-insertion improved EV association with EGFR-overexpressing tumor cells, while at the same time the incorporation of PEG chains reduced interactions with other, non-targeted cells. In addition, the insertion of PEG-lipids dramatically increased the circulation time of intravenously administered EVs in mice. While this behavior is common to PEGylated liposomes and other nanoparticles [82, 83], we are the first to show that this mechanism also applies to EVs. Such elongation of EV circulation time through surface engineering may prove to be crucial for the further development of EV-based drug delivery systems, given that unmodified exogenously administered EVs are rapidly cleared from circulation by cells from the reticulo-endothelial system (RES) (i.e. within 10-30 min [11]), which greatly limits their exposure to, and accumulation in targeted diseased cells and tissues. It should be noted however, that the drawbacks of PEGylation observed for liposomes, including impaired endosomal escape and transfection efficiency [82], likely also apply to PEGylated EVs. Hence, although insertion of shielding polymers into EVs is a promising advance towards the development of efficient EV-based drug delivery systems, careful optimization of this technique (e.g. PEG and ligand density, PEG chain and acyl length) is required to preserve the unique properties for efficient cargo delivery harnessed by EVs.

Alternatively, it is possible to decorate isolated EVs with targeting ligands while preserving the interactions of other EV membrane proteins with recipient cells (which is partly lost when applying chemical conjugation or post-insertion techniques). To achieve this,

Table 2: Overview of advantages and disadvantages of EV targeting strategies discussed in this thesis.

Targeting strategy	Advantages	Disadvantages
Cell engineering		
Conventional ligand fusion with EV membrane proteins	• Stable ligand incorporation • Predictable ligand orientation in EV membrane • EV cargo delivery potential is likely maintained	• Time-consuming • Producer cell modification required • Possibility of ligand degradation and low expression levels in EVs • Possibly impairs function of EV membrane fusion partners • Not applicable to all ligands/ therapeutic proteins (e.g. producer cell-targeting peptides or toxic proteins)
Ligand fusion with GPI-anchors	• Ligand enrichment compared with parent cells • EV cargo delivery potential is likely maintained • Likely no impairment of EV protein functions • Possibly higher complexity of targeting ligands allowed than for fusion with EV membrane proteins	• Time-consuming • Producer cell modification required • Possibility of ligand degradation and low expression levels in EVs • Ligand orientation may be (partially) incorrect • Not applicable to all ligands/ therapeutic proteins (e.g. producer cell-targeting peptides or toxic proteins)
Isolated EV engineering		
Chemical conjugation of ligands with EV membrane proteins	• Quick and easy to perform • No modification of EV producer cells required • Applicable to a broad range of targeting ligands, including toxic proteins and antibodies • Applicable to EVs from various sources • High ligand densities can be obtained	• EV membrane protein functions required for cell association, immune evasion and intracellular routing may be compromised • Limited specificity of conjugation reactions • Conjugation profile and efficiency may be dependent on EV source
Post-insertion of ligand-PEG-lipids	• Quick and easy to perform • No modification of EV producer cells required • Applicable to a broad range of targeting ligands, including toxic proteins and antibodies	• PEG shielding properties may impair intracellular routing in recipient cells and cargo delivery efficiency • Stringent purification required for removal of micelles

Isolated EV engineering (continued)		
Post-insertion of ligand-PEG-lipids	• Applicable to EVs from various sources • Dramatically improves EV circulation time due to PEG incorporation	• Possibly low ligand incorporation, prone to optimization • PEG-lipid stability in EV membranes unknown
Decoration with recombinant 'plug-and-play' ligand-C1C2 fusion proteins	• 'Plug-and-play' method to target EVs (once purified proteins are obtained) • No modification of EV producer cells required • Applicable to EVs from various sources • No impairment of EV protein functions	• Time-consuming production process of C1C2-fusion proteins • Possibility of immunogenicity of C1C2 domains due to aggregation tendency • Only applicable to PS-exposing EV subsets • Not applicable to all ligands/ therapeutic proteins (e.g. aptamers or toxic proteins)

in **Chapter 6** we developed and evaluated recombinantly produced nanobodies fused with the phosphatidylserine (PS)-binding C1C2 domains of lactadherin (also termed MFG-E8). PS, which is normally exclusively localized in the inner leaflet of the plasma membrane, is often found to be externalized in EV membranes [11, 84-88]. This externalization possibly results in the accumulation of lactadherin on the EV surface, as shown by the recurrent detection of lactadherin in proteomic analyses of EVs from various sources [89-93]. Inspired by this mechanism, the EV-associating capabilities of lactadherin (and in particular its C1C2 domains) have previously been exploited by others through engineering of EV-producing cells to express recombinant lactadherin fusion proteins, which were subsequently secreted onto EVs [94-100]. However, given the fact that lactadherin is a soluble protein, we reasoned that the potential of C1C2-based EV decoration could be expanded by the use of purified recombinant C1C2-fused proteins (i.e. C1C2-nanobodies). This would theoretically allow for 'plug-and-play' nanobody decoration of PS-exposing EVs after EV isolation, regardless of EV source, and provide a biocompatible yet high-affinity decoration mechanism. However, we experienced that purification and storage of the C1C2 fusion proteins was hampered by rapid and irreversible precipitation of the proteins, presumably due to the high hydrophobicity of the C1C2 domains. To overcome these issues, a stabilizing mixture of bovine serum albumin (BSA) and negatively, positively and neutrally charged amino acids was developed. The optimized formulation adequately prevented protein precipitation and allowed large-scale protein production and long-term storage at -20°C. We showed that the stabilized C1C2-nanobodies possessed high-affinity and high specificity for both PS and EGFR. These characteristics allowed spontaneous nanobody association with PS-exposing erythrocyte- as well as tumor cell-derived EVs, targeting these EVs to EGFR-expressing tumor cells and dramatically improving tumor cell-specific EV uptake. Importantly, EV integrity, morphology and protein marker expression were

unaltered after decoration with C1C2-nanobodies. Hence, it is conceivable that native EV protein functions are preserved through this process, which, as mentioned above, could prove to be essential for functional cargo (RNA) delivery. Moreover, decoration of EVs with C1C2-nanobodies could have the additional advantages of masking PS-recognition by coagulation factors (e.g. Factors V and VIII [101]) and PS-binding receptors expressed by macrophages [102-104], possibly inhibiting thrombogenic side-effects and premature clearance by the RES. However, it should be noted that the stability of the interaction of C1C2-nanobodies with EVs in plasma has not been investigated. It could be that the C1C2-nanobodies are readily expelled from EV surfaces in the presence of other PS-binding molecules in circulation, or alternatively the C1C2-nanobodies may translocate to other PS-positive surfaces. Furthermore, the time-consuming protocol of producing C1C2-proteins may limit its versatility for other applications (e.g. other targeting ligands or reporter proteins). Nevertheless, the biocompatible nature and broad applicability to EVs from various sources make the C1C2-fusion strategy appealing for future research.

While this thesis mainly focuses on strategies to improve EVs for drug delivery purposes, it should be noted that native EVs could also serve as a rich source of inspiration for the improvement of synthetic drug delivery systems. EVs are believed to comprise a multitude of constituents which facilitate delivery of their cargo to recipient cells. Intracellular cargo delivery is arguably predominantly mediated by EV surface molecules (including bioactive lipids and proteins), which may play roles in cell adhesion, immune evasion, membrane fusion and intracellular routing. The incorporation of such moieties in synthetic drug delivery systems could be a viable approach to increase the biocompatibility and *in vivo* transfection efficiency of such systems. This hypothesis is reviewed in detail in **Chapter 7**. Liposomes, which resemble EV structure and size, would form a logical basis for the development of 'EV-mimetics'. Decades of liposome engineering and characterization should theoretically provide an extensive toolbox for the reproducible incorporation of EV components into liposomes. In addition, current pharmaceutical expertise allows for rapid transition to controllable large-scale production for (pre)clinical testing. Furthermore, the use of predefined components to generate EV-mimetics could facilitate approval of such systems by regulatory agencies (e.g. Food and Drug Administration), which could be less straightforward for native or engineered EVs due to their rather complex and variable compositions.

However, despite such advantages of EV-mimetics over native EVs, it should be stated that the crucial components that drive EV functioning remain to be elucidated, and it is well possible that their activity is orchestrated by a large variety of effector molecules. The reproducible incorporation of such variety of constituents (especially membrane proteins) into liposomes is currently still hampered by significant technical challenges.

Perspectives

In this thesis, several techniques to tailor the content and targeting capacity of EVs are

described. When further optimized and applied to a suitable EV type (e.g. autologous EVs or EVs with inherent immunosuppressive properties), these could prove to be powerful tools for the generation of EV-based drug delivery systems. Still, significant challenges exist for the pharmaceutical development of engineered EVs [72, 105-107]. EVs are typically heterogeneous structures with variable composition, depending on cell culture conditions, cell status, the presence of stimulators and other parameters. This can result in large batch-to-batch variability and corresponding differences in pharmaceutical effectiveness, which hinders clinical approval by regulatory agencies. Furthermore, protocols for large-scale EV manufacturing required for (pre)clinical applications, as well as current good manufacturing practice (CGMP) guidelines stating criteria for EV products, are currently lacking. To maximize the potential of EVs and to produce EV batches with limited heterogeneity, it may be required to isolate specific subtypes of EVs (e.g. only those modified with targeting ligands and/or loaded with therapeutic cargoes). To overcome these challenges, several important technological advances have to be made by the EV research field.

Despite these challenges, an increasing number of publications show remarkable effects of EVs, and their associated cargo, over long distances *in vivo*, and confirm that EV-based intercellular communication is not simply a myth. These inspiring reports will increase the recognition of EVs as candidate drug delivery systems, and improve the chance that EV-inspired drug delivery systems will eventually transition from the bench to the bedside. The range of available tools for in-depth analysis of EV constituents, (large-scale) EV isolation, and suitable readout systems for functional cargo delivery is currently expanding, hopefully allowing the EV research community to unravel the delivery mechanisms harnessed by EVs. Ultimately, these may be exploited for the design and development of 'Trojan horse' EVs for biocompatible, efficient and targeted delivery of (biological) therapeutics.

REFERENCES

1. Y. Li, J. Wang, M. Guillaume Wientjes, J.L. Au, Delivery of nanomedicines to extracellular and intracellular compartments of a solid tumor, *Adv Drug Deliv Rev*, (2012) 29-39.
2. R. van der Meel, L.J. Vehmeijer, R.J. Kok, G. Storm, E.V. van Gaal, Ligand-targeted particulate nanomedicines undergoing clinical evaluation: current status, *Adv Drug Deliv Rev*, 65 (2013) 1284-1298.
3. S. Svenson, Clinical translation of nanomedicines, *Curr Opin Solid State Mater Sci*, 16 (2012) 287-294.
4. T.M. Allen, P.R. Cullis, Liposomal drug delivery systems: from concept to clinical applications, *Adv Drug Deliv Rev*, 65 (2013) 36-48.
5. V.J. Venditto, F.C. Szoka Jr, Cancer nanomedicines: so many papers and so few drugs!, *Adv Drug Deliv Rev*, (2013) 80-88.
6. S.M. Ryan, D.J. Brayden, Progress in the delivery of nanoparticle constructs: towards clinical translation, *Curr Opin Pharmacol*, 18 (2014) 120-128.

7. V. Sainz, J. Conniot, A.I. Matos, C. Peres, I.E. Zupan, L. Moura*, et al.*, Regulatory aspects on nanomedicines, *Biochem Biophys Res Commun*, 468 (2015) 504-510.

8. A. Wicki, D. Witzigmann, V. Balasubramanian, J. Huwyler, Nanomedicine in cancer therapy: challenges, opportunities, and clinical applications, *J Control Release*, 200 (2015) 138-157.

9. R. Duncan, R. Gaspar, Nanomedicine(s) under the microscope, *Mol Pharm*, 8 (2011) 2101-2141.

10. J.L. Au, B.Z. Yeung, M.G. Wientjes, Z. Lu, Delivery of cancer therapeutics to extracellular and intracellular targets: Determinants, barriers, challenges and opportunities. , (2015) 280-301.

11. M. Yanez-Mo, P.R. Siljander, Z. Andreu, A.B. Zavec, F.E. Borras, E.I. Buzas*, et al.*, Biological properties of extracellular vesicles and their physiological functions, *J Extracell Vesicles*, 4 (2015) 27066.

12. H. Valadi, K. Ekstrom, A. Bossios, M. Sjostrand, J.J. Lee, J.O. Lotvall, Exosome-mediated transfer of mRNAs and microRNAs is a novel mechanism of genetic exchange between cells, *Nat Cell Biol*, 9 (2007) 654-659.

13. A. Zomer, C. Maynard, F.J. Verweij, A. Kamermans, R. Schafer, E. Beerling*, et al.*, In Vivo imaging reveals extracellular vesicle-mediated phenocopying of metastatic behavior, *Cell*, 161 (2015) 1046-1057.

14. C.P. Lai, E.Y. Kim, C.E. Badr, R. Weissleder, T.R. Mempel, B.A. Tannous*, et al.*, Visualization and tracking of tumour extracellular vesicle delivery and RNA translation using multiplexed reporters, *Nat Commun*, 6 (2015) 7029.

15. M. Mittelbrunn, C. Gutierrez-Vazquez, C. Villarroya-Beltri, S. Gonzalez, F. Sanchez-Cabo, M.A. Gonzalez*, et al.*, Unidirectional transfer of microRNA-loaded exosomes from T cells to antigen-presenting cells, *Nat Commun*, 2 (2011) 282.

16. A. Montecalvo, A.T. Larregina, W.J. Shufesky, D. Beer Stolz, M.L. Sullivan, J.M. Karlsson*, et al.*, Mechanism of transfer of functional microRNAs between mouse dendritic cells via exosomes, *Blood*, 119 (2012) 756-766.

17. D.M. Pegtel, K. Cosmopoulos, D.A. Thorley-Lawson, M.A. van Eijndhoven, E.S. Hopmans, J.L. Lindenberg*, et al.*, Functional delivery of viral miRNAs via exosomes, *Proc Natl Acad Sci U S A*, 107 (2010) 6328-6333.

18. M.T. Le, P. Hamar, C. Guo, E. Basar, R. Perdigao-Henriques, L. Balaj*, et al.*, miR-200-containing extracellular vesicles promote breast cancer cell metastasis, *J Clin Invest*, 124 (2014) 5109-5128.

19. K. Bryniarski, W. Ptak, A. Jayakumar, K. Pullmann, M.J. Caplan, A. Chairoungdua*, et al.*, Antigen-specific, antibody-coated, exosome-like nanovesicles deliver suppressor T-cell microRNA-150 to effector T cells to inhibit contact sensitivity, *J Allergy Clin Immunol*, 132 (2013) 170-181.

20. K. Bryniarski, W. Ptak, E. Martin, K. Nazimek, M. Szczepanik, M. Sanak*, et al.*, Free Extracellular miRNA Functionally Targets Cells by Transfecting Exosomes from Their Companion Cells, *PLoS One*, 10 (2015) e0122991.

21. L. Alvarez-Erviti, Y. Seow, H. Yin, C. Betts, S. Lakhal, M.J. Wood, Delivery of siRNA to the mouse brain by systemic injection of targeted exosomes, *Nat Biotechnol*, 29 (2011) 341-345.

22. J. Wahlgren, L.K.T. De, M. Brisslert, F. Vaziri Sani, E. Telemo, P. Sunnerhagen*, et al.*, Plasma exosomes can deliver exogenous short interfering RNA to monocytes and lymphocytes, *Nucleic Acids Res*, 40 (2012) e130.

23. S. El-Andaloussi, Y. Lee, S. Lakhal-Littleton, J. Li, Y. Seow, C. Gardiner*, et al.*, Exosome-mediated delivery of siRNA in vitro and in vivo, *Nat Protoc*, 7 (2012) 2112-2126.

24. J.M. Cooper, P.B. Wiklander, J.Z. Nordin, R. Al-Shawi, M.J. Wood, M. Vithlani, *et al.*, Systemic exosomal siRNA delivery reduced alpha-synuclein aggregates in brains of transgenic mice, *Mov Disord*, 29 (2014) 1476-1485.

25. S. Bala, T. Csak, F. Momen-Heravi, D. Lippai, K. Kodys, D. Catalano, *et al.*, Biodistribution and function of extracellular miRNA-155 in mice, *Sci Rep*, 5 (2015) 10721.

26. F. Momen-Heravi, S. Bala, T. Bukong, G. Szabo, Exosome-mediated delivery of functionally active miRNA-155 inhibitor to macrophages, *Nanomedicine*, 10 (2014) 1517-1527.

27. A.B. Banizs, T. Huang, K. Dryden, S.S. Berr, J.R. Stone, R.K. Nakamoto, *et al.*, In vitro evaluation of endothelial exosomes as carriers for small interfering ribonucleic acid delivery, *Int J Nanomedicine*, 9 (2014) 4223-4230.

28. V. Gujrati, S. Kim, S.H. Kim, J.J. Min, H.E. Choy, S.C. Kim, *et al.*, Bioengineered bacterial outer membrane vesicles as cell-specific drug-delivery vehicles for cancer therapy, *ACS Nano*, 8 (2014) 1525-1537.

29. J.L. Hood, M.J. Scott, S.A. Wickline, Maximizing exosome colloidal stability following electroporation, *Anal Biochem*, 448 (2014) 41-49.

30. K.B. Johnsen, J.M. Gudbergsson, M.N. Skov, G. Christiansen, L. Gurevich, T. Moos, *et al.*, Evaluation of electroporation-induced adverse effects on adipose-derived stem cell exosomes, *Cytotechnology*, (2016).

31. A. Schroeder, C.G. Levins, C. Cortez, R. Langer, D.G. Anderson, Lipid-based nanotherapeutics for siRNA delivery, *J Intern Med*, 267 (2010) 9-21.

32. S.D. Laufer, T. Restle, Peptide-mediated cellular delivery of oligonucleotide-based therapeutics in vitro: quantitative evaluation of overall efficacy employing easy to handle reporter systems, *Curr Pharm Des*, 14 (2008) 3637-3655.

33. A. Detzer, C. Engel, W. Wunsche, G. Sczakiel, Cell stress is related to re-localization of Argonaute 2 and to decreased RNA interference in human cells, *Nucleic Acids Res*, 39 (2011) 2727-2741.

34. J.R. Chevillet, Q. Kang, I.K. Ruf, H.A. Briggs, L.N. Vojtech, S.M. Hughes, *et al.*, Quantitative and stoichiometric analysis of the microRNA content of exosomes, *Proc Natl Acad Sci U S A*, 111 (2014) 14888-14893.

35. L. Stevanato, L. Thanabalasundaram, N. Vysokov, J.D. Sinden, Investigation of Content, Stoichiometry and Transfer of miRNA from Human Neural Stem Cell Line Derived Exosomes, *PLoS One*, 11 (2016) e0146353.

36. M.J. Haney, N.L. Klyachko, Y. Zhao, R. Gupta, E.G. Plotnikova, Z. He, *et al.*, Exosomes as drug delivery vehicles for Parkinson's disease therapy, *J Control Release*, 207 (2015) 18-30.

37. G. Fuhrmann, A. Serio, M. Mazo, R. Nair, M.M. Stevens, Active loading into extracellular vesicles significantly improves the cellular uptake and photodynamic effect of porphyrins, *J Control Release*, 205 (2015) 35-44.

38. M.S. Kim, M.J. Haney, Y. Zhao, V. Mahajan, I. Deygen, N.L. Klyachko, *et al.*, Development of exosome-encapsulated paclitaxel to overcome MDR in cancer cells, *Nanomedicine*, (2015).

39. Y. Tian, S. Li, J. Song, T. Ji, M. Zhu, G.J. Anderson, *et al.*, A doxorubicin delivery platform using engineered natural membrane vesicle exosomes for targeted tumor therapy, *Biomaterials*, 35 (2014) 2383-2390.

40. H. Saari, E. Lazaro-Ibanez, T. Viitala, E. Vuorimaa-Laukkanen, P. Siljander, M. Yliperttula, Microvesicle- and exosome-mediated drug delivery enhances the cytotoxicity of Paclitaxel in autologous prostate cancer cells, *J Control Release*, 220 (2015) 727-737.

41. X. Zhuang, X. Xiang, W. Grizzle, D. Sun, S. Zhang, R.C. Axtell, *et al.*, Treatment of brain inflammatory diseases by delivering exosome encapsulated anti-inflammatory drugs from the nasal region to the brain, *Mol Ther*, 19 (2011) 1769-1779.

42. D. Sun, X. Zhuang, X. Xiang, Y. Liu, S. Zhang, C. Liu, *et al.*, A novel nanoparticle drug delivery system: the anti-inflammatory activity of curcumin is enhanced when encapsulated in exosomes, *Mol Ther*, 18 (2010) 1606-1614.

43. D.J. Gibbings, C. Ciaudo, M. Erhardt, O. Voinnet, Multivesicular bodies associate with components of miRNA effector complexes and modulate miRNA activity, *Nat Cell Biol*, 11 (2009) 1143-1149.

44. L. Li, D. Zhu, L. Huang, J. Zhang, Z. Bian, X. Chen, *et al.*, Argonaute 2 complexes selectively protect the circulating microRNAs in cell-secreted microvesicles, *PLoS One*, 7 (2012) e46957.

45. Z. Lv, Y. Wei, D. Wang, C.Y. Zhang, K. Zen, L. Li, Argonaute 2 in cell-secreted microvesicles guides the function of secreted miRNAs in recipient cells, *PLoS One*, 9 (2014) e103599.

46. N. Kosaka, H. Iguchi, Y. Yoshioka, F. Takeshita, Y. Matsuki, T. Ochiya, Secretory mechanisms and intercellular transfer of microRNAs in living cells, *J Biol Chem*, 285 (2010) 17442-17452.

47. Q. Pan, V. Ramakrishnaiah, S. Henry, S. Fouraschen, P.E. de Ruiter, J. Kwekkeboom, *et al.*, Hepatic cell-to-cell transmission of small silencing RNA can extend the therapeutic reach of RNA interference (RNAi), *Gut*, 61 (2012) 1330-1339.

48. S.D. Olson, A. Kambal, K. Pollock, G.M. Mitchell, H. Stewart, S. Kalomoiris, *et al.*, Examination of mesenchymal stem cell-mediated RNAi transfer to Huntington's disease affected neuronal cells for reduction of huntingtin, *Mol Cell Neurosci*, 49 (2012) 271-281.

49. A. Mizrak, M.F. Bolukbasi, G.B. Ozdener, G.J. Brenner, S. Madlener, E.P. Erkan, *et al.*, Genetically Engineered Microvesicles Carrying Suicide mRNA/Protein Inhibit Schwannoma Tumor Growth, *Mol Ther*, 21 (2013) 101-108.

50. J. Skog, T. Wurdinger, S. van Rijn, D.H. Meijer, L. Gainche, M. Sena-Esteves, *et al.*, Glioblastoma microvesicles transport RNA and proteins that promote tumour growth and provide diagnostic biomarkers, *Nat Cell Biol*, 10 (2008) 1470-1476.

51. J.P. Tosar, F. Gambaro, J. Sanguinetti, B. Bonilla, K.W. Witwer, A. Cayota, Assessment of small RNA sorting into different extracellular fractions revealed by high-throughput sequencing of breast cell lines, *Nucleic Acids Res*, 43 (2015) 5601-5616.

52. Y. Liu, L. Zhao, D. Li, Y. Yin, C.Y. Zhang, J. Li, *et al.*, Microvesicle-delivery miR-150 promotes tumorigenesis by up-regulating VEGF, and the neutralization of miR-150 attenuate tumor development, *Protein Cell*, 4 (2013) 932-941.

53. S. Ohno, M. Takanashi, K. Sudo, S. Ueda, A. Ishikawa, N. Matsuyama, *et al.*, Systemically Injected Exosomes Targeted to EGFR Deliver Antitumor MicroRNA to Breast Cancer Cells, *Mol Ther*, 21 (2013) 185-191.

54. M. Yang, J. Chen, F. Su, B. Yu, F. Su, L. Lin, *et al.*, Microvesicles secreted by macrophages shuttle invasion-potentiating microRNAs into breast cancer cells, *Mol Cancer*, 10 (2011) 117.

55. Y. Zhang, D. Liu, X. Chen, J. Li, L. Li, Z. Bian, *et al.*, Secreted monocytic miR-150 enhances targeted endothelial cell migration, *Mol Cell*, 39 (2010) 133-144.

56. P. Mocharla, S. Briand, G. Giannotti, C. Dorries, P. Jakob, F. Paneni, *et al.*, AngiomiR-126 expression and secretion from circulating CD34+ and CD14+ PBMCs: role for proangiogenic effects and alterations in type 2 diabetics, *Blood*, 121 (2013) 226-236.

57. Y. Yin, X. Cai, X. Chen, H. Liang, Y. Zhang, J. Li, *et al.*, Tumor-secreted miR-214 induces regulatory T cells: a major link between immune evasion and tumor growth, *Cell Res*, 24 (2014) 1164-1180.

58. Y. Akao, A. Iio, T. Itoh, S. Noguchi, Y. Itoh, Y. Ohtsuki*, et al.*, Microvesicle-mediated RNA molecule delivery system using monocytes/macrophages, *Mol Ther*, 19 (2011) 395-399.

59. D. Koppers-Lalic, M. Hackenberg, I.V. Bijnsdorp, M.A. van Eijndhoven, P. Sadek, D. Sie*, et al.*, Nontemplated nucleotide additions distinguish the small RNA composition in cells from exosomes, *Cell Rep*, 8 (2014) 1649-1658.

60. M.F. Bolukbasi, A. Mizrak, G.B. Ozdener, S. Madlener, T. Strobel, E.P. Erkan*, et al.*, miR-1289 and "Zipcode"-like Sequence Enrich mRNAs in Microvesicles, *Mol Ther Nucleic Acids*, 1 (2012) e10.

61. A.O. Batagov, V.A. Kuznetsov, I.V. Kurochkin, Identification of nucleotide patterns enriched in secreted RNAs as putative cis-acting elements targeting them to exosome nano-vesicles, *BMC Genomics*, 12 Suppl 3 (2011) S18.

62. M.L. Squadrito, C. Baer, F. Burdet, C. Maderna, G.D. Gilfillan, R. Lyle*, et al.*, Endogenous RNAs modulate microRNA sorting to exosomes and transfer to acceptor cells, *Cell Rep*, 8 (2014) 1432-1446.

63. N. Szostak, F. Royo, A. Rybarczyk, M. Szachniuk, J. Blazewicz, A. del Sol*, et al.*, Sorting signal targeting mRNA into hepatic extracellular vesicles, *RNA Biol*, 11 (2014) 836-844.

64. B.W. van Balkom, A.S. Eisele, D.M. Pegtel, S. Bervoets, M.C. Verhaar, Quantitative and qualitative analysis of small RNAs in human endothelial cells and exosomes provides insights into localized RNA processing, degradation and sorting, *J Extracell Vesicles*, 4 (2015) 26760.

65. C. Villarroya-Beltri, C. Gutierrez-Vazquez, F. Sanchez-Cabo, D. Perez-Hernandez, J. Vazquez, N. Martin-Cofreces*, et al.*, Sumoylated hnRNPA2B1 controls the sorting of miRNAs into exosomes through binding to specific motifs, *Nat Commun*, 4 (2013) 2980.

66. J.D. Arroyo, J.R. Chevillet, E.M. Kroh, I.K. Ruf, C.C. Pritchard, D.F. Gibson*, et al.*, Argonaute2 complexes carry a population of circulating microRNAs independent of vesicles in human plasma, *Proc Natl Acad Sci U S A*, 108 (2011) 5003-5008.

67. A. Turchinovich, L. Weiz, A. Langheinz, B. Burwinkel, Characterization of extracellular circulating microRNA, *Nucleic Acids Res*, 39 (2011) 7223-7233.

68. A. Turchinovich, A.G. Tonevitsky, W.C. Cho, B. Burwinkel, Check and mate to exosomal extracellular miRNA: new lesson from a new approach, *Front Mol Biosci*, 2 (2015) 11.

69. H. Izumi, M. Tsuda, Y. Sato, N. Kosaka, T. Ochiya, H. Iwamoto*, et al.*, Bovine milk exosomes contain microRNA and mRNA and are taken up by human macrophages, *J Dairy Sci*, 98 (2015) 2920-2933.

70. L. Cheng, X. Sun, B.J. Scicluna, B.M. Coleman, A.F. Hill, Characterization and deep sequencing analysis of exosomal and non-exosomal miRNA in human urine, *Kidney Int*, 86 (2014) 433-444.

71. S. Rana, S. Yue, D. Stadel, M. Zoller, Toward tailored exosomes: the exosomal tetraspanin web contributes to target cell selection, *Int J Biochem Cell Biol*, 44 (2012) 1574-1584.

72. G. Fuhrmann, I.K. Herrmann, M.M. Stevens, Cell-derived vesicles for drug therapy and diagnostics: Opportunities and challenges, *Nano Today*, 10 (2015) 397-409.

73. D. Zech, S. Rana, M.W. Buchler, M. Zoller, Tumor-exosomes and leukocyte activation: an ambivalent crosstalk, *Cell Commun Signal*, 10 (2012) 37.

74. L.A. Mulcahy, R.C. Pink, D.R. Carter, Routes and mechanisms of extracellular vesicle uptake, *J Extracell Vesicles*, 3 (2014) 24641.

75. K.J. Svensson, H.C. Christianson, A. Wittrup, E. Bourseau-Guilmain, E. Lindqvist, L.M. Svensson*, et al.*, Exosome uptake depends on ERK1/2-heat shock protein 27 signaling and lipid Raft-mediated endocytosis negatively regulated by caveolin-1, *J Biol Chem*, 288 (2013) 17713-17724.

76. D. Feng, W.L. Zhao, Y.Y. Ye, X.C. Bai, R.Q. Liu, L.F. Chang, *et al.*, Cellular internalization of exosomes occurs through phagocytosis, *Traffic*, 11 (2010) 675-687.

77. M.E. Hung, J.N. Leonard, Stabilization of exosome-targeting peptides via engineered glycosylation, *J Biol Chem*, 290 (2015) 8166-8172.

78. C.P. Lai, O. Mardini, M. Ericsson, S. Prabhakar, C.A. Maguire, J.W. Chen, *et al.*, Dynamic biodistribution of extracellular vesicles in vivo using a multimodal imaging reporter, *ACS Nano*, 8 (2014) 483-494.

79. T. Smyth, K. Petrova, N.M. Payton, I. Persaud, J.S. Redzic, M.W. Graner, *et al.*, Surface functionalization of exosomes using click chemistry, *Bioconjug Chem*, 25 (2014) 1777-1784.

80. P.S. Uster, T.M. Allen, B.E. Daniel, C.J. Mendez, M.S. Newman, G.Z. Zhu, Insertion of poly(ethylene glycol) derivatized phospholipid into pre-formed liposomes results in prolonged in vivo circulation time, *FEBS Lett*, 386 (1996) 243-246.

81. K. Sou, T. Endo, S. Takeoka, E. Tsuchida, Poly(ethylene glycol)-modification of the phospholipid vesicles by using the spontaneous incorporation of poly(ethylene glycol)-lipid into the vesicles, *Bioconjug Chem*, 11 (2000) 372-379.

82. J.S. Suk, Q. Xu, N. Kim, J. Hanes, L.M. Ensign, PEGylation as a strategy for improving nanoparticle-based drug and gene delivery, *Adv Drug Deliv Rev*, (2015).

83. O.K. Nag, V. Awasthi, Surface engineering of liposomes for stealth behavior, *Pharmaceutics*, 5 (2013) 542-569.

84. A. Llorente, T. Skotland, T. Sylvanne, D. Kauhanen, T. Rog, A. Orlowski, *et al.*, Molecular lipidomics of exosomes released by PC-3 prostate cancer cells, *Biochim Biophys Acta*, 1831 (2013) 1302-1309.

85. M. Record, K. Carayon, M. Poirot, S. Silvente-Poirot, Exosomes as new vesicular lipid transporters involved in cell-cell communication and various pathophysiologies, *Biochim Biophys Acta*, 1841 (2014) 108-120.

86. M. Colombo, G. Raposo, C. Thery, Biogenesis, secretion, and intercellular interactions of exosomes and other extracellular vesicles, *Annu Rev Cell Dev Biol*, 30 (2014) 255-289.

87. N. Arraud, C. Gounou, R. Linares, A.R. Brisson, A simple flow cytometry method improves the detection of phosphatidylserine-exposing extracellular vesicles, *J Thromb Haemost*, 13 (2015) 237-247.

88. N. Arraud, R. Linares, S. Tan, C. Gounou, J.M. Pasquet, S. Mornet, *et al.*, Extracellular vesicles from blood plasma: determination of their morphology, size, phenotype and concentration, *J Thromb Haemost*, 12 (2014) 614-627.

89. C. Thery, A. Regnault, J. Garin, J. Wolfers, L. Zitvogel, P. Ricciardi-Castagnoli, *et al.*, Molecular characterization of dendritic cell-derived exosomes. Selective accumulation of the heat shock protein hsc73, *J Cell Biol*, 147 (1999) 599-610.

90. V. Luga, L. Zhang, A.M. Viloria-Petit, A.A. Ogunjimi, M.R. Inanlou, E. Chiu, *et al.*, Exosomes mediate stromal mobilization of autocrine Wnt-PCP signaling in breast cancer cell migration, *Cell*, 151 (2012) 1542-1556.

91. K. Hassani, M. Olivier, Immunomodulatory impact of leishmania-induced macrophage exosomes: a comparative proteomic and functional analysis, *PLoS Negl Trop Dis*, 7 (2013) e2185.

92. B. Fevrier, D. Vilette, F. Archer, D. Loew, W. Faigle, M. Vidal, *et al.*, Cells release prions in association with exosomes, *Proc Natl Acad Sci U S A*, 101 (2004) 9683-9688.

93. R.J. Simpson, S.S. Jensen, J.W. Lim, Proteomic profiling of exosomes: current perspectives, *Proteomics*, 8 (2008) 4083-4099.

94. A. Delcayre, A. Estelles, J. Sperinde, T. Roulon, P. Paz, B. Aguilar, *et al.*, Exosome Display technology: applications to the development of new diagnostics and therapeutics, *Blood Cells Mol Dis*, 35 (2005) 158-168.

95. Z.C. Hartman, J. Wei, O.K. Glass, H. Guo, G. Lei, X.Y. Yang, *et al.*, Increasing vaccine potency through exosome antigen targeting, *Vaccine*, 29 (2011) 9361-9367.

96. R.B. Rountree, S.J. Mandl, J.M. Nachtwey, K. Dalpozzo, L. Do, J.R. Lombardo, *et al.*, Exosome targeting of tumor antigens expressed by cancer vaccines can improve antigen immunogenicity and therapeutic efficacy, *Cancer Res*, 71 (2011) 5235-5244.

97. I.S. Zeelenberg, M. Ostrowski, S. Krumeich, A. Bobrie, C. Jancic, A. Boissonnas, *et al.*, Targeting tumor antigens to secreted membrane vesicles in vivo induces efficient antitumor immune responses, *Cancer Res*, 68 (2008) 1228-1235.

98. C. Sedlik, J. Vigneron, L. Torrieri-Dramard, F. Pitoiset, J. Denizeau, C. Chesneau, *et al.*, Different immunogenicity but similar antitumor efficacy of two DNA vaccines coding for an antigen secreted in different membrane vesicle-associated forms, *J Extracell Vesicles*, 3 (2014) 24646.

99. Y. Takahashi, M. Nishikawa, H. Shinotsuka, Y. Matsui, S. Ohara, T. Imai, *et al.*, Visualization and in vivo tracking of the exosomes of murine melanoma B16-BL6 cells in mice after intravenous injection, *J Biotechnol*, 165 (2013) 77-84.

100. M. Morishita, Y. Takahashi, M. Nishikawa, K. Sano, K. Kato, T. Yamashita, *et al.*, Quantitative analysis of tissue distribution of the B16BL6-derived exosomes using a streptavidin-lactadherin fusion protein and iodine-125-labeled biotin derivative after intravenous injection in mice, *J Pharm Sci*, 104 (2015) 705-713.

101. J. Shi, G.E. Gilbert, Lactadherin inhibits enzyme complexes of blood coagulation by competing for phospholipid-binding sites, *Blood*, 101 (2003) 2628-2636.

102. M. Miyanishi, K. Tada, M. Koike, Y. Uchiyama, T. Kitamura, S. Nagata, Identification of Tim4 as a phosphatidylserine receptor, *Nature*, 450 (2007) 435-439.

103. R. Hanayama, M. Tanaka, K. Miwa, A. Shinohara, A. Iwamatsu, S. Nagata, Identification of a factor that links apoptotic cells to phagocytes, *Nature*, 417 (2002) 182-187.

104. K.S. Ravichandran, Beginnings of a good apoptotic meal: the find-me and eat-me signaling pathways, *Immunity*, 35 (2011) 445-455.

105. S. El-Andaloussi, I. Mager, X.O. Breakefield, M.J. Wood, Extracellular vesicles: biology and emerging therapeutic opportunities, *Nat Rev Drug Discov*, 12 (2013) 347-357.

106. R. van der Meel, M.H. Fens, P. Vader, W.W. van Solinge, O. Eniola-Adefeso, R.M. Schiffelers, Extracellular vesicles as drug delivery systems: lessons from the liposome field, *J Control Release*, 195 (2014) 72-85.

107. J.A. Smith, K.S. Ng, B.E. Mead, S. Dopson, B. Reeve, J. Edwards, *et al.*, Extracellular vesicles: Commercial Potential As Byproducts of Cell Manufacturing for Research and Therapeutic Use, *BioProcess International*, [internet] (2015).

APPENDICES

Nederlandse samenvatting

Dankwoord

Curriculum Vitae

List of publications

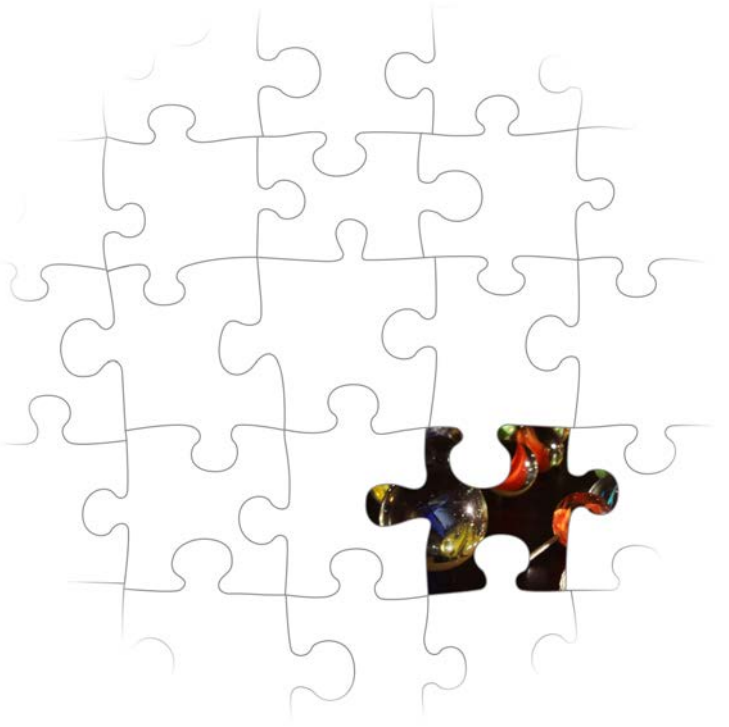

Nederlandse samenvatting

Inleiding

Bijna iedereen kent wel iemand, direct of indirect, die aan kanker is overleden. Ondanks grote vooruitgang in het onderzoek naar kanker, is deze aandoening wereldwijd nog steeds een van de meest voorkomende doodsoorzaken. De beschikbare therapie kan ernstige bijwerkingen veroorzaken en is vaak niet toereikend om het ziekteverloop te remmen. De effectiviteit van dergelijke behandelingen kan mogelijk verbeterd worden door de medicijnen te verpakken in synthetische nanodeeltjes, zoals liposomen en polymere micellen. Deze nanodeeltjes zijn gemiddeld tienduizend keer kleiner dan de dikte van een vingernagel. Het gebruik van nanodeeltjes als verpakking voor geneesmiddelen heeft een aantal voordelen, namelijk:

- Bescherming van het geneesmiddel tegen stoffen in de bloedsomloop die het geneesmiddel kunnen inactiveren en afbreken.
- Verbetering van belangrijke farmaceutische eigenschappen (zogenaamde 'farmacokinetiek') van het geneesmiddel. Nanodeeltjes met een diameter kleiner dan 200 nanometer (nm) kunnen langer in de bloedsomloop blijven circuleren en zich ophopen in ontstoken weefsels, zoals tumoren.
- Een oppervlak dat kan worden aangepast. Hierdoor kunnen bijvoorbeeld coatings worden aangebracht die ongewenste immuunreacties kunnen tegengaan en de opname van de deeltjes door het beoogde weefsel kunnen verbeteren.

Ondanks deze voordelen is het aantal nanogeneesmiddelen dat daadwerkelijk wordt toegepast in de praktijk vooralsnog zeer beperkt. Eén van de verklaringen hiervoor is het feit dat nanodeeltjes die in eerste instantie veelbelovende eigenschappen lijken te hebben, uiteindelijk toch ongeschikt blijken te zijn voor patiënten. Dit is vaak te wijten aan hun toxiciteit, het veroorzaken van schadelijke immuunreacties, het binden van eiwitten in het bloed waardoor ze inactief worden, en/of ophoping in de verkeerde (gezonde) weefsels, waardoor bijwerkingen (bijv. haaruitval) kunnen ontstaan. De toepasbaarheid van nanogeneesmiddelen wordt dus veelal belemmerd door de ongewenste reactie van ons lichaam op deze kunstmatige deeltjes.

Extracellulaire vesicles: een natuurlijk communicatienetwerk

Het afgelopen decennium is het duidelijk geworden dat de natuur zelf ook gebruik maakt van nanodeeltjes. Deze nanodeeltjes worden uitgescheiden door bijna elke cel in ons lichaam en bevatten een breed scala aan eiwitten, lipiden en genetische informatie. Dergelijke informatiepakketjes, ook wel extracellulaire 'vesicles' (letterlijk vertaald: membraanblaasjes) genoemd, hebben een grootte die vergelijkbaar is met die van synthetische nanogeneesmiddelen (50-200 nm). Ze zijn in staat hun inhoud te beschermen tegen afbraak

in de bloedsomloop en deze te transporteren naar andere cellen in het lichaam. Extracellulaire vesicles (hierna afgekort tot EVs) vormen hiermee dus een systeem waarmee cellen onderling kunnen communiceren, zelfs op grote afstand.

De ontdekking van dit natuurlijke communicatienetwerk heeft belangrijke gevolgen voor de verdere ontwikkeling van nanogeneesmiddelen. Als de natuur al nanodeeltjes heeft ontwikkeld waarmee complexe boodschappen binnen het lichaam kunnen worden verstuurd, waarom zouden we ons dan richten op de ontwikkeling van synthetische systemen die soortgelijke (therapeutische) boodschappen moeten afleveren? Zou het mogelijk zijn om EVs te gebruiken als 'Trojaanse paarden' (zie ook **Hoofdstuk 1**) om geneesmiddelen efficiënt op de juiste plek in het lichaam af te leveren? Op deze manier zouden de nadelen van synthetische nanodeeltjes kunnen worden omzeild en de effectiviteit van geneesmiddelen kunnen worden verhoogd. Deze vraagstelling vormt de basis van het onderzoek dat beschreven is in dit proefschrift.

EVs zijn van nature 'voorgeprogrammeerd' met verschillende eigenschappen die ervoor zorgen dat ze hun boodschap kunnen overdragen naar specifieke cellen en weefsels. Om deze vesicles in te kunnen zetten voor het transport en de bezorging van geneesmiddelen, moeten dergelijke eigenschappen wellicht worden aangepast. Zo dient het oppervlak van natuurlijke EVs gemodificeerd te worden om hun opname door gezond weefsel te remmen en tegelijkertijd hun opname door 'zieke' cellen (bijv. tumorcellen) te bevorderen. Daarnaast is het uiteraard belangrijk om de vesicles te beladen met geschikte therapeutische stoffen. Het laden van geneesmiddelen in EVs en het sturen van EVs naar de juiste weefsels vormen de twee kernthema's binnen dit proefschrift.

Beladen van EVs met therapeutische stoffen

Eén van de meest veelbelovende therapeutische stoffen van de afgelopen decennia is 'small interfering RNA' (siRNA). Dit zijn kleine stukjes genetische informatie, die heel nauwkeurig de activiteit van ontregelde genen, die betrokken zijn bij ziekteprocessen (waaronder kanker), kunnen verlagen. Door deze genen uit te schakelen met siRNA (een proces dat ook wel gentherapie wordt genoemd), kunnen deze aandoeningen beter worden behandeld, en mogelijk zelfs worden genezen. Er kleven echter ook nadelen aan siRNA. Ten eerste wordt het extreem snel afgebroken in het bloed, waardoor het weinig kans heeft bij de beoogde cellen te komen. Daarnaast zijn siRNA-moleculen relatief groot en negatief geladen, waardoor ze niet uit zichzelf door cellen kunnen worden opgenomen. Om gen-activiteit te kunnen beïnvloeden, is het echter wel noodzakelijk dat siRNA moleculen de cel binnenkomen. Het verpakken van siRNA in nanodeeltjes kan hierbij helpen.

EVs bevatten van nature genetisch materiaal dat qua grootte en samenstelling lijkt op siRNA. Ze zijn in staat om dit materiaal over te brengen naar cellen, waar het vervolgens gen-activiteit kan beïnvloeden. Mogelijk kunnen deze vesicles dus ook gebruikt worden om siRNA af te leveren. Het is echter nog onduidelijk hoe siRNA het best in EVs kan worden verpakt.

EVs bevatten, net als cellen, een negatief geladen celmembraan. Hierdoor kan siRNA niet uit zichzelf EVs binnendringen. Onderzoek heeft echter uitgewezen dat dit wel mogelijk is als de vesicles worden blootgesteld aan elektrische pulsen (een proces genaamd 'elektroporatie'). Elektroporatie wordt verondersteld tijdelijk gaatjes te maken in het EV membraan, waardoor het siRNA naar binnen kan. Als de gaatjes weer sluiten, wordt het siRNA ingesloten. Hoe dit echter precies in zijn werk gaat, is onbekend.

In **Hoofdstuk 2** hebben we geprobeerd een veelgebruikte elektroporatiemethode verder te optimaliseren, om zoveel mogelijk siRNA in EVs te laden. Tot onze verbazing kwamen we erachter dat elektroporatie lang niet zo goed werkt voor het laden van siRNA in EVs als voorheen gedacht. We lieten zien dat elektroporatie voornamelijk leidt tot samenklontering van het siRNA met metaalionen afkomstig van de elektroporatie-elektroden, maar niet tot het laden van siRNA in EVs. De siRNA-aggregaten waren ongeveer even groot als EVs, waardoor ze makkelijk konden worden verward met vesicles die daadwerkelijk waren geladen met siRNA. We veronderstelden dat, als de vorming van siRNA-aggregaten tijdens elektroporatie zou worden tegengegaan, de hoeveelheid siRNA die in de EVs terecht zou komen, verhoogd zou kunnen worden. Om dit te testen hebben we verschillende technieken toegepast om het vrijkomen van metaalionen tijdens elektroporatie tegen te gaan. Hierdoor kon inderdaad de vorming van siRNA-aggregaten worden voorkomen. Het bleek echter onder deze omstandigheden nog steeds onmogelijk om meetbare hoeveelheden siRNA in EVs te laden. Deze studie toonde daarmee aan dat het laden van siRNA in EVs lastiger is dan voorheen gedacht en benadrukt dat er nieuwe, betrouwbare methoden ontwikkeld moeten worden om dit te bewerkstelligen.

Een aantal andere strategieën om siRNA te laden in EVs is besproken in **Hoofdstuk 3**. Het is bijvoorbeeld mogelijk om de cellen die EVs uitscheiden te manipuleren, zodat deze zelf siRNA gaan produceren. Een deel van het siRNA zal dan vaak automatisch in EVs worden verpakt. Het is echter nog onduidelijk hoe cellen bepalen welke genetische informatie in EVs terecht komt. Het kan daarom voorkomen dat sommige siRNA moleculen wel door cellen worden verpakt in EVs, terwijl andere worden buitengesloten. Er is meer onderzoek nodig naar dergelijke selectiemechanismen om een robuuste siRNA-beladingsmethode ontwikkelen.

Modificatie van het oppervlak van EVs om opname in specifieke weefsels te bevorderen

Naast het beladen van EVs met therapeutische stoffen, is het belangrijk dat de vesicles deze stoffen op de juiste plek in het lichaam afleveren. Wanneer dit niet gebeurt, zijn hogere doses nodig om het juiste effect te bereiken en kunnen bijwerkingen ontstaan. De gerichte opname van nanodeeltjes door specifieke cellen en weefsels (bijvoorbeeld tumorcellen) kan in het algemeen bereikt worden door het oppervlak van de deeltjes te bekleden met moleculen die binden aan kenmerkende eiwitten op dergelijke weefsels. Het is bijvoorbeeld bekend dat veel tumorcellen het eiwit 'epidermal growth factor receptor' (EGFR) op hun oppervlak dragen, terwijl dit minder voorkomt bij gezonde cellen. Door EVs te bekleden met moleculen

die specifiek aan EGFR binden, kunnen ze specifiek naar tumorcellen worden gestuurd. Het is echter nog onduidelijk op welke manier het koppelen van dergelijke moleculen (ook wel 'targeting liganden' genoemd) aan EVs het best kan worden uitgevoerd, zonder de EVs te beschadigen.

In **Hoofdstuk 4** hebben we een nieuwe methode beschreven om EVs te bekleden met zogenaamde 'anti-EGFR nanobodies'. Nanobodies zijn kleine fragmenten van antistoffen die door kameelachtige dieren (bijvoorbeeld lama's) worden gemaakt. Ze binden zeer sterk aan specifieke eiwitten (in dit geval EGFR) en kunnen daardoor gebruikt worden als targeting liganden voor tumorcellen. Onze hypothese was dat als we het oppervlak van EVs zouden bekleden met deze nanobodies, de binding van de EVs aan tumorcellen sterk zou toenemen. Om dit te testen, hebben we cellen genetisch gemodificeerd, zodat deze nanobodies zouden maken waaraan glycolipiden (een combinatie van vetten en suikers) vast zaten. Dergelijke glycolipiden komen erg veel voor op het oppervlak van EVs. Het gevolg van deze modificatie was dat de cellen EVs produceerden waarop grote hoeveelheden nanobodies aanwezig waren. Vervolgens hebben we bepaald of het gedrag van de nanobody-EVs ten opzichte van tumorcellen was veranderd. Hieruit bleek dat de binding van de nanobody-EVs aan tumorcellen die EGFR op hun oppervlak droegen sterk was verbeterd in vergelijking met natuurlijke EVs, terwijl dit niet het geval was voor cellen waarop geen EGFR aanwezig was. Daarnaast was er ook sprake van een sterkere interactie van nanobody-EVs met tumorcellen wanneer de EV-houdende vloeistof in beweging werd gehouden. Dit suggereert dat de versterkte interactie van EVs met tumorcellen, na bekleding met nanobodies, ook in het menselijk lichaam (waarin vloeistoffen continu in beweging zijn) kan plaatsvinden.

De hierboven beschreven strategie om targeting liganden op EVs te plaatsen heeft helaas ook nadelen. Het is bijvoorbeeld niet altijd mogelijk om de cellen die de benodigde EVs uitscheiden, genetisch te manipuleren. Daarnaast is de modificatieprocedure erg tijdrovend en kan het in sommige gevallen voorkomen dat de targeting liganden niet goed door de cel worden geproduceerd, waardoor ze niet, of slechts in beperkte mate op EVs terecht komen.

Om deze redenen hebben we in **Hoofdstuk 5** ook een andere manier onderzocht om anti-EGFR nanobodies op EVs te plaatsen. In deze studie hebben we anti-EGFR nanobodies via een chemische reactie gekoppeld aan het wateroplosbare polymeer polyethyleen glycol (PEG), dat op zijn beurt gekoppeld was aan lipiden. We kwamen erachter dat, wanneer we de ontstane nanobody-PEG-lipiden mengden met EVs en het mengsel verhitten, de lipiden automatisch werden ingebouwd op het oppervlak van de vesicles (dat ook hoofdzakelijk uit een laag van lipiden bestaat). Het gevolg hiervan was dat de nanobodies op het oppervlak van de EVs werden gezet. Dit gebeurde zonder dat de EVs beschadigd werden. Het voordeel van deze methode was bovendien dat de EV-producerende cellen niet gemodificeerd hoefden te worden. De methode kon daarom ook gebruikt worden voor het plaatsen van nanobodies op het oppervlak van EVs van bloedplaatjes, die doorgaans zeer lastig te manipuleren zijn.

Het plaatsen van nanobodies en PEG-polymeren op het oppervlak van EVs veranderde

de interacties van EVs met cellen. De binding van EVs aan tumorcellen met EGFR nam sterk toe door de modificatie, terwijl de binding aan cellen die dit eiwit niet op hun oppervlak droegen (kenmerkend voor de meeste gezonde cellen) juist *afnam*. Dit laatste kan verklaard worden door het feit dat de polymeren een beschermende laag vormen om de EVs, die ervoor zorgt dat de EVs niet meer goed in contact kunnen komen met de cellen. De nanobodies zorgen ervoor dat dit effect wordt opgeheven, maar alleen voor tumorcellen. Door deze combinatie van polymeren en nanobodies aan te brengen op het oppervlak van de EVs kon dus de 'voorkeur' van de EVs voor tumorcellen worden vergroot.

Het coaten van EVs met polymeren bracht echter nog een voordeel met zich mee, dat zichtbaar werd toen de EVs werden geïnjecteerd in muizen. Op verschillende tijdstippen na injectie werd de hoeveelheid EVs dat zich nog in het bloed bevond, gemeten. Het bleek dat natuurlijke EVs binnen tien minuten niet meer te detecteren waren in het bloed, waarschijnlijk doordat ze uit het bloed werden weggevangen door immuuncellen. De EVs waarop de polymeren waren aangebracht bleven echter vele malen langer circuleren en konden soms zelfs nog vier uur na injectie in het bloed worden teruggevonden. De polymeren zorgden er dus voor dat de EVs minder goed werden herkend door het immuunsysteem van het lichaam, waardoor ze minder snel werden opgeruimd. Dit is erg voordelig, want de bloedvaten rond ontstoken weefsel (zoals tumoren) bevatten doorgaans kleine gaatjes. Hierdoor kunnen nanodeeltjes op deze plekken uit de vaten lekken en het ontstoken weefsel binnentreden. Hoe langer de nanodeeltjes in het bloed aanwezig blijven, hoe groter de kans is dat ze daadwerkelijk uit de vaten lekken voordat ze worden opgeruimd door het lichaam. Door de verblijftijd in de bloedsomloop te verlengen met de polymeren, hebben we er dus voor gezorgd dat de ophoping van EVs in tumorweefsel kan worden verhoogd. Vervolgonderzoek moet uitwijzen of dit ook daadwerkelijk het geval is. Daarnaast is het belangrijk te onderzoeken of de gecoate EVs net zo efficiënt hun boodschap aan tumorcellen over kunnen dragen als natuurlijke EVs. Er bestaat namelijk een kans dat de polymeren hiermee interfereren.

Dit probleem kan waarschijnlijk voorkomen worden door de nanobodies op een andere manier op EVs te plaatsen, zonder gebruik te maken van polymeren. Een dergelijke strategie is beschreven in **Hoofdstuk 6**. In deze studie hebben we gebruik gemaakt van het eiwit 'lactadherine', dat van nature in ons lichaam aanwezig is. Dit eiwit bindt sterk aan een specifiek negatief geladen lipide, genaamd phosphatidylserine (PS). PS komt vaak voor op het oppervlak van EVs, waardoor lactadherine in staat is aan EVs te binden. De binding van lactadherine aan PS wordt mogelijk gemaakt door twee specifieke delen van lactadherine, genaamd 'C1' en 'C2' (verder afgekort tot 'C1C2'). We redeneerden dat, wanneer we C1C2 aan nanobodies zouden koppelen, deze nanobodies vervolgens aan PS op EVs zouden kunnen hechten. Om dit te testen, hebben we met behulp van biotechnologische technieken fusie-eiwitten gemaakt, die bestonden uit een C1C2-deel en een nanobody-deel (zogenaamde 'C1C2-nanobodies'). Het bleek dat deze eiwitten in staat waren om aan zowel EGFR te binden (met hun nanobody-deel), als aan PS (met hun C1C2-deel). Door de eiwitten simpelweg te

mengen met EVs, werd het oppervlak van de EVs automatisch bekleed met C1C2-nanobodies, zonder de EVs aan te tasten. Deze modificatie was mogelijk met EVs van twee verschillende celtypen (rode bloedcellen en tumorcellen), wat suggereert dat dit een universele manier is om EVs met targeting liganden te bekleden. Het bekleden van EVs met C1C2-nanobodies zorgde er ook hier voor dat de binding van de EVs aan tumorcellen met EGFR op het oppervlak sterk werd verbeterd. Daarnaast zagen we een verbetering van de hoeveelheid EVs die door de tumorcellen werd opgenomen.

Naast deze belangrijke verbeteringen van het gedrag van EVs ten opzichte van tumorcellen, heeft het bekleden van EVs met C1C2-nanobodies wellicht een ander voordeel. Het PS op het oppervlak van EVs staat bekend als een 'eet mij' signaal, dat ook aanwezig is op dode cellen. Cellen van ons immuunsysteem herkennen dit signaal en zorgen ervoor dat dergelijke cellen en EVs worden vernietigd en opgeruimd. Uiteraard is dit geen gunstige eigenschap wanneer EVs ingezet worden om kanker te behandelen. Doordat de C1C2-nanobodies aan PS binden, kunnen ze er mogelijk voor zorgen dat het PS op EVs wordt afgeschermd voor het immuunsysteem. Hierdoor zouden ze minder snel worden opgeruimd en dus meer kans hebben om bij hun doel (de tumor) te komen. Het is echter nog onduidelijk of de C1C2-nanobodies hiertoe werkelijk in staat zijn. Daarnaast is het ook in deze studie nog niet opgehelderd of de C1C2-nanobodies de EVs belemmeren in hun vermogen om hun boodschap naar tumorcellen over te dragen. Vervolgonderzoek zal hier waarschijnlijk meer duidelijkheid over geven.

Het onderzoek in dit proefschrift is vooral gericht op het inzetten van (gemodificeerde) EVs voor antikankertherapie. EVs kunnen echter ook als een grote bron van inspiratie dienen voor de verbetering van synthetische nanodeeltjes. Ze bezitten unieke eigenschappen, waardoor ze in staat zijn genetisch materiaal van de ene naar de andere cel te transporteren. Het is tot nu toe echter onduidelijk welke onderdelen van EVs hiervoor verantwoordelijk zijn. Als dit opgehelderd wordt, zouden we dergelijke onderdelen kunnen inbouwen in synthetische systemen (bijvoorbeeld liposomen, die qua structuur al erg op EVs lijken), waardoor de therapeutische effectiviteit van dergelijke systemen sterk kan worden verbeterd. Een bijkomend voordeel is dat synthetische systemen vaak een simpele, duidelijk gedefinieerde samenstelling hebben, terwijl de samenstelling van EVs erg complex is. Hierdoor kunnen ze makkelijker op grote schaal geproduceerd worden en sneller worden toegepast in de praktijk. Het idee om veelgebruikte synthetische systemen te verbeteren met cruciale onderdelen van EVs is uitgebreid besproken in **Hoofdstuk 7**. Er wordt ingegaan op een breed scala aan eiwitten, lipiden en genetische informatie in EVs die vanwege hun biologische functie interessant kunnen zijn om hiervoor te gebruiken.

Conclusies

EVs kunnen worden gezien als een natuurlijk communicatiesysteem, waarmee cellen in ons lichaam over grote afstand genetische informatie naar elkaar versturen. Het versturen

van dergelijke informatie naar zieke cellen is tevens het doel van gentherapie, maar door een gebrek aan efficiënte afleversystemen wordt deze therapie in praktijk nog nauwelijks toegepast. Wellicht kunnen EVs worden ingezet om gentherapie mogelijk te maken, aangezien ze hier van nature voor lijken te zijn uitgerust. Het is echter wel noodzakelijk om een aantal eigenschappen van natuurlijke EVs aan te passen, zodat ze de juiste therapeutische boodschap vervoeren en deze op de juiste plek in het lichaam afleveren. In dit proefschrift zijn een aantal nieuwe methoden beschreven om dit te bewerkstelligen. Daarnaast is onderzocht wat de invloed van dergelijke aanpassingen is op het gedrag van EVs en wordt besproken hoe EVs gebruikt kunnen worden om synthetische afleversystemen te verbeteren. Hiermee draagt dit onderzoek bij aan de ontwikkeling van veilige, efficiënte en doelgerichte therapie van kanker gebaseerd op EVs.

Dankwoord

Gefeliciteerd, je bent door mijn proefschrift heen en nu mag je beginnen aan het toetje! Je vraagt je inmiddels vast af hoe het toch mogelijk is dat ik meer dan vier jaar van mijn leven aan dit promotieonderzoek heb gewijd, maar toch nog kan lachen. Dat zal ik je vertellen. Ik ben tijdens deze periode van alle kanten bijgestaan door mensen die ervoor hebben gezorgd dat mijn onderzoek niet alleen (enigszins) nuttig en van hoge kwaliteit was, maar ook vooral heel leuk om uit te voeren. Ik ga in het komende stuk tekst proberen al deze mensen te bedanken, maar vergeef me als ik iemand vergeet. Heb je het gevoel dat je vergeten bent, dan is deze voor jou: Bedankt voor alles, gezellig dat je erbij was!

Beste **Ray(mond)**, het was en is nog steeds een eer om in jouw team te mogen werken. Onder jouw leiding als promotor heb ik een geweldige tijd gehad. Je eeuwige optimisme werkt erg aanstekelijk en heeft ervoor gezorgd dat ik beter in staat was om met tegenvallende resultaten om te gaan. Je hebt er zelfs voor gezorgd dat we negatieve data konden omtoveren tot een publicatie (hoofdstuk 2)! Daarnaast heb ik erg veel gehad aan je out-of-the-box ideeën, die vaak erg waardevol bleken te zijn en de basis van dit proefschrift hebben gevormd. Ik neem graag op wetenschappelijk gebied een voorbeeld aan je, maar ook op sociaal gebied. Als graag geziene (en gehoorde) gast op borrels, congressen en andere festiviteiten zorg je ervoor dat iedereen het naar zijn/haar zin heeft. Jouw persoonlijkheid heeft ook zijn weerklank op de sfeer binnen je groep, die altijd open en gezellig is. Bedankt voor dit alles, ik hoop dat we onze samenwerking nog erg lang kunnen voortzetten. Proost!

Beste **Wouter**, ook al was je door andere verplichtingen in het UMC niet veel in beeld tijdens mijn promotieonderzoek, toch was je tijdens onze ontmoetingen altijd open, geïnteresseerd en betrokken. Ik wil je bedanken dat je mijn tweede promotor bent geweest en dat je me de kans hebt gegeven dit onderzoek bij het LKCH uit te voeren.

Beste **Pieter**, wat ben ik blij dat jij mijn co-promotor bent geweest. Jouw droge humor en wijze woorden wanneer ze nodig waren hebben me erg geholpen om mijn promotieonderzoek tot een goed einde te brengen. Ik waardeer je kritische blik op de wetenschap en je goede ideeën wanneer ik om inspiratie verlegen zat. Ik heb ontzettend veel van je geleerd, binnen de wetenschap maar ook daarbuiten. Je bent altijd goed gezelschap, of het nu bij een borrel is, op congressen in gedeelde hotelkamers met transparante toilet- en douchedeuren, in de celkweek of tijdens het ontleden van muizen. Kortom: ik ben erg blij en dankbaar dat ik dit promotietraject onder jouw begeleiding heb mogen voltrekken. Ik hoop dat onze samenwerking nog lang niet ophoudt en dat we samen nog vele papers mogen publiceren.

Ondanks dat je niet direct bij mijn onderzoek betrokken bent, wil ik ook jou, **Gerard**, bedanken voor je steun tijdens de periode dat er onzekerheid was over mijn vervolgcarrière. Daarnaast waardeer ik je interesse en enthousiasme tijdens de werkbesprekingen op de vrijdagochtend, bedankt daarvoor!

Ik wil ook graag de leden van de **leescommissie**, prof. dr. Storm, prof. dr. van den Bosch,

prof. dr. Egberts, prof. dr. Engbersen en dr. van Rheenen bedanken voor het kritisch beoordelen van mijn proefschrift.

Gedeelde smart is halve smart, dat is maar weer gebleken! **Susan**, ik ben blij dat jij gezellig in hetzelfde schuitje als ik zat en we heerlijk onze frustraties en ingevingen eruit konden gooien tijdens onze kampvuursessies! Next to dat I muts endjoid the conversaties in bed Engels (and in het Netherlands) in de celkweek, op de borrels, congressen en feestjes waar we als Jut en Jul van het LKCH te vinden waren. Ik heb erg gelachen en ik ga onze tijd samen zeker missen! Toppie dat je mijn paranimf wil zijn (en dat ik de jouwe mag zijn), we gaan er een mooi feestje van maken! Bedankt voor alles!

Zonder goede hoofdanalist was de helft van het onderzoek in dit proefschrift in het water gevallen, dat weet ik zeker. **Arnold**, jouw probleemoplossend vermogen heeft een hoop van mijn gestuntel goed gemaakt, van verstopte ÄKTA's tot een opgeblazen celkweeklab. Daarnaast ben je een geweldige metgezel voor borrels en andere festiviteiten, en was je nooit te beroerd om me in allerlei commissies te betrekken (gewild en ongewild). Bedankt voor alle hulp gedurende de mooie tijd bij het LKCH en uiteraard bedankt dat je mijn paranimf wil zijn. Ik hoop dat we, ondanks je nieuwe uitdaging van het vaderschap, nog vaak een borreltje kunnen doen (en af en toe een ÄKTA repareren ;)).

Uiteraard mogen ook de leermeesters in het onderzoek, de post-doctoralen, niet ontbreken in dit dankwoord. **Marcel**, ook al ben je pas tijdens de tweede helft van mijn onderzoek bij ons komen werken, ben ik erg blij dat ik je alsnog heb leren kennen. Je bent uitstekend gezelschap tijdens een borrel (ik waardeer een goede muziekkenner) en ik bewonder je vaardigheid om met iedereen, maar dan ook echt iedereen, goed op te schieten. Zelden heb ik een socialer persoon ontmoet. Daarnaast weet ik niet wat er van Chapter 5 zou zijn geworden zonder jouw uitstekende vivo-skills. Bedankt voor alles en ga vooral zo door! In dezelfde lijn wil ik ook jou, **Roy**, bedanken voor jouw prominente aanwezigheid binnen de groep en binnen mijn onderzoek. Jouw input en ervaring met nanobodies hebben de basis gevormd van veel experimenten in dit proefschrift en je was een onmisbaar onderdeel van Team Vivo. Als echte gangmaker met harde grappen en tegelijk magnifieke sociale skills wist je ervoor te zorgen dat er nooit een borrel of feestje inkakte. Ondanks al die katers die ik eraan heb overgehouden, heb ik van je aanwezigheid genoten! Bedankt!

Naast hoofdanalist ben ik ook gezegend geweest met de aanwezigheid van een topteam van ondersteunende analisten. Beste **Jerney**, bedankt voor al het noeste en uiterst nauwkeurige pipetteerwerk dat je voor me hebt uitgevoerd, dat moet toch een mooie publicatie gaan opleveren. Daarnaast deel ik je voorliefde voor grove humor en goede TV-series en heb ik erg gelachen tijdens onze gesprekken die gemiddeld binnen 86 seconden tot bedenkelijk niveau waren gezakt (uiteraard niet mijn schuld). Ik had me geen betere analist kunnen wensen! **Silvie**, als echte lab 1 mascotte heb jij redelijk wat tirades moeten verduren als mijn experiment weer eens niet lukte, respect daarvoor (en uiteraard sorry). Ik heb genoten van onze goede gesprekken, popduel deelnames, en random geouwehoer op lab 1 en vind

het altijd een gemis als er je een dagje niet bent. Bedankt en we drinken een pintje en/of vegabrouwsel op Lowlands! Ook wil ik graag een ander vast onderdeel van lab 1 bedanken. **Annet**, jij hebt me veel geleerd. Uiteraard heeft 99% daarvan niks met wetenschap te maken, maar er zaten zeker belangrijke levenslessen tussen. Je kon me altijd bijpraten over alles wat er speelde binnen het LKCH en zorgde voor een fantastische sfeer op het lab. Daarnaast wil ik ook jou, **Arjan**, bedanken voor je gortdroge humor, pintvaardigheid, muzieksmaak en je vermogen om van de meest slechte borrelthema's een nog slechtere borrelposter te maken. Ik heb veel met je gelachen, en ik vermoed dat we samen nog niet uitgelachen zijn. **Brigit**, bedankt voor alle gereedschap en oude verstofte apparaten waar je mee aan kwam zetten als ik weer eens iets nodig had. Erg fijn en gezellig om je in de buurt te hebben! **Sandra**, **Liesbeth**, **Tesy** en **Simone**, jullie wil ik bedanken voor jullie geduld om mijn geouwehoer de hele dag aan te horen en voor alle hulp die ik van jullie heb gehad in verschillende facetten van mijn onderzoek. Top! In het elektronenmicroscopie-hoekje wil ik ook jullie, **Cor** en **George**, hartelijk bedanken voor alles wat jullie me hebben geleerd over dit ambacht. Cor, ik waardeer daarnaast je humor en je initiatieven om deze ook bij de rest van het LKCH kenbaar te maken. **Ruud**, altijd gezellig om het celkweeklab met je te delen. Ik heb me lang verwonderd over de combinatie van een fetisj voor alientatoeages met het opgroeien van cellen in een flesje, maar nu ik er zo over nadenk, maakt het eigenlijk wel sense.

Mijn dank gaat ook uit naar mijn mede-AIO's van het LKCH. **Steven**, zonder jou had ik een groot deel van de moleculaire biologie die dit proefschrift rijk is, wel kunnen vergeten. Bedankt voor alle keren dat je me hebt geholpen om een zinkend schip weer tot drijven te brengen. Daarnaast was je goed gezelschap bij een pintje! **Rick**, altijd lachen met jou (of om jou). Ik heb grote bewondering voor de gigantische chaos die je op je bench creëert, om er vervolgens omheen te pipetteren. Maar ach, misschien is dit wel de beste weg naar de Nobelprijs. Ik gok dat je nieuwe job als biercommissaris je beter af gaat, maar wie weet, hou vol! **Jessica** (spreek uit: Djezz-i-kee), als stille kracht op het lab promoveer jij vast als één van de weinigen wél binnen vier jaar. Respect en ga zo door! **Anil**, thanks a lot for your sparkling presence on lab 1, it is fantastic to see how quickly you integrated in the Dutch culture! I love how you bring a bit of Bollywood to the lab, and wish you the best of luck in your PhD! **Ivar**, mooi om te zien hoe jij na al je tegenstribbelingen toch in de borrelcommissie terecht bent gekomen. Ik hoop dat je het lab nog van veel borrels zult voorzien, en wens je veel succes met het afronden van je PhD. **Marco**ooooo! Jouw ad rem woordgrappen zorgden altijd voor de nodige luchtigheid tijdens borrels en uiterst serieuze aangelegenheden (vraag me niet welke), bedankt daarvoor en ga zo door! **Mirjam**, mooi om te zien hoe je als vreemde eend in de LKCH-bijt toch goed bent geïntegreerd. Succes met je onderzoek naar nare parasieten (liever jij dan ik ;))! **Aida**, thank you for your happy and relaxed presence in our group. Good luck with your studies, I'm sure they will end well! **Tesse**, fijn dat je af en toe even in ons lab komt pipetteren, altijd goed gezelschap! Ik vind het knap dat je in traditionele chirurgenkledij toch reclame kunt maken voor Andrélon perfecte krul. **Pim** (ook al ben je geen AIO maar CEO, ik moet je

ergens neerzetten), ik heb erg met je gelachen tijdens congressen en op het lab. Jouw bizarre, maar toch waargebeurde verhalen spreken altijd tot de verbeelding. Als ik ooit inspiratie voor een 'date' nodig heb zoek ik je op. Veel succes met je avontuur in Afrika! **Stephanie**, ook al ben je nog maar net toegetreden tot de borrelcommissie, je hebt je strepen al ruimschoots verdiend. Jouw enthousiasme werkt aanstekelijk en ik hoop dat je deze de komende jaren erin kan houden. Daar kan alleen maar goeds uit komen. **Minke** en **Zonne**, jullie zijn de toekomst van het lab! Jullie aanwinst zorgt er vast voor dat die er rooskleurig uit komt te zien. Succes met jullie PhDs! **Sara**, thank you for all your help in translating Italian forms and for getting me integrated in Italy, I much appreciate it. I hope you still like research after too many disappointing results, and I look forward to work together with you in the future. **Linglei**, I think you are my biggest (and probably only) fan, thank you for that! I enjoy your presence and love the way you get yourself settled in the Netherlands. I think all the hard work you put in your PhD will pay off one day, keep up the good work!

Uiteraard mogen ook (oud)stafleden hier niet ontbreken. **Coen**, bedankt voor al je out-of-the-box ideeën en discussies, die hebben zeker bijgedragen aan dit proefschrift. Ik bewonder je vermogen om beurzen binnen te slepen en deze om te zetten in dikke papers, hou dat vol! Voor een pintje en grove humor kan ik ook altijd bij jou terecht. **Rolf**, **Mark, Maarten, Susan** en **Joost**, de discussiepunten die jullie aandroegen tijdens werkbesprekingen hebben me vaak aan het denken gezet, bedankt hiervoor! Ik hoop dat ik ook in de toekomst nog eens bij jullie kan aankloppen. **Richard**, ik bewonder hoe je jezelf hebt opgewerkt tot dé rode bloedcel-goeroe van Nederland en wil je graag bedanken voor je input in mijn onderzoek. Succes met het managen van de lading verse AIO's! **Harry**, bedankt voor de elektronenmicroscopie-expertise die je, in uitgebreide gesprekken, met me hebt gedeeld. Zonder jou waren nanobodies op vesicles misschien wel nooit zichtbaar geworden. Bedankt! **Karen**, bedankt voor je ideeën tijdens de werkbesprekingen. Daarnaast denk ik dat jij van de hele afdeling het meest overtuigend *I was made for loving you* kan playbacken.

Ik heb het geluk gehad een aantal fijne studenten te begeleiden tijdens mijn onderzoek. **Lies**, als eerste student was jij mijn oefenproject, maar ik denk dat dit project zeer zeker geslaagd is. Het was erg leuk om met je samen te werken, en het heeft zeker zijn vruchten afgeworpen. Succes met je PhD bij Biofarmacie, hopelijk kunnen we in de toekomst nog eens samenwerken. **Rick**, het was geinig om te ervaren wat er gebeurt als je een farmaceut en een scheikundige laat samenwerken. Ik denk dat het zeker creatieve ideeën heeft opgeleverd! Succes met je master en je vervolgcarrière. **Michael**, het was gezellig om je in mijn team te hebben. Bedankt voor alle moeite die je in een ambitieus project hebt gestoken, ook al viel het soms tegen. Ik hoop dat je ook buiten het onderzoek je draai kunt vinden en wens je alle geluk voor de toekomst! **Clara**, it was great to get to know you and to work with you! I much appreciate all the hard work and long days you put in my project, thanks! In addition, I think the Spanish touch you brought into the group was very nice. Good luck with your future career!

Mijn cardio-kamergenoten verdienen hier ook een eervolle vermelding. **Lena** en

Patricia, bedankt voor het opfleuren van onze kamer, die er met alleen mannen toch wat steriel uit had gezien. Ik vond het altijd gezellig om bij jullie op de kamer te zitten. Succes met het afronden van jullie PhD's! **Peter-Paul**, jij stuitert tegen alle muren op en zorgt voor een prettige achtergrondruis in de kamer. Het getik, gekraak en geklop dat je veroorzaakt is af en toe gekmakend, maar aan de andere kant denk ik dat je je geen betere cardioloog kunt wensen, die altijd de boel aan het tikken houdt. Ik heb respect voor de lange dagen die je maakt en ik wens je veel succes in je vervolgcarrière.

Ik wil daarnaast graag de AIO's en postdocs van de vorige generatie bedanken. **Eelo**, **Thijs**, **Claudia**, **Agon**, **Vivian**, **Esther**, **Marije**, **Jonas**, **Peter-Paul**, **Eszter**, **Krijn** en **Bert,** bedankt dat jullie mij de weg om een goede AIO te worden hebben laten zien. Ik heb genoten van de korte tijd die we samen in de oldskool AIO-kamer en in de labs hebben doorgebracht. De feestjes en borrels waren zonder jullie ongetwijfeld minder gezellig geweest, en jullie hebben me vaak geïnspireerd voor mijn onderzoek. ik wens jullie veel succes in de toekomst, en hoop dat we samen nog eens een borreltje kunnen drinken.

Mede-borrelcommissieleden **Eline** en **Jasper** , bedankt voor jullie inzet en input tijdens de borrels en de overleggen! Jullie zijn uitstekend borrelgezelschap, ga zo door!

Het ondersteunend personeel van het LKCH verdient hier ook zeker vermelding. **Joukje**, jouw inzet om alles tot in de puntjes te regelen is bewonderenswaardig. Ik had me geen betere assistent kunnen wensen voor de voorbereidingen van mijn promotie en voor alle contractuele strubbelingen die ik heb moeten doormaken. Een dikke pluim, bedankt! **Michel**, bedankt dat je me altijd hebt geholpen om het ICT-systeem van het UMC te omzeilen en computerproblemen binnen no-time te fixen. **Arno**, erg fijn dat jij het magazijn beheert. Zonder jouw inzet om de continue stroom van celkweekflessen die we nodig hadden in stand te houden, had ik niet zoveel experimenten uit kunnen voeren. Ik drink graag nog eens een whisky met je! **Carin** en **Sonja**, bedankt voor het snel bijvullen van mijn budget nadat de borrelboodschappen er een gat in hadden geslagen ;)

Ik heb ook steun gehad van mensen buiten het LKCH. Ik wil daarom graag de (oud) collega's van Biofarmacie (onder wie **Erik O**, **Kristel**, **Markus**, **Erik T**, **Albert**, **Işil**, **Emmy**, **Kimberley**, **Joep**, **Mies** en **Enrico**) van harte bedanken voor de gezellige en leerzame tijd die ervoor heeft gezorgd dat ik überhaupt ben gaan promoveren. Daarnaast vond ik het erg fijn dat ik tijdens mijn promotie af en toe stiekem kon aansluiten bij jullie borrels. Ook wil ik even de mensen noemen die de ISEV congressen en vesicle-meetings altijd tot een feestje hebben gemaakt. **Olivier**, **Marijke**, **Els**, **Bas**, **Niek**, **Tom**, **Eduard** en talloze andere vesicle-vriendjes, bedankt voor alle gezelligheid! Mijn dank gaat daarnaast uit naar de collega's in het Kruyt gebouw: **Paul**, **Raimond**, **Sabrina** en **Remko.** Bedankt voor jullie input en het delen van jullie nanobody-expertise!

Zonder ontspanning kan er natuurlijk geen fatsoenlijk promotieonderzoek worden gedaan. Daarom wil ik graag **Rob**, **Rodney**, **Mark**, **Diederik**, **Rozemarijn**, **Joost**, **Jorg**, **Else**, **Erik**, **Emma**, **Niels**, **Lotte**, **Beb**, **Luc**, **Kido**, **Jurgen** en **Maikel** (en vast nog een aantal die ik

vergeet, maar die zijn minstens zo belangrijk) bedanken voor alle feestjes, festivals, concerten en alle andere algemene random gezelligheid die jullie in mijn leven hebben gebracht. Ik hoop dat we nog lang zo door kunnen gaan! **Wendy**, bedankt dat je mijn kapsel al die jaren in vorm hebt gehouden!

Ook de familie mag hier uiteraard niet ontbreken. **Sjors**, **Nienke**, **Lex** en **Christel** en al jullie kinders, bedankt voor alle gezelligheid en support tijdens mijn onderzoek! Daarnaast een speciaal bedankje voor Nienke en Sjors voor het gebruik van hun mooie camera, die mede verantwoordelijk is voor de cover van dit proefschrift! **Marieke** en **Alexis**, **pap** en **mam**, ondanks dat voor jullie promoveren toch een beetje een raadselachtig beroep is gebleven, vind ik het fijn dat jullie altijd geïnteresseerd waren en me steevast hebben gesteund. Pa, bedankt voor je hulp bij het bewerken van knikkers voor de cover en Marieke, bedankt voor het begrijpelijk maken van de Nederlandse samenvatting! Bitte sehr voor alles!

Naast een plek om te promoveren, heeft het LKCH me iets gegeven dat veel meer waard is. Lieve, knappe **Maaike**, dit stukje tekst is compleet ontoereikend om uit te drukken hoe blij ik ben dat wij elkaar hebben gevonden en nu bij elkaar zijn. Jij maakt me compleet en geeft me de kracht om te doen wat ik leuk vind. Met jou aan mijn zijde kan ik alles aan. We moeten misschien nog wat moeilijke tijden door waarin we elkaar moeten missen, maar ik weet zeker dat ons verhaal uiteindelijk gaat eindigen met de magische zin "en ze leefden samen nog lang en gelukkig". Love you!

Sander

Curriculum Vitae

Sander Kooijmans was born on the 3rd of February, 1988 in Wamel (Gelderland), The Netherlands. In 2006 he finished his pre-university gymnasium education at the RSG Lingecollege in Tiel, and started his Bachelor's program in Pharmacy at the Utrecht University. He obtained his degree in 2009 and started a Master's program in Drug Innovation at the Utrecht University. During his Master's, he completed a 9-month research project at the Department of Pharmaceutics at the Utrecht University. This project was aimed at the development of a novel method to construct randomized gene libraries, which could be used to screen for efficient peptide-based gene delivery vectors. After this, he moved to Australia for a 6-month research project at the Department of Drug Delivery, Disposition and Dynamics at the Monash University in Melbourne. There he focused on the identification of transporters responsible for transport of adamantane-derived drugs across the blood-brain barrier. He obtained his Master's degree in 2011 and started a PhD project at the Department of Clinical Chemistry and Haematology at the University Medical Center Utrecht under supervision of prof. dr. Raymond Schiffelers and prof. dr. Wouter van Solinge. In his project he worked on the engineering of extracellular vesicles for drug delivery purposes. The results of this work are presented in this thesis. He continued his career as a postdoctoral researcher at the Bioindustry Park Silvano Fumero in Turin, Italy, where he investigates the therapeutic application of stem cell-derived extracellular vesicles after kidney injury.

List of publications

Publications from this thesis

S.A.A. Kooijmans, P. Vader, S.M. van Dommelen, W.W. van Solinge and R.M. Schiffelers. Exosome mimetics: a novel class of drug delivery systems. *Int J Nanomedicine*. 7 (2012) 1525-41.

S.A.A. Kooijmans*, S. Stremersch*, K. Braeckmans, S.C. de Smedt, A. Hendrix, M.J.A. Wood, R.M. Schiffelers, K. Raemdonck# and P. Vader#. Electroporation-induced siRNA precipitation obscures the efficiency of siRNA loading into extracellular vesicles. *J Control Release*. 172 (2013) 229-38.

S.A.A. Kooijmans*, S. Stremersch*, K. Raemdonck# and P. Vader#. New considerations in the preparation of nucleic acid-loaded extracellular vesicles. *Ther Deliv*. 5 (2014) 105-7.

S.A.A. Kooijmans, L.A.L. Fliervoet, R. van der Meel, M.H.A.M. Fens, H.F.G. Heijnen, P.M.P. van Bergen en Henegouwen, P. Vader and R.M. Schiffelers. PEGylated and targeted extracellular vesicles display enhanced cell specificity and circulation time. *J Control Release*. 224 (2016) 77-85.

S.A.A. Kooijmans, C. Gómez Aleza, S.R. Roffler, W.W. van Solinge, P. Vader and R.M. Schiffelers. Display of GPI-anchored anti-EGFR nanobodies on extracellular vesicles promotes tumour cell targeting. *J Extracell Vesicles*. 5 (2016) 31053.

*These authors contributed equally to this work

# These authors contributed equally to this work

Other publications

S.A.A. Kooijmans, D. Senyschyn, M.M. Mezhiselvam, J. Morizzi, S.A. Charman, B. Weksler, I.A. Romero, P.O. Couraud and J.A. Nicolazzo. The involvement of a Na^+- and Cl^--dependent transporter in the brain uptake of amantadine and rimantadine. *Mol Pharm*. 9 (2012) 883-93.

S.M. van Dommelen, P. Vader, S. Lakhal, **S.A.A. Kooijmans**, W.W. van Solinge, M.J.A. Wood and R.M. Schiffelers. Microvesicles and exosomes: Opportunities for cell-derived membrane vesicles in drug delivery. *J Control Release*. 161 (2012) 635-44.

T.M. Hinton, P. Monaghan, D. Green, **S.A.A. Kooijmans**, S. Shi, K. Breheney, M. Tizard, J.A. Nicolazzo, A.N. Zelikin and K. Wark. Biodistribution of polymer hydrogel capsules for the delivery of therapeutics. *Acta Biomater*. 8 (2012) 3251-60.

M. de Raad, **S.A.A. Kooijmans**, E.A. Teunissen and E. Mastrobattista. A Solid-Phase Platform for Combinatorial and Scarless Multipart Gene Assembly. *ACS Synth Biol*. 2 (2013) 316-26.

L.N. Borgheti-Cardoso, L.V. Depieri, **S.A.A. Kooijmans**, H. Diniz, R.A.J. Calzzani, F.T.M. Vicentini, R. van der Meel, M.C. Fantini, M.M. Iyomasa, R.M. Schiffelers and M.V.L.B. Bentley. An *in situ* gelling liquid crystalline system based on monoglycerides and polyethylenimine for local delivery of siRNAs. *Eur J Pharm Sci*. 74 (2015) 103-17.

Selected abstracts

S.A.A. Kooijmans, M.J. A. Wood, R.M. Schiffelers and P. Vader. Loading of siRNA into extracellular vesicles by electroporation is accompanied by extensive siRNA aggregate gormation. Podium presentation at the annual conference of the International Society of Extracellular Vesicles, Boston, USA, April 2013.

S.A.A. Kooijmans, L.A.L. Fliervoet, R. van der Meel, S. Oliveira, R. Heukers, P.M.P. van Bergen en Henegouwen, P. Vader and R.M. Schiffelers. Retargeting of extracellular vesicles by introduction of anti-EGFR nanobodies: lessons from the liposome field. Podium presentation at the annual conference of the International Society of Extracellular Vesicles, Rotterdam, The Netherlands, April 2014.

S.A.A. Kooijmans, L.A.L. Fliervoet, R. van der Meel, M.H.A.M. Fens, P.M.P. van Bergen en Henegouwen, P. Vader and R.M. Schiffelers. Comparison of two novel strategies for (re)targeting of extracellular vesicles with anti-EGFR nanobodies. Podium presentation at the annual conference of the International Society of Extracellular Vesicles, Washington D.C., USA, April 2015.

S.A.A. Kooijmans, J.J.J.M. Gitz-François, P. Vader and R.M. Schiffelers. Recombinant phosphatidylserine-binding proteins for targeting of extracellular vesicles to tumor cells: A plug-and-play approach. Poster presentation at the annual conference of the International Society of Extracellular Vesicles, Rotterdam, The Netherlands, May 2016.